Roles of organic-inorganic interactions in the generation of petroleum as exemplified by Lower Palaeozoic petroleum systems, Europe

vorgelegt von
M.Sc. Geologe
Shengyu Yang
geb. in Liaoning, China

von der Fakultät VI - Planen Bauen Umwelt
der Technischen Universität Berlin
zur Erlangung des akademischen Grades

Doktor der Naturwissenschaften
Dr. rer. nat.

genehmigte Dissertation

Promotionsausschuss:

Vorsitzender: Prof. Dr. Wilhelm Dominik
Berichter: Prof. Dr. Brian Horsfield
Berichter: Prof. Dr. Reinhard Sachsenhofer

Tag der wissenschaftlichen Aussprache: 07.09.2017

Berlin 2017

Für meine Eltern

献给父母

“So lange Vater und Mutter auf der Welt sind, solltest Du nicht in die Ferne reisen – tust Du es dennoch, so gib wenigstens Dein Reiseziel bekannt.”

Konfuzius (551 BC – 479 BC)

父母在，不远游，游必有方。

孔子

ACKNOWLEDGEMENTS

It was 2011 when I met Prof. Dr. Brian Horsfield and Dr. Hans-Martin Schulz in Beijing for the first time. Their courteous and affable characters besides profound knowledge attracted me here in Germany, 7000+ km away from home. My first gratitude goes to Brian who opened the gate of geochemistry world to me and showed me the way (cited from a self-made song Hotel Organic Geochemistry). His constructive suggestions on academic topics and enlightenments on life always inspire me to be a good researcher and enjoy the life at the same time. Hans-Martin is another mentor to be greatly acknowledged which is not merely attributed to the fact that we are both Borussia Dortmund fans. His elaborate attitude toward science and humility to people act as great examples for me. I also benefited greatly from his abundant suggestions and efficient corrections on my manuscripts, some of which were even finished in the weekend.

My sincere gratitude is extended to Dr. Nicolaj Mahlstedt, Dr. Niels Hemmingsen Schovsbo, Prof. Dr. Rolando di Primio, Dr. Mareike Noah, and Dr. Stefanie Pötz for fruitful discussions. It's impossible to carry out my research without the professional and reliable technical supports from Ferdinand Perssen, Cornelia Karger, Anke Kaminsky, and Kristin Günther.

Chinese Scholarship Council is greatly acknowledged for sponsoring my Ph.D. study.

I am grateful to be a member of an NGO (non-governmental organization) called "cyclopentane" which consist Janina Stapel, Sascha Kuske, Seyed Hossein Hosseini Baghsangani, and Volker Ziegs, in addition to me. The five "carbon atoms" bonded together ends in never-ending entertainment, friendship, and trust.

Gratitude to my beloved father Yang Desan and mother Song Yuying is beyond words. More than 30 years of constant love and expectations from them provide me an infinite power forward. My two sisters and brother are also gratefully acknowledged for their love and encouragement. Due to limited space here, my endless thanks to my wife Zhang Yu will be presented in detail in the rest of my life.

LIST OF PUBLICATIONS

Articles:

(1) **S. Yang**, B. Horsfield, N. Mahlstedt, M. H. Stephenson, and S. F. Könitzer, 2015, On the primary and secondary petroleum generating characteristics of the Bowland Shale, northern England: Journal of the Geological Society, v. 173, p. 292-305 (postprint), doi: 10.1144/jgs2015-056.

(2) **S. Yang**, and B. Horsfield, 2016, Some predicted effects of minerals on the generation of petroleum in nature: Energy & Fuels, v. 30, p. 6677-6687 (postprint), doi: 10.1021/acs.energyfuels.6b00934.

(3) **S. Yang**, H.-M. Schulz, N. H. Schovsbo, and J. A. Bojesen-Koefoed, 2017, Oil-source rock correlation of the Lower Palaeozoic petroleum system in the Baltic Basin (northern Europe), (in press; preliminary version published online Ahead of Print May 22, 2017): AAPG Bulletin (postprint), doi: 10.1306/02071716194.

(4) **S. Yang**, H-M. Schulz, B. Horsfield, and N.H. Schovsbo, H. Rothe and K. Hahne Impact of uranium irradiation on the petroleum potential of the Cambro-Ordovician Alum Shale, Northern Europe (preprint). Submitted to Geochimica et Cosmochimica Acta on 27 Jul 2017.

Poster and Presentation:

(1) **S. Yang**, B. Horsfield, and M. H. Stephenson, 2015, Kinetics of primary and secondary petroleum generation of the Bowland Shale: IMOG, Czech Republic. Poster.

(2) **S. Yang**, H.-M. Schulz, N. H. Schovsbo, and J. A. Bojesen-Koefoed, 2016, Oil-source rock correlation of the Lower Palaeozoic petroleum system in the Baltic Basin: AAPG Geosciences Technology Workshop, Lithuania. Oral presentation.

ABSTRACT

The clay-rich Lower Carboniferous Bowland Shale (England) and the uranium-rich Cambro-Ordovician Alum Shale (Northern Europe), both deposited in marine environments, are characterized by dominating gaseous and aromatic compounds in pyrolysates. Therefore, the kerogens in both of these shales can be classified as type III from classical perspectives, which is not consistent with the depositional environment. This dissertation aims to investigate the organic-inorganic interactions in changing the petroleum formation and occurrence. Special efforts were made to validate the interactions in geological environments, besides the findings derived from laboratory experiments.

Interdisciplinary geochemical techniques covering pyrolytic methodologies, e.g., Rock-Eval pyrolysis, pyrolysis gas chromatography (Py-GC), bulk kinetics, micro-scale sealed vessel-Py-GC (MSSV-Py-GC), and high resolution experiments based on extractions, e.g., GC-Flame Ionization Detector (GC-FID), GC-mass spectrometry (GC-MS), and Fourier Transform Ion Cyclotron Resonance MS (FT-ICR-MS) are employed in unravelling the organic-inorganic interactions. Furthermore, mass-balances, PhaseKinetics, and 1D modelling are also carried out to predict the occurrence and behaviour of petroleum.

The mineral matrix effect (MME) does not only influence basic geochemical parameters, e.g. a decrease in HI and increases in T_{max}, OI and gas generation, but also changes the hydrocarbon generation kinetics and phase behaviour. Accordingly, significant errors can be induced by MME when basin modelling approaches are applied to predict secondary gas generation. The extent of MME in shale varies according to the mineralogical composition. In contrast to the clay-rich Bowland Shale, the calcite-rich Toolebuc Oil Shale and the quartz-rich Alum Shale are only slightly and not affected by MME, respectively. Furthermore, the size of the interface area between clay minerals and organic matter could be another factor that influences the extent of MME.

The MME is found heating rate dependent, i.e., a lower heating rate weakens the MME on pyrolysate aromaticity and generation quantity. Therefore, the catalytic and retention effects of clay minerals are speculated to only exist in the laboratory environment and not in a geological maturation process. This is further supported by the fact that the kerogen pyrolysates resemble natural products more than products derived from whole rock pyrolysis as revealed by FT-ICR MS experiments.

Robust correlations can be established between uranium contents and pyrolysate GOR and aromaticity on the immature Alum Shale samples, indicating a strong uranium irradiation effect on petroleum generation. Also, the aromaticity and GOR of free hydrocarbons from thermovaporization-GC are proportional to those in pyrolysates which validates that the uranium irradiation does influence the petroleum generation in nature. The FT-ICR MS data reveal that the macro-molecules in the uranium-rich Alum Shale samples are less alkylated and could be responsible why such kind of samples tend to generate gaseous products.

Basin modelling results reveal that most Alum Shale horizons reached peak oil generation between Late Devonian to Early Carboniferous (360-385 Mya) which means kerogens have had experienced about a quarter of irradiation until peak oil generation compared with radiation measured from nowadays core samples which have received full irradiation since their formation (478-500 Mya). Kerogen structures during the oil window time were reconstructed based on the fact that both irradiation time and uranium contents are linearly correlated with irradiation damages. The kerogens are much more oil-prone and tend to generate more aliphatic hydrocarbons back to Devonian time compared with nowadays samples. In addition, the gas sorption capacity of the Alum Shale is supposed to be less strong during Palaeozoic time in contrast to sorption experiments.

The unique distribution of triaromatic steroids in uranium-rich Alum Shale samples, i.e., decreased concentrations of C_{26}-C_{28} triaromatic steroids with increasing uranium contents, was found in oil samples sourced from the Alum Shale. This parameter could act as an oil-source-correlation proxy, especially when aliphatic biomarkers are normally destroyed in the uranium-rich Alum Shale.

In summary, catalytic effects under high temperatures and hydrocarbon retention induce the MME, and the uranium irradiation works in condensation and cross-linking reactions. The MME is a laboratory induced artefact and does not exist in geological environments. The kerogen structures are not changed by minerals during diagenesis. In contrast, uranium irradiation significantly alters kerogen structures, and furthermore changes the quantity and quality of petroleum generation in both laboratory and geological environments. The removal of minerals by acidic dissolution is an efficient way to avoid misleading information caused by MME. A reconstruction of kerogen structures back to the time of petroleum generation is crucially important to correctly evaluate the hydrocarbon generation characteristics of uranium-rich source rocks.

ZUSAMMENFASSUNG

Die Ton-reichen Schichten des Unterkarbonischen Bowland-Schiefers (England) und des Uran-reichen Kambroordovizischen Alaunschiefers (Nordeuropa), die unter marinen Bedingungen abgelagert wurden, zeichnen sich durch gasförmige und aromatische Komponenten in ihren Pyrolysaten aus. Somit wird das Kerogen nach klassischen Gesichtspunkten als Typ III beschrieben, was nicht mit den Ablagerungsbedingungen im Einklang steht. Diese Dissertation hat zum Ziel, die organisch-anorganischen Interaktionen zu untersuchen, welche die Erdölgenese und -vorkommen beeinflussen. Besonderes Augenmerk wurde auf die Validierung der Prozesse unter geologischen Bedingungen gelegt, sowie auf deren Vergleich mit Laborexperimenten.

Zur detaillierten Erkundung organisch-anorganischer Interaktionen wurden interdisziplinäre geochemische Verfahren angewandt, die von pyrolytischen Methoden reichen, z.B. Rock-Eval-Pyrolyse, gekoppelte Pyrolyse-Gaschromatographie (Py-GC), Bulk-Kinetik, micro-scale sealed vessel-Pyrolyse-Gaschromatographie (MSSV-Py-GC), und hochauflösende Experimente an Muttergesteinsextrakten, z.B. Gaschromatographie mit Flammenionisierungsdetektor (GC-FID), gekoppelte Gaschromatographie-Massenspektrometrie (GC-MS), und Fourier Transform Ion Cyclotron Resonance MS (FT-ICR-MS). Weiterhin wurden zur Vorhersage von Vorkommen und Phasenverhalten des gebildeten Erdöls Massenbilanzierungsberechnungen, PhaseKinetics und 1D-Modellierung durchgeführt.

Der Mineralmatrix-Effekt (MME) wirkt sich nicht nur auf grundlegende geochemische Parameter aus, verursacht z.B. einen Abfall des Wasserstoff-Indizes (HI) und einen Anstieg des T_{max}, Sauerstoff-Indizes (OI) und der Gasgenese, sondern beeinflusst die Kinetik der Kohlenwasserstoffgenese und deren Phasenverhalten. Daraus können sich signifikante Fehler in der Beckenmodellierung zur Vorhersage der Sekundärgasgenese ergeben, welche hauptsächlich zur thermogenen Schiefergasproduktion beiträgt. Das Ausmaß der MME in Schiefergesteinen variiert mit der Mineralzusammensetzung. Im Gegensatz zum Ton-reichen Bowland-Schiefer sind der Kalzit-reiche Toolebuc Ölschiefer und der Quarz-reiche Alaunschiefer durch den MME nur wenig bzw. nicht beeinflusst. Ein weiterer Faktor, der sich auf den MME auswirkt, können Grenzflächeninteraktionen zwischen Tonmineralen und organischer Materie sein.

Der Mineralmatrixeffekt ist Heizraten-abhängig; eine niedrige Heizrate vermindert die Aromatizität der Pyrolysate und die Menge der gebildeten Produkte. Hieraus wird geschlussfolgert, dass die katalytischen Effekte von und Retention an Tonmineralen lediglich im Labor entstehen, jedoch nicht unter geologischen Reifebedingungen. Eine höhere Ähnlichkeit von Kerogenpyrolysaten mit Mutter-gesteinsextrakten als mit deren Pyrolysaten in FT-ICR-MS-Experimenten unterstützt diese These.

Unreife Alaunschiefer-Proben zeigen robuste Korrelationen zwischen Uranium-Gehalten und Gas-Öl-Verhältnis (GOR) bzw. Aromatizität der Pyrolysate und deuten auf einen starken Strahlungseffekt von Uranium auf die Erdölgenese. Weiterhin sind Aromatizität und GOR von freien Kohlenwasserstoffen aus Thermovaporisationsexperimenten proportional zu denen in Pyrolysaten, und unterstützt den Strahlungseffekt auf die Erdölgenese unter natürlichen Bedingungen. FT-ICR-MS-Daten zeigen, dass Makromoleküle im Uranium-reichen Alaunschiefer weniger alkylisiert sind, was die erhöhte Gasgenese derartiger Proben verursachen kann.

Die Beckenmodellierung zeigt, dass der Großteil der Alaunschieferschichten den Höhepunkt der Ölgenese zwischen Spätem Devon und Frühem Karbon (360-385 Mill. Jahren vor heute, Ma) erreichten. Dies bedeutet, dass das Kerogen zu jener Zeit nur ungefähr ein Viertel der Strahlung erhalten hat als dies an heutigen Kernproben gemessen wurde, welche die volle Strahlungsmenge seit ihrer Bildung (478-500 Ma) erhalten haben. Die Kerogenstruktur zur Zeit der maximalen Erdölgenese wurde, basierend auf linearen Korrelationen von Strahlungsschäden mit Strahlungsdauer bzw. Uranium-Gehalten, rekonstruiert. Das modellierte Kerogen generiert wesentlich höhere Mengen an Öl, welches aliphatischer ist, als heute vorzufindende Proben. Zusätzlich wird angenommen, dass die Gassorptionskapazität des Alaunschiefers im Paläozoikum weniger stark war als heutzutage.

Die bseondere Verteilung von triaromatischen Steroiden in Uranium-reichen Alaunschiefer-Proben, z.B. verringerte Konzentrationen von C_{26}-C_{28} triaromatischen Steroiden mit steigendem Uranium-Gehalt, wurde ebenfalls in genetisch verwandten Ölen gefunden. Dieser Parameter könnte als Korrelationsproxy für Öle und Muttergesteine dienen, besonders da aliphatische Biomarker im Alaunschiefer normalerweise zerstört sind.

Katalytische Effekte bei hohen Temperaturen und die Retention von Kohlenwasserstoffen lösen MME aus, und die Uranium-Strahlung verursacht Kondensationsreaktionen und Querverbindungen. Der MME ist ein Effekt, der sich auf Laborexperimente beschränkt,

und existiert nicht unter natürlichen Bedingungen. Kerogenstrukturen werden während der Diagenese nicht durch Minerale verändert. Im Gegensatz dazu beeinflusst Uranium-Strahlung Kerogenstrukturen signifikant und determiniert Menge und Beschaffenheit generierter Erdöle, sowohl unter Labor- als auch natürlichen Bedingungen. Eine effektive Methode die irreführenden Informationen durch den MME zu vermeiden ist die azide Demineralisierung der Muttergesteine. Eine Rekonstruktion der originären Kerogenstruktur zur Zeit der maximalen Erdölgenese ist entscheidend für die korrekte Evaluation der Kohlenwasserstoff-genesecharakteristika Uranium-reicher Muttergesteine.

CONTENTS

LIST OF FIGURES

Fig 5.8. The terpane biomarker cross-plot can efficiently separate Llandovery source rocks from the rest. C_{24} TeT and C_{26} TT are abbreviations for C_{24} tetracyclic terpane and C_{26} tricyclic terpane respectively. The extended tricyclic terpane ratio (ETR) (Holba et al., 2001) is calculated from $(C_{28}+C_{29})/(C_{28}+C_{29}+T_s)$ in *m*/z191. The size of the dot demonstrates the maturity of each sample to evaluate the maturity dependency of the biomarkers.

Fig. 5.9. Ternary diagram showing the relative distribution of C_{27}, C_{28} and C_{29} *iso*-steranes [5α,14β,17β(H) 20S+20R]. The Llandovery shale extracts and oil sample Gec are featured by high concentrations in C_{29} *iso*-sterane.

LIST OF TABLES

LIST OF ABBREVIATIONS

A	Frequency factor
CPI	Carbon Preference Index
Ea	Activation energy
ETR	Extended Tricyclic-terpane Ratios
FID	Flame Ionization Detector
FT-ICR	Fourier Transform Ion Cyclotron Resonance
GC	Gas Chromatography
GOR	Gas to Oil Ratio
HC	Hydrocarbon
HCA	Hierarchical Cluster Analysis
HI	Hydrogen Index, HI = S_2/TOC × 100 (mg HC/g TOC)
MPLC	Medium Pressure Liquid Chromatography
MS	Mass Spectrometry
MSSV	Micro Scaled Sealed Vessel
m/z	mass to charge ratio
NSO	Nitrogen, Sulfur and Oxygen
OI	Oxygen Index, OI = S_3/TOC × 100 (mg CO_2/g TOC)
OEP	Odd to Even Predominance
PCA	Principal Component Analysis
PI	Production Index
Py	Pyrolysis
Pr/Ph	Pristane/ Phytane
S_1	Amount of Volatized Hydrocarbons at Rock Eval
S_2	Amount of Generated Hydrocarbons during Pyrolysis at Rock Eval
T_{max}	Temperature of maximum Pyrolysis Yield
TOC	Total Organic Carbon
TR	Transformation Ratio
Ts/Tm	C_{27}-trisnorneohopane/C_{27}-trisnorhopane
T_{vap}	Thermovaporisation Gas Chromatography
R_o	Vitrinite Reflection

1. INTRODUCTION

1.1 Development of Petroleum Formation Theories

Petroleum is a collective term for any subsurface material that can be produced as oil or gas (including some associated non-hydrocarbons) (Mackenzie et al., 1988). The history of petroleum utilisation can be traced back four thousand years to when asphalt was used for construction in Babylon (Al-Sammerrai et al., 1987). The earliest known oil well was drilled in China using bamboo in 347 AD (Groysman, 2014). The modern history of petroleum began in the 19th century with the drilling of exploration wells in Pennsylvania and Poland, and refining of crude oil to obtain paraffins. Later on, the invention of the internal combustion engine was the major influence in the rise of the petroleum industry. While the enormous economic impact of petroleum is self-evident, its origin has been a topic of great and ongoing debate.

1.1.1 Biogenic vs. Abiogenic

It was during the renaissance that the first reasonable theories about the origin of petroleum were developed. In 1546, Georgius Agricola, a German physician who coined the term "petroleum", proposed that bitumen is condensed from sulphur (Walters, 2006). Andreas Libavius, another German physician, hypothesised in 1597 that bitumen formed from the resins of ancient trees. These early discussions mark the beginnings of one of the longest running scientific debates: whether petroleum is formed by abiogenic processes that occur deep within the Earth, or from sedimentary organic matter derived from once living organisms.

As fossil evidences emerged during the 18th century that coals were derived from plant remains, Mikhailo Lomonosov proposed petroleum was formed from coal through underground heat and pressure in 1763 (Hedberg, 1964). Modern theories that petroleum originated from organic-rich rocks, and not necessarily coal, emerged during the 19th century (Hunt, 1863). Meanwhile, the famous Russian scientist Mendeleev (1877) proposed that petroleum was created in the depths of the Earth from chemical reactions between water and iron carbides in the hot upper mantle.

The beginning of the 20th century marks the development of modern petroleum geology. The biogenic origin of petroleum gained major recognition among geologists (Arnold and

van Vleck Anderson, 1907; Pompeckj, 1901), especially after Treibs (1934) discovered porphyrin pigments in petroleum with structures originating from chlorophylls in petroleum. Meanwhile, Fischer and Tropsch (1930) successfully synthesised long-chain hydrocarbons using inorganic reactants, i.e., carbon monoxide and hydrogen.

Starting in the 1950s, Kudryavtsev (1951) and other subsequent publications (Rudakov, 1967) from the former Soviet Union proposed a modernised version of Mendeleev's theory, relying on thermodynamic equilibrium for chemical reactions that only allows spontaneous formation of methane at high temperature and pressure, comparable to those of the upper mantle region. This abiogenic theory was appealing because it offered an explanation for the presence of petroleum deposits in metamorphic rocks of the basement. However, with the development of analytical techniques, overwhelming evidence strongly argues that petroleum is actually originated from biologically derived organic source materials, and that therefore the oil stored in basement rocks was allochthonous, ostensibly because it had simply migrated from overlying shale layers. (1) Oakwood et al. (1952) showed that oils retain fractions are optically active, just like biological matter; (2) stable carbon isotope compositions in oil were found to be in line with a biogenic origin (Craig, 1953) as living organisms favour certain carbon isotopes more than others; (3) biomarkers, e.g., steranes and terpanes, found in the petroleum can be traced to their biological predecessors (Eglinton and Calvin, 1967), some of which can even correlate oil to specific geological ages (Hoffmann et al., 1987; Moldowan et al., 1994); (4) hydrocarbons resembling petroleum can be formed through thermal cleavage of kerogen (Horsfield et al., 1989). However, the fundamental dispute continues. The astronomer Gold (1985) believes that there is a huge amount of primordial methane within the Earth since hydrocarbons were found in chondrites and other planetary bodies, including asteroids, comets, and moons. However, the utter failure of two deep wells drilled in the Siljan Ring (Sweden) where was supposed to be an ideal place to gain inorganic sourced gas (Gold and Soter, 1982) made the abiogenic origin theory remain unproven and less plausible. Even today, people who believe that petroleum has migrated upward from the mantle have not been deterred by this setback. Kenney et al. (2001) who was the drilling manager of the Sijan Ring wells claimed that: "natural petroleum has no connection with biological matter". High-temperature and high-pressure experiments, simulating mantle environment, are still running in Russian labs to synthesise inorganic origin petroleum (Belonoshko et al., 2015; Kolesnikov et al., 2009).

In summary, the abiogenic origin theory is mainly based on theoretical studies and laboratory verifications. It is ironic that this theory is advocating that the mass of petroleum is essentially infinite on Earth (Kolesnikov et al., 2009), yet only traceable amount of abiotic oil have been discovered (Walters, 2006). Geochemists do not deny the existence of a very small amount of abiogenic hydrocarbons on Earth. Nevertheless, it is irrefutable that over 99.99% of the petroleum has been found in sedimentary basins and all commercial findings are guided by the modern biogenic origin theory.

1.1.2 Deep vs. Shallow

Although most geologists agree that petroleum was formed from organic matter, there were debates within the framework of biogenic theory from the 1940s to 1960s: is the petroleum formed at shallow depths and then preserved, or is burial an essential element (roughly 1-5 km)? In other words, how and when are oil and gas generated from organic matter?

During the middle and late 1940s, the idea of shallow origin and migration of oil began to gain favour. Expansion of modern sediment studies reflected the importance attached to depositional processes and early diagenesis in understanding geologic processes. Zobell (1945) found that bacteria can produce methane and heavier hydrocarbons which resemble petroleum and thus concluded petroleum was formed in shallow areas with low temperatures. (Pratt, 1947) proposed that petroleum accumulation is completed soon after deposition of the source beds based on the occurrence of oil in continental shelves. The discovery of hydrocarbons in recent sediments from the Gulf of Mexico gave support to the shallow generation theory (Smith, 1952). Corbett (1955) suggested that humic material may be washed by meteoric water into shallow sandstone reservoirs where transformation to oil take place. Baker (1959) and Meinschein (1961) proposed that there is no chemical reaction involved in the petroleum formation, oil and gas being hydrocarbon-rich fluids that were selectively washed out from modern sediments by solubilizers-containing water.

The counterargument was that petroleum was formed through the thermal cracking of organic matter and thus requires a considerable depth to reach the temperature. (Gussow, 1954) emphasised the concept that oil globules could only migrate out of the source beds into reservoirs once overburden pressures are sufficiently high as to overcome capillary pressures. Emery and Hoggan (1958) realised that the hydrocarbons in modern sediment are compositionally significantly different from those in oil fields by virtue of their very

high methane percentage and the absence of gasoline hydrocarbons. Bray and Evans (1961) reported the Carbon Preference Index (CPI) in crude oil resembles that of ancient sedimentary rocks and are far lower than CPI values in modern sediments. Shimoyama and Johns (1971) further proved that the odd to even predominance (OEP) n-fatty acids decreases from high values to near unity from modern to ancient sediments and petroleum reservoir water. Philippi (1965) suggested that petroleum is generated at depths where the subsurface temperature is above 115°C.

After the 1970s, the debate gradually settled down and a broad consensus was reached: in shallow depth, dry gas can be generated through bacterial and microbial mechanisms, while oil and gas would be formed in deeper areas by the thermal degradation of organic precursor molecules in sediments. Carbon isotope acts an efficient tool to differentiate gas generated through different mechanisms (Schoell, 1980; Stahl and Carey, 1975). The gas formed by microbial activity was termed *biogenic gas*. Favourable conditions for biogenic gas generation include (1) sequential elimination of oxygen and the electron acceptor sulphate from the sediment, (2) moderate temperature (<75 °C), and (3) sufficient space available for the bacterial bodies (Rice and Claypool, 1981). Most of the biogenic gas was generated from dead biomass which contains degradable biomolecules, e.g., proteins and lipids, but new research manifests that it can also be formed from long-chain alkanes by anaerobic microorganisms (Zengler et al., 1999). Shale gas found in the Devonian Antrim Shale (USA) acts as a successful example of exploiting biogenic gas (Curtis, 2002). In comparison, thermogenic oil and gas require a much deeper burial history to achieve the temperatures needed for cracking the organic matter. Thermal cracking of kerogen via free radicals (Rice, 1931) or the acidic catalyst related cracking (Whitmore, 1934) serve as the two main mechanisms of the generation of thermogenic petroleum. Most of the petroleum found in oil field reservoirs is formed by a thermogenic mechanism.

In addition to these two "orthodox" mechanisms, Mango (Mango, 1990, 1992, 1994, 1997, 2010) advocated the formation of light hydrocarbons as result of catalysis of transition metals. He suggested that transition metals (e.g., V, Ni, Ti, Co, and Fe) are mainly captured from sedimentary waters by the tetrapyrrole nucleus of chlorophyll and act in a steady-state reaction to form light hydrocarbons. This theory has drawn the attentions of geologists for at least two reasons. (1) The gas wetness of pyrolysates in all thermal cracking-based pyrolysis experiments is much higher than reservoired gas (Behar et al., 1992; Horsfield et al., 1989; Lewan et al., 1979), while the metal catalysed reaction is more consistent with the

observations of producing gas wetness. (2) Some light isoparaffins remain virtually invariant through the course of oil generation (Mango, 1987) which can hardly be explained by the routine cracking theory. The invariance was interpreted to be related to cyclopropyl intermediates formed by metal catalysts (Mango, 1990) and was supported by kinetic models based on these ring closure reactions (van Duin and Larter, 1997; Xiao and James, 1997). Even though the metal catalysis hypothesis appears to explain some "contradictions" of the classical thermal cracking theory, counterarguments on this theory are based on many aspects. (1) It is suggested that gas wetness in reservoirs described by Mango does not necessarily represent the gas composition when the gas was generated because fractionation during migration would change it significantly. Price and Schoell (1995) reported that in the Bakken Shale, which serves as a closed system of both source and reservoir, associated methane accounts for ~45 wt.%, which is consistent with laboratory simulations of thermal cleavage. Snowdon (2001) advocated that gas wetness of cutting samples gives a better representative of the naturally generated gas wetness rather than conventional reservoir production data. (2) Hydrous pyrolysis experiments delivered evidence revealing that transition metals have no effect on methane enrichment or $\delta^{13}C$ changes (Lewan et al., 2008). Thus the metal catalysis theory would not be a realistic option if the source rock is initially water-saturated. (3) The contact of kerogen with transition metals in natural environments is very limited, and NiO normally used as a catalyst in Mango's experiments (Mango, 2007; Mango and Hightower, 1997) is very rare in source rocks. (4) Furthermore, some assumptions in Mango's theory appear to be questionable. For examples, olefins are important intermediates during catalytic reactions (Mango, 1987; Mango, 1994) and it was suggested that petroleum should be at least three orders of magnitude more stable than the kerogen precursors under catagenic conditions (Mango, 1991), but olefins are rarely found in natural petroleum (Curiale and Frolov, 1998) and petroleum in natural reservoirs can be secondarily cracked between 160 ^{o}C-190 ^{o}C (Horsfield et al., 1992c). Nevertheless, the transition metal catalysis theory provides the best explanation for the isoparaffin invariances and acts as an alternative petroleum generation pathway despite being a general matter of debate.

1.1.3 Fatty Acid vs. Kerogen

Another matter of contention was related to what kind of organic matters are the precursors of petroleum? Fatty acids and kerogen which is insoluble in common chemical solvents are the two candidates.

Much early pyrolysis work was concentrated on molecules soluble in organic solvents, especially fatty acids. In the 1960s, Cooper and Bray (1963) and Jurg and Eisma (1964) generated petroleum-like hydrocarbons, with a CPI around unity, through heating fatty acids. Kvenvolden (1966) speculated hydrocarbons were formed through decarboxylation of fatty acids. Welte and Waples (1973) and Douglas et al. (1975) suggested dehydration and reduction of fatty alcohols can also lead the formation of alkanes from fatty acids. Based on these extensive experiments, it is no wonder that the fatty acids were considered as an important precursor of petroleum.

Abelson (1963) pointed out fatty acids would disappear rapidly in geological environments and only kerogen can be considered capable of quantitatively accounting for the petroleum found in reservoirs. It comprises by far the largest organic matter pool on Earth, i.e., 10^{14} tons of carbon in kerogen compared to ca. 10^{12} tons in living biomass (Welte, 1970). Later research found that the kerogen is formed from proteins, carbohydrates, lipids, and lignin through degradation-recondensation (Tissot and Welte, 1984) or by selective preservation (Tegelaar et al., 1989). It is now firmly established that petroleum is primarily formed from the maturation, over time and with burial at elevated temperatures, of kerogen.

1.2 Characterisation of Kerogen Structure

The kerogen structure and the maturation process it experienced are the initial factors that control the thermogenic petroleum composition, followed by secondary processes like migration fractionation, phase separation, biodegradation, water washing, etc. The structural features of kerogen describe the elemental constitution, chemical bond connection, and the stability of the structures, and thus define the quality, quantity, and kinetics of petroleum generation.

1.2.1 Generation quality and quantity

1.2.1.1 Elemental analysis and Rock-Eval

Pioneering studies by Down and Himus (1941) attributed kerogen compositional differences to variation in plant sources, depositional environment and bacterial reworking. Now it is widely accepted that four types of kerogen can be recognised by elemental analysis (Durand and Espitalié, 1973; Van Krevelen, 1950) and Rock-Eval pyrolysis (Espitalie et al., 1977). These kerogen types can provide information not only about past environments and biota, but also petroleum generation characteristics.

Source rocks deposited in anoxic lakes or anoxic shallow marine basins tend to contain a very hydrogen-rich kerogen derived from plankton (type I or II) and are oil-prone. Those deposited in fluvial and deltaic facies usually contain hydrogen-leaner kerogen (type III) derived from higher land plants and predominantly generate gas-rich products or high-wax oils. Type IV kerogen which is dominated by inertinite has a very little petroleum generation potential. Although such general correlations between depositional environments, kerogen type and hydrocarbon generation are fulfilled in most scenarios, exceptions exist. The generation potential of source rocks is reflected by the Hydrogen Index (HI), this being the discriminator for kerogen type recognition. Type I (HI>600 mgHC/gTOC) and type II (200 mg HC/gTOC<HI<600 mg HC/gTOC) contain great hydrocarbon generation abilities and sourced most of the commercial petroleum reservoirs in the world. Type III kerogen which has low HI enabled only limited petroleum discoveries. Nevertheless, gas fields in Mid-European Basin(Lutz et al., 1975), waxy crude oils in Asia (Peters et al., 1999), and coal bed methane (Law, 1988) are examples of petroleum generated by type III kerogen.

1.2.1.2 Pyrolysis-GC

Although the gross hydrocarbon generation ability and general oil vs. gas preference can be estimated through calibrated kerogen typing, little exploration-oriented information can be derived, e.g., GOR, aromaticity, and sulphur contents. Pyrolysis, defined as a chemical degradation reaction that is induced by thermal energy alone (Ericsson and Lattimer, 1989), when interfaced with GC, is able to provide compositional information on a molecular level.

Kerogens degrade upon pyrolysis to yield many compound types including hydrocarbons, ketones, alcohols, nitriles and thiols, as represented by cyclic and acyclic, saturated and unsaturated carbon skeletons (Dembicki et al., 1983; Van de Meent et al., 1980). Of these the most commonly occurring major identifiable components seen by pyrolysis-GC are doublets of normal alk-1-enes and alkanes, alkylphenols, alkylbenzenes, alkylnaphthalenes and alkylthiophenes. It was proven that the structural information contained within the readily identifiable and major components of kerogen pyrolysis products are coincident with aromaticity data gained by ^{13}C-NMR which is a non-destructive technique (Horsfield, 1989). It's now widely accepted that the abundances and distributions of resolved pyrolysis products give clues as to the bulk compositions of natural petroleums, such as paraffinicity and aromaticity (Damsté et al., 1993; Espitalie et al., 1988). In according, not only the

aromaticity (Larter, 1984), and sulphur contents (di Primio and Horsfield, 1996; Eglinton et al., 1990) of the petroleum which could be generated from the source rock can be inferred from pyrolysates, the type of petroleum can also be predicted. For example, five major types of petroleum can be predicted according to the kerogen pyrolysate length distributions, namely, Gas and Condensate, Paraffinic-Naphthenic-Aromatic oil with high/low wax content, and Paraffinic Oil with high/low wax content (Horsfield, 1989). At the same time, these kerogens can be related in a general way to terrestrial, deltaic, marine and lacustrine depositional environments (Horsfield, 1997).

1.2.2 Kinetics

The kinetics of a source rock defines its thermal reaction to heating time, temperature and/or pressure. Bulk kinetics which describes the generation of the primary products as a whole are well established (Braun and Burnham, 1987; Quigley et al., 1987). More advanced kinetic models are also available. For examples, secondary kinetics of source rocks (Behar et al., 1997; Pepper and Dodd, 1995; Ungerer et al., 1988), secondary kinetics in reservoirs (Horsfield et al., 1992c; Waples, 2000) are especially important in evaluating areas experienced high maturation processes and in the exploration of shale gas. Compositional kinetics (Behar et al., 1992; di Primio and Horsfield, 2006; Dieckmann et al., 2000a; Düppenbecker and Horsfield, 1990) provide much more detailed information in simulating the generation of petroleum.

Quasi-first-order reactions are generally applied for the investigation of kinetics and the result is typically shown as a variable frequency factor and a distribution of activation energy (Burnham et al., 1987; Quigley et al., 1987), in which the frequency factor is related to the vibration frequency of the reaction. Although a compensation effect (Constable, 1925) occurs in the kinetics results which shows a clear correlation between frequency factor and average activation energy (Lakshmanan et al., 1991; Stainforth, 2009) the most intuitive way to compare kinetic features of different samples is to extrapolate the results to a typical geological heating rate (2-4 °C/Ma) and to compare the transformation rate curves (Schenk et al., 1997; Tegelaar and Noble, 1994).

The stabilities of chemical bonds and kerogen heterogeneities together define the frequency factor and activation energy distributions. Thus the kinetic characteristics of source rocks, especially the values and the shapes of the activation energy distributions, are initially controlled by the organic facies (Pepper and Dodd, 1995). Typically, type I kerogen

tends to have a very concentrated activation energy distribution due to the homogenous distribution of C-C bonds and the heterogeneous type III kerogen is normally featured by a very broad activation energy distribution (Ungerer and Pelet, 1987). The marine type II kerogen generally shows an intermediate distribution, but it can be variable according to depositional environment and/or precursors. For examples, the enrichment of *Gloeocapsamorpha Prisca* in an Ordovician marine shale would focus the activation energy distribution as for a type I kerogen (Waples, 2010) and the kinetics can be very active when the shale is sulphur-rich (Tegelaar and Noble, 1994). The kinetic features of marine shale also change with sedimentary facies and geological age of the samples (Mahlstedt, 2012; Waples and Marzi, 1998).

1.3 Influence from Inorganic Materials

As stated above, pyrolysis plays a crucially important role in evaluating kerogen structures and providing practical information for petroleum exploration. The fact that some inorganic materials also influence pyrolysate compositions, sometimes overprinting the initial control of pyrolysates from kerogen structure, raises the question as to whether organic-inorganic reactions control petroleum yields and compositions in active source rocks. Similarly, the presence or absence of water influences pyrolysate characteristics. In addition to these pyrolysis-inspired lines of research, the role of radioactive bombardment on source rock generating characteristics is still under investigation.

1.3.1 Minerals

1.3.1.1 Mineral and petroleum occurrence

Quartz, clay, and calcite are generally the main minerals in shale (Shaw and Weaver, 1965). Other minor constitutes include feldspar, pyrites, phosphate, mica, and siderite. For example, the Mississippian Barnett Shale has average quartz, clay, and calcite contents of 34.3%, 24.2%, and 16.1%, respectively (Loucks and Ruppel, 2007), while the Cretaceous Eagle Ford Shale is typically featured by a carbonate content over 60% and relatively low quartz concentration (Mullen, 2010).

The significant concomitance of clay minerals with oil production has drawn the attention of the importance of mineral in searching for petroleum (Frost, 1945; Grim, 1947). For example, Weaver (1960) found oil production in different geological periods is statistically correlated to the montmorillonite proportion of layers developed in the periods although

carbonate source rocks were not taken into consideration at that time. In general, clay minerals have been believed to play important roles in kerogen preservation and the catalytic formation of petroleum. Furthermore, the process of illitization is also related to oil generation and expulsion in time and space (Burst, 1969).

Degradation-recondensation (Tissot and Welte, 1984) and selective preservation (Tegelaar et al., 1989) are classical pathways in interpreting kerogen formation, while natural sulphurization (Sinninghe Damsté et al., 1989) and clay sorptive protection (Salmon et al., 2000) are also important supplementary mechanisms. Clay minerals, acting as natural adsorbents in sedimentary systems, can adsorb and then protect amorphous, labile and dissolved organic components (e.g., amino acids and simple sugars) from complete microbial degradation. As a result, the presence of clay minerals might play a significant role in organic matter accumulation and the subsequent concentration reactions to kerogen in sedimentary rocks (Wu et al., 2012). This hypothesis is supported by the fact that TOC is inversely proportional to the grain size in most continental shelf sediments (Mayer, 1994) which was ascribed to a monolayer adsorption of organic compounds onto minerals (Salmon et al., 2000).

Besides the thermal cracking of kerogen *via* free radical in generating petroleum (Rice, 1931), the acid catalytic cracking mechanism *via* carbonium intermediates is an alternative (Whitmore, 1934). The carbonium-ions are primarily generated on the Brønsted and Lewis acid sites of clay minerals. In chemistry, the Brønsted acid is viewed as a proton donor and the Lewis acid can act as an electron acceptor. The acid catalytic mechanism affects isomerization, polymerization, and disproportion of hydrogen (Frost, 1945; Kissin, 1987), and might, therefore, be responsible for the presence of aromatic hydrocarbons and the absence of olefins in natural petroleum (Brooks, 1948).

Smectite can be transformed into illite in the illite/smectite (I/S) mixed-layer during diagenesis and catagenesis stages (Burst, 1969; Powers, 1967). The illitization process can be related to petroleum generation and expulsion. For examples, smectite alters to illite at a temperature between 80 to 120 °C (Burst, 1969) which corresponds to the oil generation peak in the same temperature range. The illite percentage in the I/S layer has a good correlation with the T_{max} value (Burtner and Warner, 1986) and is applied in evaluating petroleum generation stages (Foscolos et al., 1976; Lindgreen and Drits, 2000). Illitization is accompanied with dehydration from interlayers and the release of pore water (Perry Jr and Hower, 1972). The expelled water may create overpressure (Powers, 1967) and serves

as primary migration driving force (Bruce, 1984), although Osborne and Swarbrick (1997) counterargued that the small water volume released during illitization is not sufficient to create overpressure.

Petroleum generated from source rocks with different mineralogical compositions can vary in many aspects. For example, oil originated from carbonate source rocks are generally heavier, richer in sulphur more naphthenic, and with a lower Carbon Preference Index (CPI) than petroleum generated from shale (Hughes, 1984; Jones, 1984). Furthermore, at a molecular level, pristane/phytane, diasterane/sterane, and Ts/Tm ratios are higher in shale samples compared with carbonate rocks at equivalent thermal maturities (Didyk, 1978; McKirdy et al., 1981; Rubinstein et al., 1975). It has to be pointed out that although these differences are superficially related to the mineralogical composition, the redox conditions, precursors as well as other factors during deposition are also important to explain compositional variations of oil sourced from carbonate and shale.

1.3.1.2 Mineral matrix effect (MME)

Espitalie et al. (1980) and Horsfield and Douglas (1980) firstly reported the influence of minerals on Rock-Eval and pyrolysis gas chromatography (Py-GC) products, respectively. The so-called mineral matrix effect can cause changes in HI, Oxygen Index (OI) and T_{max} in the Rock-Eval analysis, as well as gas-oil ratio and aromaticity in the case of Py-GC, and even can influence the hydrocarbon generation kinetics (Dembicki, 1992).

Espitalie et al. (1980) found that illite and montmorillonite can adsorb the generated heavy hydrocarbons in open system pyrolysis and hinder elution, thus leading to shifts of the T_{max} values toward high temperatures and decreases in S_1, S_2 and HI values. Tarafa et al. (1983) further reported that the retaining mechanism could also delay some hydrocarbons from S_1 into S_2 and therefore cause an erroneous Production Index (PI). Besides the physical adsorption, minerals also have selective catalytic impacts on the pyrolysates. For example, CO_2 generation could be enhanced by the existence of carbonate minerals and may lead to an increase of OI values (Katz, 1983). In brief, when MME is an efficient factor, then the whole rock is always lower in HI and higher in OI compared with its kerogen counterpart after demineralisation. Calibrated by Van Krevelen diagram based on elemental data, it was found that kerogen data plotted in the pseudo-Van Krevelen diagram are more reliable in kerogen type identification than whole rock data (Katz, 1983).

Detailed compositional information revealed by Py-GC and Py-GC-MS also demonstrates that the MME exists in laboratory pyrolytic experiments. In general, montmorillonite and kaolinite are catalysts to generate more gas-rich and more aromatic hydrocarbons from kerogen (Dembicki et al., 1983; Horsfield and Douglas, 1980), indicating the activity of Lewis acids. Tannenbaum and Kaplan (1985b) further reported that branched, alicyclic, and aromatic hydrocarbons in the pyrolysates are consistently higher in the presence of montmorillonite compared with any other minerals can be attributed to the carbonium-ion cracking mechanism. The release of aliphatic biomarkers (Lu et al., 1989) and diamondoids (Wei et al., 2006) through pyrolysis can also be enhanced by the presence of montmorillonite. By comparison, the catalytic effect of illite and calcite on hydrocarbon generation are negligible (Tannenbaum et al., 1986a). Recently, Lewan et al. (2014) found that bitumen would enter smectite interlayers before illitization and undergoes cross-linking to form pyrobitumen instead of thermally cracking into oil, and hence leads to a decrease in petroleum generation rates and expulsion efficiencies.

The MME on kinetic effects was discussed by Dembicki (1992) who determined bulk kinetic data on mixtures of kerogens and different minerals. However, only activation energy distributions were compared leaving out the variable frequency factors, this leads to critical reviews by Pelet (1994) and Burnham (1994b). A reply to these two comments from Dembicki (1994), after extrapolating the kinetic data to a simplified geological situation, showed that quartz and calcite can hinder kerogen transformation in contrast to bentonite. A similar trend was reported by Reynolds and Burnham (1995), but the degree of the MME on kinetics is concluded to be minor when modelling petroleum generation.

In summary, clay minerals are especially important in simulating MME, and two main mechanisms are discussed. (1) The high surface area of clay minerals (Sing, 1985) leads to adsorption of heavy compounds generated during pyrolysis, and hence influences T_{max}, GOR, S_2 and HI, as well as the kinetics of the reactions. The adsorption ability of different minerals generally decreases in the following order: illite > montmorillonite > calcite > and kaolinite (Espitalie et al., 1980). (2) The selective catalysis induced by the active acid cites leads to a carbonium-ion cracking and influences the isomerization and aromatization processes. Thus the hydrocarbon composition and biomarker generation can be changed. The catalytic ability of minerals decreases in the order of montmorillonite > kaolinite > calcite > illite (Hu et al., 2014).

It has to be pointed out that not every source rock necessarily undergoes MMEs in pyrolysis experiments. Horsfield and Douglas (1980) and Katz (1983) concluded that the MME varies according to the TOC content and mineralogical composition of the samples. A very high TOC content (> 6%) or a low clay content can decrease or even avoid the MME (Peters, 1986). The presence of water is supposed to decrease the contact between organic matter and minerals, and thus significantly attenuates the activity of the clay catalysing function (Huizinga et al., 1987; Lewan et al., 2014; Pan et al., 2007; Tannenbaum and Kaplan, 1985a).

1.3.1.3 Water influence on MME

Tannenbaum and Kaplan (1985a) and Pan et al. (2007) emphasized that the presence of liquid water in the pyrolysis system could significantly attenuate the activity of the clay-catalyzing function, counterarguments from Eglinton et al. (1986) and Behar et al. (2010) noted that the function of water in pyrolysis is very limited.

The importance of water in petroleum generation was highlighted by Jurg and Eisma (1964) who achieved petroleum-like products by heating fatty acid with and without water. Lewan et al. (1979) claimed that hydrous pyrolysates are more resemble to natural petroleum compared with products from other pyrolytic techniques because they basically contain no alkene, less aromatic and polar compounds and more liquid fractions than anhydrous pyrolysates (Lewan et al., 1985). It is suggested that water acts as an exogenous source of hydrogen (Hoering, 1984) and reduces the rate of decomposition, promotes thermal cracking and inhibits carbon-carbon bond cross-linking (Lewan, 1997).

Hydrous pyrolysis was also applied in bulk kinetic research (Hunt et al., 1991; Lewan and Ruble, 2002), but the results are very different from the well-established anhydrous kinetic models, e.g., the hydrous-kinetic parameters result in very narrow oil windows with significant heterogeneities among samples (Burnham, 2015; Lewan and Ruble, 2002). The samples used in hydrous pyrolysis experiments are typically 0.2-2 cm in length (Lewan et al., 1985; Lewan et al., 2014) which are significantly coarse-grained and larger than finely powdered samples (micrometre level) used in anhydrous system kinetic tests. This would increase the temperature errors caused by thermal transients and hinder the efficient expulsion of generated products (Peters, 1986; Stainforth, 2009). Expulsion efficiency research would benefit from this big samples size (Lewan et al., 2014), but great errors would be induced in kinetic research which requires accurate temperature determinations.

Furthermore, the gas/oil ratios (GOR) of type I, II, II-S and III kerogens through hydrous pyrolysis reveals that GOR initially decreases with increasing temperatures (Lewan and Henry, 1999) which is inconsistent with geological observations (Hunt, 1996).

The influence of water on MME in petroleum generation is not further discussed in this dissertation for the following reasons. (1) The excessive water applied in experiments does not always match the geological situation as the water saturation in a shale layer can be very low due to compaction and clay dehydration (Foscolos and Powell, 1979). On the other hand, Michels et al. (1995) suggested that water is self-sufficient in shale through de-oxygenation and can provide enough protons to saturate the generated hydrocarbons. (2) Anhydrous close-system pyrolysis can also generate petroleum-like hydrocarbons without alkenes (Horsfield et al., 1989; Michels et al., 1995) because a certain pressure plays a more important role than water in removing the alkenes (Monthioux et al., 1985). (3) Most of the routine pyrolysis related techniques are anhydrous systems, e.g., Rock-Eval (Espitalie et al., 1977), open pyrolysis (Horsfield, 1989; Van de Meent et al., 1980), bulk kinetics (Braun and Burnham, 1987), micro-scale sealed vessel (MSSV) (Horsfield et al., 1989), and some golden tube pyrolysis (Behar et al., 1992). Thus, detailed investigations of MME in anhydrous systems would make this contribution of more practical importance.

1.3.2 Uranium

1.3.2.1 The Uranium enrichment in shale

Uranium is one of the most common elements in the Earth's crust, being 40 times more common than silver and 500 times more common than gold (Vine and Tourtelot, 1970). It can be found almost everywhere in soil, rivers, and oceans, for example, the average uranium contents in a river is 0.6 ppb and 3.3 ppb in sea water (Bloch, 1980). Sedimentary rocks are estimated to have an average uranium content of four ppm (Alloway, 2013; Swanson, 1960). In black shales the uranium concentration is higher, i.e., the average contents are eight ppm for shales and 20 ppm for organic-rich marine shales (Swanson and Swanson, 1961). However, high uranium concentrations can be found in some black shale, ranging from 50 to 500 ppm. Black shale-related uranium mineralisation includes marine and terrestrial shales, containing uranium adsorbed onto the organic material and clay minerals. Examples include the uraniferous Alum Shale (Sweden and Estonia), the Chattanooga shale (USA), the Chanziping shale (China), and the Gera-Ronneburg deposit (Germany).

Uranium in black shale is generally proposed to be initially derived from sea water by synsedimentary processes, although Anderson et al. (1989) suggested that uranium is mainly precipitated within the sediments rather than the removal from water. Primary mechanisms of uranium fixation and remobilization in shale are summarised here.

(1) Reducing Environment

Uranium in shale is believed to be precipitated in reducing environments, and the concepts date back to the 1930s (Goldschmidt, 1937). This is furthermore validated by modern sedimentology research which revealed that uranium was precipitated on the Baltic Sea shelf where oxygen deficiency was induced by biological activity (Koczy et al., 1957). Uranium in seawater is soluble in a oxidizing environment and its solubility is significantly decreased in reducing environments (Durand, 2003). Therefore, a combination of uranium-rich sea water and reducing environment can lead to uranium precipitation from the water and enrichment in the sediments (Breger and Brown, 1962; Disnar and Sureau, 1990; Vine and Tourtelot, 1970). Similarly, Leventhal (1991) emphasised the importance of euxinic bottom water and slow sedimentation rate in controlling the uranium concentration in the Alum Shale.

(2) Water Circulation

In contrast to underline the reducing environments as a controlling factor, Leckie et al. (1990) found that the uranium-rich Shaftsbury Formation (Cretaceous) in Canada was deposited in relatively shallow water based on palynological, micropalaeontological and geochemical results. Schovsbo (2002) also reported that the uranium concentration in the Alum Shale is inversely correlated to the layer thickness which implied that uranium is more enriched in the inner-shelf instead of the outer-shelf facies. This type of uranium concentration is explained by a higher degree of bottom water circulation resulting in enhanced supply of uranium in the sediment/water interface where the uranium removal from the sea water took place (Schovsbo, 2002).

(3) Humic Organic Matter.

Swanson (1960) found that humic organic matter contains far more uranium than sapropelic type does in U.S.A shales. Thus, it was concluded that uranium in shales is concentrated from sea water within, on, or near the humic organic matter by one or a combination of the following processes: (1) direct precipitation of uranium, probably by

hydrogen sulfide; (2) removal of uranium ions from solution by adsorption and complexing on solid humic material; and (3) adsorption or complexing of uranium by humic acids while in solution. In contrast, Breger and Brown (1962) argued that uranium is only correlated with TOC irrespective of the organic types. This is based on the fact that some marine shales (e.g., Alum Shale) which contain little humic organic matter can also be enriched in uranium.

(4) Hydrothermal Activity

Migration of hydrothermal fluid into sea water causes changes in temperature and pressure, and thus leads uranium precipitation into the shale (Fisher and Bostrom, 1969; Oliver et al., 1999). The abnormal metal composition of the Alum Shale (Oslo Region) may be a result of interactions of submarine hydrothermal activity with an anoxic bottom water during deposition (Berry et al., 1986). This local volcanic influence may be taken as an explanation why shales isochronously deposited with Alum Shale in Wales, Northern America, and South America lack such high uranium contents.

(5) Phosphorites

Phosphorite laminae or nodules in shale are normally rich in uranium, similar to the hosting shale (Veeh et al., 1974). However, only some certain phosphorite minerals are characterised by high uranium concentrations and point to early diagenetic and selective fixation from the pore water (Schovsbo, 2002; Veeh et al., 1974).

(6) Remobilisation

After synsedimentary fixation in the shale, the uranium can be remobilized and locally concentrated. For example, the Silurian graptolitic black shale in Gera-Ronneburg (Germany) is rich in stockwork uranium which was further enriched by hydrothermal and supergene processes (Dahlkamp, 2013; Lange and Freyhoff, 1991).

1.3.2.2 Uranium and petroleum generation

The most common isotopes in natural uranium are ^{238}U (99.27%) and ^{235}U (0.72%) (Osmond and Cowart, 1976). Most of the radiation resulting from ^{238}U decay in natural systems will be emitted in the form of α-radiation, which has a shallow penetration depth of <100 μm, followed by less intensive γ-radiation which penetrates several decimetres (Jaraula et al., 2015). Alpha particles were suggested to be important in petroleum

generation for a long time (Lind and Bardwell, 1926). Experimental research has manifested that fatty acids can be decarboxylated by alpha particle radiation at 130^{o} to form hydrocarbons (Sheppard and Burton, 1946). It was proposed that the radiolytic cracking of kerogen can be an alternative maturation pathway besides the thermal and microbial mechanisms (Jaraula et al., 2015).

The TOC content in shale is generally proportional to the uranium content (Bates, 1958; Leventhal, 1981) and this correlation is applied while using gamma-ray spectral logging in finding shales (Schmoker, 1981; Serra, 1983). A positive relation between oil yield and uranium concentrations was suggested by Swanson (1960) for the Chattanooga shale (USA). Furthermore, the effects of uranium irradiation on the organic matter are a matter of debate for a long time, and are outlined as follows.

(1) Extractability and Biomarker

Intensive uranium radiolysis was suggested to cause hydrocarbon polymerization through a free radical crosslinking mechanism (Charlesby, 1954), or by the gradual construction of methane (Court et al., 2006). This process was considered to significantly change the organic matter solubility and biomarker distribution.

Atomic pile radiation on petroleum revealed that paraffins would turn into an insoluble gel after a certain dose of radiation is reached (Charlesby, 1954). In Alum Shale, the bitumen extractability and high molecular (C_{26}-C_{28}) triaromatic biomarkers are reversely correlated with the uranium content (Dahl et al., 1988a, b; Lewan and Buchardt, 1989). Hoering and Navale (1987) speculated that the absence of biomarkers in some Alum Shale horizons was caused by irradiation damage. Lewan and Buchardt (1989) concluded that the irradiation-induced crosslinking would convert the single hydrocarbons into insoluble complexes and that the longer side chains of the triaromatic steroids are more susceptible to the polymerization.

(2) Pyrolysates

The ratio of aromatic compounds (toluene and naphthalene) to *n*-alkanes during pyrolysis of the Chattanooga shale was reported to be positively correlated to the uranium content by Leventhal (1981). Similar results from Horsfield et al. (1992a) revealed that the uranium-rich Alum Shale tends to generate very gas-rich and aromatic products and that "dead carbon " get enhanced with increasing maturation, findings that were further confirmed by

Bharati et al. (1995) and Sanei et al. (2014). However, the Alum Shale is still a key target to answering questions about the influence of uranium irradiation on organic matter in sediments, and recent investigations showed that the uranium concentration in Alum Shale is proportional to the quantity of gas generation and inversely correlated to oil generation (Kotarba et al., 2014a). Other Py-GC-MS studies demonstrated that uranium-rich bitumen tends to generate less diverse hydrocarbons with smaller and less alkylated PAHs compared with samples with lower uranium contents (Court et al., 2006).

(3) Element Ratios

The atomic H/C and O/C ratios which are proxies to define the kerogen type and thermal maturity (Durand and Espitalié, 1973) are also susceptible to uranium irradiation, i.e., H/C is decreased and O/C is increased when the uranium content in the shale is high (Pierce et al., 1958). This general trend revealed by elemental analyses is further supported by other techniques including Rock-Eval (Landais, 1996; Leventhal et al., 1986) and ^{13}C NMR spectroscopy (Bharati et al., 1995). The liberation of hydrogen by uranium ionising radiation (Colombo et al., 1964; Dole, 1958) is one explanation for the H/C decrease (Dahl et al., 1988b). The increased oxygen content is presumably derived from hydroxyl radicals, formed by the radiolysis of water (Court et al., 2006).

(4) Stable Carbon Isotopes

Leventhal and Threlkeld (1978) firstly reported that the $^{13}C/^{12}C$ ratios of Upper Jurassic Morrison Formation samples are correlated to the log of the U concentrations. This was attributed to a preferential loss of isotopically light volatiles, formed by radiolysis of the organic matter, leaving a ^{13}C-enriched residue. Further investigations of shale and bitumen samples also confirmed this irradiation effect on stable carbon isotopes (Court et al., 2006; Dahl et al., 1988b).

(5) Maturity Indicators

The vitrinite reflectance of humic coal can be enhanced by the crosslinking caused by uranium irradiation irrespective to the geological heating (Breger, 1974). T_{max} was also reported to be shifted to higher values when uranium contents are high (Forbes et al., 1988; Landais, 1996). In contrast, Dahl et al. (1988b) reported T_{max} values decrease with increasing uranium contents. Today, it is widely accepted that decarboxylation occurs

during irradiation at low temperatures leading to higher values for maturity indicators (Jaraula et al., 2015; Landais, 1993).

(6) Olefins

The unsaturated olefins are thermally unstable in geological environments. They typically contribute less than 1% to crude oil but can be as high as 10% in some Siberian oils (Curiale and Frolov, 1998). The high temperature of hydrothermal activity can generate olefins (Simoneit and Lonsdale, 1982) which is similar to anhydrous pyrolysis experiments in the laboratory (Horsfield, 1989). Alpha radiolytic dehydration is another main process to cause the occurrence of olefins in nature (Frolov and Smirnov, 1994). The hypothesis behind this phenomenon is that all C-C *n*-alkane bonds are similarly sensitive for the dehydration to *n*-alkenes in response to alpha particle radiation (Frolov et al., 1996).

1.4 Research Perspectives and Objectives

The fundamentals of petroleum geochemistry in exploration are now well established (Hunt, 1996; Killops and Killops, 2013; Tissot and Welte, 1984) thanks to a basic understanding of the processes controlling yield, quality and maturation characteristics, and the development of modelling protocols for assessing rates of physical and chemical change in time and space in sedimentary basins. Yet, there are still gaps in our level of understanding of organic-inorganic interactions in source rocks, namely, the adsorptive and catalytic effects of clay minerals and bombardment of organic matter by the radioactive decay of uranium. This dissertation seeks to remedy these deficiencies. The clay-rich Lower Carboniferous Bowland Shale of northern England was the focus of research on MME, while the the Cambro-Ordovician Alum Shale of Northern Europe was studied to evaluate the effects of uranium irradiation. Special efforts were made to examine whether laboratory simulation resembles the catalytic effects of inorganic matter in nature and how these organic-inorganic interactions influence petroleum exploration.

1.4.1 MME

The hydrocarbon retaining function and the catalytic effect of clay minerals in petroleum generation have been well documented by previous works. Two main issues related to MME are discussed in this dissertation.

(1). Most of the previous investigations of the MME focused on Rock-Eval and Py-GC experiments to show its effects and mechanisms. However, the influence on petroleum exploration concepts is not systematically reported. A comprehensive comparison of isolated kerogen material and whole rock samples, covering organic type identification, kinetics determination, and the application in petroleum system modelling, would unravel scenarios how much uncertainty can be induced when samples w/o minerals were used in laboratory experiments.

(2). The validity of MME in nature is still a matter of debate. On the one hand, the catalytic effects of clay minerals serve as the premise of the carbonium-ion cracking theory (Frost, 1945; Grim, 1947), and Tannenbaum and Kaplan (1985b) suggested that the MME works efficiently in nature and would change the composition of generated petroleum. Hill et al. (2007) proposed that the secondary gas in Barnett Shale could be formed by the combination of hydrocarbon retention on the mineral surface and subsequent catalytic cracking. On the other hand, Welte (1965) pointed out that petroleum generated in clay catalytic reactions has a tendency to show a thermodynamic equilibrium, which, however, is not observed in crude oils with respect to the iso- and *n*-paraffin ratio. Espitalié et al. (1984) suggested that the MME is induced by high temperatures in the absence of water and that a less drastic effect is expected in geological reality. Vandenbroucke and Largeau (2007) doubted the mineral catalytic theory in nature based on the fact that the primary cracking mainly occurs in the organic network of kerogen, where minerals are absent.

To achieve these two goals, the Carboniferous Bowland Shale from Northern England was a key target of the investigations of this dissertation. Taken as the most prospective shale gas play in England, the Bowland Shale was deposited in a marine environment with significant organic carbon content. This shale is widely distributed in several sedimentary basins in Northern England. The conceptual research outline is as follows:

(1). This dissertation will not only investigate the MME on the routine Rock-Eval and Py-GC basis but also its effect on the phase behaviour prediction and 1-D basin modelling. Comparison of data derived from whole rock and their kerogen counterpart shall present how different the petroleum type, quantity, and phase behaviour predictions would be. Therefore, how the MME influences source rock evaluation and pre-drill petroleum prediction can be systematically evaluated.

(2). To examine the validity of MME in nature, a series of pyrolysis experiments were carried out applying different heating rates as one of the most significant differences between laboratory pyrolysis and geological maturation lies in the heating rate. Geological heating rates normally fall in the range 10^{-10} to 10^{-12} K/min, while a typical laboratory pyrolysis heating rate is not slower than 10^{-1}K/min. The heating rate dependency of MME would allow interpretations whether the effect is ubiquitous or will be attenuate in the slow geological heating environment. A naturally matured sample as calibration would also help in determining whether the pyrolysis of kerogen or whole rock better simulate petroleum generation and thus to conclude if the MME exists in nature or not.

1.4.2 Uranium

Although many pyrolysis, isotope, and biomarker studies have been carried out in exploring how uranium changes the organic matter and influences the petroleum occurrence, there are still several major puzzles which need to be solved.

(1). Some marine Alum Shale horizons tend to generate gas-rich and very aromatic hydrocarbons (Bharati et al., 1995; Horsfield et al., 1992a; Lewan and Buchardt, 1989; Sanei et al., 2014). High uranium concentration serve as an explanation for the atypical petroleum production characteristics, but the influence of precursor still can not be excluded (Bharati et al., 1995; Horsfield et al., 1992a). For example, some marine algae, e.g., *Chlorella marina*, can also yield aromatic-rich hydrocarbons (Derenne et al., 1996). Furthermore, the trilobite chitin which can produce aromatic pyrolysates (Arthur Stankiewicz et al., 1996) could also serves as an explanation why such marine shales generate very aromatic products.

(2). Previous pyrolysis work to investigate uranium irradiation effect was mostly based on laboratory tests on source rock samples. However, there is a lack of validation of these experimental results by natural petroleum. Uncertainties still exist whether the high GOC and aromaticity of the uranium-rich shale pyrolysates are merely induced by organic-uranium interactions under the artificially high-temperature exposure or whether such features are true in real natural products. Outcrop samples used in previous studies, which were heavily weathered and hydrocarbon depleted, turned out to be non-relevant.

(3). The impact of uranium irradiation on kerogen stability is not clear. The maturity indicator T_{max} changes in the response of uranium contents are contradictory, as shown in various studies (Dahl et al., 1988b; Forbes et al., 1988), and was not supported by kinetic studies yet.

(4). Previous hydrocarbon generation property evaluations based on pyrolytic researches are problematic. Because, when petroleum generation occurred in Palaeozoic time, the kerogen structures of the source are expected to be very different from those in nowadays samples due to different exposure times to irradiation. Therefore, a reconstruction of the oil window time kerogen structure is necessary for predicting petroleum generation.

(5). Aliphatic biomarkers in the uranium-rich shale samples are normally not detectable (Dahl et al., 1988a), thus, the oil-source rock correlation using established biomarkers is challenging. Important to note is that the distribution of triaromatic steroids in uranium-rich shales is unique (Dahl et al., 1988a; Lewan and Buchardt, 1989). However, whether this feature can be observed in producing oil and whether it may serve as a correlation tool has not been reported so far.

The Middle Cambrian – Lower Ordovician Alum Shale which holds the biggest low-grade uranium resource in Europe was investigated in this dissertation. A freshly drilled well in Saint Petersburg (Russia) provides unweathered shale samples with different uranium contents. Results about scattered outcrop samples from the Scandinavian area are also presented as supplements. Crude oils produced from Lower Palaeozoic petroleum systems were collected from the Baltic Basin to enable biomarker correlations with the Alum Shale. This research concept includes the application of a wide range of methodologies:

(1). The relationship between uranium content, pyrolysate composition, and thermovaporisation composition was well examined using immature Dictyonema (Lower Ordovician Alum Shale) core samples. Thus, influences from maturity, weathering, and precursor can be safely excluded. Accordingly, the uranium irradiation effect leading to differences in hydrocarbon generation in pyrolysis experiments, as well as in the natural petroleum occurrence, can be examined.

(2). Bulk kinetic investigations were carried out on Alum Shale samples with various uranium contents and facilitates a proper evaluation how different uranium contents influence petroleum generation. This is important in further petroleum system studies using basin modelling approaches to determine the timing of petroleum generation.

(3). The application of ESI mode FT-ICR MS on the Alum Shale bitumen is helpful in revealing the molecular characteristics of nitrogen, sulphur, and oxygen (NSO) compounds which can also reflect the kerogen structure. Based on the structural changes of kerogen

induced by uranium, the mechanisms of ionising irradiation in petroleum generation can be elaborated.

(4). Since the irradiation damage to organic matter is linear to both uranium contents and irradiation time, a back-calculation of the kerogen structure during the Palaeozoic time is possible based on the experiment derived correlation between uranium content and irradiation damage.

(5). Aromatic biomarkers in extracts gained from the Alum Shale and from producing oil samples were compared. Possible aromatic steroids biomarkers can be applied in oil-uranium-rich source rock correlation studies.

1.5 The Structure of the Dissertation

After this INTRODUCTION in CHAPTER 1, the mineral matrix effect in Bowland Shale samples will be discussed in CHAPTER 2 and 3, and the uranium influence on petroleum generation from the Alum Shale are presented in CHAPTER 4 and 5.

CHAPTER 2 reveals how clay minerals affect the quality, quantity, kinetics, and phase behaviour of hydrocarbons generated by Bowland Shale samples based on laboratory pyrolysis experiments.

CHAPTER 3 is focused on the heating rate dependency of MME, and thus speculated the effectiveness of MME in geological environment.

CHAPTER 4 compiles results how uranium irradiation changes petroleum generation from Alum Shale using natural samples for calibration. The original kerogen structures are also reconstructed.

CHAPTER 5 describes how uranium irradiation modifies biomarker patterns in producing oil and Alum Shale extracts. A comprehensive oil-source rock correlation was achieved in the Baltic Basin.

SUMMARY and PESPECTIVES are given in the last CHAPTER.

2. MINERAL MATRIX EFFECT (MME)

2.1 Abstract

The Carboniferous Bowland Shale of northern England has drawn considerable attention because it has been estimated to have 1329 trillion cubic feet hydrocarbons in-place (gas and liquids) resource potential (Andrews, 2013). Here we report on the oil and gas generation characteristics of three selected Bowland Shale whole rock samples taken from a core and their respective kerogen concentrates. Compositional kinetics and phase properties of the primary and secondary fluids were calculated through the PhaseKinetics and GORfit approaches and PVT modelling software. The three Bowland Shale samples contain immature, marine Type II kerogen. Pyrolysate compositions infer primary generation of Paraffinic-Naphthenic-Aromatic (PNA) Oil with low contents of wax and sulphur. Bulk kinetic parameters share many similarities to productive American Palaeozoic marine shale plays. The secondary gas generation potential of Bowland Shale is bigger than primary gas potential although it requires 14 kcal/mol activation energy higher to achieve peak production. Primary oil, primary gas and secondary gas reach their maximum generation at 137, 150 and 230°C respectively for a 3°C/Ma heating rate. Different driving forces of expulsion including the generation of hydrocarbon and overpressure caused by phase separation during sequential periods of subsidence and uplift could be inferred.

2.2 Introduction

It was in the nineteen eighties that Selley (1987) drew attention to the high shale gas potential of organic-rich shales in the U.K. (Selley, 1987; Selley, 2005; Smith, 1995). He suggested that the most prospective candidates were the Lower Carboniferous basins in northern Britain. Concerted exploration with a view to exploitation was never seriously considered until twenty or so years later, when horizontal drilling and hydraulic fracturing revolutionized unconventional gas production in the USA and directly led to the rapid emergence of the shale gas industry (Bowker, 2007; Curtis, 2002; Pollastro, 2007). Indeed,

---

This chapter has been published as: Yang, S., B. Horsfield, N. Mahlstedt, M. H. Stephenson, and S. F. Könitzer, 2015, On the primary and secondary petroleum generating characteristics of the Bowland Shale, northern England: Journal of the Geological Society, v. 173, p. 292-305 (postprint), doi: 10.1144/jgs2015-056.

it was after the UK's 13th Onshore Licensing Round in 2008 that companies and government made a concerted effort in shale gas assessment and exploration (DECC, 2011). EIA (2011) evaluated that the Bowland Shale system possesses a risked GIP of 95 trillion cubic feet (tcf) and made a risked recoverable resource estimate of 19 tcf. Gas-in-place has been estimated by the British Geological Survey (BGS) to lie in the range of 822-2281 (tcf) (Andrews, 2013). Known as a conventional source rock in the Bowland Basin and elsewhere in northern England (Lawrence et al., 1987), the Carboniferous Bowland Shale is also the prime shale gas target in UK (Selley, 2012; Smith et al., 2010). The first U.K. shale gas well (Preese Hall No.1) drilled by Cuadrilla Resources in 2010 targeted the play as having the highest shale gas potential in the country (Green et al., 2012).

The integration of outcrop, well and seismic data have shown that the Bowland Shale can be divided into lower and upper parts. The upper Bowland Shale is thinner but possesses a higher organic matter content and exhibits better lateral continuity than the lower part (Andrews, 2013). The organic-rich upper part of the Bowland Shale is hemi-pelagic in origin and is dominated by clay-rich mudstone intercalated with very thin calcareous mudstones (Chisholm et al., 1988). The average thickness of this formation is 150 m (locally reaches 890 m). The upper Bowland Shale, focus of the current investigation, was deposited in several adjoining basins (Widmerpool Gulf, North Staffordshire Basin, Edale Basin, etc.) separated by the emergent East Midlands Shelf (Fig. 2.1). The lower shale layer (age from late Chadian to Brigantian), which was interbedded with mass-flow limestones and sandstones (Waters et al., 2009), is considerably thicker, reaching 3000 m in its depocentres (Andrews, 2013). The sedimentology and structural geology of the Bowland Shale have been studied by many authors (Barrett, 1988; Fraser and Gawthorpe, 2003; Lawrence et al., 1987; Leeder, 1988; Waters et al., 2009). Biomarkers and stable carbon isotopes have established likely precursor biota of the organic matter (Armstrong et al., 1997; Ewbank et al., 1993). Also, Konitzer et al. (2014) have used TOC and carbon isotope composition to differentiate various depositional environments vertically. The mass of in-place gas can be evaluated using a combination of forward (includes kinetic) and inverse (includes mass balance) modelling. Because shales are extremely heterogeneous, both laterally (tens to hundreds of kilometres) and vertically (metres to decimetres), the exploration equation has to be applied at appropriate intervals for regional and reservoir scale applications

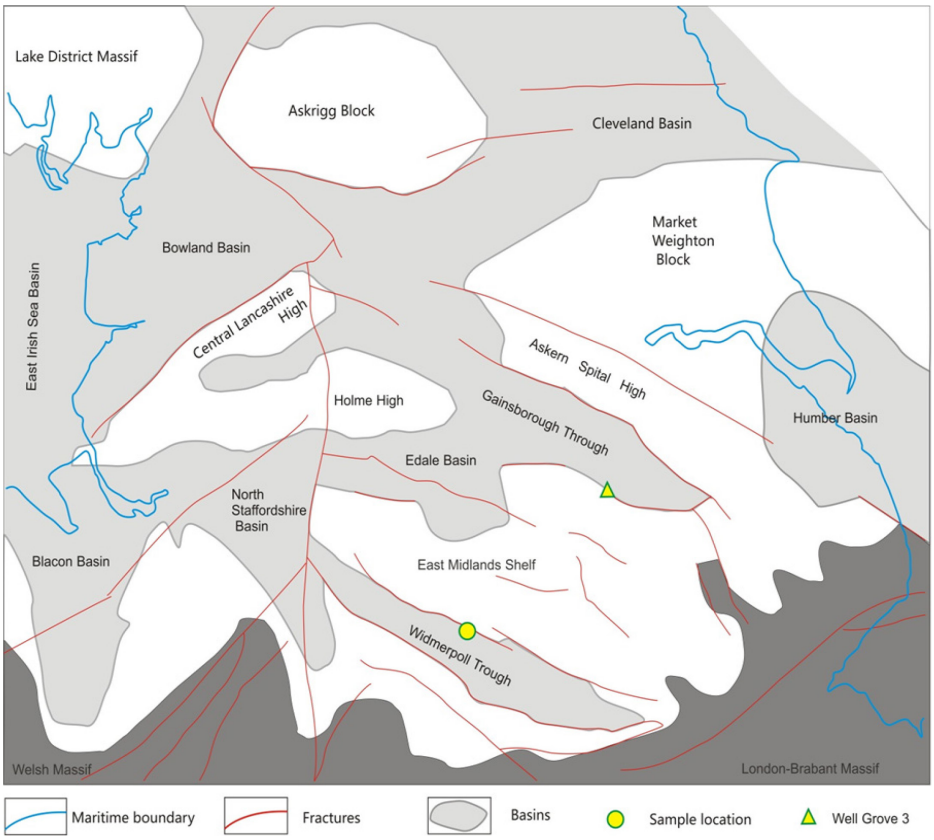

Fig. 2.1. Locations of samples and 1 D basin modelling well. Namurian basin distribution after Fraser and Gawthorpe (2003)

To date, mainly inverse modelling has been applied to the Bowland Shale; thus, its shale gas potential (Raji et al., 2013; Selley, 2005; Selley, 2012; Smith et al., 2010) and total energy resource potential (Andrews, 2013; DECC, 2011; EIA, 2011; Hough and Vane, 2014) have been calculated using basic geochemical data, including TOC and Rock-Eval. Gross et al. (2015) concluded that the high average TOC content and large thicknesses of the mudstone lithofacies point to a significant shale gas/liquid potential in areas with appropriate maturity (1.2-3.5 $\%R_o$), but that a relatively low average HI and high clay content may be seen as detrimental to shale gas potential. (Green et al., 2012), Imber et al. (2014) and Pater and Baisch (2011) have recently documented the orientation of fractures in the Bowland Shale and evaluated the formation's frackability (ease with which the rock can be fractured) using rock mechanical experiments and seismic data. The Bowland Shale consists mainly of impermeable, brittle rock (varying according mineralogy), with many faults and fractures. The maximum horizontal stress orientation of 8°NNW agrees with the regional stress orientation.

Little or no kinetics-related work has been published on the Bowland Shale; that means neither "conversion" using bulk kinetics nor "% gas" using compositional kinetics/physical

property prediction, as a function of organic matter type and/or facies. Kinetic models basically describe the "ease" with which the substituents in the kerogen breakdown to form hydrocarbons via assumed pseudoreactions (Braun and Burnham, 1987; Burnham et al., 1988; Schenk et al., 1997). Utilising specific kinetic parameters for the target shale is imperative whenever possible (Dieckmann and Keym, 2006; Peters et al., 2006). Compositional kinetics provide compositional information on the generated fluids; surface GOR and gas dryness prediction are of great importance, because both have big influences on the quality of the produced oil and gas. The PhaseKinetics model characterizes the compositional evolution of the fluids generated with increasing thermal stress, as well as the phase behaviour of the petroleum at different maturity levels (di Primio and Horsfield, 2006). Predictions of bulk petroleum compositions and physical properties have already been published for basins in South Africa (Hartwig et al., 2012), North Dakota (Kuhn et al., 2012), Norway (Duran et al., 2013), Eastern Canada (Baur et al., 2010), Brazil (di Primio and Horsfield, 2006) and China (Tan et al., 2013), in several cases with confirmation of correct prediction using local calibration. In the current study we employed the PhaseKinetics approach on both whole rock samples and kerogen concentrates to predict the properties of fluids generated from Bowland Shale, also taking into consideration the impact of rock-fluid interactions (mineral matrix effects, considered to be laboratory artefects) on the results (Espitalie et al., 1980; Horsfield and Douglas, 1980).

The contribution of secondary gas at high levels of thermal stress, determined to be dominant in the majority of shale gas "sweet spots" (Jarvie et al., 2007) also needs to be qualitatively and quantitatively evaluated. The GOR-Fit model (Mahlstedt et al., 2013) discriminates between primary gas, primary oil (both from kerogen breakdown) and secondary gas (from the breakdown of primary oil) has been successfully applied to marine and lacustrine shales in Germany (Ziegs, 2013). In the current study we employed the GOR-Fit kinetic model to predict secondary gas formation in the Bowland Shale.

In the current contribution we have focussed on the specific kinetic parameters themselves, utilising a 1D basin model to demonstrate how fluid properties change as a function of organic maturity and reservoir conditions. We have then considered the evolution of expulsion mechanisms during different geological times, and thereafter considered the degree of secondary gas formation, comparing our model with default kinetics models derived from published studies in Petromod©.

2.3 Samples and Analytical Procedure

2.3.1 Samples

The shallow Carsington Dam Reconstruction C4 borehole (SK 244 503) which targeted upper Bowland Shale, was drilled in Derbyshire, Northern England. Both hemi-pelagic marine shale and pro-deltaic turbidites deposited in deep-basin water were recognized using micropetrography and TOC-bulk $\delta^{13}C_{org}$ data (Konitzer et al., 2014). Thick intervals of marine Bowland Shale are relatively homogeneous on a metre-scale, whereas intervals of interbedded shales and turbiditic sandstones are relatively more heterogeneous, as revealed by petrophysical (Hough and Vane, 2014), geochemical (Gross et al., 2015) and lithological (Konitzer et al., 2014) properties. Three unweathered core shale samples as well as their kerogen concentrates from the marine part of that well were tested in this study. Thin section observation and mineralogy had previously shown that sample No.1 and No.3 represent thin-bedded carbonate-bearing clay-rich mudstones and sample No.2 is lenticular clay-dominated mudstone. All the three samples have $\delta^{13}C_{org}$ values between -28.0‰ and -28.4 ‰ indicating that the kerogen is derived from marine planktonic algae, so the three samples are representative of the thick hemi-pelagic mudstones, and these lithofacies dominate the succession at Carsington. (Fig. 2.2) (Konitzer et al., 2014).

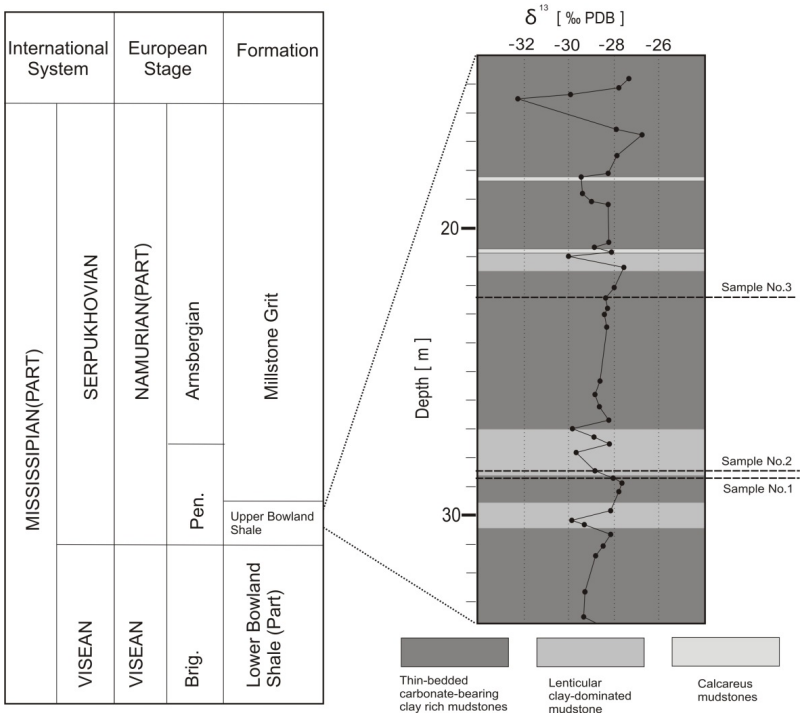

Fig. 2.2. Stratigraphy of the study area. Depth, lithology, TOC and bulk δ^{13}Corg data of the Carsington C4 core samples (Konitzer et al., 2014) as well as the locations of the 3 shale samples investigated in this paper.

2.3.2 Analytical procedure

2.3.2.1 Kerogen isolation and screening

Kerogen concentrates were obtained by (1) crushing the shale to millimetre size, (2) treating with hydrofluoric acid for one week at room temperature and (3) sieving to 10-500 microns. TOC and Rock-Eval analyses were performed using a Leco SC-632 Analyser and Rock-Eval 6 instrument respectively following established procedures (Espitalie et al., 1977).

2.3.2.2 PhaseKinetics (compositional kinetics)

The PhaseKinetics approach of di Primio and Horsfield (2006) has four stages:

(1). Pyrolysis-gas chromatography (PyGC), providing a quick evaluation of the kerogen structure characteristics in terms of Petroleum Type Organofacies, was performed using the Quantum MSSV-2 Thermal Analysis System® interfaced with an Agilent GC-6890A (Horsfield et al., 2014). Briefly stated, milligram quantities (whole rock: 14-16 mg, kerogen: 2-4 mg) of each sample were loaded into a small open glass tube and heated under flowing helium; free hydrocarbons were vented for 3 minutes during an isothermal purge at 300°C, after which the C_2+ pyrolysis products generated during heating from 300°C to 600°C were collected in a cryogenic trap (liquid nitrogen). Methane passed through the trap and passed through the GC column to the Flame Ionisation Detector (FID). Trapped products were liberated by removing the cooling agent and heating the trap to 300°C. AHP-Ultra 1 dimethylpolysiloxane capillary column (50 m length, inner diameter of 0.32 mm, film thickness of 0.52 mm) connected to a FID was used to with helium as carrier gas. Quantification of individual compounds and boiling range splits was conducted by external standardisation with *n*-butane.

(2). Bulk kinetic parameters were assessed by subjecting samples to open-system, non-isothermal pyrolysis at four different linear heating rates (0.7, 2, 5, 15 °C/min) using a Source Rock Analyser® (SRA) following established procedures (Braun and Burnham, 1987). The discrete activation-energy (Ea) distribution optimization with a single, variable frequency factor (A) as well as geological extrapolation were performed using the KINETICS 2000® and KMOD® programs.

(3). Non-isothermal closed-system micro scale sealed vessel (MSSV) pyrolysis (Horsfield et al., 1989) is a micro-analytical method to artificially mature sedimentary organic matter to

different stages of conversion and to quantify the composition of generated products. It provides the possibility of determining primary and secondary reaction kinetics of specific compound groups and to extrapolate their generation to geological heating rates (Horsfield et al., 2014). For each experiment, milligram quantities of samples were sealed in glass capillaries and artificially matured at 0.7℃/min to temperatures corresponding to 10, 30, 50, 70 and 90 transformation ratio (TR) as defined by bulk kinetic results. The tubes were then cracked open using a piston device coupled with the injector, and the released products were swept into the GC using a flow of helium. Quantification was performed by external standardisation using *n*-butane.

(4). Compositional kinetics and physical property modelling were fulfilled in the last step. The hydrocarbons generated during MSSV are divided into 14 pseudo compositions. Seven of them are in the gas fraction (C_1, C_2, C_3, i-C_4, n-C_4, i-C_5, n-C_5) and the gas composition was corrected based on a GOR- gas-wetness correlation from natural black oil. The other seven compounds describe the liquid phase consisting of C_6 and pseudo boiling ranges of $C_{7\text{-}15}$, $C_{16\text{-}25}$, $C_{26\text{-}35}$, $C_{36\text{-}45}$, $C_{46\text{-}55}$, $C_{56\text{-}80}$. According to the weight percentage of the 14 pseudo compositions, each bulk kinetic potential which has the same activation energy was populated into 14 parts, afterward these compositional kinetics models are ready to be applied to basin modelling software (especially the IES PetroMod® which has a module for inputting these) which make this method very convenient. Physical property modelling was carried out using PVT-Sim® based on the 14 pseudo compounds determined by MSSV. Standard temperature and pressure (STP) GOR was calculated through separator simulator module in the software and phase envelopes were also drawn.

2.3.2.3 GOR-Fit

The GOR-Fit model based on open-system SRA and closed-system MSSV pyrolysis consists of three main steps (Mahlstedt et al., 2013). In the first one, the MSSV - generation of $C_{1\text{-}5}$, C_{6+} and the total C_{1+} boiling fractions are normalized to the maximum MSSV-yields. Since the normalized C_{1+} MSSV yields curve and SRA-TR curves are identical (Schenk and Horsfield, 1993) and only primary cracking takes place in the open-system SRA pyrolysis, the primary oil and gas splines can be deduced from the SRA-TR curve by multiplying by an oil and gas ratio assumed fixed and derived from pyrolysis gas chromatography after a small temperature adjustment to fit the measured MSSV oil and gas generation curves better. The second step is to calculate the secondary gas amount by subtracting primary gas from measured MSSV oil yields at corresponding temperatures. A secondary gas spline is

again approximated by "factorising" the SRA-curve (factor derived from multiplication of the C_{6+} spline factor by 0.7 assuming that 70% of C_{6+} compounds are degraded to gas and 30% to coke) which is then temperature shifted to match calculated secondary gas yields. After obtaining the generation characteristics of primary oil, primary gas and secondary gas in 3 heating rates, the kinetics models and geological extrapolations were achieved by using KINETICS 2000® and KMOD® in the last step.

2.3.2.4 1-D Basin modelling

1-dimensional basin modelling was carried out on well Grove 3 from the East Midlands Shelf using IES PetroMod®2013. Lithology and depth inputs in the modelling came from the drilling , and stratigraphic ages were taken from International Commission on Stratigraphy (Cohen et al., 2013) and Gradstein et al. (. A Kerogen-Oil-Gas kinetics model with secondary reaction developed on kerogen No.3 in this research was used as kinetics input. Two periods of uplift of the Bowland Shale in the late Carboniferous/early Permian and after the Late Cretaceous have been recognised by (Leeder, 1988) and (Barrett, 1988), and the heat flow model was modified after (Jarvis and McKenzie, 1980). Calibration on vitrinite reflectance is after the report from BGS which also produced a 1 D model on well Grove 3 (Andrews, 2013).

2.4 Results and Discussion

2.4.1 Primary generation

Here we compare the results for whole rock samples with those of kerogen concentrates. Significant differences in composition are reported, the causes discussed, and the ramifications for petroleum composition outlined.

2.4.1.1 Whole rock

All three whole rock samples have TOC contents higher than 2% (Table 2.1) fitting the minimum TOC requirement for shale gas development (Curtis, 2002; Muntendam-Bos, 2009), but the S_2 and HI values are low (Table 2.1). Rock-Eval crossplots confirm that the three whole rock samples generate and release pyrolysates with a type III composition (Fig. 2.3 a). Samples 1 and 3 are immature samples while sample 2 is marginally mature (Fig. 2.3 b).

In cases where analytical artefacts are excluded (e.g. mineral-organic interactions occurring during pyrolysis;(Horsfield and Douglas, 1980) the proportion of resolved and identifiable compounds in the GC trace reflects the kerogen structure as a whole (Horsfield et al., 1989; Larter, 1984). Their GC traces show that the whole rock samples analysed here tend to generate high percentages of low molecular weight compounds (C_1 – C_5) and high concentrations of aromatic compositions like ethylbenzene, xylenes, trimethylbenzene, and naphthalene (Fig. 2.4). The average alkyl chain length distribution of the pyrolysates from whole rocks 1 and 3 are of the Gas and Condensate type whereas whole rock 2 falls in Low Wax Paraffinic-Naphthenic-Aromatic (P-N-A) Crude Oil field (Fig. 2.5). Two additional ternary diagrams were used to characterize the pyrolysate in terms of aromaticity, paraffinicity and either sulphur content (Eglinton et al., 1990) or phenol content (Larter, 1984). They clearly show that the whole rock pyrolysate is very aromatic (Fig. 2.6 a and b); sulphur-containing compounds and phenols are in low abundance (Fig. 2.6 a and b).

Table 2.1. Rock-Eval and TOC data.

Sample Number	GFZ Number	Depth (meter)	S_1 (mg/g)	S_2 (mg/g)	S_3 (mg/g)	T_{max} (°C)	HI (mg TOC)	OI HC/g (mg TOC)	PI CO_2/g $(S_1/(S_1+S_2))$	TOC (%)
Whole rock 1	G013218	28.68	0.18	1.71	1.67	429	62	61	0.0952	2.75
Whole rock 2	G013219	28.42	0.16	4.88	0.7	438	188	27	0.0317	2.6
Whole rock 3	G013220	22.36	0.37	6.46	0.49	430	206	16	0.0542	3.14
Kerogen 1	G013688	28.68	1.36	60.89	1.20	430	329	6	0.0218	18.5
Kerogen 2	G013689	28.42	0.39	14.13	0.48	432	318	11	0.0269	4.45
Kerogen 3	G013690	22.36	1.18	33	0.83	426	324	8	0.0345	10.2

S_1: quantity of free hydrocarbons (gas + oil). S_2: quantity of thermally generated (cracked) hydrocarbons. S_3: quantity of CO_2 generated during pyrolysis of the sample. HI (hydrogen index)=(S_2*100)/TOC. OI (oxygen index)=(S_3*100)/TOC. PI (production index) = $S_1/(S_1+S_2)$

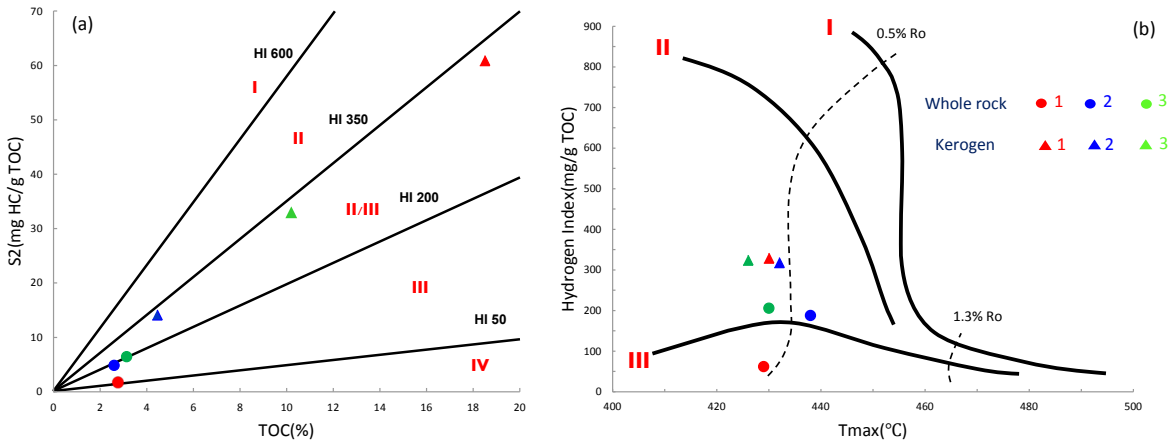

Fig. 2.3. Rock-Eval and TOC diagrams for kerogen type and maturity identification.

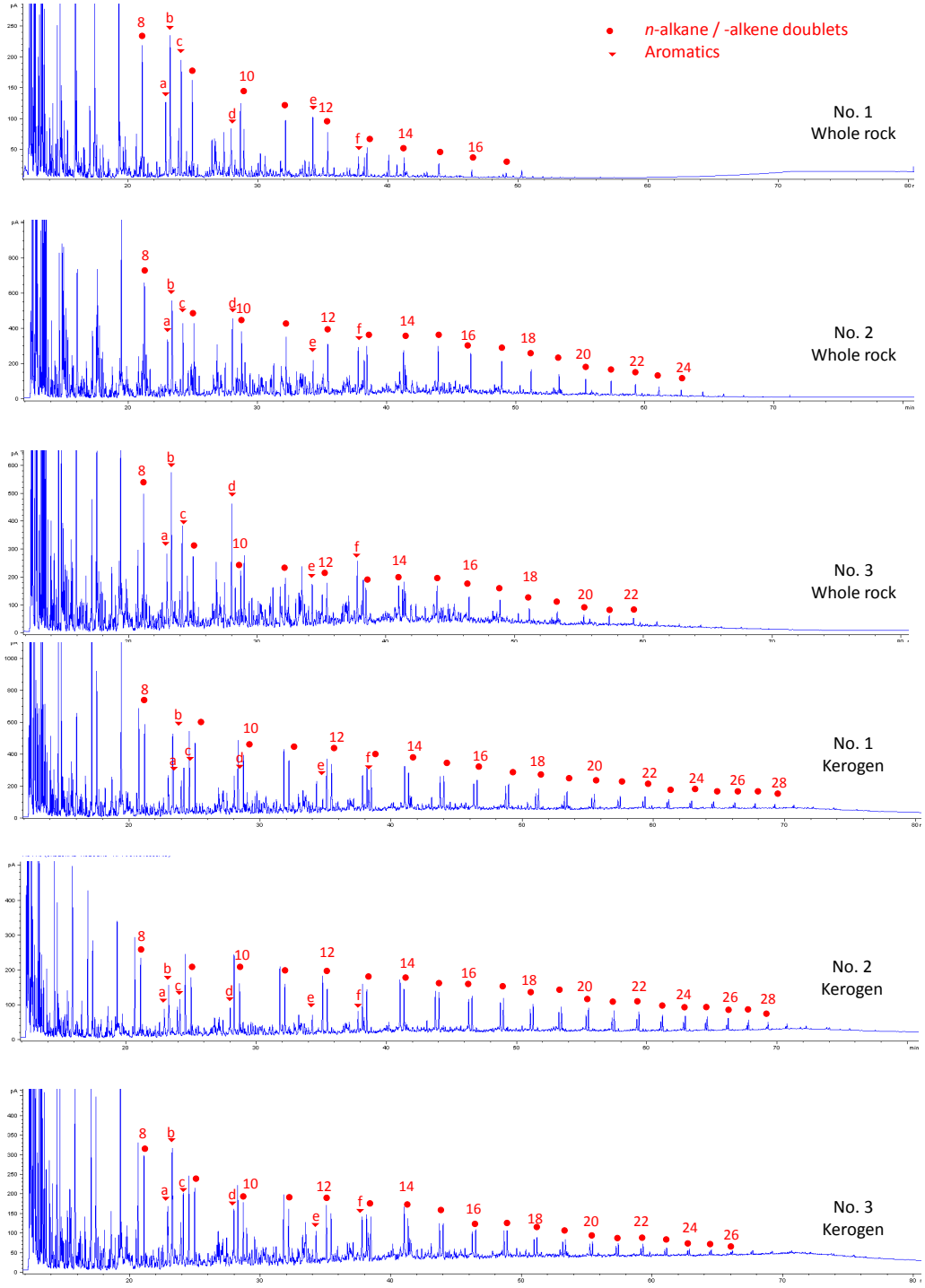

Fig. 2.4. PyGC chromatograms of the 6 samples. Normal alkane and alkene peaks have been highlighted and selectively numbered. Representative aromatic compounds are ethylbenzene (a), meta- and paraxylenes (b), orthoxylene (c), 1,2,4-trimethylbenzene (d), naphthalene (e) and 2-methylnaphtalen (f).

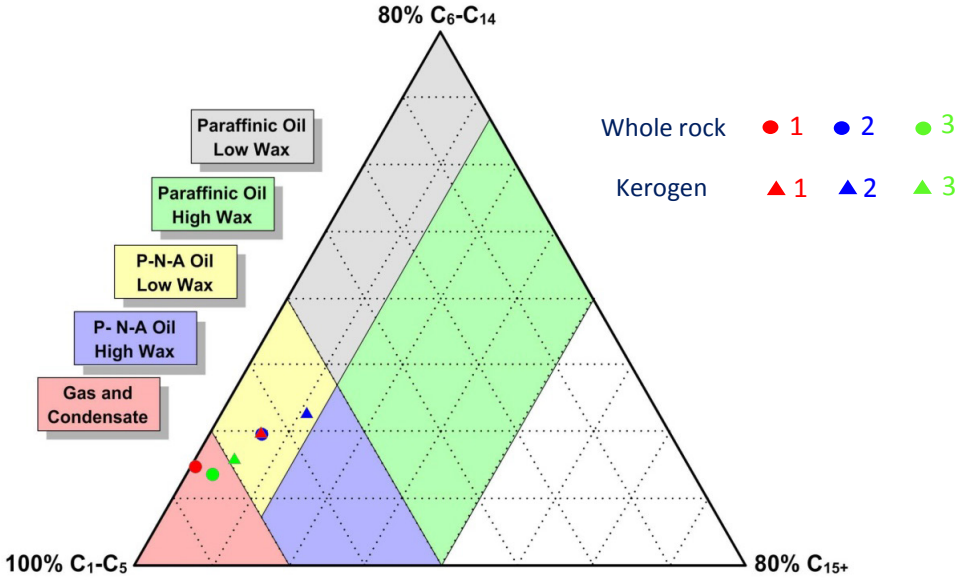

Fig.2.5. Pyrolysate chain length distribution and Petroleum Type Organofacies classification (Horsfield, 1989)

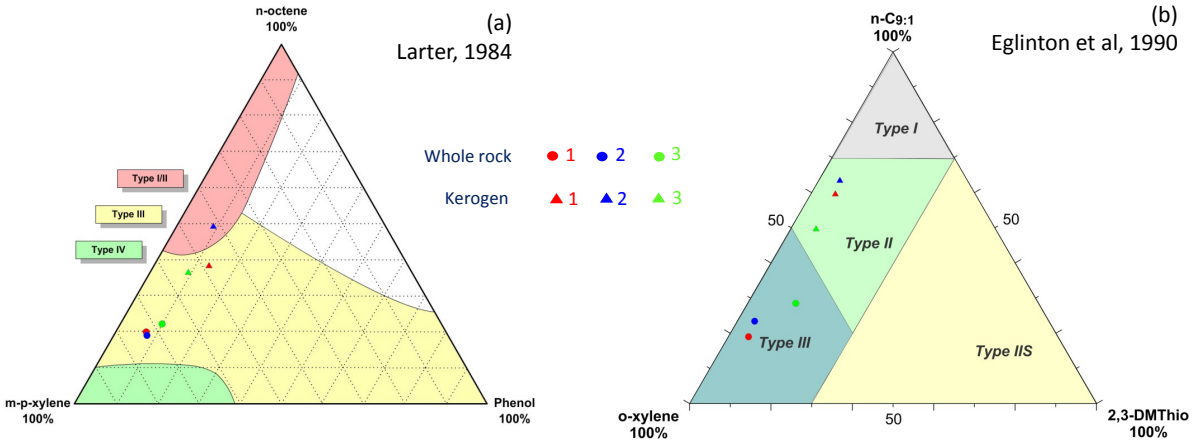

Fig. 2.6. Petroleum composition predictions from PyGC results according Larter (1984) and Eglinton et al. (1990)

As far as thermal response is concerned, whole rock Bowland Shales have peak activation energies between 55-57 kcal/mol and frequency factors exceed 2.85×10^{14} (Fig. 2.7). Applying these values to natural maturation using a typical geological heating rate (3°C/ma), the whole rock samples 1 and 3 reach 50%TR at about 150°C (Fig. 2.8), whereas whole rock sample 2 needs around ten more degrees to reach that TR. These kinetics characteristics of the whole rock samples are unusual, in that the samples require higher temperatures for kerogen breakdown than most known Palaeozoic marine shales (Mahlstedt, 2012).

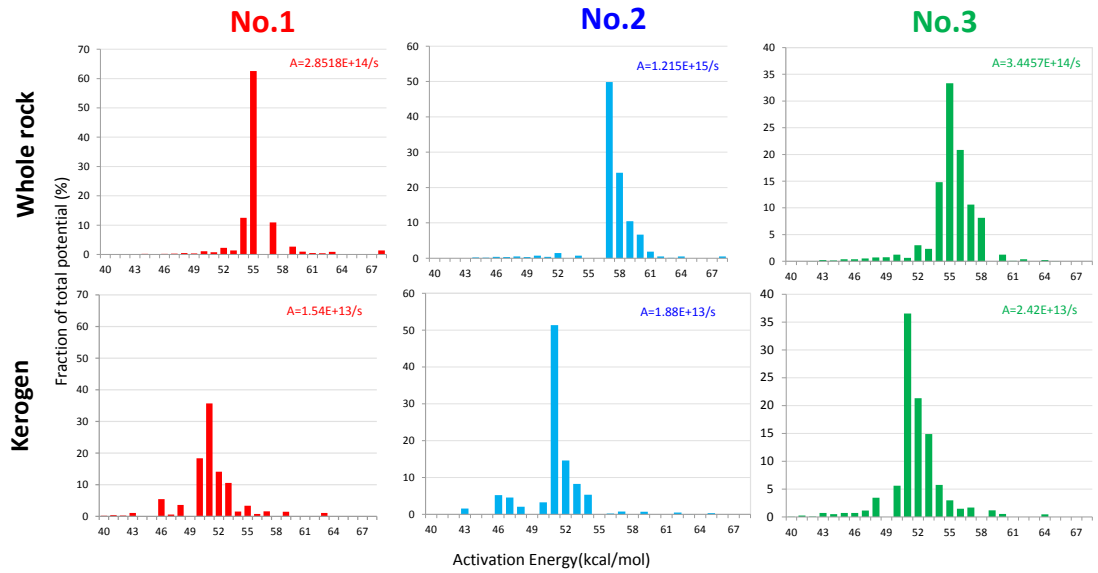

Fig. 2.7. Bulk kinetics models of the whole rock samples and kerogen concentrates.

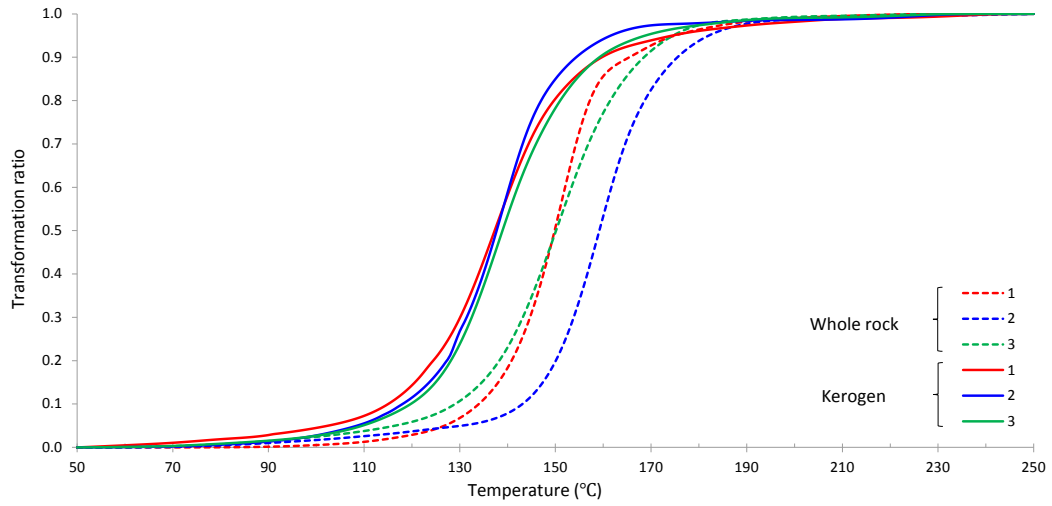

Fig. 2.8. Transformation ratio variations in geological heating rate (3°/ma).

Two compositional kinetics models for whole rock samples are shown in Fig. 2.9. These were built by populating the bulk kinetic potentials with MSSV pyrolysis data (di Primio and Horsfield, 2006). Cumulative GORs in surface environment of whole rock samples get enhanced with increasing thermal maturation except 2 slight deviant values from sample No.1 and No.2 at 50% TR (Fig. 2.10). The maximum GOR can be as high as 498Sm^3/Sm^3 of sample 1 at 90% percentage which is very similar to the GOR behaviour of Arang coal (organic type III) of Indonesia (di Primio and Horsfield, 2006). The pressure-temperature phase envelope for multicomponent mixture gives the region of temperatures and pressures at which the mixture forms two phases. Generally speaking, the envelope in

temperature axis direction is controlled by molecular weight, while GOR and gas wetness control the pressure axis direction (Amyx et al., 1960). Phase envelopes of whole rock sample 3 reflect the fact that the primary generated fluids are dominated by low molecular weight compounds. For a hypothetical reservoir at 100℃ and 200 bar, the critical point of hydrocarbons accumulating up to 90% TR is very close to that reservoir condition, and the fluids can be termed volatile oil (McCain, 1990).

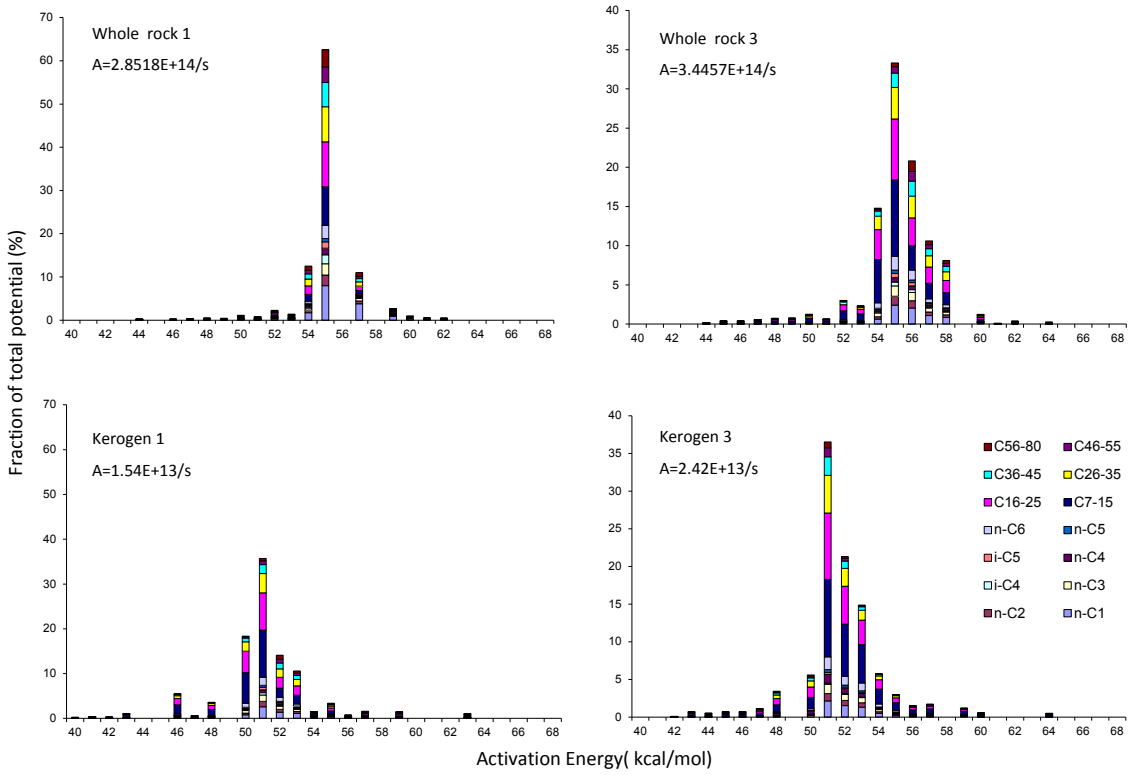

Fig. 2.9. Compositional kinetic models of selected samples.

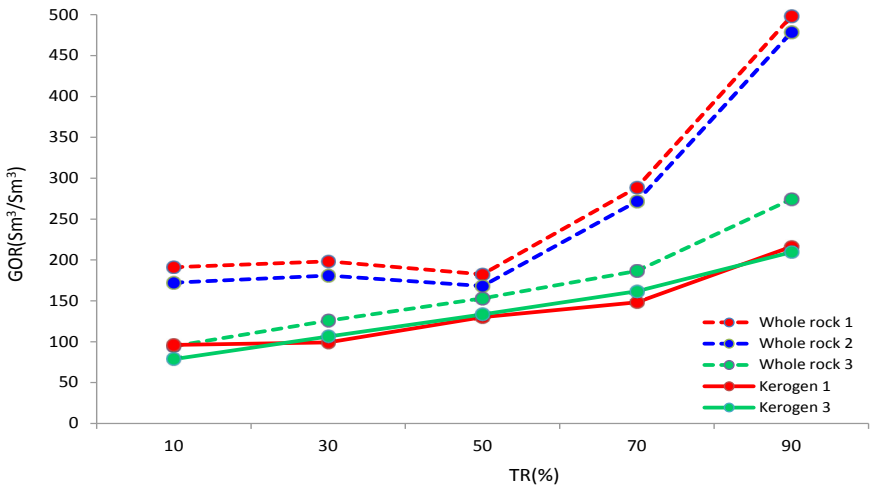

Fig. 2.10. Gas:oil ratio of the samples analyzed as a function of increasing transformation ratio.

2.4.1.2 Kerogen

Although the three kerogen concentrates have quite different TOC contents and S_2 values (Table 2.1), they share very similar HIs. With the HI values range of 318-329 mgHC/gTOC the three kerogen concentrates are classified as type Ⅱ (Fig. 2.3a). The maturity indicator T_{max} implies that the three kerogen concentrates are immature (Fig. 2.3b).

The pyrolysates of kerogen are dominated by normal alkanes/enes, subsidiary aromatics and other resolved peaks are generated (Fig. 2.4). All three concentrates fall in the Low Wax P-N-A Oil area (Fig. 2.5), which manifests the typical characteristics of many marine shales (Horsfield, 1997). Fig. 2.6 suggests that hydrocarbons generated by kerogen are richer in paraffinic compounds than aromatic ones. In addition, the sulphur content is also very low (Fig. 2.6a).

Peak activation energies of the three kerogen concentrates are 51 kcal/mol and their frequency factors range from $1.54\text{-}2.42\times10^{13}$ (Fig. 2.7). The geological extrapolation curves fall closely together as regards TR variations according to temperature (Fig. 2.8). The Bowland Shale kerogen generation kinetics are more stable than sulphur-rich marine shale (Dieckmann, 2005) and closely resemble those reported for productive unconventional shale plays from the US including Barnett shale (Jarvie et al., 2010), Bakken shale (Kuhn et al., 2012) and Woodford shale (Mahlstedt, 2012).

Due to the limited amount of sample available MSSV experiments were not carried out on kerogen No.2. Compositional kinetics results of sample No.1 and 3 show that about half of the hydrocarbons in peak generation (activation energies ranges between 50-54 kcal/mol) are contributed by compounds between C_7-C_{25} and gases make up only small proportions of the total products (Fig. 2.9).

Cumulative GOR variations as a function of increasing TR for kerogens 1 and 3 are closely similar (Fig. 2.10). GOR increases steadily from less than 100 m^3/Sm^3 at 10% TR to about 200 m^3/Sm^3 at the highest TR and this GOR variation pattern is very similar as those of the Woodford Shale and Kimmeridge Clay (di Primio and Horsfield, 2006). The cumulative hydrocarbon phase envelopes imply that fluids generated by Bowland kerogen concentrates are typical black oil (McCain, 1990) and the systematic decrease in cricondentherms and increase in cricondenbars together with the shift of the critical point towards higher pressures and lower temperatures with increasing TR consistent with critical points shift pathways of fluids from Snorre Fields during maturation (di Primio et al., 1998).

2.4.1.3 Comparison and discussion

Clearly, there are significant compositional differences between the respective pyrolysates of whole rock and kerogen concentrate pairs. The whole rock samples show low HI values and are classified as containing type III organic matter, while the kerogen concentrates have higher HI and are classified as comprising type II organic matter (Fig. 2.3). Whole rock samples tend to generate higher percentages of low molecular weight compounds (C_1-C_5) and alkylaromatics (Fig. 2.4), whereas the equivalent kerogen pyrolysate is dominated by normal alkanes and alkenes (Fig. 2.4). Ternary plots also demonstrate differences of organic facies and paraffinicity between these two materials (Fig. 2.5 and 2.6). From the kinetic perspective, whole rock samples are more refractory and heterogeneous than the kerogen (Fig. 2.7 and 2.8). More light compounds were generated during pyrolysis from whole rock samples, which is responsible for that they have higher GORs (Fig. 2.10) and lower cricondentherms in the phase envelopes (Fig. 2.11) than their kerogen counterparts.

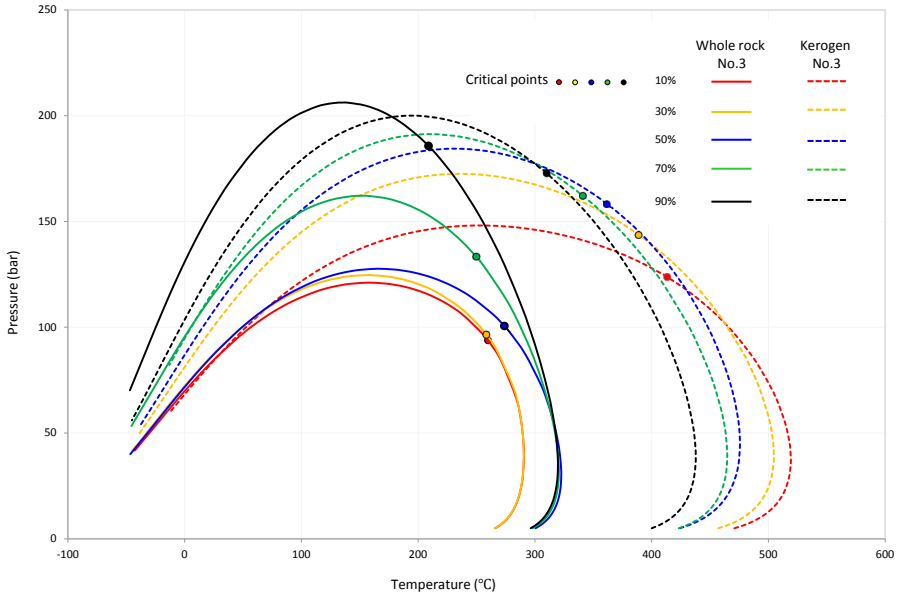

Fig. 2.11. Phase envelopes of whole rock and kerogen of sample No.3 during artificial maturation.

The differences between kerogen and whole pyrolysates have been discussed over decades. Saxby (1970) and Robl and Davis (1993) reported that the treatment of whole rock by hydrofluoric acid during mineral dissolution and kerogen concentration does not change kerogen structure significantly. Differences in pyrolysate compositions have been attributed to the Mineral Matrix Effect. The effect occurs in many open- and closed system pyrolysis experiments including Rock-Eval (Espitalie et al., 1980; Espitalié et al., 1984; Makadi, 1983), pyrolysis GC (Horsfield and Douglas, 1980; Karabakan and Yürüm, 1998), bulk kinetics

determination (Burnham, 1994a; Dembicki, 1992; Dessort et al., 1997; Pelet, 1994) and hydrocarbon expulsion efficiency calculations (Lewan et al., 2014), and is brought about by sorption followed by catalytic thermal degradation. Because of their high surface area (Sing, 1985), clay minerals (especially smectite) have the ability to strongly adsorb pyrolysate (Espitalie et al., 1980; Espitalié et al., 1984), especially the heavy compounds (Katz, 1983). Clay mineral tends to catalyze the kerogen to generate more CO_2, light hydrocarbons and aromatic compounds (Espitalié et al., 1984; Larter, 1984; Lu and Kaplan, 1989; Tannenbaum et al., 1986b). A disproportionation of hydrogen occurs in the pyrolyser, enhancing C_1-C_5 yield, while simultaneously depositing dead carbon, bringing about diminished HIs and lower yields of heavy compounds in Py-GC data, and being more refractory from a kinetic perspective. The overall outcome as far as bulk petroleum is concerned, is that genetic potential is diminished (Fig. 2.3 and 2.6), inherent oil potential is lowered relative to gas and in absolute terms (Fig. 2.5, 2.10) and phase envelopes change their shape accordingly (Fig. 2.11).

Sedimentological, organic petrological and stable carbon isotope studies (Armstrong et al., 1997; Fraser and Gawthorpe, 2003; Konitzer et al., 2014) have shown that the 3 upper Bowland Shale in this research is marine shale from predominantly hemi-pelagic deposition and organic matter is derived from planktonic phytoclasts. These attributes are better represented by the isolated kerogen pyrolysis data (Rock-Eval, PyGC and bulk kinetic results) than by the equivalent whole rock data. It should be pointed out that the mineral matrix effects shown here are thought to only exist in artificial pyrolysis experiments and not during natural catagenesis. Fast heating rates, high temperatures, a dry pyrolysis environment and enhanced contact of the organic matter with minerals after grinding are considered as the main reasons that lead the mineral matrix effect in laboratory pyrolysis (Makadi, 1983; Vandenbroucke and Largeau, 2007). Another important thing is that not every source rock necessarily has to suffer from this effect. Horsfield and Douglas (1980) and Katz (1983) concluded that the matrix effect varies according to mineralogy and TOC content of the rocks under investigation. A very high TOC or low clay content can decrease or avoid the effect (Reynolds et al., 1995). Tannenbaum and Kaplan (1985a), and Lewan et al. (2014) also reported that the existence of water in the pyrolysis experiments can hinder the excessive formation of coke and catalyzing function of clay minerals. However, since the TOC content of Bowland Shale ranges from 1.3% to 9.1% (Gross et al., 2015), clay contents are considered to be medium/high (EIA, 2011) and all pyrolysis experiments employed here are anhydrous systems, the mineral matrix effect is likely

inevitable in the Bowland Shale (except those samples with TOC content higher than 6%) pyrolysis experiments. If whole rock samples are used in the Bowland Shale PhaseKinetics research here, the cumulative GOR can be greatly over-estimated and leads to erroneous conclusions in phase prediction and resource evaluation.

2.4.2 Secondary cracking

GOR-Fit was applied to kerogen 3 to explore the generation characteristics and kinetics of primary oil, primary gas and secondary gas formation. As the 5℃/min heating rate MSSV experiments shows, the C_{6+} fraction starts to decrease at around 460℃ with increasing temperature (Fig. 2.12) as a result of secondary cracking. The decrease of C_{1+} generation and C_{1-5} products after 510℃ and 540℃ (Fig. 2.12) manifests the formation of coke or pyrobitumen (Dieckmann et al., 1998). Small scale secondary cracking occurs when temperature reaches 420℃ in the MSSV and significantly more secondary gas was formed after 460℃ where is the onset of the decrease of C6+ compounds in the MSSV (Fig. 2.12). The excellent identical trend of secondary gas in MSSV and calculated secondary gas (Fig. 2.12) attest to the robustness of the GOR-Fit approach.

By combining the generation spline under three heating rates (0.7, 2.0, 5.0 ℃/min), the kinetics of primary oil, primary gas and secondary cracking can be drawn (Fig. 2.13). The activation energy distribution of primary oil (Fig. 2.13) is very similar to the bulk kinetic distribution (Fig. 2.7). Compared with primary gas, the peak activation energy of secondary gas is 14 kcal/mol higher, and frequency factor also increased 2 degrees (Fig. 2.13).

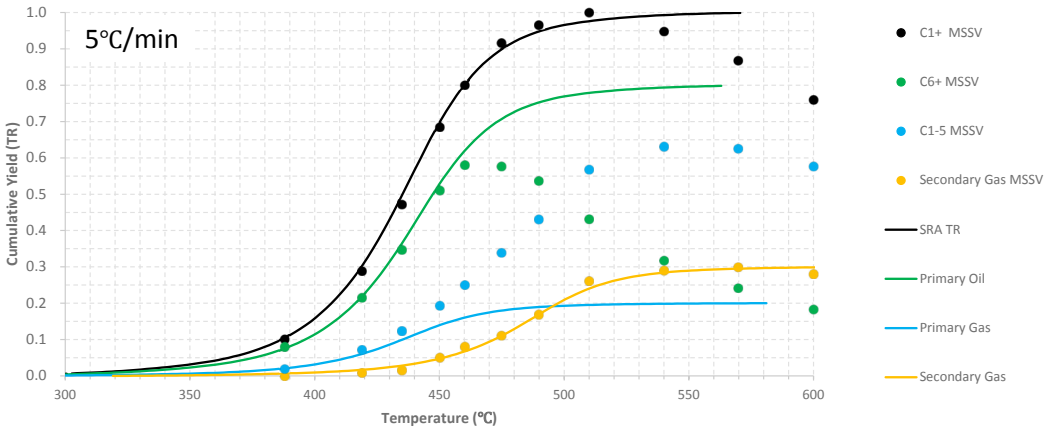

Fig. 2.12. Measured MSSV pyrolysis data of kerogen No.3 for boiling ranges C1+, C6+ and C1-5 normalized to the maximum C1+ yield and fitted spline curves for calculated primary and secondary gas generation using the heating rates of 5.0°/min, compared with normalized SRA TR curve.

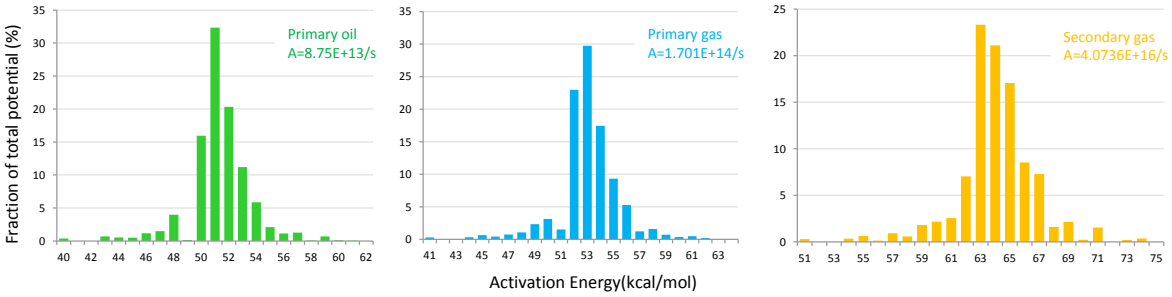

Fig. 2.13. Kinetics models of primary oil, primary gas and secondary gas generation of kerogen No.3.

The generation rate of bulk primary hydrocarbons (SRA), primary oil, primary gas, and secondary gas at a linear heating rate of 3K/Ma is shown in Fig. 2.14. Both the primary oil and gas generation curve are within the SRA range. About 80% of the primary hydrocarbon was contributed by primary oil, and this partly explains why both the SRA and primary oil reach peak generation rates between 136-138℃ (Fig. 2.14). When the temperature has reached 150℃ and the Ro is 1.2% the primary gas reaches its maximum generation rate. The secondary gas generation capability of the sample a crucial important in shale gas potential evaluation, as seen in e.g. the Fort Worth Basin (Jarvie et al., 2007).Much higher maturity is required to achieve the secondary gas compared with the primary gas, for the peak secondary generation temperature reaches 230℃ which is 80℃ higher than primary gas and vitrinite reflectance is as high as 2.85% (Fig. 2.14).

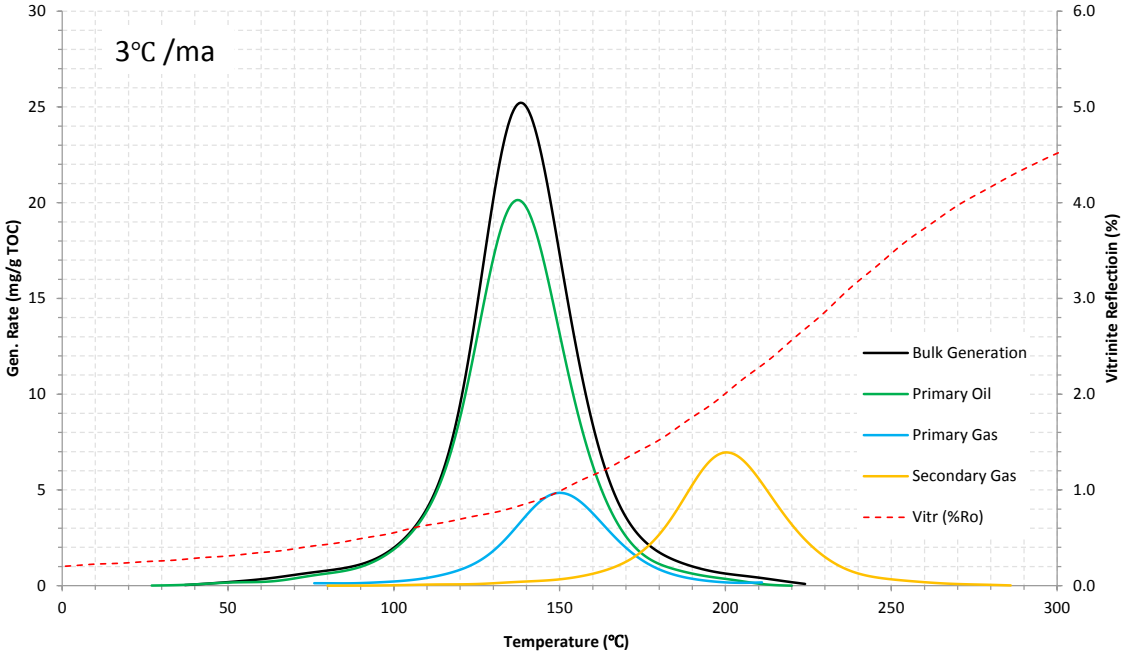

Fig. 2.14. Computed generation rate curves as a function of temperature at a geological heating rate of 3 ℃/ma and vitrinite reflectance for kerogen No.3.

2.5 Application

2.5.1 Primary generation

The upper Bowland Shale in well Grove 3 lies in the lower part of Namurian stage and was overlaid by the Millstone Grit. Since the target layer is very thin in the borehole, here we use Namurian layer to represent it in the 1 D basin modelling for illustrative purpose. Modelling result demonstrates that the upper Bowland Shale had experienced a rapid burial in the late Carboniferous and the kerogen attained about 26% TR at the end of Carboniferous (roughly equivalent to R_o:0.6%) (Fig. 2.15 a) when the primary oil reached a high generation level (Fig. 2.14). During this period, the main driving force for hydrocarbon expulsion would be pressure-driven flow as kerogen degradation and rapid compaction took place (Tissot and Welte, 1984). Fluids generated at TR 30% fall into the one-phase field in reservoir conditions (Fig. 2.15 c) indicating that in-situ primary hydrocarbons would exist as an undersaturated liquid in the source rock. The uplift that happened during late Carboniferous to early Permian not only stopped the rapid organic maturation but also changed the reservoir conditions significantly (point A has a temperature of 90 ℃ and pressure of 186 bar, the temperature and pressure of point B are 51 ℃ and 72 bar respectively) (Fig. 2.15 a). If we use 30% TR fluids to roughly represent the hydrocarbon generated at point A, it can be predicted that when petroleum in the source rock was shifted from point A to point B the decrease in temperature and pressure would cause a phase separation and gas composition would contribute 8% in volume of the whole fluids (Fig. 2.19 c). This sudden gas-exsolution in the very tight shale reservoir would cause an abnormal pressure in the source rock and increase the expulsion efficiency greatly (Momper, 1979). Thus the driving force for expulsion in this period would be changed to the abnormal pressure caused by volumetric expansion induced by phase separation. After then the shale was deeply buried again between Jurassic and Cretaceous time and the TR of the organic matter reached as high as 92% at a maximum burial of 2900m (Fig. 2.15 a). By the end of the Mesozoic was reached (roughly equivalent to R_o:1.4%) primary generation entered its late stage (Fig. 2.14). Expulsion should have been driven by continuous burial and vast hydrocarbon generation. A major uplift happened in the Cenozoic which reduced the temperature and pressure of the Bowland Shale reservoir again (point C has a temperature of 160 ℃ and pressure of 283 bar, the temperature and pressure of point D are 73 ℃ and 187 bar respectively). However, this time phase separation would not be likely to occurduring the uplift when reservoir conditions of TR

90% fluids were changed from point C to D (Fig. 2.15 f). Practically, if petroleum under reservoir conditions (point D in Fig. 2.15 a and f) was produced to the surface (point E in Fig. 2.15 a and f) a gas-exsolution would happen again, and the vapour phase would hold about 25% of the total fluid.

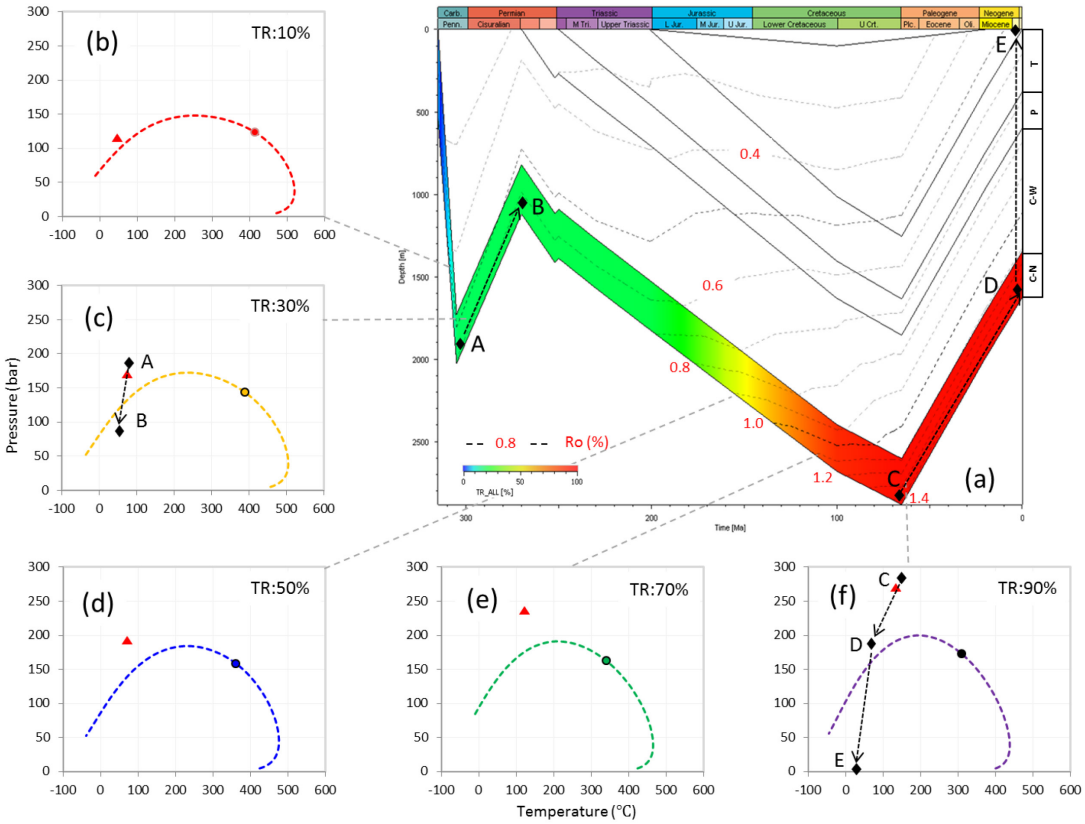

Fig. 2.15. Transformation ratio and Ro evolution histories of well Grove 3 and phase envelopes of primarily generated fluids in according maturities by upper Bowland Shale. The well location can be found in Fig. 2.1. C-N and C-W in stratigraphy part represent Namurian and Westphalian in Carboniferous respectively. Red triangle in each of the phase envelop represents reservoir condition in geological burial history respectively. Black diamonds in 1D modelling map and phase envelops stand for the temperatures and pressures of point A, B, C, D, and E, and the black dash lines linking the points simulate the processes of the fluids being migrated among different reservoir conditions with the arrows imply the moving directions.

In the combination of burial history and phase properties of hydrocarbons generated in geological time, different dominant expulsion driving forces can be proposed and the surface GOR can be assessed. Different expulsion driving forces and mechanisms lead to varying expulsion efficiency and define the amount and property of the unconventional resource left in the source rock. Although only primary hydrocarbon is addressed here, any further secondary cracking, migration or biodegradation would act upon this first-formed composition. The produced GOR prediction is very important in oil field strategy making,

because different fluids varies in economic perspective and engineering requirement. Unfortunately, there are no production data in this well to verify the phase prediction results. Nevertheless, this systematic approach including hydrocarbon composition simulation, phase variation prediction, basin modelling application could be a new thinking in unconventional system production prediction and resource evaluation.

2.5.2 Secondary cracking

Kinetics results shown in Fig. 2.13 can be converted as a Kerogen-Oil-Gas kinetics input model in the basin modelling software, thus gas generated under secondary cracking by upper Bowland Shale in well Grove 3 can be simulated (Fig. 2.16 a). The maximum generation of secondary gas is 151169 tons of secondary gas/km^2 (Table 2.2) and about 90000 tons in the area (Fig. 2.16 a), however, if a default Kerogen-Oil-Gas kinetics model developed by (Quigley et al., 1987) was applied, the secondary gas products are predicted to be only 30492 ton/km^2 (Table 2.2) and about 20000 tons in the area (Fig. 2.16 b). A more comprehensive comparison of maximum secondary gas generation in Grove 3 predicted by kinetics developed in this research and other 9 type Ⅱ source rock default kinetics models (Abu-Ali et al., 1999; Behar et al., 1997; Dieckmann et al., 2000b; Dieckmann et al., 1998; Pepper and Corvi, 1995; Quigley et al., 1987; Ungerer, 1990; Vandenbroucke et al., 1999; Waples et al., 1992) manifests that the result can be very enormously different (Fig. 2.17. and Table 2.2). A maximum secondary generations of 226920 ton/km^2 predicted by Waples et al. (1992) is more than 70 times bigger than the (Burnham and Sweeney, 1989) model which is only 3182 ton/km^2 (Fig. 2.17. and Table 2.2). Relatively speaking, secondary kinetics model developed in this research provides a moderately high production of secondary gas and share many similarities with the prediction of the (Pepper and Corvi, 1995) model (Fig. 2.17. and Table 2.2). It has to be pointed out that the vitrinite reflectance of upper Bowland Shale in well Grove 3 is only 1.4%, which implies that the shale only experienced a low degree of secondary cracking. Thus more significant differences in secondary gas predictions must exist at higher maturity areas when different kinetics models are applied in the basin modelling.

Kinetics parameters defines in which period of secondary cracking the shale is , for example a certain maturity is in the beginning of secondary cracking in one kinetics model, but might be in peak generation in another model. Every target source rock must be approached with a unique secondary kinetics model, huge errors might be induced if default models are selected which plays very important role in shale gas in-place assessment.

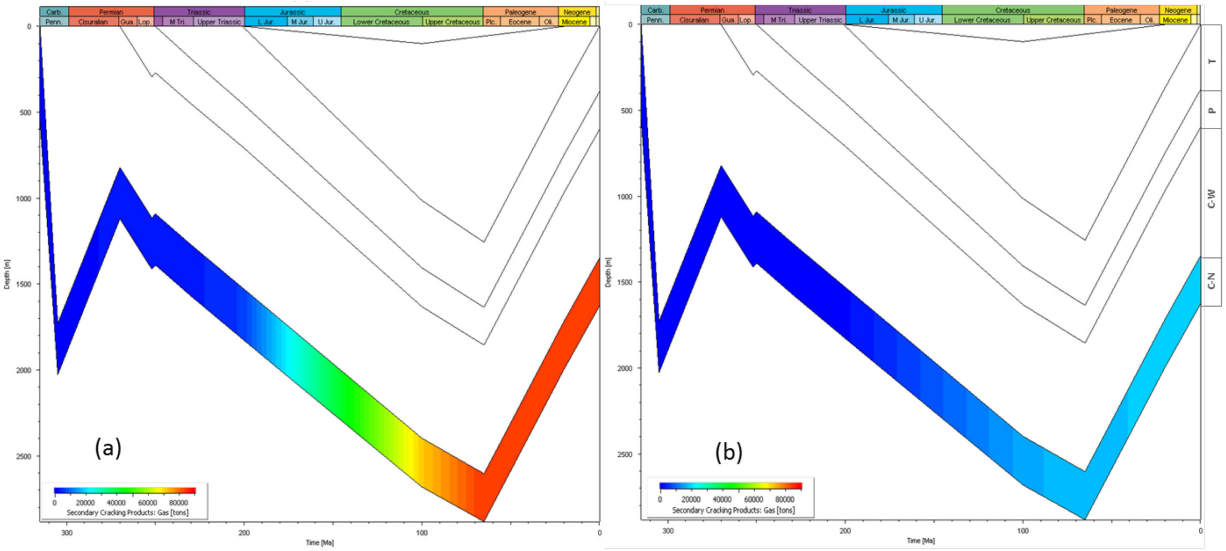

Fig. 2.16. A comparison of secondary gas generation per km2 of upper Bowland Shale in well Grove 3 if (a) secondary cracking kinetics model in this research and (b) kinetics model from Quigley et al. (1987) are applied in the basin modelling respectively.

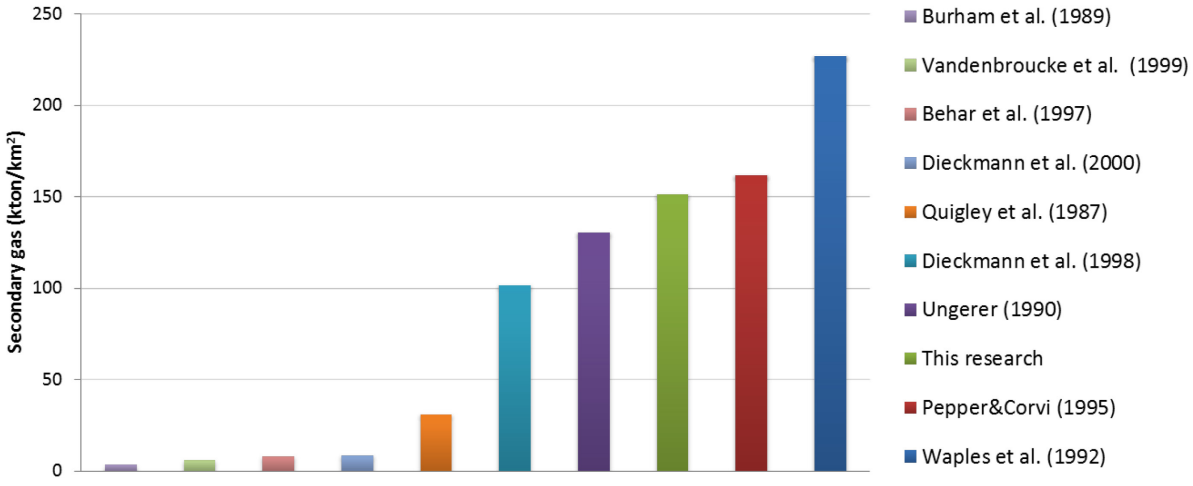

Fig. 2.17. The maximum secondary gas generation per km2 of upper Bowland Shale in well Grove 3 when secondary kinetics of this research was applied as well as the predictions from 9 other default Kerogen-Oil-Gas kinetic models in the PetroMod 2013.

Table 2.2. Detailed information about default Kerogen-Oil-Gas kinetics models shown in Fig. 2.17.

Author and year	Kerogen type	Lithology	Location of sample	Age of sample	Secondary gas/ton
Burnham and Sweeney. (1989)	II	/	/	/	3182
Vandenbroucke et al. (1999)	II	Shale	North Sea	Kimmeridge	5597
Behar et al. (1997)	II	Shale	Paris Basin	Toarcian	8028
Dieckmann et al. (2000)	II	Lime mudstones	Western Canada Basin	Upper Devonian	8226
Quigley et al. (1987)	II	/	/	/	30492
Dieckmann et al. (1998)	II	Shale	Lower Saxonian Basin	Toarcian	101124
Ungerer (1990)	II	Shale	North Sea	Kimmeridge	130254
This research	II	Shale	Northern England	Lower Carboniferous	151169
Pepper&Corvi (1995)	II	Siliciclastic	mixed	/	161430
Waples et al. (1992)	II	Artificial	/	/	226920

2.6 Conclusions

Although the mineral matrix effect is a laboratory induced artefact and may not occur on every shale, the three Bowland Shale researched here suffered from this effect severely. If whole rock samples are used in pyrolysis experiments instead of kerogen concentrates, the hydrocarbon generation potential as defined by HI is under-estimated, bulk kinetic parameter indicate higher thermal stabilities, and the inferred natural GOR is over-estimated.

The three upper Bowland Shale samples are immature (equivalent Ro less than 0.5%) marine shales and comprise type Ⅱ kerogen. Kerogens generate pyrolysates diagnostic of Paraffinic-Naphthenic-Aromatic Oil with low content of wax and sulphur. The bulk kinetic frequency factors range from 1.54×10^{13} to 2.42×10^{13} and main activation energies range from 50 to 53 kcal/mol. All these characteristics of Bowland Shale are quite similar to productive Palaeozoic marine shale in the US such as Bakken, Barnett and Woodford shale.

The Bowland Shale possesses a high secondary gas generation potential and primary oil, primary gas and secondary gas reach their maximum generation at 137, 150 and 230℃ respectively in geological time.

In the combination of phase properties and burial history, different driving forces of expulsion can be concluded and produced GORs are predicted. Expulsion efficiency varies

with the organic maturity and reservoir conditions, and the amount and property of the unconventional resource left in the source rock change accordingly.

Vast differences can be found in secondary gas amount prediction when varying default kinetics models are chosen which emphasizes the significance of a targeted secondary kinetics model in shale gas resource basin modelling evaluation.

2.7 Acknowledgements

The authors thank Ferdinand Perssen for technical assistance. We are also grateful to editors and two anonymous reviewers for their constructive comments and suggestions. This project was funded by China Scholarship Council.

3. HEATING RATE DEPENDENCY OF MME

3.1 Abstract

The presence of some minerals can strongly influence the composition of laboratory pyrolysates. The question is whether similar effects may also occur in nature, thereby influencing the gas-oil ratio and other bulk compositional characteristics. A series of experiments have been conducted at varying heating rates to examine this issue. Three source rocks that vary significantly in mineralogy (a quartz-rich, a calcite-rich and a clay-rich sample), namely the Alum Shale, Bowland Shale, and Toolebuc Shale, respectively, were tested by Rock-Eval pyrolysis, open-system pyrolysis gas chromatography (PyGC) and bulk kinetics parameters to check for the existence or otherwise of mineral matrix effects (MME). Kerogen and whole-rock samples were then pyrolyzed at three heating rates using closed-system pyrolysis to examine the heating rate dependency on hydrocarbon aromaticity, gas-oil ratio and total yield. The solvent extract of one Bowland Shale sample was used as a reference material for the natural system when extrapolating the results from laboratory experiments to nature. A comparison of the natural reference sample with kerogen- and whole-rock pyrolysates using Fourier Transform - Ion Cyclotron Resonance Mass Spectrometry was also made, providing insights into NSO compounds in laboratory and natural environments. The MME in Alum Shale, Toolebuc Oil Shale and Bowland Shale has negligible, weak and strong influences on Rock-Eval, PyGC and bulk kinetic results, respectively. MME on the hydrocarbon aromaticity total yield are heating rate dependent, with decreasing heating rates, the effect is weakened. Bowland kerogen pyrolysate resembles natural products more in certain NSO class ratios compared with its whole-rock counterpart. The MME is speculated to be induced by the fast heating rates and higher temperatures in the laboratory, and it is concluded that the effects do not occur in the geological maturation process.

Reprinted with permission from Yang, S., and B. Horsfield, 2016, Some predicted effects of minerals on the generation of petroleum in nature: Energy & Fuels, v. 30, p. 6677-6687 (postprint), doi: 10.1021/acs.energyfuels.6b00934.

3.2 Introduction

Petroleum consists of an exceedingly complex mixture of hydrocarbons and non-hydrocarbons, extending from methane to macromolecular aggregates. The relative proportions of these components are quite variable and depend initially upon the nature of the kerogen in the parent source rock and its level of maturity at the time of expulsion, and subsequently upon the pressure and temperature conditions of the source-carrier-reservoir system during expulsion, migration and accumulation. While the role played by diagenetic minerals on reservoir quality is well known, for example the formation of clays from feldspars or the conversion of smectite to illite (Bethke et al., 1986; Velde and Espitalié, 1989), it remains unclear as to whether bulk petroleum composition is strongly influenced by retention and/or catalytic processes in source rocks. It has been suggested that clay minerals can be used in the search for oil as a result of its importance in petroleum generation and expulsion (Weaver, 1960). For instance, clay can effect isomerization, disproportion of hydrogen and polymerization of unsaturated hydrocarbons (Frost, 1945; Grim, 1947), and might, therefore, be responsible for the presence of aromatics and the absence of olefins in petroleum (Brooks, 1948, 1952). Mango (1990) proposed that the transition metals, captured from sedimentary waters by chlorophyll, are the catalytic agents that convert *n*-alkane biolipids into the rearranged light hydrocarbons in petroleum. At the molecular level, diasterane/sterane ratios for biomarkers are commonly related to clay content (Rubinstein et al., 1975; van Kaam-Peters et al., 1998), because clays catalyse the formation of diasterane precursors. The high heterogeneity of both organic matter and minerals in gas shales argues that organic-inorganic interactions may be quite different depending upon the depositional environment (Bernard et al., 2012).

The purported importance of organic-inorganic interactions during petroleum formation in nature stems largely from pyrolysis experiments. For example, Jurg and Eisma (1964) produced hydrocarbons by decarboxylating a fatty acid mixed with kaolinite in the presence and absence of water; Shimoyama and Johns (1971) produced the same using montmorillonite. β cleavage produced a hydrocarbon with two carbon atom atoms less than the parent fatty acid when pyrolysis was conducted in the presence of calcium carbonate (Johns and Shimoyama, 1972). The so called Mineral Matrix Effects (MME) (Espitalie et al., 1980) can bring about changes in the gas-oil ratio, gas wetness and fluid aromaticity pyrolysates, as reported from laboratory open- and closed-system experiments including Rock-Eval (Espitalié et al., 1984; Katz, 1983), pyrolysis-GC (Horsfield and

Douglas, 1980), pyrolysis-FT IR (Öztaş and Yürüm, 2000), pyrolysis-GC/MS (Tannenbaum et al., 1986b), bulk kinetics determination (Dembicki, 1992; Dessort et al., 1997), PhaseKinetics modelling (Yang et al., 2015) and hydrocarbon expulsion simulation (Lewan et al., 2014). For clay minerals, two main mechanisms are active: (1) due to the high surface area (Sing, 1985), they tend to adsorb heavy compounds generated in pyrolysis, hence influence the pyrolysis maturity indicator (T_{max}), composition and quantity of the pyrolysate (Horsfield et al., 1983), as well as the kinetics of the reaction, (2) a selective catalytic feature of the clay minerals can change the gas-oil ratio (GOR), aromaticity, oxygen index (OI) and other compositional features of the products (Dembicki, 1990; Wu et al., 2012). It has to be pointed out that not every source rock in pyrolysis experiments necessarily has to suffer from the MME. Horsfield and Douglas (1980), Horsfield et al. (1983) and Katz (1983) concluded that MME varies according to the TOC content and mineralogy of the samples under investigation. A very high TOC (>6%) or low clay content can decrease even avoid the MME (Reynolds and Burnham, 1995). Tannenbaum and Kaplan (1985a), Pan et al. (2010) and Lewan et al. (2014) emphasized that the presence of liquid water in the pyrolysis system could significantly attenuate the activity of the clay catalysing function , although Eglinton et al. (1986) and Behar et al. (2010) noted that the function of water in pyrolysis is limited.

One of the most significant differences between laboratory pyrolysis and geological maturation lies in the heating rate. Geological heating rates normally fall in the range 10^{-10} to 10^{-12} K/min, while a typical laboratory pyrolysis heating rate is not slower than 10^{-1}K/min. With that being said, the slowest experimental heating rate is 300°C over 6-years, or 10^{-5}K/min (Saxby and Riley, 1984) which is not realistic for a routine test. Retort yield from Green River Shale is reported to decrease at lower heating rates (Burnham and Singleton, 1983). From a petroleum generating kinetics perspective, during non-isothermal pyrolysis of immature oil shale and coal, the onset and T_{max} of organic transformation reactions are shifted to higher temperatures with increasing rate of heating (Burnham et al., 1987; Schenk et al., 1997). For the MSSV pyrolysis of Duvernay Shale, aromaticity and the unresolvable GC "hump" decrease with decreasing heating rates (Dieckmann et al., 2000a). Similarly, pyrolysates are always richer in polar and aromatic compounds than petroleums (Horsfield, 1997) and are higher in gas wetness (di Primio and Horsfield, 2006) compared with natural products irrespective of the type of pyrolysis being employed. Karabakan and Yürüm (1998) reported the influence of heating rate to MME, but instead of using kinetic derived temperatures they simply heated samples to certain fixed temperatures under

different heating rates which is less meaningful in a geological sense. The comparison of these pyrolysates does not reflect the heating rate dependency in pyrolysis; it is mainly controlled by maturity instead. Only the products that were generated at the same TR are directly comparable.

It would represent a significant step forward if MME in pyrolysis experiments could be extrapolated to geological systems by consideration of heating rate as a parameter. In this paper, we evaluate the MME on three types of source rocks which have significantly different mineralogies (a quartz-rich, a calcite-rich and a clay-rich sample) using Rock-Eval, open pyrolysis and bulk kinetic modelling. Two types of samples with strong MME were applied to a closed-system (MSSV) pyrolysis to investigate the heating rate dependency of MME on aromaticity, GOR and bulk generation amounts. The projected changes in MME as a function of heating rate were firstly extrapolated from laboratory to nature, and the predictions compared with the results of thermovaporisation of a natural bitumen sample. The ultrahigh-resolution Fourier transform ion cyclotron resonance mass spectrum (FT-ICR MS) technique, which has been applied to identify acids and heteroatom compounds in crude oil (Hughey et al., 2002), asphaltene (Klein et al., 2006), oil sand (Barrow et al., 2004) and coal extracts (Wu et al., 2003), etc., was first induced into MME research here to compare the major compound classes present in whole-rock and kerogen pyrolysates with those in natural bitumen to elucidate whether MME occurs in nature.

3.3 Samples and Analytical Methods

3.3.1 Samples

Three immature whole-rock samples from the Alum Shale, Toolebuc Oil Shale and Bowland Shale, as well as their kerogen concentrates were studied in this research using pyrolysis (Table 3.1). The solvent extract of one Bowland Shale was used as a reference.

The Alum Shale sample taken from a core drilled in Central Sweden is of Early Ordovician age. This marine shale was deposited in an inner shelf facies and is characterized by an enrichment of uranium (>200ppm) which was diffused from seawater across the sediment/water interface (Schovsbo, 2002). Quartz (80%) is a major mineralogical component, together with K-feldspar (18%) (Schulz et al., 2015).

As one of the most important oil shale plays in Australia, the marine Toolebuc Formation of Early Cretaceous age underlies about 484,000 km^2 of the Eromanga and Carpenteria Basins (Dyni, 2006). The outcrop Toolebuc Oil Shale samples studied here comes from Julia Creek where the oil shale was deposited in an epicontinental sea environment (Boreham and Powell, 1987) and has a calcite content over 45% (Patterson et al., 1986).

Table 3.1. Generalized information and Rock-Eval & TOC data of the samples tested in the research.

Sample Name	Location	Age	Mineralogy	Sample type	Tmax (°C)	HI (mg HC/g TOC)	OI (mg CO2/g TOC)	TOC (%)
Alum Shale	Middle Sweden	Early Ordovician	Quartz-rich (80%)	whole-rock	418	357	4	16.7
				kerogen	420	356	6	41.1
Toolebuc Oil Shale	Northeastern Australia	Early Cretaceous	Calcite-rich (+45%)	whole-rock	417	457	24	13.1
				kerogen	421	426	31	52.5
Bowland Shale	Northern England	Late Carboniferous	Clay-rich (+50%)	whole-rock	431	194	10	3.17
				kerogen	426	302	4	24.2

The Namurian (Late Carboniferous) Bowland Shale sample is from 31.02m in the Carsington Dam Reconstruction C4 borehole, which was drilled in the Widmerpool Trough, Northern England. Thin section observation and carbon isotope research have previously shown that this Bowland Shale sample is a thin-bedded carbonate-bearing clay-rich mudstone, its bulk δ^{13}Corg value of -28.8 ‰ indicating that the kerogen is derived from marine planktonic algae (Konitzer et al., 2014). The mineralogy of the marine Namurian Bowland Shale in Northern England is characterized by a high concentration of clay (+50%) and a moderate content of quartz (22.1±3.9 %) (Spears and Amin, 1981). Among the clay minerals, kaolinite is the most abundant, constituting 20.8±7.5 % of the total minerals; montmorillonite and illite contents are low.

The reference Bowland Shale core sample was taken from 1,404 metres depth in Old Dalby. The whole-rock sample has an HI of 188 mg/g TOC which is similar to the pyrolyzed whole-rock (HI: 194 mg/g TOC; see results section). With a T_{max} of 437°C, the shale is considered to be an early oil-window matured sample which is suitable as a reference for comparing artificial and natural products.

3.3.2 Analytical Methods

3.3.2.1 Kerogen isolation and screening

Kerogen concentrates were isolated from whole-rock samples by (1) crushing the shale sample to sub-millimetre size, (2) treating with hydrochloric acid/6N hydrofluoric acid [2:1] for one week at room temperature and (3) sieving to 10-500 microns.

Rock-Eval and TOC analyses were performed using a Rock-Eval 6 and Leco SC-632 Analyser respectively following established procedures.

3.3.2.2 Pyrolysis gas chromatography (PyGC)

PyGC was performed using the Quantum MSSV-2 Thermal Analysis System® interfaced with an Agilent GC-6890A (Horsfield et al., 2014). Milligram quantities of each sample were loaded into a small open glass tube and heated under flowing helium; free hydrocarbons were vented for 3 minutes during an isothermal purge at 300°C, after which the C_{2+} pyrolysis products generated during heating from 300°C to 600°C were collected in a cryogenic trap (liquid nitrogen). Methane passed through the trap and passed through the GC column to the Flame Ionisation Detector (FID). Trapped products were then liberated by removing the cooling agent and heating the trap to 300°C. An HP-Ultra 1 dimethylpolysiloxane capillary column connected to the FID was employed using helium as carrier gas. Quantification of individual compounds and boiling range splits was conducted by external standardisation with n-butane.

3.3.2.3 Bulk kinetics

Bulk pyrolysis was performed using a Source Rock Analyser® (SRA) at three different heating rates (0.7, 2 and 5 K/min) following established procedures (Burnham et al., 1987). The discrete activation-energy (Ea) distribution optimization with a single frequency factor (A) as well as geological extrapolation were performed using the KINETICS 2000® and KMOD® programmes. The corresponding temperatures of Transformation Ratio (TR) 30%, 50% and 70% for each of the three different heating rates (0.7, 2 and 5 K/min) were selected for MSSV pyrolysis and measurement of pyrolysate composition.

3.3.2.4 Micro scale sealed vessel (MSSV) pyrolysis-GC

As described by Horsfield et al. (2014), milligram quantities of samples were sealed in glass capillaries and artificially matured to temperatures corresponding to 30, 50 and 70 TR for

each of the heating rates 0.7, 2 and 5 K/min respectively. The tubes were then cracked open using a piston device coupled with the injector, and the released products were swept into the GC using a flow of helium. Quantification was performed by external standardisation using *n*-butane.

3.3.2.5 Thermovaporisation-GC

Around 10 mg of coarsely crushed reference shale was weighed into MSSV glass capillary tubes, which were then sealed by an H_2 flame after having reduced the internal volume with pre-cleaned quartz sand. After introduction into the Quantum MSSV-2 Thermal Analysis System, the external surfaces of the tube were purged for 5 min at 300°C, during which time volatiles were mobilised within the tube; thereafter the tube was cracked open by a piston device to transfer the products into a liquid nitrogen-cooled trap. The composition of these volatiles was analysed as described under PyGC.

3.3.2.6 MSSV-FT-ICR MS

Aliquots of MSSV pyrolysates were extracted using dichloromethane and methanol (V/V 9:1). Mass analyses were performed in negative ion ESI mode with a 12 T FT-ICR mass spectrometer equipped with an Apollo II ESI source, both from Bruker Daltonik GmbH. Nitrogen was used as drying gas at a flow rate of 4.0 L/min and a temperature of 220 °C and as nebulizing gas with 1.4 bars. The sample solutions were infused at a flow rate of 150 µL/h. The capillary voltage was set to 3000 V and an additional CID (collision-induced dissociation) voltage of 70 V in the source was applied to avoid cluster and adduct formation (Poetz et al., 2014).

3.3.2.7 Analysis of reference material

A Soxhlet extractor was used for extraction of the reference sample bitumen. Core sample material (20 g) was filled in an extraction tube and extracted with a solvent mixture of dichloromethane and methanol (v/v = 99:1) at 40 °C for 24 h. The bitumen was then analysed by FT-ICR MS as described above.

3.4 Result and Discussion

3.4.1 The existence of MME

3.4.1.1 Rock-Eval and TOC

Significant differences in maturity parameters and organic matter type identification indices can be found between Bowland and Toolebuc whole-rock-kerogen pairs while Alum Shale sample pairs seem to be less influenced by MME (Table 3.1 and Fig. 3.1). The clay-rich Bowland whole-rock sample manifests higher T_{max} (Fig. 3.1a), higher OI (Fig. 3.1b) and lower HI (Fig. 3.1b) than its kerogen counterpart and these make the Bowland whole-rock samples seem to be more mature and more terrestrial in origin as when compared with the kerogen. By comparison, the calcite-rich Toolebuc Oil Shale whole-rock sample was influenced by a less significant MME, and in the opposite way to that of the Bowland samples, namely the Toolebuc whole-rock signature looks less mature and has a better organic matter type (Fig. 3.1). A negligible MME in T_{max} and OI was noted for the quartz - dominated Alum Shale samples.

The MME induced by clay minerals in these Rock-Eval tests resemble those reported by Dembicki et al. (1983),Espitalié et al. (1984)and Heller-Kallai et al. (1984) who concluded (1) the retention of relatively heavy compounds on clay minerals is responsible for the increase of T_{max} and decrease of HI in whole-rock samples and (2) the selective catalytic effect of acid minerals in generating CO_2 (Larsen and Hu, 2006) explains why the OI of whole-rock sample was shifted to higher values. The impact of MME on the calcite-rich Toolebuc Oil Shale samples supports the work of Katz (1983) who reported carbonate mineral can enhance the HI and hinder the OI.

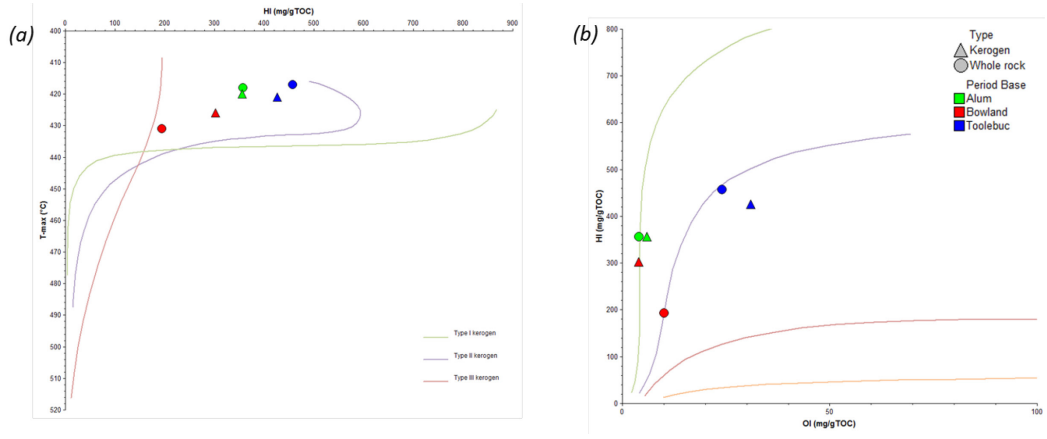

Fig. 3.1. Basic geochemical screening based on Rock-Eval & TOC of whole-rock and kerogen samples.

3.4.1.2 PyGC

The PyGC analysis of source rocks is a technique which can make a quick evaluation of kerogen structure (Dembicki et al., 1983; Van de Meent et al., 1980) and relate that structure to bulk petroleum composition by means of Petroleum Type Organofacies (Horsfield, 1989). As a Lower Palaeozoic marine shale, it is not typical for the Alum Shale to be rich in low molecular weight and aromatic pyrolysis products, e.g., xylene and toluene (Fig.3. 2 and 3.3), this unique characteristic could be induced either by an unusual precursor biota or by effects related to the presence of uranium (Horsfield et al., 1992b). Negligible differences in the pyrolysates of Alum whole-rock and kerogen can be observed which implies the quartz does not bring about MME because of its inert nature, possibly combined with the already aromatic nature of the pyrolysate (Fig. 3.2 and 3.3).

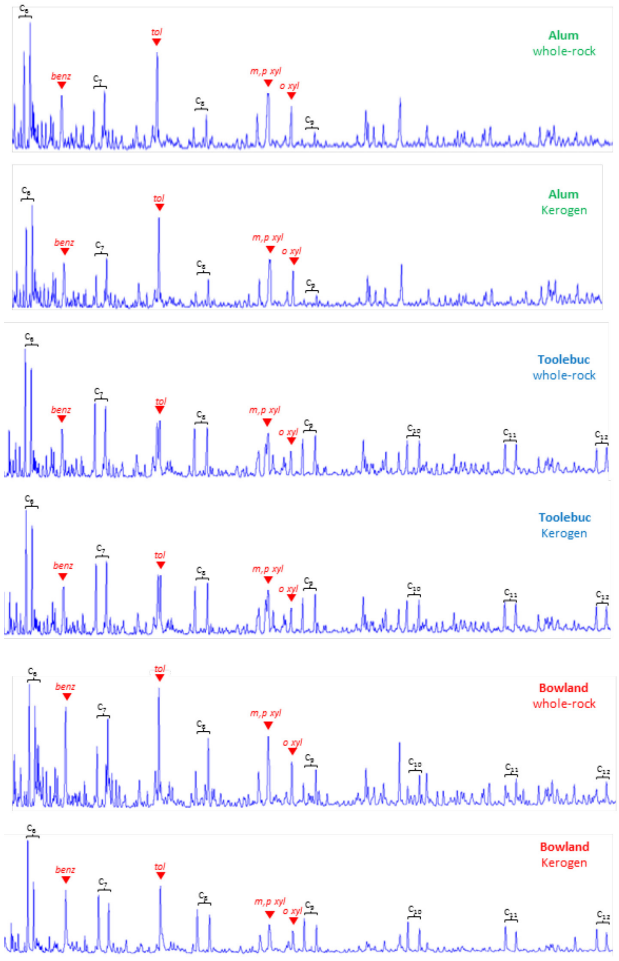

Fig. 3.2. Comparison of PyGC maps on whole-rock and kerogen pairs. Bowland Shale pyrolysate shows an obviously higher aromatic compounds concentration compared with its kerogen counterpart. (benz: benzene, tol: toluene, m,p xyl: meta- and para-xylene, o xyl: ortho-xylene.)

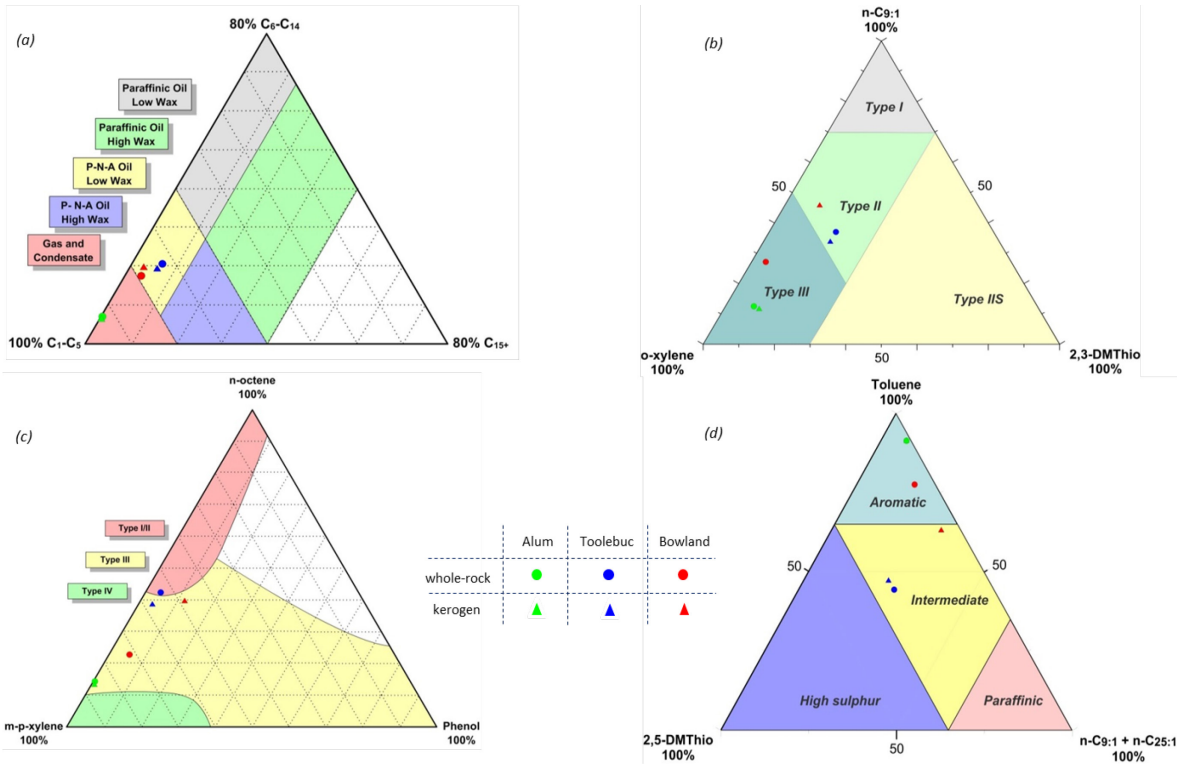

Fig. 3.3. Quick classification on the pyrolysates of both whole-rock and kerogen concentrates.

The pyrolysate of Toolebuc Oil Shale belongs to the Low Wax P-N-A (Paraffinic-Naphthenic-Aromatic) oil Petroleum Type Organofacies (Fig. 3.3. a)(Horsfield, 1989). Thiophenic sulphur compounds generated from the carbonate oil shale are more abundant than in either of the two clastic sediments (Fig. 3.3. b, d). Although the differences of kerogen and whole-rock pyrolysates are not significant (Fig. 3.2), it still can be recognised that the kerogen products are more aromatic than the whole-rock counterpart (Fig. 3.3).

In contrast, pronounced differences can be found between the clay-rich Bowland Shale whole-rock pyrolysis products and its kerogen pyrolysate, i.e., aromatic compounds are more abundant, and there is an increased complexity of the compound mixture in whole-rock products, when compared with kerogen that was heated alone (Fig. 3.2). Different from the calcite-rich Toolebuc Oil Shale, Bowland Shale kerogen generates more high molecular (Fig. 3.3a) and aliphatic products (Fig. 3.3 b-d).

The preferential catalytic effect of clay minerals on low molecular weight aromatic and branched hydrocarbons has been attributed to cracking *via* a carbonium-ion intermediate which forms on the Lewis acid sites of the clay (Tannenbaum and Kaplan, 1985b). The MME induced by carbonate minerals was considered as less significant and opposite to clay minerals (Hu et al., 2014; Tannenbaum et al., 1986b).

3.4.1.3 Bulk kinetics

The activation energy distribution and frequency factor of Alum Shale kerogen degradation seem not to be influenced by the intimate presence of minerals during pyrolysis (Fig. 3.4). Toolebuc kerogen shows slightly more refractory characteristics compared with the whole-rock, and the Bowland Shale kerogen's activation energy distribution was shifted to obviously lower values when MME was eliminated (Fig. 3.4). These preferential shift features of illite, calcite and clay minerals on bulk kinetic parameters are in agreement with the stated effects of mineral matrices when building kinetic models (Dembicki, 1992), (Dessort et al., 1997).

An instructive way of comparing the differences in kinetic parameters noted above is to apply them to a geological heating rate, here chosen to be 3K/million year (Fig. 3.5). Considering a TR of 50% for example, the geological temperature shifts between whole-rock-kerogen pairs of Toolebuc Oil Shale and Bowland Shale are 5°C and 17°C, respectively (Fig.3. 5). It is clear that these variations can lead to huge differences in the estimated timing of hydrocarbon generation, expulsion and accumulation.

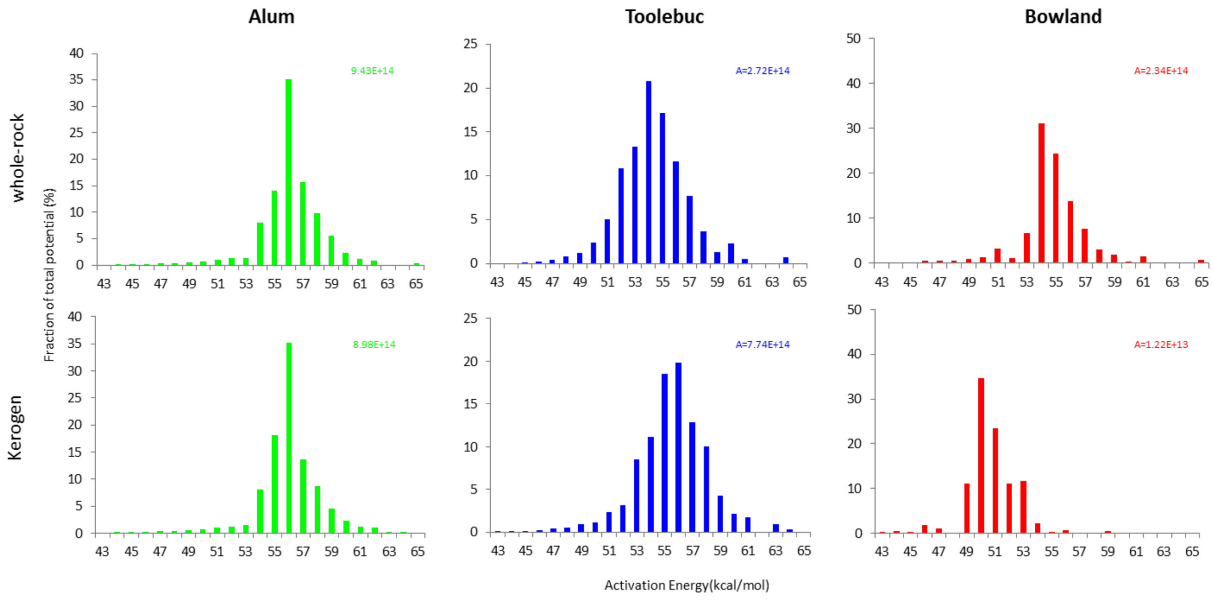

Fig. 3.4. Bulk kinetic parameters of whole-rock and kerogen samples. Negligible (Alum Shale), Small (Toolebuc Oil Shale) and significant (Bowland Shale) differences can be figured out.

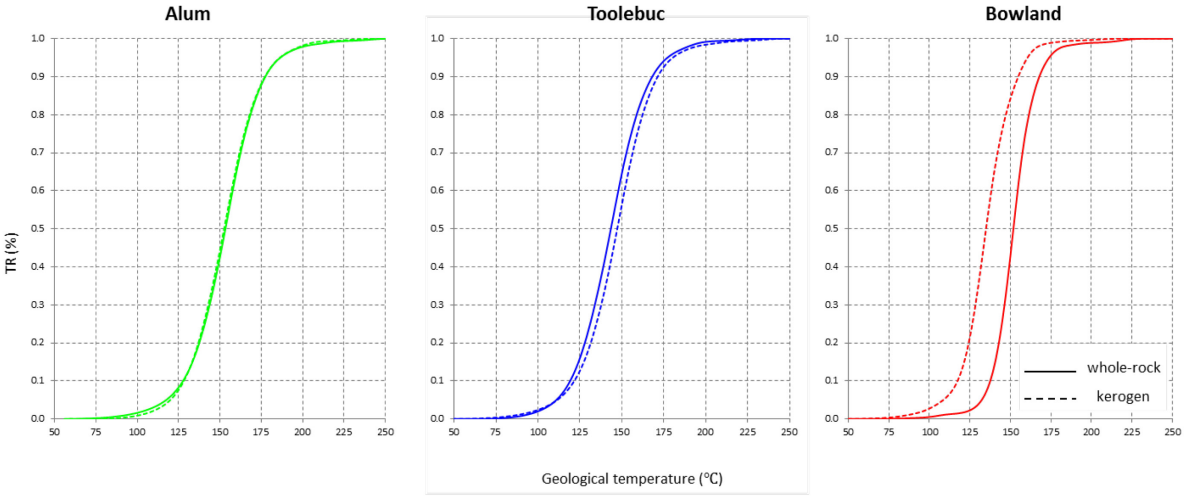

Fig. 3.5. Geological extrapolation (heating rate: 3K/million year) of bulk kinetics parameters and comparison of comparison on whole-rock and kerogen samples.

3.4.2 The heating rate dependence of MME

With decreasing heating rates, the GC "hump" (unresolved complex mixture) and alkene/alkane ratios of both Toolebuc and Bowland pyrolysates decrease, which is in agreement with previous studies on the heating rate dependency of pyrolysis products (Dieckmann et al., 2000a; Williams et al., 1990). Here, we discuss how aromaticity, GOR and total yield were influenced by heating rates with and without minerals.

3.4.2.1 Aromaticity

For the pyrolysates of samples artificially matured to TR 50%, the lower the heating rate is, the lower is the aromaticity (benzene, toluene, xylenes and tetramethylbenzene compared with nearby normal alkanes). The biggest change is seen for the Bowland Shale whole-rock sample (Fig. 3.6). Changes of the Bowland whole-rock pyrolysates are bigger than those of their kerogen counterparts, pointing to the stronger heating dependence on organic-inorganic interactions than on the thermal degradation of kerogen. By way of contrast, the aromaticities of Toolebuc whole-rock and kerogen samples seem to not be strongly controlled by heating rates at all, ostensibly because MME are weak (Fig. 3.7a).

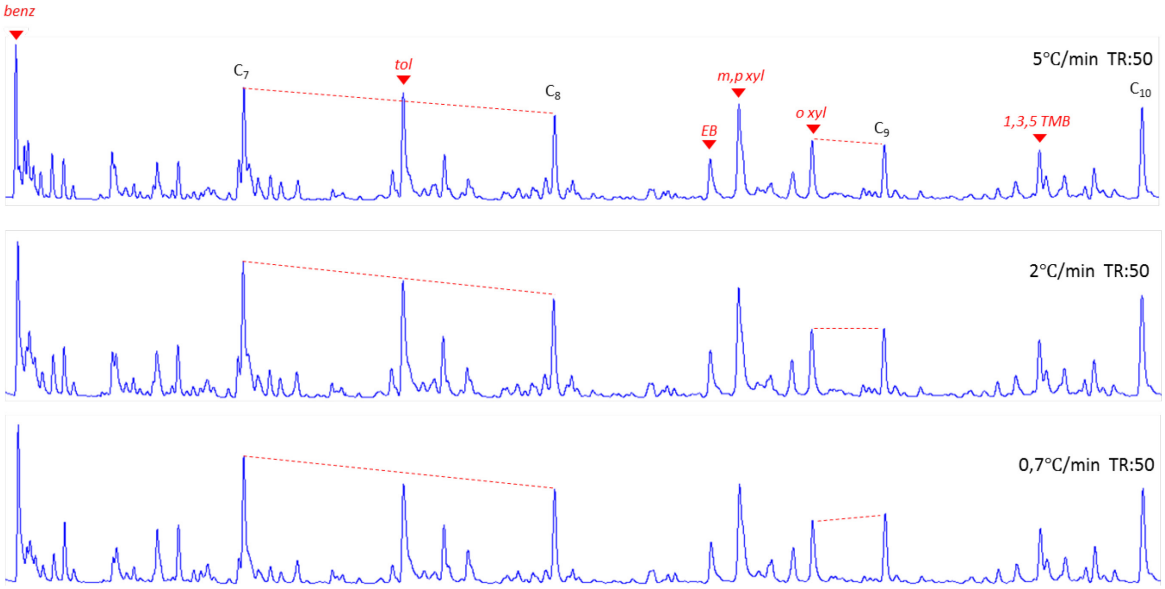

Fig. 3.6. Pyrolysate GC traces of Bowland whole-rock sample at different heating rates when heated to TR 50%. The data manifests that the slower the heating rate is, the more aliphatic the products would be generated. benz: benzene, tol: toluene, EB: ethylbenzene, xyl: xylene, TMB: tetramethylbenzidine.

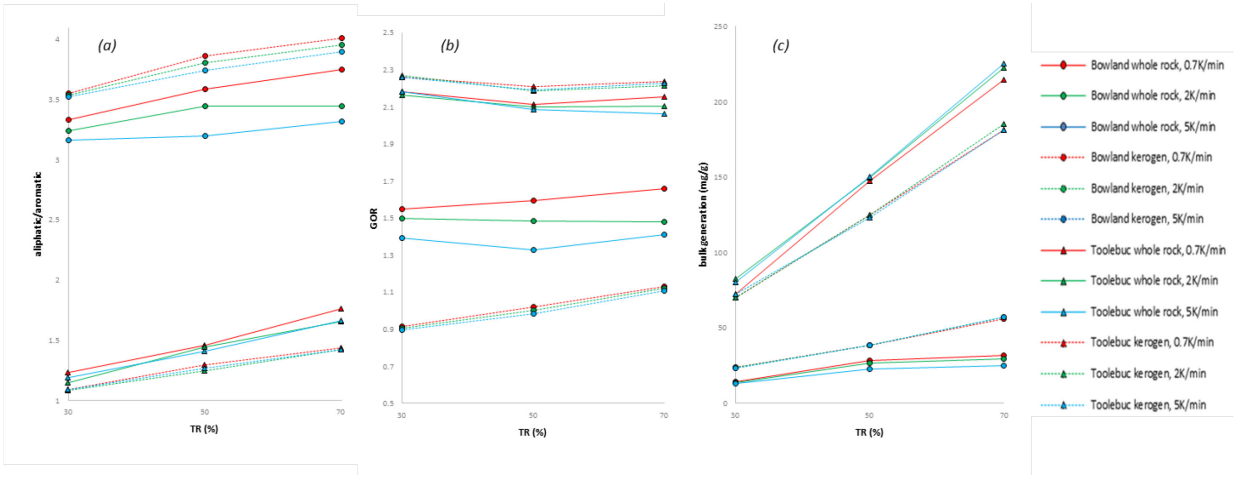

Fig. 3.7. Aliphatic/aromatic compounds ratio, GOR and bulk hydrocarbon generation/TOC variations of Bowland Shale and Toolebuc Oil Shale samples in all three heating rates. Aliphatic compounds include all normal alkenes and alkanes from C1-C30. Aromatic compounds are composed of benzene, toluene, ethyl benzene, xylenes, tetramethylbenzidines, naphthalene, and branched naphthalenes.

3.4.2.2 Gas-oil ratio

Differences in GOR between the whole-rock and kerogen samples is another important compositional influence caused by MME (Horsfield and Douglas, 1980). The GOR of both Toolebuc and Bowland samples increase with decreasing heating rate (Fig. 3.7b). The volatile generation in closed system pyrolysis was contributed by kerogen and oil cracking, a slower heating rate which allows longer time for cracking is possibly the reason why GOR is elevated with decreasing heating rate (Gibbins-Matham and Kandiyoti, 1988). GOR of the clay-rich Bowland whole-rock sample changes much more significantly with varying heating rates compared with the other pairs (Fig. 3.7b) because of MME.

3.4.2.3 Generated Product Yield

Significant differences in bulk generation product yields (including unresolved complex mixture in the GC "hump", normalized by TOC) can be found between whole-rocks and kerogen concentrates of Toolebuc and Bowland samples (Fig. 3.7c). Whole-rocks of the Toolebuc Oil Shale possess higher bulk generation/TOC than their kerogen counterparts while Bowland Shale samples show the opposite trend (Fig. 3.7c), which correlates with HI changes caused by the MME (Fig. 3.1). Gross hydrocarbon generation by kerogen samples is roughly independent of heating rate, which is consistent with the prerequisite of kinetic theory (Braun and Burnham, 1987; Dieckmann et al., 2000a). In contrast, the quantity of whole-rock product depends on heating rate especially in the case of the Bowland Shale samples (Fig. 3.7c). It seems that with decreasing heating rate, the MME on bulk generation amount can be diminished, and whole-rock generation yields can approach those of its kerogen counterpart. It has to be pointed out that the "pseudo HI" in MSSV pyrolysis (Fig. 3.7c) is not directly comparable to Rock-Eval derived HI because: (1) the highest TR in MSSV pyrolysis is 70% in this research, while Rock-Eval HI is achieved when TR has reached 100%; (2) MSSV products were introduced to the GC column where part of the pyrolysate is retained at the GC-interface, whereas very little pyrolysate is lost during direct FID ignition in Rock-Eval (Horsfield, 1997); and it should be noted that (3), coke can be formed in the low-pressure closed-system MSSV pyrolysis but only at high TR. The first two of these factors explain why "pseudo HI" in MSSV is much lower than the HI provided by Rock-Eval. Anyway, the gross hydrocarbon quantity variation induced by MME in both of these systems should be similar.

3.4.3 Geological Calibration

The aliphaticity of thermal extracts from the natural bitumen in Bowland Shale is always higher than artificial pyrolysis products generated from the immature starting material (Fig. 3.8a). With slower heating rates, aliphaticities of both whole-rock and kerogen pyrolysates increase. In the logarithmic coordinates system, the changing rate of whole-rock products is obviously faster than kerogen pyrolysates which implies that in a geological heating rate the differences between these two materials become smaller, in another words, the aliphaticity difference is very likely to have disappeared completely. Geological extrapolation trend lines from artificial pyrolysis show that the prediction of aliphaticity roughly matches that of the natural rock bitumen chosen here for calibration, although, geometrically speaking, there are many possibilities for smoothing the trend lines from the limited dataset shown here.

From the perspective of gross hydrocarbon yield, the heating rate independency of kerogen breakdown implies that the quantity predicted in the laboratory using kerogen is comparable to the geological situation (Fig. 3.8b). Obviously, this is not the case for direct measurements on whole-rock samples; but using extrapolated data, the slower the heating rate, the closer the generation amount of Bowland whole-rock is to its kerogen counterpart (Fig. 3.8b). This observation could be explained by deducing that the MME on gross hydrocarbon generation is quantitatively heating rate dependent and a slower pyrolysis heating rate could reduce the effectiveness of MME on hydrocarbon retention.

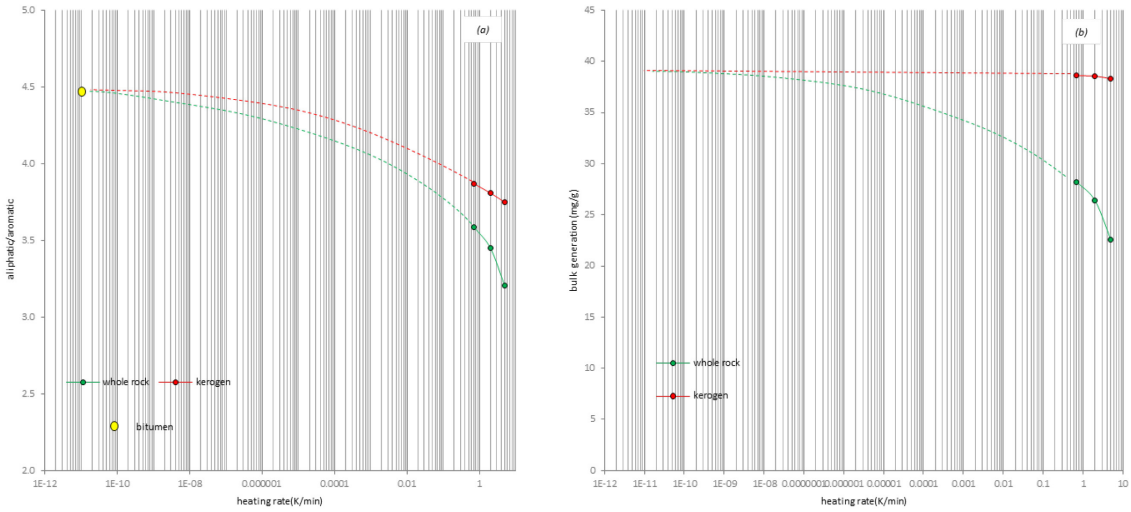

Fig. 3.8. The variation trends of aliphatic/aromatic ratios and bulk generation according to changing heating rates on Bowland Shale samples when they are heated to TR 50%. Natural bitumen reference was shown in Fig. 3.8a.

3.4.4 Insights into Hetero-element Geochemistry

The distribution of elemental classes in source rock extracts and crude oil revealed by FT-ICR MS is largely determined by deposition environment (Chiaberge et al., 2013; Hughey et al., 2002), maturity (Oldenburg et al., 2014; Poetz et al., 2014) and secondary alteration effects such as migration fractionation (Liu et al., 2015), biodegradation (Kim et al., 2005; Pan et al., 2013) and thermochemical sulphate reduction (Walters et al., 2015). Here we examined pyrolysates to see if MME affects heteroelement distributions.

The pyrolysates of Bowland kerogen and whole-rock samples show a decrease in oxygen and increase in nitrogen compounds with increasing TR (Fig. 3.9) thereby resembling changes noted for natural solvent extracts of Type II source rocks with increasing thermal maturity (Poetz et al., 2014). The gross oxygen, nitrogen and sulphur composition of kerogen and whole-rock pyrolysates are rather similar which is surprising considering that significant MMEs have described earlier. However, a detailed comparison of the compound class ratios of O_1/O_2, $N_1/N_{2\text{-}4}$ and N_1O_1/N_1O_2 demonstrates significant differences do indeed occur (Fig. 3.10). Kerogen pyrolysates show much higher ratios in O_1/O_2, $N_1/N_{2\text{-}4}$ and a lower N_1O_1/N_1O_2 ratio. Although it was reported that O_2 class distribution can be changed by contamination and biodegradation (Kim et al., 2005; Pan et al., 2013), all samples were tested by the sample instrument on the same day, these factors can be safely excluded. Since the values of the compound class ratios are small and relatively constant with increasing TR, it can be demonstrated that no significant heating rate dependency occurs within either kerogen or whole-rock samples. More importantly, the O_1/O_2, $N_1/N_{2\text{-}4}$ and N_1O_1/N_1O_2 ratios of the natural Bowland Shale extract being used for calibration are 0.31, 0.30 and 0.59 respectively which are rather close to kerogen products but not whole-rock pyrolysates (Fig. 3.10). Since the reference sample is in the early oil window maturity and occurs within a thick shale layer (over 20m), very limited expulsion is anticipated. The low ratios of O_1/O_2 and $N_1/N_{2\text{-}4}$ of whole-rock sample appear to be caused by the catalytic effect of minerals which tends to bring about condensation of oxygen and nitrogen atoms into aromatic ring systems.

The great resemblance of kerogen pyrolysates and shale extract in the three compound class ratios implies that though kerogen MSSV pyrolysis can't accurately reflect the occurrence of NSO compounds in natural bitumens, it does provides better prediction than whole-rock pyrolysis. The vast differences between artificially heated whole-rock and naturally matured shale extract on both elemental gross compounds and compound class

ratios manifest that MME caused by clay minerals on NSO generation is heating rate related, and that is why the extreme slow geological heating generates similar product as kerogen pyrolysate although there are minerals in the shale. In brief, MME on both hydrocarbon and NSO compounds generation are obviously heating rate dependent and the slower the heating rate is, the weaker the effects of MME. Thus, it can be speculated that the MME only exists in a laboratory environment, but is not significant in the geological maturation process.

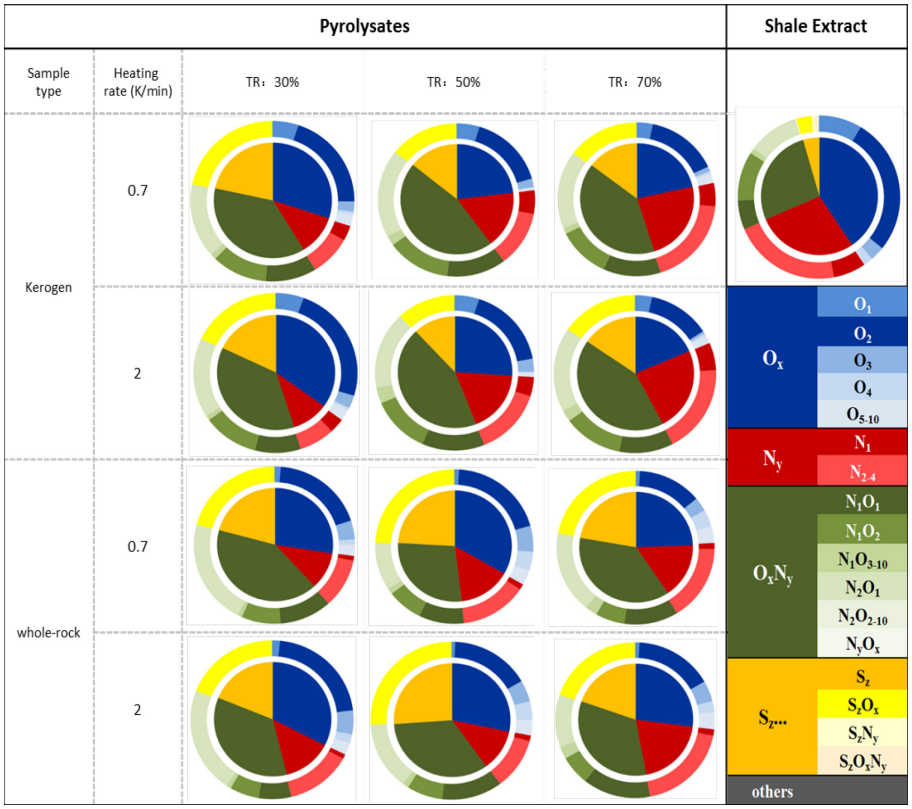

Fig. 3.9. Elemental class distribution pie charts of pyrolysates and matured shale extract in the negative ESI spectra assigned with molecular formulas.

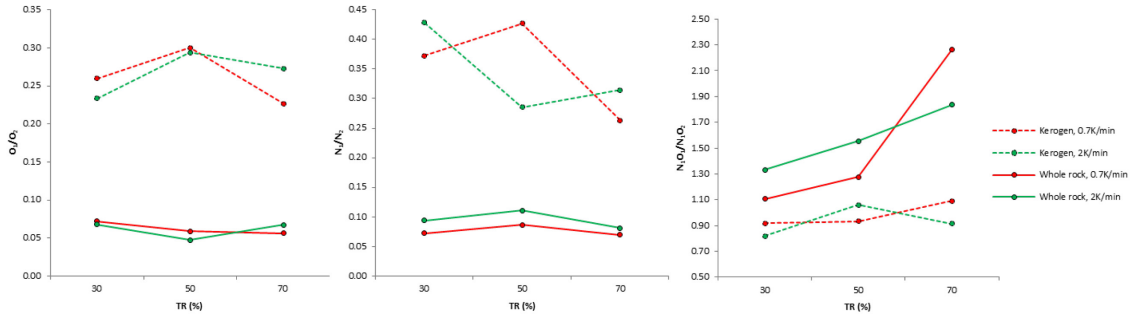

Fig. 3.10. "Class" comparison of Bowland kerogen and whole-rock pyrolysates. The O_1/O_2, N_1/N_2 and N_1O_1/N_1O_2 ratios of the reference matured Bowland Shale extract are 0.31, 0.30 and 0.59, respectively, which are more resemble to kerogen rather than whole-rock sample.

3.5 Conclusions

1. The MME in the quartz-rich Alum Shale, calcite-rich Toolebuc Oil Shale and clay-rich Bowland Shale has negligible, week and strong effluence on Rock-Eval, PyGC and bulk kinetics result respectively. Kerogen type, maturity, organic facies and kinetics can be influenced accordingly.

2. MME on the hydrocarbon aromaticity and generation amount are heating rate dependent, with decreasing heating rate, the effect is weakened. The heating rate dependency of whole-rock pyrolysate GOR is stronger than MME and gets enhanced when heating rate is slowed down.

3. Neither the Bowland kerogen nor the whole-rock pyrolysates show similar gross elemental composition as natural products. However, kerogen pyrolysate resembles natural products more in certain NSO class ratios compared with whole-rock pyrolysate, which implies MME on NSO compounds is diminished in a geological situation.

4. The MME is speculated to only exist in the laboratory environment, not in a geological maturation process. The MME doesn't change kinetic of hydrocarbon generation nor the composition of products in nature; it only affects laboratory pyrolysis results in assessing kerogen type, maturity, organic facies or kinetics.

3.6 Acknowledgments

This study is financially supported by the Chinese Scholarship Council. The authors wish to thank Prof. Michael Stephenson (BGS), Dr. Christopher Vane (BGS), Dr. Chris Boreham (Geoscience Austrilia) and Grippen Oil & Gas, Sweden for providing shale samples. Cornelia Karger and Ferdinand Perssen in GFZ are acknowledged for their technical support. We also thank three anonymous referees for their insightful reviews of the manuscript.

4. URANIUM IRRADIATION ON PETROLEUM GENERATION

4.1 Abstract

An interdisciplinary geochemical study covering Rock-Eval pyrolysis, pyrolysis-gas chromatography, thermovaporisation-gas chromatography and Fourier Transform Ion Cyclotron Resonance mass spectrometry (FT-ICR MS) was carried out to unravel the organic-inorganic interactions caused by radiogenic decay of uranium in immature organic-rich Alum Shale (Middle Cambrian-Lower Ordovician).

The uranium content is correlated with the gas-oil ratios as well as the aromaticity of the pyrolysates of immature samples, indicating a strong uranium irradiation effect on the quantity and quality of the petroleum potential. Also, the gas-oil ratios and aromaticity of thermovaporisation results resemble those in pyrolysates, and proves that the influence of uranium irradiation on the petroleum generation is valid in nature. The FT-ICR MS data reveal that the macro-molecules in the uranium-rich Alum Shale samples are less alkylated and provide evidences for kerogen structures alteration by irradiation to a more gas- and aromatic-prone though geological time.

The radiation dosage resulting from the decay of uranium is linearly correlated with uranium content and impact time, whereas the kerogen structure changes exponentially since labile structures react early and become stabilized in later stages. As a result, the gas percentage and aromaticity of petroleum generated during the oil window time were calculated pointing to more oil- and aliphatic-prone characteristics than those in pyrolysis experiments. In addition, the gas sorption capacity of the Alum Shale is assumed to be less developed during Palaeozoic times in contrast to result suggested by sorption experiment preformed present day. The kerogen restructuring avoids over-estimation on gas generation and gas retention in the Alum Shale and can reduce exploration risks significantly.

This chapter has been submitted to Geochimica et Cosmochimica Acta on 27 Jul 2017 (pretprint).

4.2 Introduction

The potential role played by uranium (U) in petroleum generation was recognised a long time ago. Alpha particles, which are the main products of uranium decay, were suggested to be important (Lind and Bardwell, 1926). Experimental data showed that fatty acids can be decarboxylated by alpha particle radiation at 130°C to form hydrocarbons (Sheppard and Burton, 1946). A correlation between uranium concentration and oil yield in Chattanooga Shale was presented by Swanson (1960). Later, it was found that the total organic carbon (TOC) content is proportionally related to the uranium content (Leventhal, 1981; Swanson and Swanson, 1961), and this finding is routinely applied in using gamma-ray spectral logging to delineate the occurrence of organic rich shales (Schmoker, 1981; Serra, 1983).

Uranium irradiation is responsible for bringing about changes in organic matter composition. The reflectance of vitrinite in humic coal can be enhanced by the crosslinking of polymers caused by radiolytic effects from uranium (Breger, 1974). The atomic H/C and O/C ratios which are used to define the kerogen type and thermal maturity (Durand and Espitalié, 1973) were also considered susceptible to uranium irradiation (Pierce et al., 1958). The uranium enrichment can lead to decreased aliphatic biomarker concentrations (Hoering and Navale, 1987) and may furthermore influence the aromatic biomarker distributions (Dahl et al., 1988a, b; Lewan and Buchardt, 1989). Leventhal and Threlkeld (1978) showed that the $^{13}C/^{12}C$ ratios are correlated to the log of the uranium concentrations, and this finding was confirmed by further investigations on shale (Dahl et al., 1988b) and bitumen samples (Court et al., 2006). Marine shale samples with high uranium contents produce atypical pyrolysates in that there is a significantly enhanced percentage of gas and aromatic compounds relative to long chain aliphatics (Horsfield et al., 1992a; Leventhal, 1981).

These comprehensive investigations played fundamental roles in understanding the influence of uranium irradiation on petroleum generation. However, several key issues are still under debate.

(1) The actual processes leading to changes of the Hydrogen Index (HI), Oxygen Index (OI) and T_{max} in uranium-rich samples which have undergone similar maturation during burial are not clear. Forbes et al. (1988) and Landais (1996) reported that OI and T_{max} values of vitrinite in Akouta uranium deposit (Niger) tend to be increased by increasing uranium contents. In contrast, very low OI values have been reported for the uranium-rich

Alum Samples (Schulz et al., 2015) and Dahl et al. (1988b) suggested that T_{max} is inversely proportional to uranium content.

(2) Due to limited sample amounts and uranium depletion in response to surface weathering, no clear correlation could be found between uranium contents and the atypical pyrolysate characteristics of the Alum Shale in a study by Horsfield et al. (1992a). This led to the hypothesis that a unique algal biomolecule might be the precursor for the gas- and aromatic-rich properties (Bharati et al., 1995). Importantly, the mechanism of uranium irradiation in changing the petroleum generation potential is still a matter of debate. It is not known which alteration processes change the kerogen structures in response to irradiation and how these changes influence the petroleum generation and occurrence.

(3) Up until now most studies have only featured pyrolysis experiments (Court et al., 2006; Dahl et al., 1988b; Horsfield et al., 1992a; Leventhal, 1981). Studies utilising natural laboratories have not been employed to study the effect of uranium irradiation on petroleum generation. It is not known whether the atypically generated hydrocarbons represent structural moieties caused by uranium irradiation or the effects are secondary and related to the high-temperatures and fast heating rates during pyrolysis experiments.

(4) In either case pyrolysis experiments based on black shale samples in their current state could provide misleading information about petroleum generation because the kerogen structures hundreds of million years ago at the very start of the irradiation history could have been essentially the same as what we would consider typical for marine shales, with a more paraffinic character (Horsfield, 1989).

The Alum Shale (Middle Cambrian – Lower Ordovician) holds the largest low-grade uranium resource in Europe. Here, we present new interdisciplinary geochemical data from investigations of the Alum Shale followed by a discussion of the implications regarding the influence of uranium on petroleum generating potential. Fresh immature samples have been systematically investigated using inductively coupled plasma-mass spectrometry (ICP-MS), pyrolysis methods, thermovaporisation- gas chromatography (Tvap-GC), Fourier Transform Ion Cyclotron Resonance mass spectrometry (FT-ICR MS), and a new method then proposed for back-calculating the aromaticity and chain length distributions of the original kerogen structures.

4.3 Study Area and Samples

The Baltic Basin covers parts of the southern Baltic Sea, the Kaliningrad Oblast, Northern Poland and the western parts of the Baltic States (Fig. 4.1), and contains sediments ranging in age from the Early Cambrian to the present day. The basin fill is thin in the north-eastern part and thickens toward the Teisseyre-Tornquist (Ulmishek, 1990).

The Alum Shale is considered as one of the most important source rocks for oil and gas in the Baltic Basin because of its wide occurrence, considerable thicknesses and high TOC contents (Buchardt, 1999; Kotarba et al., 2014b). Named after the hydrated potassium and aluminium-bearing sulphate [$KAl(SO_4)_2 \cdot 12H_2O$], the Alum Shale Formation is a formal name for the collective of Middle Cambrian, Upper Cambrian (Furongian) and Lower Ordovician (Tremadocian) shale (Andersson, 1985; Thickpenny, 1984). This shale is widely distributed within and around the Baltic Basin, and can be as thick as 180 metres in offshore Denmark (Nielsen and Schovsbo, 2006) and 90 metres in southern Sweden (Pool et al., 2012). The TOC content of Alum shales is typically higher than 2 wt.% (Schovsbo, 2003) and up to 22 wt.% in Middle Sweden (Kosakowski et al., 2016).

34 Alum Shale samples, covering different ages, were analysed from Sweden, Estonia and Russia (Fig. 4.1). Most of the samples are from boreholes, five samples were carefully selected from outcrops (Table 4.1). These samples are of low maturity according to previous maturity assessments based on the reflectance of vitrinite-like macerals (Buchardt et al., 1997; Petersen et al., 2013), and are thus suitable for studies of petroleum potential.

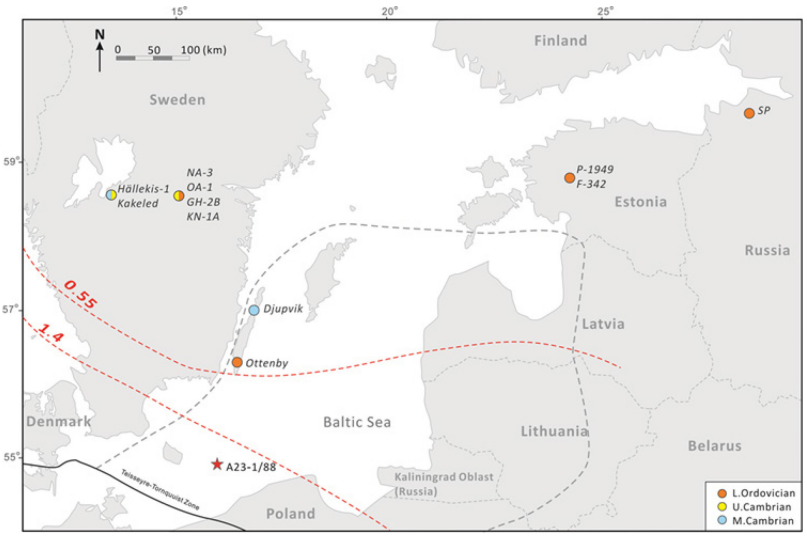

Fig. 4.1. Geographical overview of the Alum Shale sample distribution. The grey dash line depicts the boundary of the Baltic Basin, and the red dash lines represent the isolines of vitrinite-like maceral reflectance of the Alum Shale modified after Buchardt et al. (1997). Ages of the samples are given in coloured circles.

Table 4.1. Background information, uranium contents, and Rock-Eval & TOC data of the Alum Shale samples.

Age	Name	Type	Well/Place	Uranium (ppm)	TOC (%)	Rock-Eval				
						S1 (mg/g)	S2 (mg/g)	T_{max} (°C)	HI (mg HC/g TOC)	OI (mg CO_2/g TOC)
Lower Ordovician	LO-1	borehole	Saint Petersburg	74	11.1	0.3	23.7	409	214	33
	LO-2	borehole	Saint Petersburg	190	9.0	0.3	17.6	412	195	31
	LO-3	borehole	Saint Petersburg	244	13.6	0.4	21.9	411	161	30
	LO-4	borehole	Saint Petersburg	274	6.2	0.2	5.9	414	95	47
	LO-5	borehole	Saint Petersburg	110	9.4	0.1	8.4	419	59	37
	LO-6	borehole	NA-3	136	14.1	0.8	53.6	419	380	2
	LO-7	borehole	F-342	107	8.1	0.3	33.8	406	416	2
	LO-8	borehole	P-1949	119	12.4	2.5	47.6	405	385	3
	LO-9	outcrop	Ottenby	33	8.1	0.6	30.1	441	374	0
Upper Cambrian	UCm-1	borehole	OA-1	155	16.7	1.0	59.6	417	387	1
	UCm-2	borehole	GH-2B	413	21.7	1.3	73.4	426	338	2
	UCm-3	borehole	KN-1A	135	13.1	1.9	50.5	425	385	1
	UCm-4	outcrop	Kakeled	186	21.7	2.2	83.4	416	384	2
	UCm-5	outcrop	Kakeled	194	11.1	0.6	42.2	418	381	1
	UCm-6	borehole	Hällekis-1	201	11.6	1.4	57.4	413	497	10
	UCm-7	borehole	Hällekis-1	177	14.6	1.0	53.1	417	365	8
	UCm-8	borehole	Hällekis-1	50	4.1	0.2	11.6	420	284	20
	UCm-9	borehole	Hällekis-1	142	3.0	0.5	8.8	419	298	30
	UCm-10	borehole	Hällekis-1	130	14.0	0.9	60.9	420	435	11
	UCm-11	borehole	Hällekis-1	109	12.6	0.9	59.0	420	467	12
	UCm-12	borehole	Hällekis-1	97	13.4	0.9	64.1	421	479	10
	UCm-13	borehole	Hällekis-1	84	22.1	1.9	138.1	426	624	5
	UCm-14	borehole	Hällekis-1	87	10.7	1.3	52.2	424	490	10
Middle Cambrian	MCm-1	outcrop	N. Djupvik	14	9.9	1.8	33.4	421	338	4
	MCm-2	outcrop	Kakeled	35	13.5	2.0	47.7	418	353	2
	MCm-3	borehole	Hällekis-1	21	11.1	2.5	59.8	423	537	10
	MCm-4	borehole	Hällekis-1	35	11.1	3.9	56.6	420	511	4
	MCm-5	borehole	Hällekis-1	35	10.8	2.1	21.1	423	195	9
	MCm-6	borehole	Hällekis-1	43	11.3	3.2	77.3	426	686	7
	MCm-7	borehole	Hällekis-1	47	22.0	2.7	128.4	423	583	6
	MCm-8	borehole	Hällekis-1	44	10.4	2.9	52.8	416	508	7
	MCm-9	borehole	Hällekis-1	34	12.2	4.3	55.0	418	451	6
	MCm-10	borehole	Hällekis-1	11	3.3	1.4	16.3	426	498	14
	MCm-11	borehole	Hällekis-1	22	5.9	1.8	31.3	422	529	14

4.4 Experimental Methods

4.4.1 Uranium measurement

Uranium contents were measured by inductively ICP-MS as described by Romer and Hahne (2010). About 250 mg of rock powder, which had been dried at 105°C, was weighed into 15 ml teflon vials (Savillex®) and decomposed using HF, Aqua Regia (3:1 mixture of 37% HCl and 63% HNO_3), and perchloric acid ($HClO_4$). In a first step, 4 ml HF and 4 ml Aqua Regia were added to the samples. The tightly closed vials were placed into a heating block (160°C) for 14 hours. After cooling, 1 ml $HClO_4$ (70%) was added to destroy the organic material and fluorides. This solution was evaporated at 180°C to incipient dryness. The samples were re-dissolved in 1 ml 7N HNO_3 and dried. Then, the $HClO_4$ step was repeated twice. The samples were re-dissolved in 7N HNO_3 and kept at 100°C for 14 hours. This solution was brought to a volume of 50 ml for analysis. Data were acquired in peak jumping mode using a Galileo 4870 in pulse counting mode.

4.4.2 Pyrolytic techniques

Rock-Eval pyrolysis and TOC measurement were performed using Rock-Eval 6 and Leco SC-632 analysers, respectively, following established procedures. Pyrolysis-GC and thermovaporisation were performed using the Quantum MSSV-2 Thermal Analysis System interfaced with an Agilent GC-6890A (Horsfield et al., 2014). (1) For Py-GC, about 10 mg of coarsely crushed reference shale was filled into a small open glass tube and heated at 300 °C for three minutes to vent the free hydrocarbons. Hydrocarbons generated between 300 to 600 °C were collected and measured. Quantification of individual compounds was conducted by external standardisation with *n*-butane. (2) For thermovaporisation-GC, around 10 mg of sample was weighed into MSSV glass capillary tubes, which were then sealed by a hydrogen flame. After introduction into the Quantum MSSV-2 Thermal Analysis System, the external surfaces of the tube were purged for five minutes at 300°C, during which time volatiles were mobilised within the tube; thereafter the tube was cracked open by a piston device to transfer the products into a liquid nitrogen-cooled trap. The composition of these volatiles was quantified as described under Py-GC.

4.4.3 FT-ICR MS

Based on screening data, four representative Alum Shale samples, were Soxhlet-extracted using a mixture of dichloromethane and methanol (v/v = 99:1). Mass analysis of the

resulting bitumen samples was performed in negative ion Electospray Ionisation (ESI) mode with a 12 T FT-ICR mass spectrometer equipped with an Apollo II ESI source, both from Bruker Daltonik GmbH. Nitrogen was used as drying gas at a flow rate of 4.0 L/min and at a temperature of 220 °C, and acting as nebulizing gas with 1.4 bars. The sample solutions were infused at a flow rate of 150 μL/h. The capillary voltage was set to 3000 V and an additional collision-induced dissociation voltage of 70 V in the source was applied to avoid cluster and adduct formation. Ions were accumulated in the collision cell for 0.05 s and transferred to the ICR cell within 1 ms. Spectra were recorded in broadband mode using 4 megaword data sets. For each mass spectrum, 200 scans were accumulated in a mass range from m/z 147 to 1000.

An external calibration was done using an in-house calibration mixture for ESI negative mode containing fatty acids and modified polyethylene glycols. Subsequently, each mass spectrum was internally recalibrated using known homologous series. A quadratic calibration mode was chosen for all samples. The RMS errors of the calibrations were between 0.001 and 0.031 ppm. Elemental formulas were assigned to the recalibrated m/z values with a maximal error of 0.5 ppm.

4.5 Results

4.5.1 Screening data

The uranium contents in the Alum Shale are highly variable, ranging from 11 ppm to 413 ppm (Table 4.1). The Middle Cambrian samples are generally lower in uranium content compared with Upper Cambrian and Lower Ordovician Alum Shale samples (Table 4.1).

With total organic carbon (TOC) contents greater than 4.0 %, except for sample UCm-9 which contains 3.0 % (Table 4.1), most of the analysed Alum Shale samples can thus be viewed as "excellent" source rocks from the perspective of organic richness (Hunt, 1961; Peters and Cassa, 1994). The correlation between uranium and TOC contents is poor (Table 4.1), as also found in a more comprehensive study with more than 300 Alum Shale samples presented in Schovsbo (2002).

The T_{max} value of sample LO-9 from Ottenby, Southern Sweden (Fig. 4.1) is 441 °C which suggests that the organic matter is early mature with respect to oil generation whereas all other samples are immature with T_{max} values lower than 430 °C (Table 4.1). In the pseudo-van Krevelen diagram, seemingly Types I, II, III, and even type IV kerogens occur in the

Alum (Fig. 4.2a). They are, however, in conflict with the marine depositional environment (Thickpenny, 1984). Samples with low HI and high OI are mostly from a shallow well close to St. Petersburg (Russia) while the Swedish and Estonian samples are characterized by Types I and II kerogen. Low OI (<10 $mgCO_2/gTOC$) and moderate HI values (between 300-500 mgHC/gTOC) of the Alum Shale from South-Central Sweden were also reported by Sanei et al. (2014) and Schulz et al. (2015). Samples from Hällekis-1 and Saint Petersburg boreholes demonstrate inverse relationships in general between T_{max} values and uranium contents, especially those with uranium contents higher than 100 ppm (Fig. 4.2b).

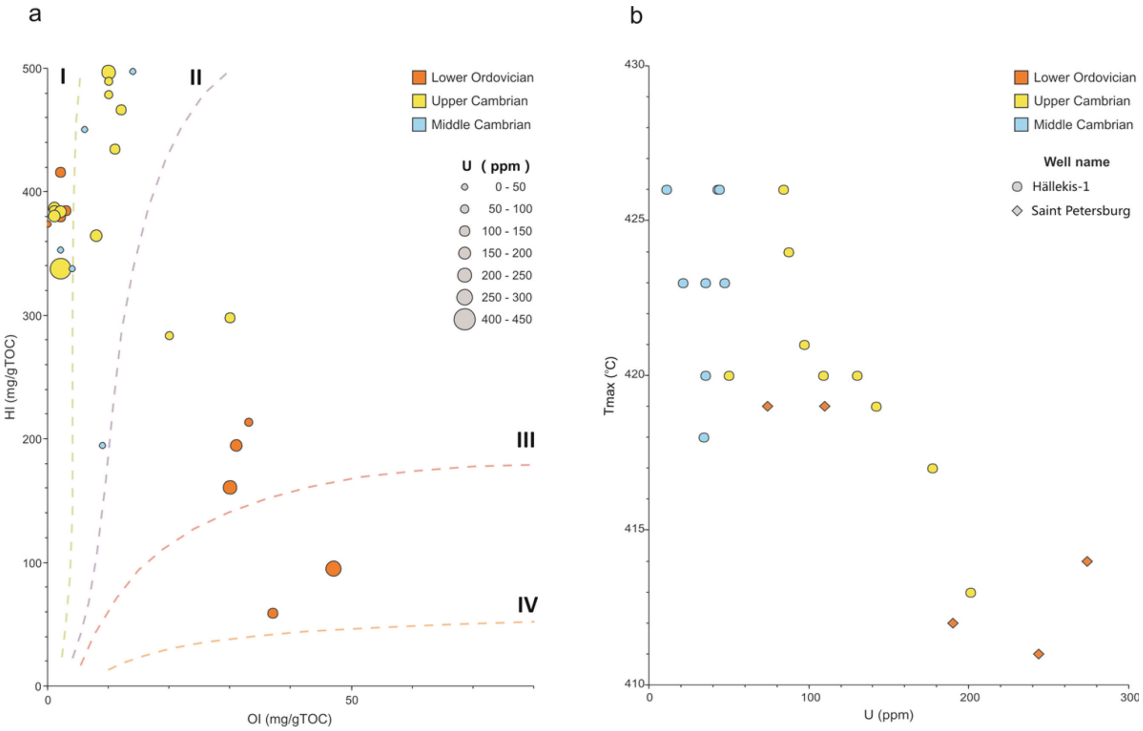

Fig. 4.2. The correlations between uranium contents and key Rock-Eval parameters. (a) Different kerogen types can be identified based on the pseudo-van Krevelen diagram (Espitalie et al., 1977). HI and OI are poorly correlated with uranium contents. (b) Tmax values of samples from two boreholes are inversely proportional to their uranium contents in general.

4.5.2 Open pyrolysis-gas chromatography and thermovaporisation

The Py-GC and Tvap-GC data unravel detailed compositional information equivalent to the Rock-Eval derived S2 and S1 components, respectively. Py-GC provides an overview of the structural characteristics of kerogen (Horsfield, 1989; Van de Meent et al., 1980), while the Tvap-GC manifests the hydrocarbons that have been generated and retained in the source rock over its geological history, minus volatile losses that have occurred during sample acquisition and storage.

16 representative samples were selected for pyrolytic analyses and significantly different pyrolysates occur among these samples (Table 4.2). The uranium-poor sample (MCm-1, U=14 ppm) which can be viewed as "typical" marine shale from the perspective of uranium concentration generates short (C_1-C_5), middle- (C_6-C_{14}) and long-chained (C_{15+}) hydrocarbons dominated by normal alk-1-enes and alkanes (Fig. 4.3a). With increasing uranium contents, the pyrolysates are less aliphatic and characterized by increasing content of aromatic compounds. This can be seen for sample LO-3 (U=244 ppm) where the oil range pyrolysates are almost exclusively consist of aromatic compounds (Fig. 4.3). For all samples, the gas percentages and aromaticity of the pyrolysates appear to be exponentially controlled by the uranium content (Fig. 4.4a and b).

Table 4.2. Py-GC and Tvap data of 16 Alum Shale samples. The ternary end members are normalized as described by Horsfield (1989) and Eglinton et al. (1990). GOR in Tvap was calculated from gas over resolved oil.

	Name	Uranium content (ppm)	PyGC						Tvap	
			Horsfield, 1989			Eglinton et al., 1990			GOR	*o*-Xyl/C_9
			C_{1-5} Bulk (%)	*n*C_{6-14} Res.(%)	*n*C_{15+} Res. (%)	2,3-dmThiophene (%)	*n*-nonene; 9:1 (%)	*o*-xylene (%)		
Lower Ordovician	LO-1	74	87.5	12.5	0.0	14.2	18.8	67.0	3.2	2.6
	LO-2	190	94.6	5.4	0.0	11.6	10.1	78.3	6.1	5.2
	LO-3	244	96.5	3.5	0.0	12.9	6.9	80.2	5.4	9.1
	LO-4	274	97.4	2.6	0.0	10.5	8.1	81.4	6.9	12.7
	LO-5	110	94.0	6.0	0.0	9.0	17.2	73.8	6.3	6.1
	LO-6	136	91.3	8.5	0.2	8.0	18.6	73.4	5.8	3.5
	LO-7	107	93.3	6.7	0.0	9.0	17.6	73.4	5.9	3.7
	LO-8	119	93.5	6.5	0.0	9.5	14.4	76.2	5.6	5.1
	LO-9	33	78.1	20.4	1.8	6.2	54.3	39.4	0.4	0.5
Upper Cambrian	UCm-1	155	92.5	7.3	0.2	8.5	13.4	78.1	6.8	3.2
	UCm-2	413	98.0	2.0	0.0	9.1	5.1	85.8	6.4	12.5
	UCm-3	135	92.0	7.8	0.2	9.3	14.9	75.8	6.6	4.4
	UCm-4	186	92.4	7.4	0.2	7.3	13.2	79.5	5.5	7.5
	UCm-5	194	94.2	5.8	0.0	10.0	10.5	79.5	4.1	8.9
Middle Cambrian	MCm-1	14	77.0	21.0	2.0	9.5	45.3	45.2	0.8	1.8
	MCm-2	35	79.2	18.8	2.0	13.4	39.2	47.4	0.6	1.1

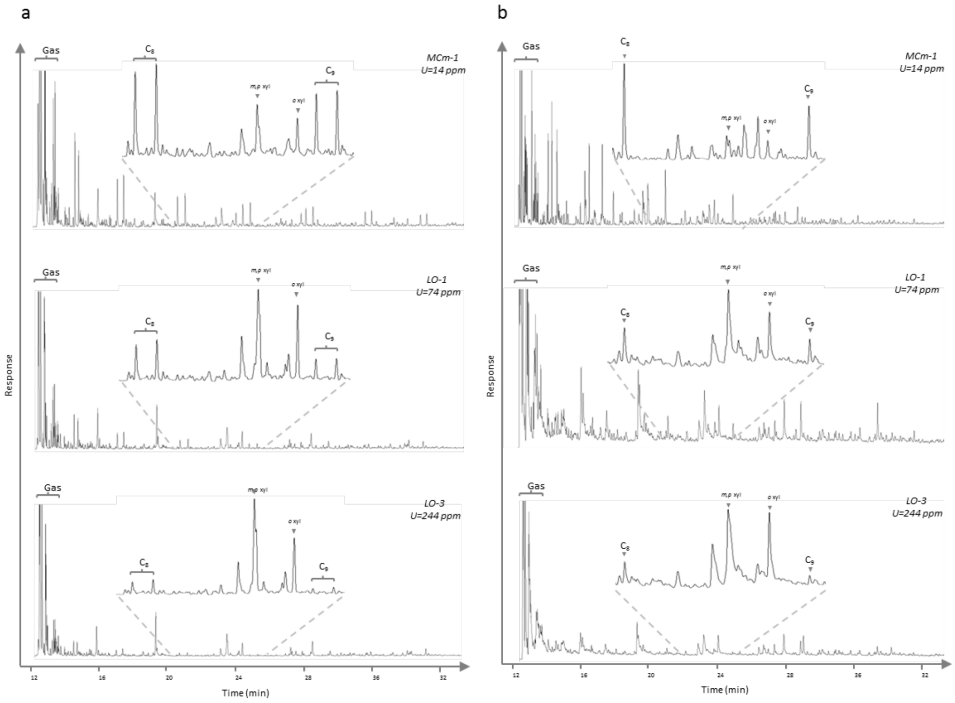

Fig. 4.3. The pyrolysis- and thermovaporisation- GC traces of three Alum Shale samples with very different uranium contents. n-alkenes and n-alkanes are named by carbon numbers, and major aromatic compounds are illustrated. (a) The pyrolysates show increasing gas/oil ratio and aromaticity in the products with increasing uranium contents from the top to bottom. (b) The Tvap products is featured by the absence of alkenes compared with Py-GC, but they still show the same trend of compositional changes in response to uranium contents as revealed by pyrolysates.

At least two groups can be identified among the samples when plotting the pyrolysate data in the classical discrimination ternary diagrams (Fig. 4.5). The organic matter in all Middle Cambrian samples and in one Lower Ordovician sample (LO-9), lean in uranium and characterised as Type II kerogen based on Rock-Eval data, have the potential to generate Paraffinic-Naphthenic-Aromatic oil with low wax contents which is similar to "classical" marine shales (Fig. 4.5a). On the other hand, the pyrolysates generated from uranium-rich Alum Shale samples are dominated by gaseous and aromatic compounds and fall in the Type III field of the pseudo-van Krevelen diagram (Fig. 4.5). Phenol and cresol which are dominant compounds in terrestrial organic matter pyrolysates (Larter, 1984; Van de Meent et al., 1980) are nearly absent when pyrolysing Alum Shale (Fig. 4.3a).

Very interestingly, the gas to oil ratio (GOR) and the *o*/xylene ratio resulting from Tvap analyses are also proportional to uranium content (Fig. 4.3b and Fig. 4.4c and d). The high sensitivity of the Tvap derived GOR to weathering and storage conditions might partly explain some inconsistencies of the correlations. Furthermore, it seems that a GOR threshold between 5.5 and 6.9 is reached in Tvap experiments and it might define the maximum gas storage capacity of finely powdered samples.

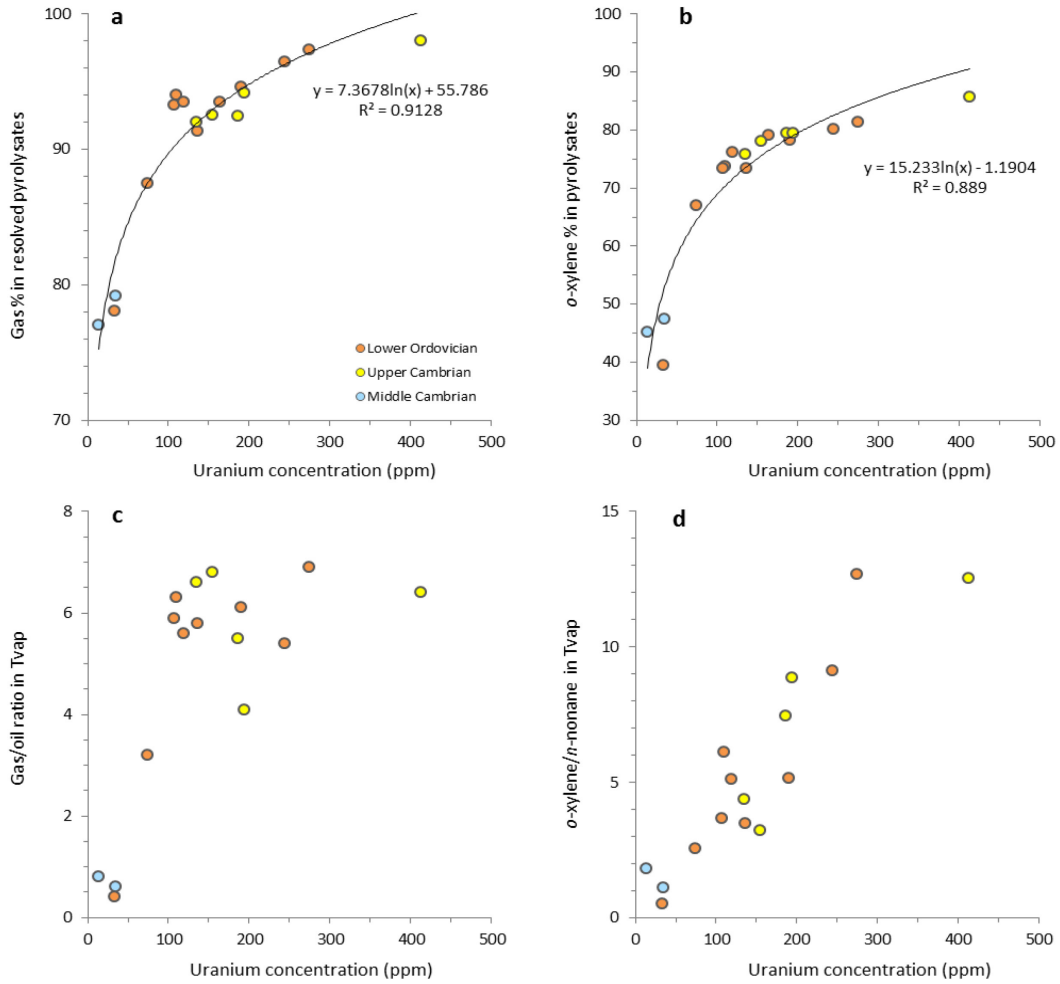

Fig. 4.4. Correlations between uranium contents with compositional information derived from pyrolysis-GC (a and b) and Tvap-GC (c and d). The gas percentage in (a) and o-xylene percentage in (b) are two end members of two classical ternary diagrams as shown in Fig. 5 which are instructive to organic facies. Gas/oil ratio in (c) is calculated from gas/resolved oil in Tvap which reflects the gas richness as (a) does. Since the 2,3-dimethylthiophene concentration in Tvap is low and can't be accurately interpreted, only o-xylene and n-nonane were used in (d). Nevertheless, both (b) and (d) represent the aromaticity of the products.

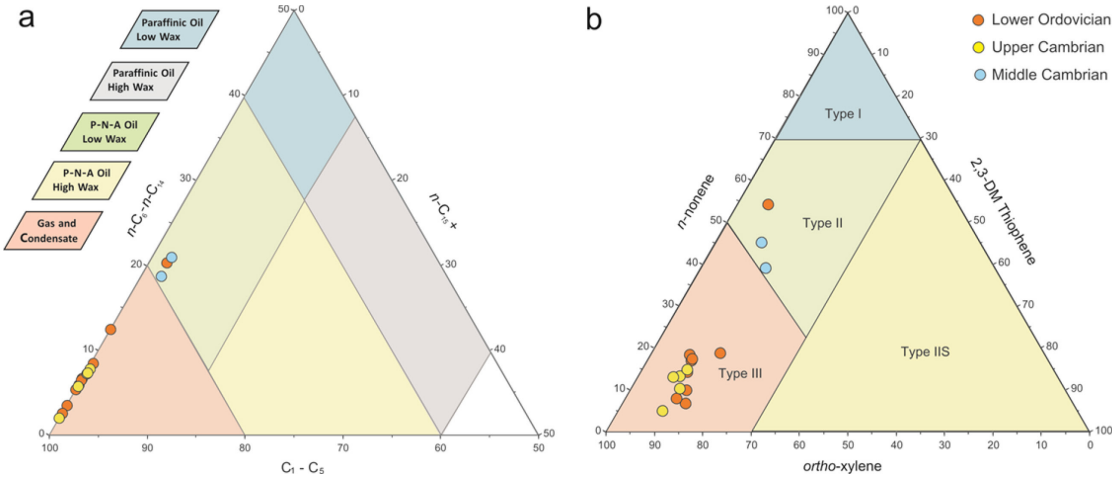

Fig. 4.5. Ternaries of the pyrolysates showing interpretations of the organic facies and kerogen structures of the shales (Eglinton et al., 1990; Horsfield, 1989).

4.5.3 FT-ICR MS

4.5.3.1 General elemental composition

The FT-ICR MS technique offers the ultra-high resolution detection of petroleum constituents (Hughey et al., 2001; Marshall et al., 1998) and is fundamental to the concept of "Petroleomics" (Marshall and Rodgers, 2004). FT-ICR MS run in ESI negative mode can identify up to 30,000 NSO-containing compounds in crude oil (Bae et al., 2010), and has been widely applied in petroleum science, e.g., oil typing (Hughey et al., 2002), biodegradation (Kim et al., 2005), maturity (Oldenburg et al., 2014; Poetz et al., 2014), thermochemical sulphate reduction (Walters et al., 2015), migration fractionation (Liu et al., 2015; Mahlstedt et al., 2016), and mineral-organic interactions (Yang and Horsfield, 2016).

In this study, total extracts from four representative Alum Shale samples were analysed. The relative total monoisotopic ion abundance (TMIA) of each NSO class was calculated by normalizing the peak area to the total. Oxygen-containing compounds are clearly more enriched in the uranium-rich samples (Fig. 4.6) although interestingly it is these samples that are exclusively low in OI (Table 4.1). Significant differences can also be found in the nitrogen class distributions (Fig. 4.6), i.e., the nitrogen-containing group exclusively consists of the N_1 class in the uranium-rich samples (LO-6 and UCm-1), while the N_2 classes only occur in the uranium-poor samples (LO-9 and MCm-2).

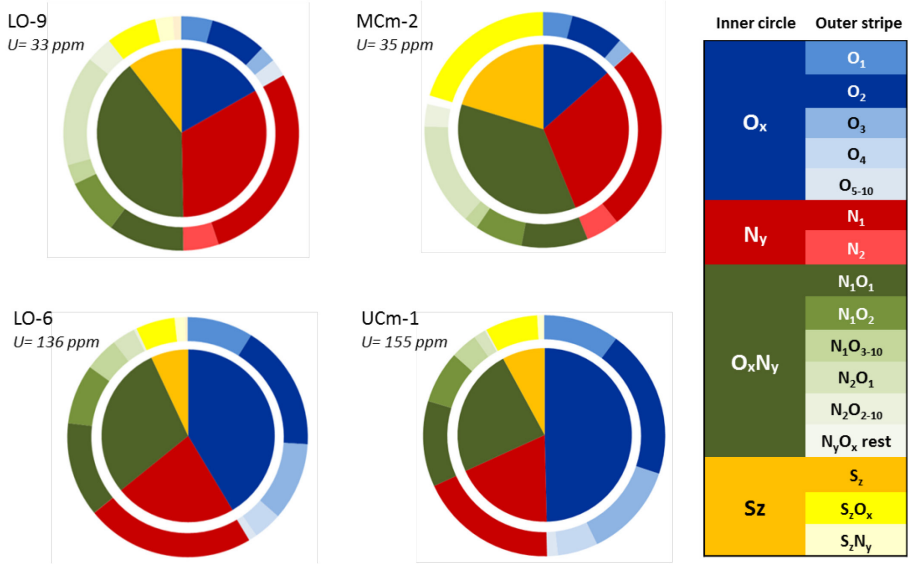

Fig. 4.6. Elemental class (inner circle) and compound class (outer circle) distribution pie charts of four representative Alum Shale samples derived from ESI(-) FT-ICR MS analyses. Uranium-poor samples (LO-9 and MCm-2) have lower oxygen contents and uranium-rich samples (LO-6 and UCm-1) are featured by the absence of N2 compounds.

4.5.3.2 Detailed N1 class characterisations

Since the oxygen compounds detectable by FT-ICR MS are highly sensitive to biodegradation (Kim et al., 2005; Liao et al., 2012) and contamination (Teräväinen et al., 2007), the N_1 class which is one of the dominating classes in each sample (Fig. 4.6) offers further investigation potential. Organic compounds containing one nitrogen atom measurable in ESI(-) FT-ICRMS are most commonly pyrrolic and indolic belonging to carbazoles (Hughey et al., 2002; Pakarinen et al., 2007).

In the vertical direction (Fig. 4.7), the DBE distribution of sample LO-9 is generally higher especially no DBE < 9 is detected. Much more pronounced differences are reflected by the carbon number distribution (Fig. 4.7) which denotes the alkylation degree of the core structures. It can be concluded that the carbon numbers range to higher values in the uranium-poor samples (Fig. 4.7a and b) compared with samples with higher uranium contents (Fig. 4.7c and d). In the case of DBE 9, sample UCm-1 (U=155 ppm) contains up to 27 carbon numbers (Fig. 4.7d) which means that maximum 15 saturated carbon atoms are attached to the core structure of carbazole ($C_{12}H_9N$). While the alkylation degree on carbazoles in sample LO-9 (U=33 ppm) is much more pronounced, the carbon number can be as high as 36 (Fig. 4.7a).

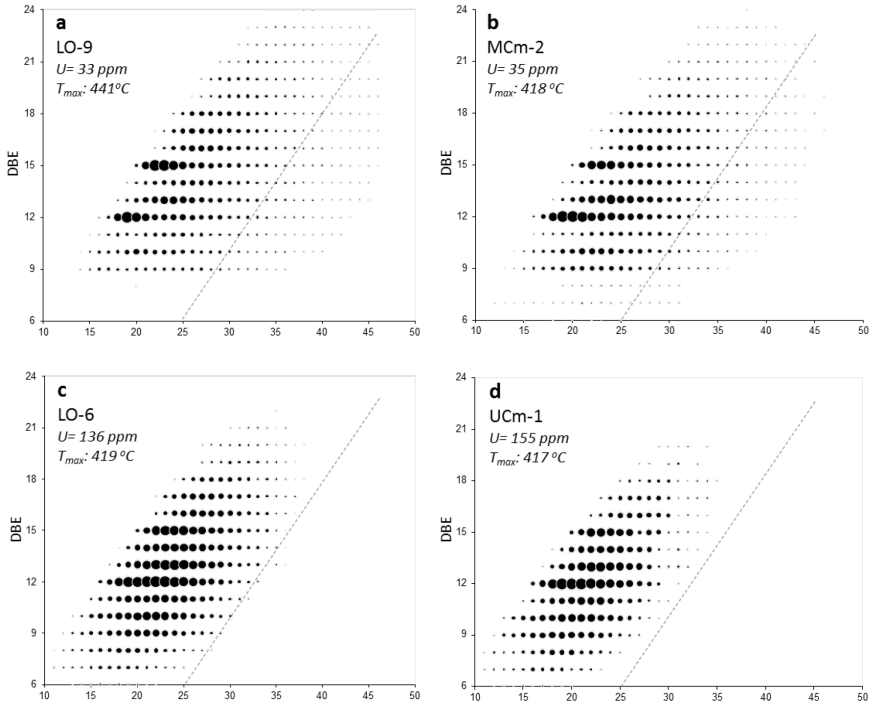

Fig. 4.7. DBE against carbon number diagrams on the N1 class of two uranium-poor (a and b) samples and two uranium-rich ones (c and d). The size of the circles denotes the relative abundance of each compound and the dash lines in the right part of each diagram enable comparison of the alkylation.

4.6 Discussion

4.6.1 The uranium enrichment

Organic-lean grey shales are estimated to have an average uranium content of four ppm (Alloway, 2013; Swanson, 1960). In organic-rich marine black shales the uranium contents are much higher averaging 20 ppm (Swanson and Swanson, 1961). For example, the Mississippian Barnett Shale has a maximum uranium content of 14 ppm (Abouelresh and Slatt, 2012; Tian, 2010), while the famous Silurian "hot shale" in the Middle East with high TOC contents (6-10%) and high gamma ray logging responses contains uranium contents of up to 25 ppm (Loydell et al., 2009; Lüning et al., 2005). Obviously, uranium concentrations in the Alum Shale, with the exceptions of Middle Cambrian samples and sample LO-9, are much higher than typical marine shale and most of other black organic rich shales (Table 4.1).

Uranium can be immobilised in sediment under a reducing depositional environment (Goldschmidt, 1937), for it is soluble in oxic seawater and the solubility significantly decreases in reducing environments (Durand, 2003). Therefore, uranium precipitation from the aqueous phase requires both uranium-rich sea water and reducing conditions which finally lead to an enrichment in sediments (Breger and Brown, 1962; Disnar and Sureau, 1990; Vine and Tourtelot, 1970).

Swanson (1960) found that humic organic matter in North American shales contains far more uranium than the sapropelic type. In contrast, Breger and Brown (1962) argued that uranium is correlated with the TOC content irrespective of the organic matter type. The poor correlation between uranium and TOC contents in the Alum Shale (Table 4.1) and in previous data sets (Schovsbo (2002) emphasises an uranium enrichment mechanism different from classical pathways. So far, there are three representative hypotheses available:

(1) Fisher and Bostrom (1969) and Oliver et al. (1999) found that hydrothermal fluids change the temperature and pressure of sea water causing uranium precipitation in fine-grained sediments. The unusual metal composition of the Alum Shale in the Oslo Graben may be a result of such interactions (Berry et al., 1986). This local volcanic influence may be taken as an explanation as to why shales contemporaneously deposited with the Alum Shale in Wales, North America, and South America lack such high uranium contents.

(2) The comparison with the Devonian Chattanooga Shale led Leventhal (1991) to conclude that the Alum shale lacks humic material. The high uranium contents in Alum Shale were attributed to a slow sedimentation rate and the long-term persistence of euxinic bottom water which may have preserved the accumulating organic matter and its associated metals.

(3) In contrast to a reducing depositional environment as a controlling factor, Leckie et al. (1990) found that the uranium-rich Shaftsbury Formation (Cretaceous) in Canada was deposited in relatively shallow water based on palynological, micropalaeontological and geochemical results. Schovsbo (2002) reported that the uranium contents of the Alum Shale are inversely correlated with the layer thickness which implied that uranium was preferentially enriched in the inner-shelf area rather than in the outer-shelf facies. Accordingly, an intensified bottom water circulation may have resulted in an enhanced supply of uranium at the sediment/water interface where the uranium extraction from the sea water took place.

In summary, during deposition of the Alum Shale, uranium was not captured by humic organic matter which developed at post-Silurian times (Kenrick and Crane, 1997). Instead, the physicochemical conditions of the depositional environment were the controlling factors.

4.6.2 Hydrocarbon precursors and products

4.6.2.1 Kerogen structure

The atomic H/C and O/C ratios which define kerogen type and thermal maturity (Durand and Espitalié, 1973) are influenced by uranium irradiation, with H/C decreasing and O/C increasing when the uranium content of the shale is high (Pierce et al., 1958). This general trend is also manifested in equivalent Rock-Eval parameters (Landais, 1996; Leventhal et al., 1986). However, uranium content is probably not the controlling factor of the HI and OI values in the current sample set (Fig. 4.2a) at least the OI is not necessarily high when the sample is rich in uranium (Table 4.1). Seemingly Types III and IV kerogen of the St. Petersburg samples could be the result of a unique depositional environment (Dronov and Holmer, 1999) or, more likely, due to biodegradation of the organic matter (Tolmacheva et al., 2001). It could be possible that the hydrocarbon potential was reduced due to the liberation of hydrogen by uranium ionising radiation (Colombo et al., 1964; Dole, 1958).

However, since the original HI values of the sample are variable, a relationship between uranium content and the current HI values is not detectable.

Middle Cambrian samples and sample LO-9 with relatively low uranium contents are predicted to produce Paraffinic-Naphthenic-Aromatic hydrocarbons which are features of classical marine shales (Horsfield, 1989). In according, it is atypical of marine shales in general that the pyrolysates of the rest samples are extremely rich in gas and aromatic compounds (Fig. 4.5). The abundance of short chain aliphatics and alkylbenzenes can be indicative of terrestrial originated organic matter (Eglinton et al., 1990; Horsfield, 1989) which, however, does not apply here. Another possible explanation could be the mineral matrix catalytic effect during pyrolysis (Espitalie et al., 1980; Horsfield and Douglas, 1980). For example, Yang et al. (2016) showed that the whole rock pyrolysate of the argillaceous marine Bowland Shale (Mississippian, UK) generates a much gassier and more aromatic pyrolysate than its kerogen concentrate does. However, the pyrolysates of a uranium-rich Alum Shale samples before and after demineralization are identical, thereby ruling out this explanation.

Using the analogue that Ordovician seas were globally and uniquely populated by the alga Gloeocapsamorpha Prisca (Fowler and Douglas, 1984), Horsfield et al. (1992a) suggested that the Cambrian might have had its own unique biota whose residues on pyrolysis yielded the unusual pyrolysates. Bharati et al. (1995) and Sanei et al. (2014) expanded the precursor hypothesis, as algae, e.g., *Chlorella marina*, can yield aromatic-rich hydrocarbons (Derenne et al., 1996). Furthermore, pyrolysis of trilobite chitin results in aromatic hydrocarbons (Arthur Stankiewicz et al., 1996) and could also serve as an explanation. Concerning the current dataset, Lower Ordovician samples with similar palaeo-biota yield very different pyrolysates (Fig. 4.5) depending on the uranium contents (Fig. 4.4a and b). The robust correlations between uranium concentrations and key pyrolysate parameters substantiate the hypothesis that irradiation is a major control on the Alum Shale products. Furthermore, with decreasing uranium contents, the pyrolysates are similar (Fig. 4.4a and b) pointing to the fact that the original kerogen structures of all Alum Shale samples are essentially uniform. It is the increasing irradiation dosage (dependent on the uranium content) that changes the basically uniform structures to be more gas-prone and aromatic.

The vitrinite reflectance of humic coal were reported to be enhanced by crosslinking of polymers caused by uranium irradiation irrespectively of the geological heating (Breger, 1974). Similarly, (Forbes et al., 1988) and (Landais, 1996) suggested the T_{max} of vitrinite in

Akouta uranium deposit (Niger) increases when the uranium contents are high. However, the reverse correlation between T_{max} and uranium contents in Alum Shale is in accordance with previous findings by Dahl et al. (1988b). Since the correlation between T_{max} and OI is poor (Table 4.1), the O-C bonds are generally stronger than C-C bonds don't serve as explanations for this. Based on molecular modelling, Claxton et al. (1993) found that the presence of aromatic rings in kerogen results in weakening the bond energies of carbon chains except for the α bond (the first carbon bond attached to the ring structure). The aromatic products-rich features of samples with high uranium contents (Table 4.2) imply that the breaking of carbon chains attached to aromatic structures occurred extensively during pyrolysis. Since such kind of bonds attached to the aromatic structures (except α bond) are generally weaker than those of the same position in a ring structure-free system, this could explain why uranium-rich samples present relatively low T_{max} values. Another possible explanation could be related to the generation and polymerisation of hydrocarbons by uranium irradiation (Court et al., 2006). These complex hydrocarbons would not be activated under the S1 temperature (up to 300 °C) and their releases during S2 temperatures (300-650 °C) would decrease the peak temperature of S2 since the vaporisation of them are anticipated to be easier than the breaking of kerogens.

4.6.2.2 Free hydrocarbons

The free hydrocarbons stored in the immature (low T_{max}) Alum Shale samples and detected by Tvap may have been formed by incipient thermal cleavage reactions or by irradiation induced maturation. Jaraula et al. (2015) reported that the odd/even carbon preference of *n*-alkanes in an immature deposit (R_o=0.26%) decreases with increasing uranium contents, and thus proposed an alternative radiolytic cracking pathway besides the thermal and microbial mechanisms of petroleum generation. It needs to be pointed out that the free hydrocarbons are quantitatively limited, especially from the uranium-rich samples, as revealed by small S1 values (Table 4.1). Nevertheless, the fit between pyrolysis results and Tvap products (Fig. 4.5) manifests that the uranium irradiation effect on compositional variation does not only work in laboratory experiments but also is effective in geological environments.

4.6.3 Heterocompounds

The gross elemental composition and detailed DBE distributions in each class of the NSO compounds of the bitumen allow further insights into changes of the organic matter structure in response to uranium irradiation.

4.6.3.1 Oxygen-containing moieties

The oxygen compounds in petroleum or source rock extracts are influenced by the depositional environment, biodegradation, and maturity. Hughey et al. (2002) found that crude oils generated from lacustrine source rocks are richer in acids (O_2 compounds) than crude oils generated from marine source rocks. Biodegradation of oils normally raises the concentrations of oxygen compounds, especially the O_2 class (Kim et al., 2005). Furthermore, extracts from Posidonia Shale (Lower Jurassic) gets more depleted in oxygen compounds during thermal maturation (Poetz et al., 2014).

Actually, the aforementioned factors play only a very minor role, if any: 1) The Alum Shale was deposited in a fully marine environment that predates the evolution of terrestrial plants. This implies that the source type variation played a very minor role for oxygen compounds variations. 2) Sample LO-6 and UCm-1 are borehole samples (Table 4.1) less prone to be biodegraded, and the outcrop samples (LO-9 and MCm-2) that a most likely to degraded show low oxygen contents (Fig. 4.6) which argue against biodegradation; (3) Sample LO-9 which is more mature among the presented four samples in Fig. 4.6 contains fewer oxygen compounds, which also contradict a possible maturation effect. Instead, the O_2 content in the Alum Shale is related to the uranium content (Fig. 4.6) and we argue that the uranium irradiation may have induced the relative oxygen enrichment in the Alum Shale bitumen as indicated by data from elemental analyses (Pierce et al., 1958). Purportedly the radiolytic cleavage of water yields highly reactive OH^- radicals which quickly react with the in-situ organic matter during diagenesis (Court et al., 2006; Jaraula et al., 2015) leading to enhanced oxygen contents in the kerogen structure . However, these high oxygen moieties do not appear to degrade into low molecular weight volatiles upon pyrolysis as shown by the low OI of many uranium-rich samples (Table 4.1 and Fig. 4.2a). Data gained by nuclear magnetic resonance spectroscopical analyses of the Alum Shale revealed that the oxygen-bearing functional groups are still intact within the kerogen macro-molecule through catagenesis stages (Bharati et al., 1995), i.e., some highly mature Alum Shale kerogens are still rich in oxygen.

N_2 class is typically present in source rocks, but is rare in oil (Bae et al., 2010), because it is preferentially retained in the source rock during expulsion as heavier compounds compared with the N_1 class (Mahlstedt et al., 2016). However, no hydrocarbon expulsion is anticipated from these immature Alum Shale samples. The absence of the N_2 compounds in uranium-rich samples (LO-6 and MCm-1) may thus be also induced by uranium irradiation.

4.6.3.2 Pyrrolic nitrogen-containing moieties

Generally, the average DBE in the N_1 class shifts toward higher values with increasing maturity of the shale (Poetz et al., 2014) or crude oil (Oldenburg et al., 2014) due to annulation and aromatisation. The DBE distribution in sample LO-9, which has the highest T_{max} value among the four samples, could be enhanced by thermal maturation. In contrast, the other three samples have comparable maturities (T_{max} values between 417 °C to 419 °C) and the influence of maturity can be excluded. Although the uranium-rich samples tend to generate more aromatic products during pyrolysis, the bitumen aromaticity is not correlated with the uranium content (Fig. 4.7c and d) and thus no induced effect here is anticipated to have happened.

Atomic pile radiation on petroleum revealed that paraffins would turn into an insoluble gel after a certain dose of radiation is reached (Charlesby, 1954). In the Alum Shale, the bitumen extractability and aliphatic biomarker concentrations are inversely correlated with the uranium content (Dahl et al., 1988a, b; Lewan and Buchardt, 1989) and were attributed to cross-linking and aromatisation by uranium irradiation (Hoering and Navale, 1987). Similar aromatisation mechanisms of the kerogen structures in response to irradiation were proposed by Forbes et al. (1988) and Kribek et al. (1999). However, the pyrrolic nitrogen compounds in the Alum Shale extracts are not obviously aromatised in the uranium rich samples (Fig. 4.7c and d). This could imply that cross-linking, rather than aromatisation, is the primary reaction path responsible for the low bitumen extractability in uranium-rich Alum Shale samples.

Mahlstedt et al. (2016) reported that alkylation of the N_1 class decreases with increasing maturity in solvent extracts of the Lower Jurassic Posidonia Shale during thermal maturation. This maturity control does not serve as an explanation for the strong alkylation reduction of the uranium-rich Alum Shale samples (Fig. 4.7c and d) since both are immature. We deduce that it is irradiation that causes side-chain cracking of alkyl chains

attached to the aromatic core structures, leaving lower levels of alkylation behind as a result. Similar damaging effects have been observed on Alum Shale biomarker distributions (Dahl et al., 1988a; Lewan and Buchardt, 1989), i.e., high molecular triaromatic steroids (C_{26}-C_{28}) are always absent in uranium-rich samples, this being atypical for extracts of immature marine shales in general (McKenzie et al., 1983). The low alkylation degree of the uranium-rich samples does not only depict the kerogen structure but may also explain why such kind of shale tends to generate gaseous products instead of long-chained oil (Fig. 4.5a).

4.6.4 Kerogen structure reconstruction

4.6.4.1 Why necessary?

The Alum Shale may hold a huge potential unconventional gas potential based on its wide occurrence, significant thickness and high TOC contents (EIA, 2015). Furthermore, the Alum Shale was suggested to have a high storage capacity, based on methane adsorption measurements in the laboratory of as much as 3.5 m^3/t (Gasparik et al., 2014). However, shale gas exploration activities in southern Sweden and northern Denmark were not successful, ostensibly due to very low gas saturation (Pool et al., 2012) and possibly gas leakage (Schovsbo et al., 2014). As far as liquid hydrocarbon potential is concerned in both conventional and unconventional "plays", the shale gas potential of the Alum Shale is said to be high, and its oil potential is anticipated to be very limited based on pyrolysis experiments (Kotarba et al., 2014a; Sanei et al., 2014). Importantly, however, petrological (Schleicher et al., 1998), carbon isotope (Więcław et al., 2010b) and biomarker (Yang et al., 2017) investigations indicate that the crude oil in Middle Cambrian sandstone reservoirs in the Baltic Basin was sourced by the Alum Shale. Thus, the composition of organic matter in the uranium-rich Alum Shale has to be evaluated carefully, with due consideration of the source rock in its present state versus that of the same shale prior to extensive radiation damage. Specifically, the kerogen in the investigated Alum Shale samples has undergone irradiation for 478-500 Myr, and must be compositionally and structurally different from that which underwent major petroleum generation in the basin centre beginning in the Early Devonian. The kerogen entering the oil window would have been less gas-prone and aromatic than current predictions suggest.

4.6.4.2 Radiation dosage

The most common isotopes of natural uranium are ^{238}U (99.27%) and ^{235}U (0.72%) (Osmond and Cowart, 1976). Most of the radiation resulting from ^{238}U decay in natural

systems is being emitted in the form of α-radiation followed by less intensive γ-radiation (Jaraula et al., 2015). With a half-life of 4.5 billion years, the ^{238}U decays exponentially (Fig. 4.8) and is independent of either temperature or pressure (Goodwin et al., 2009). However, the time span since the Cambrian is very short compared with the half-life making the curvature of the exponential curve extremely small (Fig. 4.8). Therefore, the decay can be roughly viewed as linearly correlated with time, i.e., the activity of decay in Alum Shale is considered constant.

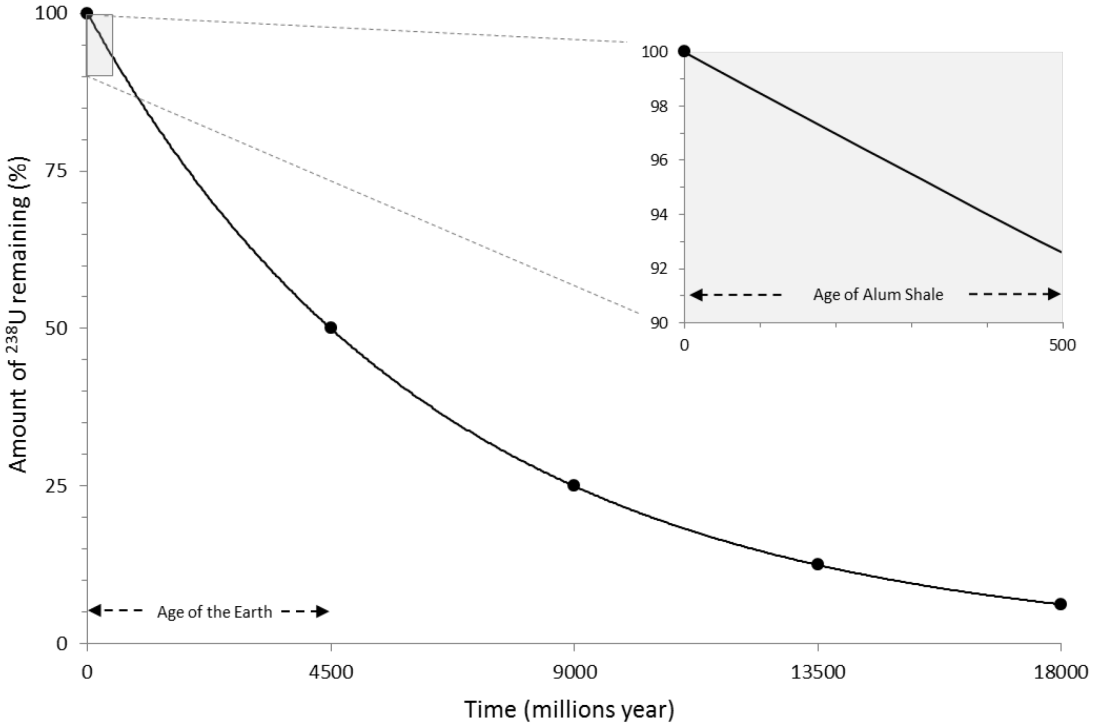

Fig. 4.8. The exponential decay curve of 238U. A zoom in on the geological time scale manifest that the decay can be roughly viewed as linearly correlated with time.

Whyte (1973) proposed that the radiation dosage (D) from a point source to a detector over times (t) can be calculated through:

$$D = E \times C \times \frac{S}{4\pi r^2} \times \mu \times t$$

where E denotes the energy per decay (MeV) which is constant for ^{238}U; C describes the activity (Bq) of decay and can also be viewed as a fixed rate as described above; S represents the area of the detector and $4\pi r^2$ is the area of a sphere with radius r, thus the

$S/4\pi r^2$ shows the probability that the radiation will reach the detector; μ is the mass energy-absorption coefficient.

Although E, C, and μ in the formula can be constant values, it is impossible to accurately measure the distance between a uranium atom and organic matter, especially the interactions must be tortuous. Nevertheless, since the uranium in Alum Shale is primarily accumulated in organic matter and marine phosphates (Lecomte et al., 2017) and the spatial relationship of uranium and organic matter is fixed through geological time, it can be concluded that the radiation dosage from one uranium atom is proportional to time. Furthermore, the gross uranium irradiation on kerogen structures within a shale sample is linearly correlated with both uranium content and time since shale deposition.

4.6.4.3 Kerogen reconstruction

The exponential relationships between uranium and pyrolysate parameters (Fig. 4.4a and b) imply that the response of kerogen structures to irradiation is not linear. Labile kerogen structures can be easily changed in the early stages; thereafter the altered structures would become less sensitive to radiation and will reach equilibrium in the end. The response curves in Fig. 4.4a and b describe a scenario that samples with different uranium contents have experienced a similar time of irradiation. These pathways should also work when the uranium content is fixed and only radiation times vary since the uranium content and radiation time are linearly complementary and the loss of ^{238}U is negligible.

In the case of sample UCm-2 (U=413 ppm), the current pyrolysate is featured by a gas content of 98% and an *o*-xylene content of 86% (Table 4.2). With decreasing radiation dosage, i.e., less radiation time, the products from this shale are less rich in gas and aromatic compounds. One-dimensional burial reconstructions presented by Kosakowski et al. (2010) indicate that the Alum Shale in the Baltic Basin centre started to generate and expel petroleum from the Early Devonian, e.g., Alum Shale in well A23-1/88 (Fig. 4.1) was in in the oil window between 420-340 Myr ago (Fig. 4.9). Accordingly, the compositional information of hydrocarbons generated during that time can be back-calculated assuming the kerogen structures in sample LO-9 (U=33 ppm) represent the primitive ones of sample UCm-2. The gas and *o*-xylene contents are calculated as 88-91% and 63-72 % (Fig. 4.9), respectively, which are still high for typical marine shales (Fig. 4.5). When the petroleum generation started in Devonian times, the Alum Shale had experienced about 1/5 time of the total irradiation compared with nowadays sample, but the kerogen alteration has

fulfilled approximately half due to the exponential response of kerogen structures to irradiation dosage. This method can also be applied to samples with lower uranium contents, and the products dated back to Palaeozoic times must be more oil-rich and aliphatic than those from sample UCm-2.

In summary, the investigated Alum Shale samples had initially a lower gas potential and a higher oil potential than previously assumed based on analysis of present day state samples. The reconstructions of the kerogen structure back to the time when oil window maturity prevailed are crucial in predicting the petroleum characteristics and thereby in reducing the hydrocarbon exploration risks.

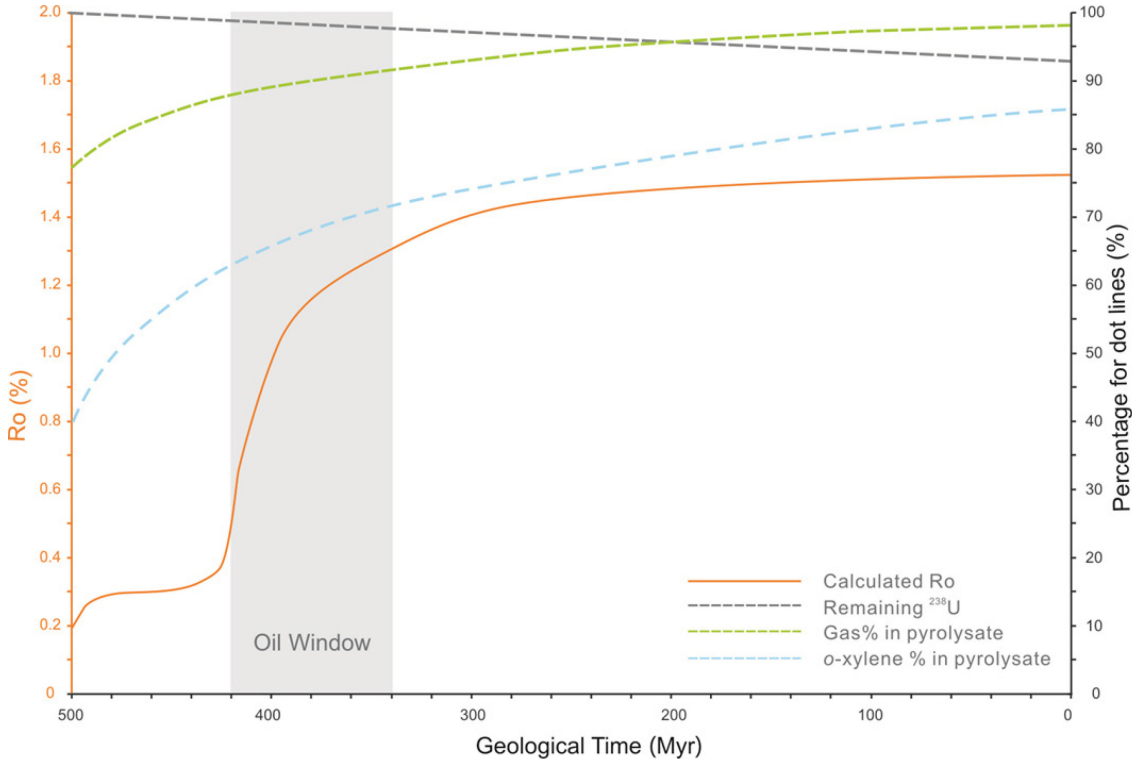

Fig. 4.9. The back-calculation of products that could be generated from sample UCm-2. Calculated vitrinite reflectance curves is based on basin modelling work on well A23-1/88 (location in Fig. 1) from Kosakowski et al. (2010). Oil window was estimated with Ro between 0.5-1.3 %. The gas and o-xylene percentages curves are based on the correlation curves in Fig. 4a and b, respectively. Pyrolysates from sample LO-9 were set as the left end members of these two curves.

4.6.4.4 Further implication

Ziegs et al. (2017) reported that the light hydrocarbon retaining ability of shale is proportional to the aromaticity of its labile kerogen, therefore, the gas adsorption capacity of the Alum Shale over geological time could also have been overestimated. The expected highest risks of gas leaks in Alum Shale are assumed to have occurred during late Caledonian uplift prior to Zechstein deposition and during Neogene uplift (Pool et al., 2012; Schovsbo et al., 2014). During the late Caledonian uplift when the aromaticity of pyrolysates were half irradiated (Fig. 4.9), the maximum gas retention capacity by the Alum Shale kerogen should be much smaller than the values suggested by adsorption experiments (Gasparik et al., 2014). Therefore, the experimental data based on nowadays Alum Shale samples should only be used as the upper bound of gas adsorption capacity in resource estimates.

The uranium irradiation effects in changing triaromatic steroids biomarker distribution (Dahl et al., 1988a; Lewan and Buchardt, 1989) can be applied in oil-source rock correlation. Yang et al. (2017) proposed reservoir oil with low C_{26}–C_{28} triaromatic steroids to be sourced from uranium-rich Alum Shale. As revealed by pyrolysis result, the compositions of Alum Shale products are related to uranium content (Fig 4.4 a and b). In this way, the kerogen structures of UCm-4 (U=231 ppm) are partly altered by uranium irradiation. However, the C_{26}–C_{28} triaromatic steroids are already completely removed (Yang et al., 2017). Similarly, Dahl et al. (1988a) documented that an Alum Shale sample with 163 ppm uranium (sample B26 in Fig. 4.9) was totally depleted in such high-molecular triaromatic steroids. These together imply that the aromatic biomarkers are much more sensitive to uranium irradiation than kerogen structures. Therefore, when the Alum Shale entered oil window during Devonian times, most of the high-molecular triaromatic biomarkers might be removed, in comparison to half of the kerogen structure was changed (Fig. 4.9). In brief, the application of triaromatic steroid biomarker distribution induced by irradiation is an important correlation tool in researching the petroleum system in the Baltic Basin, especially aliphatic biomarkers are typically absent when high-uranium content Alum Shale is involved.

In addition, the organic matter changes in response to irradiation revealed here can also be instructive to extra-terrestrial research in which strong radiation environments are ubiquitous (Allen et al., 1998) and the evaluation of the long-term impact on environment resulted from uranium waste disposal in shale (Gautschi, 2001).

4.7 Conclusion

1. Neither the HI nor the OI of the immature Alum Shale is correlated with the uranium contents. The HI could be decreased by uranium irradiation, but the diverse original HI values prevent the correlation. Oxygen compounds are enriched by the existence of uranium, but they are mainly intact in the kerogen macro-molecules.

2. Most of the Alum Shale samples generate gas-rich and aromatic products through pyrolysis experiments which are atypical for marine shale. Gas and *o*-xylene percentages in pyrolysates and natural products are both proportional to uranium contents pointing to an irradiation control on the kerogen structures.

3. The irradiation does not significantly increase the aromatisation of macro-molecules, instead, the alkylation to aromatic structures was shortened by the irradiation bombardment and this is responsible for the high production of gas.

4. Both uranium content and radiation time are linearly correlated with uranium radiation dosage. However, the response of kerogen structure to radiation is exponential; for the labial structures are altered in the early stage of irradiation.

5. About half of the irradiation induced kerogen changes occurred when the Alum Shale was in oil-window maturity. The back-calculation of kerogen structure can efficiently avoid the over-estimations of gas generation and gas retaining ability in the Alum Shale.

4.8 Acknowledgment

We thank Gripen Oil & Gas AB and the Geological Survey of Sweden for providing the samples. Dr. Nicolaj Mahlstedt is acknowledged for fruitful discussion. Kind thanks are extended to Ferdinand Perssen and Cornelia Karger for their technical support. This study is financially supported by the Chinese Scholarship Council.

5. URANIUM IRRADIATION ON BIOMARKERS

5.1 Abstract

The correlation of Lower Palaeozoic marine source rocks with reservoired oils by biomarkers is complex due to the uniform Early Phanerozoic biomass (bacteria and algae) and the lack of land plant and animal input. Accordingly, the main source rocks for the most prolific oil province in the Baltic Basin are still a matter of debate.

Ten source rocks and 15 oil samples from five north European countries bordering the Baltic Sea Basin were analysed by gas chromatography (GC) with flame ionization detector, GC-MS (mass spectrometry), and GC-MS/MS to detect acyclic isoprenoids, and aliphatic, aromatic, and NSO (nitrogen, sulphur and oxygen) biomarkers. Chemometric tools were applied to screen for meaningful source- and age-related biomarkers and to highlight genetics. Extended tricyclic terpane ratios, C_{24} tetracyclic terpane/C_{26} tricyclic terpane ratios, and relative C_{29} sterane concentrations are considered the most promising biomarkers in differentiating Llandovery shales from Cambrian to Ordovician Alum Shale and for correlation with expelled oil. The uranium irradiation related C_{26}-C_{28} triaromatic steroid concentrations provides possible distinguishing criteria for the source potential of the different Alum Shale units. Enhanced oil maturation by volcanic intrusion is highlighted by sterane biomarkers and polycyclic aromatic hydrocarbons.

The Alum Shale is here considered the main source rock for oil accumulations in Lower Palaeozoic reservoirs of the Baltic basin. Oil seepage occurring in Ordovician limestone was mainly generated by the Middle Cambrian Alum Shale, and Middle Cambrian sandstone reservoirs were mainly sourced by Upper Cambrian and Lower Ordovician Alum Shale with higher maturity. Considerations about the assessment of migration distance are based on carbazole concentrations and C_{29} sterane isomerization. Advanced studies to unravel Lower Palaeozoic oil-source rock correlations are based on

This chapter has been published as: Yang, S., H.-M. Schulz, N. H. Schovsbo, and J. A. Bojesen-Koefoed, 2017, Oil-source rock correlation of the Lower Palaeozoic petroleum system in the Baltic Basin (northern Europe), (in press; preliminary version published online Ahead of Print May 22, 2017): AAPG Bulletin (postprint), doi: 10.1306/02071716194.

meaningful biomarkers; offer approaches to significantly reduce the exploration risk in this area, and could be applied to similar Early Palaeozoic petroleum systems in other basins.

5.2 Introduction

Lower Palaeozoic successions in the Baltic Basin (northern Europe) host both conventional oil and gas accumulations, and unconventional hydrocarbons in the source rocks itself. Petroleum accumulations occur in Middle Cambrian sandstones onshore and offshore Poland (Karnkowski et al., 2010; Więcław et al., 2010b), in the Kaliningrad Oblast (Brangulis et al., 1993), and in Lithuania (Zdanavičiūtė, 2012). Scattered Upper Ordovician limestone oil reservoirs were also discovered in Latvia (Kanev et al., 1994) and around the Swedish Gotland island (Sivhed, 2004). The two most important source rocks of Lower Palaeozoic age in the Baltic Basin and surrounding areas are the Alum Shale (Middle Cambrian to Lower Ordovician) and the Llandovery (Lower Silurian) black shale which are both promising targets for shale gas exploration (Schovsbo et al., 2011; Schulz et al., 2010; Zdanavičiūtė and Lazauskienė, 2009).

Although oil is produced from Middle Cambrian sandstone and Upper Ordovician limestone in the Baltoscandian countries for decades, there is a lack of convincing evidence about the main source rock(s) since these are very alike with respect to most conventional geochemical and organic petrographic tools. All potential source rocks are marine shales containing type II kerogen (algae and bacteria originated) (Kanev et al., 1994; Nielsen and Schovsbo, 2006; Więcław et al., 2010a) and the analyses of established proxies like the pristane/phytane (Pr/Ph) ratio or routine biomarkers delivered less sufficient evidence in clearly unravelling the differences between the different marine shaly source rocks. The main complicating issue is the uniformity of shale due to the lack of higher terrigenous land plant input during the Lower Palaeozoic time and a relatively monotonous depositional environment. Although using data about light hydrocarbon distributions, selected biomarkers, and carbon isotope data then Kanev et al. (1994) and Więcław et al. (2010b) were unable to separate the shales and concluded that all shales of Middle Cambrian to Lower Silurian age are potential source rock candidates for Lower Palaeozoic petroleums reservoired in the Baltica basin. In contrast, Zdanavikiute and Bojesen-Koefoed (1997) and Pedersen et al. (2007) suggested that Llandovery shales are the main contributors for oil in Middle Cambrian sandstones according to Pr/Ph ratios and sterane data, while Schleicher et al. (1998) and Kotarba and Lewan (2013) argued that the petroleum was mainly generated by the Alum Shale based on biomarker and carbon isotope data. Dahl et al.

(1989) assumed that the oil in limestone reservoirs on Gotland was sourced from the Alum Shale which presumably was heated locally by volcanic activity, and referred to characteristic sterane, tricyclic terpane and homohopane distributions. However, the lack of Alum Shale occurrence in the near subsurface is a reasonable counterargument (Sivhed, 2004). In summary, great uncertainties exist despite previous investigations.

In this contribution we present analytical data of samples taken on a broader regional scale than previous studies in the Baltic Basin. The samples are from five Baltoscandian countries and comprise Cambrian to Silurian source rocks and oils from Middle Cambrian and Ordovician reservoirs. Conceptually, we correlated results about maturity, source, and age-specific information. Chemometric tools were applied to classify the oil samples into clusters. Specific biomarker combinations considered effectively in differentiating source rock extracts and oils from different ages in this area were introduced first. In addition, oils matured by regional deep burial versus locally from volcanic heating are differentiated. This contribution offers a practical solution for further exploration activities in the Baltic Basin by providing the best tools to differentiate source rocks and oils of Lower Palaeozoic age in general that are applicable not only in Baltic Basin but also elsewhere.

5.3 Regional Petroleum Geology

5.3.1 Regional Geodynamics and Basin Evolution

The Baltic Basin covers part of the Baltic Sea, Kaliningrad Oblast, Northern Poland and the western parts of the Baltic States (Fig. 5.1). It overlies the western margin of the East European Craton with its Precambrian crystalline basement and comprises of sediments deposited from the Early Cambrian to present day. The basin fill is thin in the north-eastern part (less than 100 m [300 ft] thickness in Estonia) and increasingly thickens south-westward towards the Teisseyre-Tornquist Zone (over 4000 m [13000 ft] thickness in northern Poland) which forms the southern boundary of the basin (Ulmishek, 1990).

Since its formation, the Baltic Basin underwent four main geodynamic evolution stages each with different burial dynamics until the Late Palaeozoic. These different episodes were the main controlling factors for the tectonic and sedimentary features of the basin (Šliaupa and Hoth, 2011).

(1). During the passive continental margin stage (Vendian-Late Ordovician) the basin started to develop as a passive margin basin from latest Vendian to Early Cambrian times

in response to the break-up of the Rodinia supercontinent (Kosakowski et al., 2010; Poprawa et al., 1999). This initial basin stage gave rise to coarse-grained siliciclastics of Ediacaran age. With progressing continental separation, marine transgressions flooded the basin, and marine shale, sandstone and carbonate sedimentation occurred from Cambrian to Ordovician periods (Nielsen and Schovsbo, 2006).

(2). The foreland basin stage (Late Ordovician-Early Devonian) developed due to the docking of the Avalonian plate to the western margin of the Baltica plate, mainly during the Late Ordovician-Silurian times (Poprawa et al., 1999; Vejbæk et al., 1994). The subsidence increased during the Silurian when up to 4500 m [14700 ft] of siliciclastic and calcareous sediments were deposited.

(3). A more continuous but slower subsidence took place during the Devonian and characterises the intra-craton basin stage (Šliaupa and Hoth, 2011). Lagoonal and deltaic deposits covered the area during that time (Ūsaityt, 2000).

(4). A thermal doming and sag basin stage developed during the Carboniferous-Permian transition. The basin subsidence ceased in the Mississippian time, thereafter, significant uplift and erosion affected the margin of the basin (Sopher et al., 2016). In response to the thinning of the lithosphere, diabase sills and dykes intruded the Baltic Basin (Motuza et al., 1994) and Scandia (Obst, 2000; Priem et al., 1968).

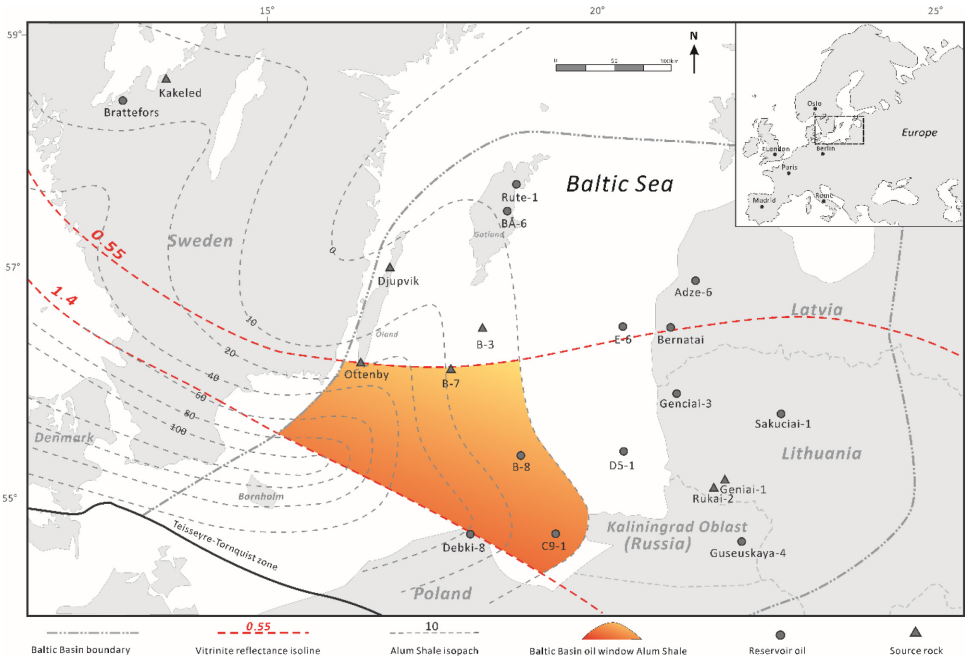

Fig. 5.1. Simplified map of the Baltic Basin and its possible oil kitchen. The thermal maturity of the Alum Shale measured on vitrinite-like macerals (Buchardt et al., 1997).

5.3.2 Source Rocks

Several marine shales with a considerable petroleum generation potential are of Early Palaeozoic age (Fig. 5.2), while carbonate deposits contain total organic carbon (TOC) contents less than 0.2 wt.% which denote them as non-source rocks (Šliaupa and Hoth, 2011). The Middle Cambrian-Lower Ordovician Alum Shale and the Llandovery shale are considered as the two most important and potential source rocks because of their wide occurrence, considerable thicknesses and high TOC contents (Kanev et al., 1994).

Named after the hydrated potassium and aluminium-bearing sulphate [$KAl(SO_4)_2 \cdot 12H_2O$], the Alum Shale consists of fine-grained, blackish mudstone and shale of Middle Cambrian, Upper Cambrian (Furongian) and Lower Ordovician (Tremadocian) age (Nielsen and Schovsbo, 2006) (Fig. 5.2). The thickness of the Alum Shale is regionally variable. To the west of the Baltic Basin, an approx. 180 m (590 ft) thick Alum Shale was found in the Danish offshore (Nielsen and Schovsbo, 2006). Within the basin, the Alum Shale reaches its maximum thickness of ca. 100 m [300 ft] in the Teisseyre-Tornquist Zone, and wedges out eastward and northward due to erosion (Buchardt et al., 1997). The Alum Shale is not present to the east and north of Kaliningrad-South Gotland line (Fig. 5.1) except for a maximum seven meter (23 ft) thick Tremadocian Alum Shale in Northern Estonia (Loog et al., 2001). Covering a time span of 23 million years (500-477 Ma), the three Alum Shale sub-stages (Middle Cambrian, Upper Cambrian and Lower Ordovician) differ in their organic and inorganic geochemical composition (Thickpenny, 1984). High TOC contents, typically up to 10 wt.% and high sulphur contents dominate in the Lower Ordovician and Middle Cambrian Alum Shale whereas the Upper Cambrian Alum Shale is featured by TOC contents of up to 22 wt.% and high silica contents (Kosakowski et al., 2016; Schovsbo et al., 2015).

Formed in a deep water environment, the Llandovery Shale is a dark grey to black shale or marlstone. This shale is rich in TOC (up to 16 %wt.) and its hydrocarbon generation potential is known in the southern and eastern part of the basin (Zdanavikiute and Bojesen-Koefoed, 1997). A typical thickness of the layer in the eastern part of the basin is 5-25 m (16-82 ft) (Kanev et al., 1994), but increases to 100 m (300 ft) in offshore Poland (Modliński and Podhalańska, 2010).

Besides these two layers, the locally distributed Caradocian age Upper Ordovician shales can also be considered as possible source rocks (Kanev et al., 1994). In Sweden and

Lithuania, the Upper Ordovcian shales are named as Fjäcka Shale and the Mossen Shale with TOC contents of up to 6 wt.%. However, these two shales have maximum thickness of 10 m (32 ft) (Högström and Ebbestad, 2004; Zdanavičiūtė and Lazauskienė, 2004), typically less than five m (16 ft) thick (Šliaupa and Hoth, 2011), and occur very locally. The equivalent shale in Poland is called Sasino Shale (Modliński and Szymański, 1997; Stouge and Nielsen, 2003). It has typical TOC between 1-2.5 wt. % with variable hydrogen index values, ranging from 11 to 359 mg hydrocarbon/gTOC, and is considered to be deposited in a sub-oxic environment (Więcław et al., 2010a). The limited distribution and hydrocarbon generation ability of the Upper Ordovician shales make them possibly regional source rocks rather than main contributors of the oil accumulations found all around the basin.

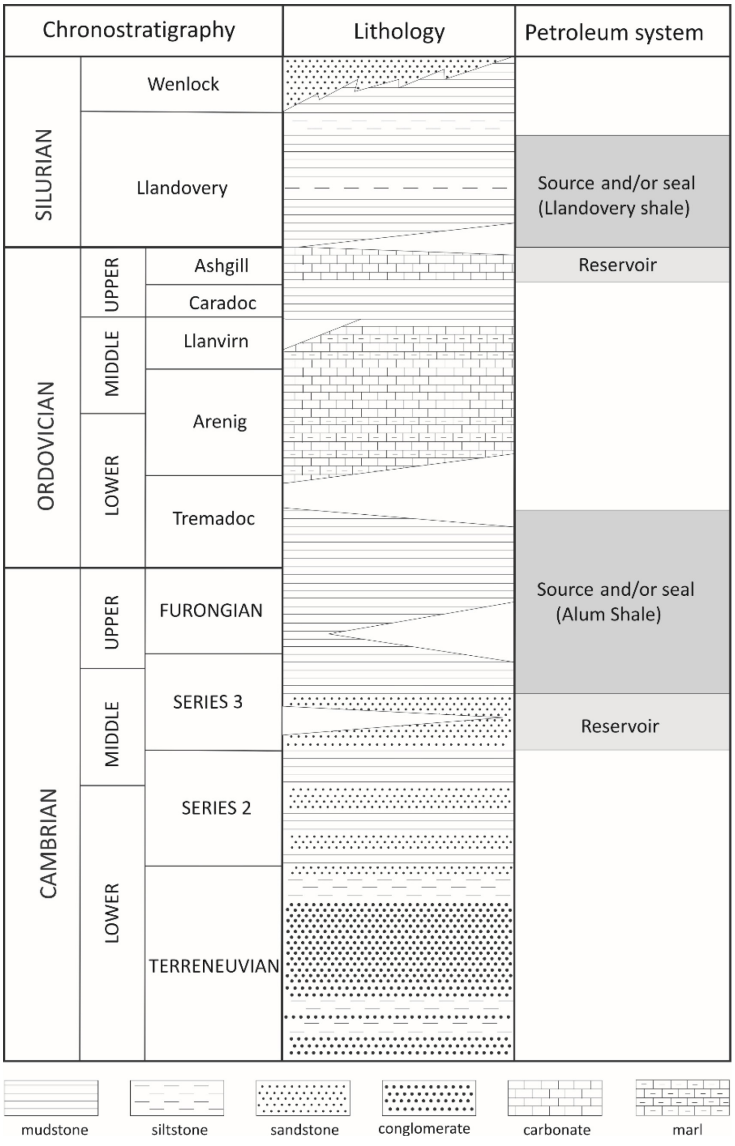

Fig. 5.2. Simplified stratigraphy of the Lower Palaeozoic petroleum system in the Polish part of the Baltic Basin.

5.3.3 Reservoirs

The Middle Cambrian sandstones and the Upper Ordovician limestone reefs are the reservoir rocks for most of the petroleums found in the Lower Palaeozoic strata in the Baltic Basin (Fig. 5.2). Petroleums trapped in sandstone occur in Poland, Russia (Kaliningrad) and Lithuania while oil reservoired in limestone reefs occur on the Swedish island of Gotland and in Latvia (offshore and onshore) (Fig. 5.1).

The trap style in the sandstone reservoirs are mosly asymmetric brachy-anticlinal domes as a result of the Caledonian orogeny. The effective porosity and permeability in the southwestern part of the Baltic Basin are generally low with values around 5-14% and 5-24 mD caused by intensive quartz cementation (Schleicher et al., 1998; Semyrka et al., 2010), whereas higher porosities characterise the eastern basin part. For instance, reservoir porosity can be as high as 20% in western Lithuania and 34% in Kaliningrad (Zdanavičiūtė, 2012).

In the northern part of the Baltic Basin, oil is produced from about 100 limestone reef structures situated in the Ordovician limestone sequence (Sivhed, 2004). In general, the reefs are located at shallow depth of only a few hundreds of metres. The onshore reefs are generally fairly small with a maximum diameter of 800 meters (2600 ft) and an height of up to 50 meters (160 ft), but can be up to two km in diameter offshore (Tuuling and Flodén, 2009). The oil is produced from fractures, cavities, and vuggy porosity of the limestone (Chatzis, 2014).

5.3.4 Maturation and Accumulation

Subsidence during the Caledonian orogeny is the main maturation control, especially in the southwestern part of the Baltic basin. Volcanic intrusions during Permo-Caboniferous times led to a localized high maturation of the Palaeozoic shales offshore Kaliningrad (Motuza et al., 1994; Motuzaa et al., 2015), island Bornholm in the Baltic Basin (Obst, 2000), and in central Sweden (Dahl et al., 1989), but only slightly contributed to the overall thermal maturation (Karnkowski et al., 2010). The 1-D burial reconstruction carried out by Kosakowski et al. (2010) and the 2-D basin modelling by Wróbel and Kosakowski (2010) indicate that the onset of petroleum generation from the lower Palaeozoic source rocks occurred from the Early Devonian through the Mississippian period. The peak of hydrocarbon generation took place from the Late Devonian to the Mississippian time and

main expulsion almost concurrently happened. During Permian and Mesozoic times tectonic activities led to remobilization with following adjustment of accumulations.

During the passive continental margin stage, normal fractures were widely developed in the basin and served as petroleum migration paths. For example, oil produced in the southwestern Baltic basin migrated eastward and northward up to shallower Ordovician limestone reservoirs through fractures, sandstones, and unconformity connections. Migration from younger source rock to older reservoirs in the Baltic Basin and into surrounding areas can also be observed. Examples are pyrobitumens found in Lower Cambrian sandstones on Bornholm island (Denmark) (Møller and Friis, 1999) as well as asphaltite in central Swedish bedrock fractures (Sandström et al., 2006) where there is no effective source rock beneath. This is caused either by downward migration due to the overpressure and abundance of fractures, or more likely due to the upward charging from younger source rocks into the tectonically uplifted older strata as suggested by Wróbel and Kosakowski (2010).

5.4 Samples and Methods

5.4.1 Samples

In the frame of this study, 15 Llandovery shales and Alum Shale samples were investigated (Table 5.1). Of these five Upper Cambrian Alum Shale samples from Sweden were also available, but did not deliver sufficient extraction amounts for geochemical investigations and were excluded.

15 oil samples from five countries have been analysed (Table 5.1). Two oil samples from the Brattefors quarry were taken directly from a fresh oil seepage after the mining company had cut a Middle Ordovician limestone which are similar to Fig. 20b as described by Buchardt et al. (1997). The other samples are from boreholes in the basin area.

The oil samples cover most of the oil producing areas in the Baltic Basin (Fig. 5.1). Previous geochemical results of analysed oil samples from the Baltic States were reported by Bojesen-Koefoed et al. (2001). This basic data set provides a meaningful geographic and stratigraphic distribution, and is used in this study to build on with further conceptual approaches and techniques to unravel the oil-source correlation of the Early Palaeozoic petroleum system in the Baltic Basin.

5.4.2 Methods

Soxhlet extraction was carried out on powdered shale and solid bitumen samples for 24 hrs at 50 °C. A dichloromethane and methanol mixture (99:1) was used as solvent. In a next step, asphaltenes were precipitated from the extracted bitumen as well as from the crude oil samples before medium pressure liquid chromatography (MPLC) fractionation. Aliphatic and aromatic hydrocarbons, and NSO (nitrogen, sulphur and oxygen) compounds were separated from the maltene fraction after MPLC as described by Radke et al. (1980).

Gas chromatography with flame ionization detector (GC-FID) was carried out on the aliphatic hydrocarbon fractions of all samples. The instrument was equipped with a HP Ultra 1 capillary column. The oven temperature was programmed from 40 °C to 300 °C with a 5 °C/min heating rate.

Biomarkers from aliphatic, aromatic, and NSO compounds were detected by gas chromatography-mass spectrometry (GC-MS). Gas chromatography-mass spectrometry-mass spectrometry (GC-MS/MS) was applied to detect aliphatic biomarkers for better peak separation. GC-MS test runs were based on a Trace GC Ultra system coupled to a DSQ mass spectrometer. The GC was equipped with a programmed temperature vaporizer (PTV) injection system and a fused silica capillary column, and was heated from 50 °C to 310 °C at a rate of 3 °C/min. GC-MS/MS measurements were performed on a Finnigan MAT 95XL mass spectrometer coupled to a HP 6890A gas chromatograph with a PTV injection system. The GC oven temperature was programmed from 50 °C to 310 °C with a heating rate of 3 °C/min, followed by an isothermal phase of 30 min.

5.5 Results

5.5.1 GC-FID

All samples show very high signal/noise ratios for normal alkanes and acyclic isoprenoids, and pristane/nC$_{17}$ and phytane/nC$_{18}$ ratios are generally low (Table 5.1 and Fig. 5.3). The biodegradation scale by Peters and Moldowan (1991) suggests that all samples are non- to slightly biodegraded (Table 5.1). Thus, a very weak impact from biodegradation on the following oil-source correlation is expected.

No significant odd or even carbon number predominance of *n*-alkanes pattern was observed in the samples. Most of them have Pr/Ph ratios between 1.0-3.0, except the three Llandovery Shale extracts from the B3 well with Pr/Ph ratios higher than 3.0 (Table 5.1).

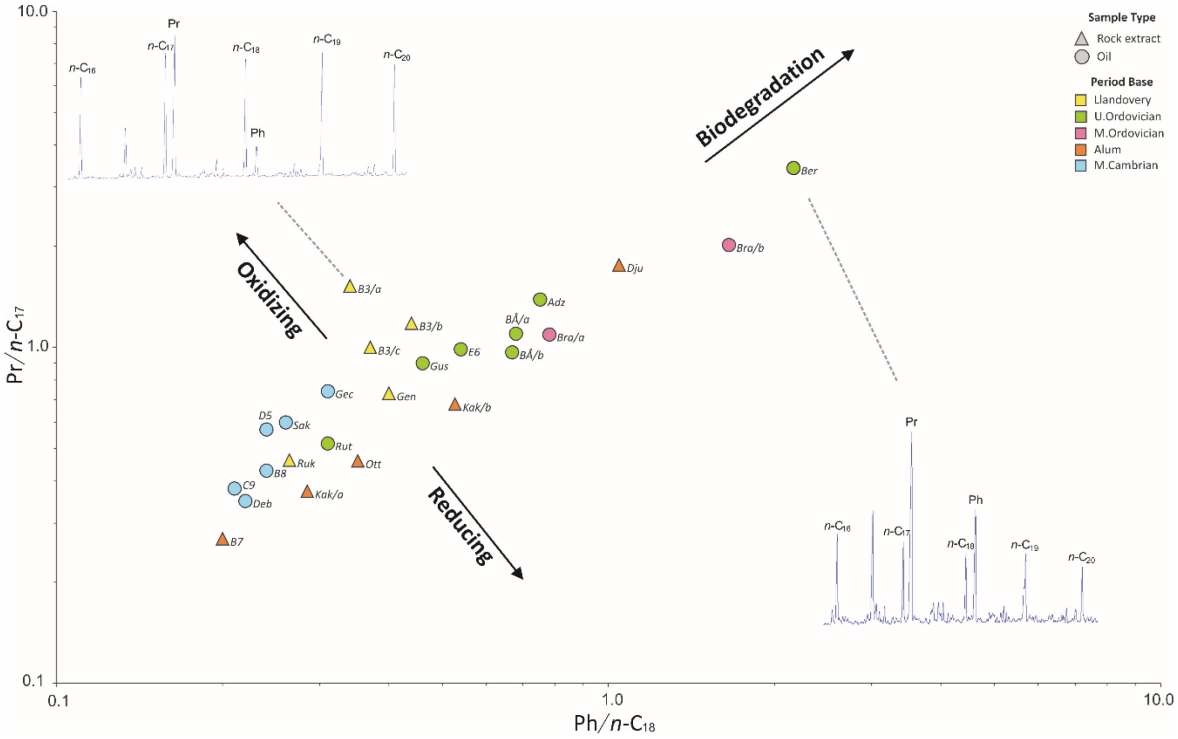

Fig. 5.3. Diagram of pristane/n-C_{17} vs.phytane/n-C_{18} with two representative GC-FID traces. Depositional environment and biodegradation can be evaluated accordingly (Peters et al., 1999).

5.5.2 Aliphatic Biomarkers

Based on the *m/z* 191 and *m/z* 217 traces of aliphatic biomarkers, at least two endmember types can be identified. For example, the Llandovery shale extracts are characterized by higher concentrations of C_{24} tetracyclic terpane and C_{28}-C_{29} tricyclic terpane peaks are significantly smaller than T_s and T_m (Fig. 5.4A). The sterane and diasterane biomarkers of the Llandovery shale samples are dominated by C_{27} and C_{29} homologues (Fig. 5.4B). In contrast, the C_{24} tetracyclic terpane contents in the Alum Shale extracts and reservoir oil are very low, and T_s and T_m peaks are less predominant. Furthermore, these samples show obviously higher C_{28}/C_{29} steranes ratio in comparison with the Llandovery shale extracts (Fig. 5.4B).

All samples have low concentrations in gammacerane and C_{35} homohopane. Accordingly, confident interpretations of these biomarkers can only be achieved in a few samples (Table 5.1). Other redox-, precursor-, and age-related biomarkers, like 28,30-Bisnorhopane, dinosteranes, and 24-norcholestanes were not identified applying through GC-MS/MS analysis from any of the samples. 24-*iso*-/*n*-propylcholestanes were only recognized in sample "Deb".

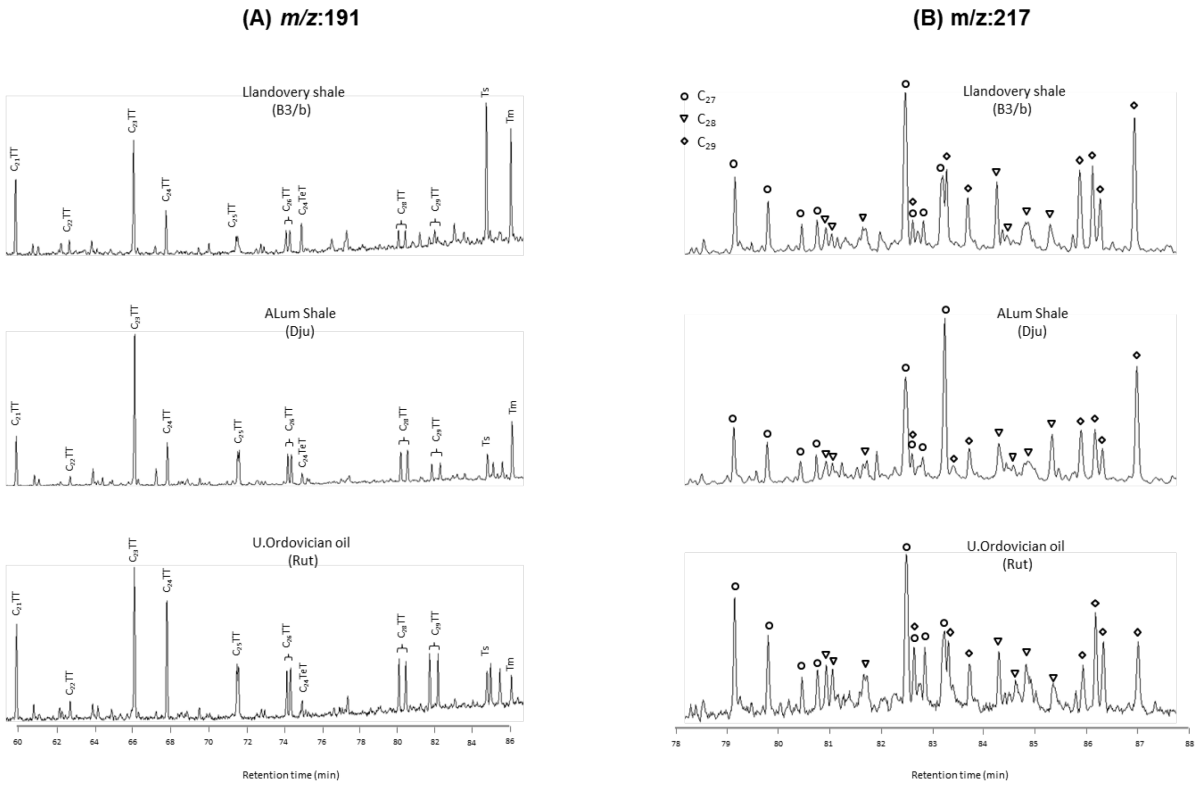

Fig. 5.4. Comparison of terpane and sterane traces of three representative samples. Traces shown here were provided by GC-MS for direct visual comparison purpose. T_s/T_m ratios and sterane biomarkers presented in table 5.1 and figures were interpreted from GC-MS/MS to ensure better data quality.

5.5.3 Aromatic and NSO Biomarkers

Naphthalenes, phenanthrenes, and dibenzothiophenes can be clearly identified in all samples, while the aromatic steroid concentrations differ significantly (Fig. 5.5). The Lower Ordovician and Upper Cambrian Alum Shale samples show no or very little C_{26}-C_{28} triaromatic steroid distribution patterns and all oils from Middle Cambrian reservoirs are also depleted in these compounds (Table 5.1 and Fig. 5.5). When comparing the polycyclic aromatic hydrocarbons (PAHs), most samples are featured by very low pyrene/phenanthrene ratios, only oil samples from the Brattefors quarry are characterized by pyrene concentrations higher than phenanthrene.

In the investigated NSO fractions, the carbazole concentrations vary among the samples. In general, shale extracts are always rich whereas only four oil samples from Middle Cambrian sandstone and oil seepage in the Brattefors quarry show identifiable carbazoles signals (Table 5.1).

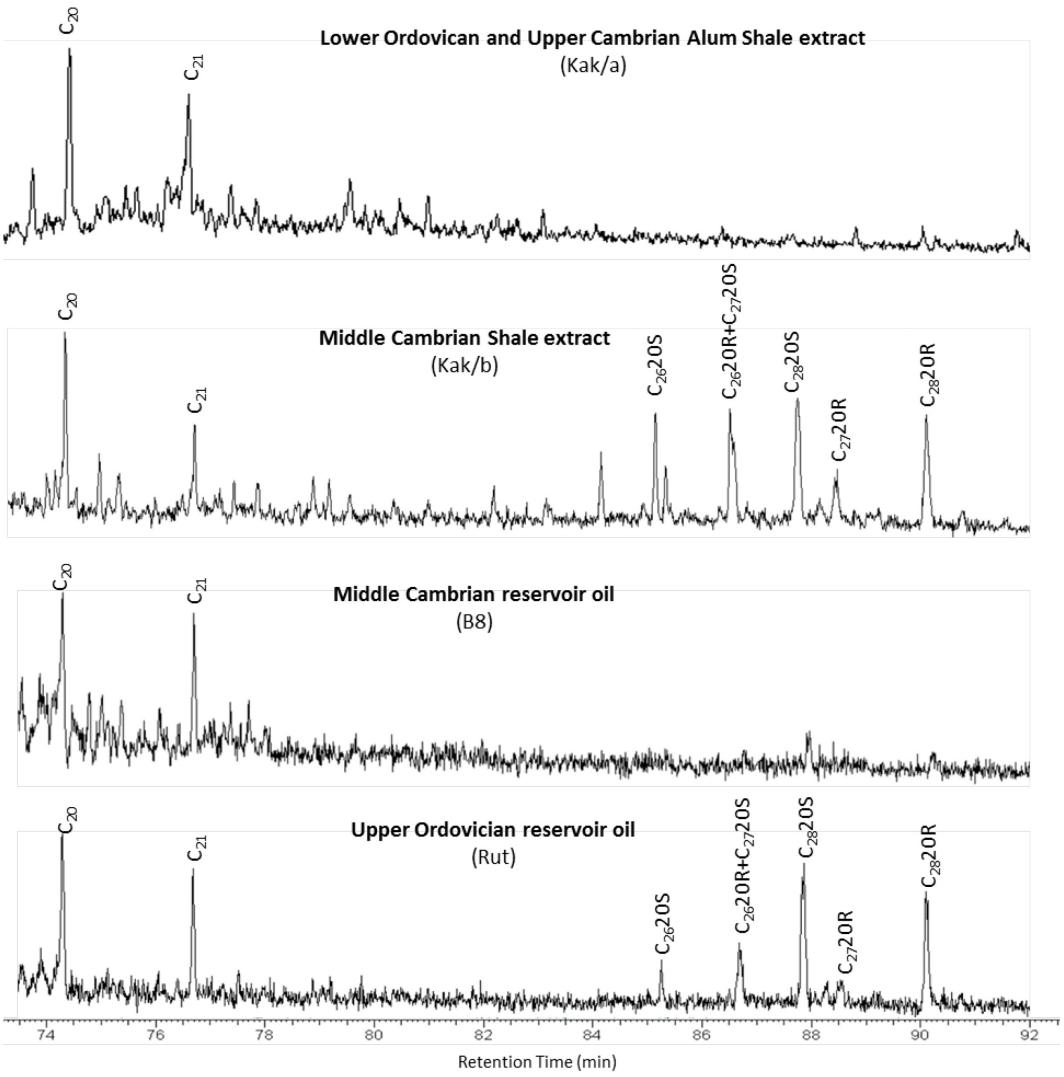

Fig. 5.5. The distributions of triaromatic steroids (m/z=231) in three Alum Shale extracts and two typical oil samples. C_{20}-C_{21} triaromatic steroids can be detected from all samples, but some samples show no/very low C_{26}-C_{28} responses.

5.5.4 Oil Family Assignments

Chemometric tools which use multivariate statistics to remove noise and to show affinities among samples are very helpful in oil-source correlations (Peters et al., 2013; Peters et al., 2016). Depositional environment-, precursor-, and age-related biomarkers were chosen to as meaningful input parameters for principal component analysis (PCA) and hierarchical cluster analysis (HCA), instead maturity dependent parameters were not integrated (Table 5.1).

The gained PCA results point to differences between Llandovery shale extracts and the rest of the samples. The key signals for correlation are extended tricyclic terpane ratios (ETR),

C_{24}TeT/C_{26}TT, and C_{29} sterane distributions, whereas other ratios are relatively less significant (Fig. 5.6A). Two main clusters can be grouped by HCA data (Fig. 5.6B), and the Llandovery shale extracts are clearly separated from the Alum Shale extracts and the oils. However, additional sub-clusters can be identified within cluster I: the Alum Shale extracts and two oil samples from the Brattefors quarry are closely related, and the oil sample Gec appears to be a mixture of the two end members (Fig. 5.6).

It has to be pointed out that almost none of the source-related and age-related biomarkers used here are totally maturity independent and vertical and horizontal heterogeneities of the source rock can also significantly influence the result of the oil-source correlation. Thus, detailed discussions on the results are necessary.

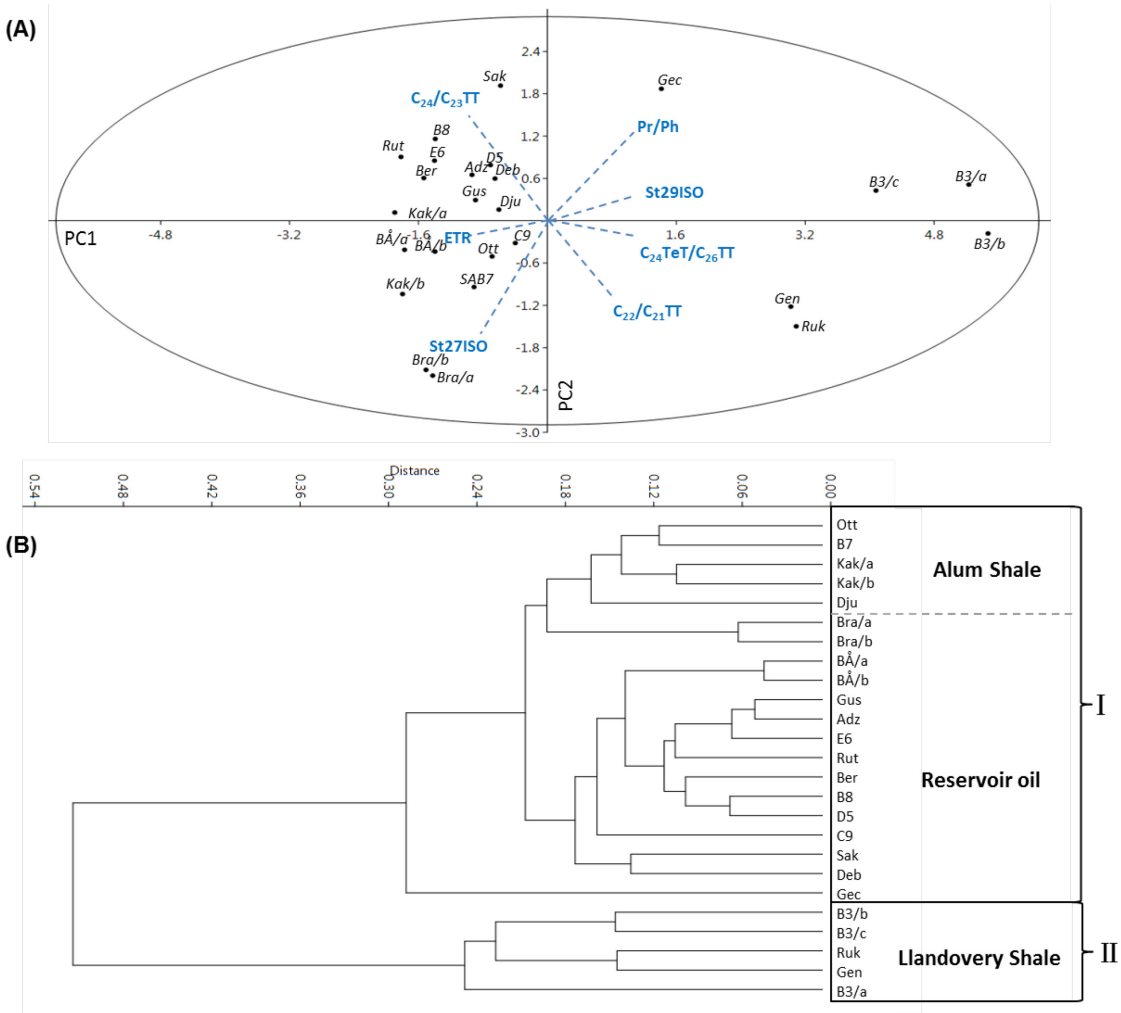

Fig. 5.6. (A) Principal component analysis on oil samples based on representative biomarkers and (B) hierarchical cluster result in grouping the oils into two groups.

5.6 Discussion

5.6.1 Maturity

The maturity assessment is not only important in evaluating the influence of local hydrothermal overprints, but also helpful in unravelling the impact of maturity on oil-source correlations. A good correlation can be found between the maturity biomarker ratios diasterane/sterane and Ts/Tm (Fig. 5.7A). It has to be pointed out that both of these two maturity parameters can be influenced by mineralogy (McKirdy et al., 1981; Rubinstein et al., 1975), for example, carbonate-rich source rocks are characterized by small values of these ratios. However, the mineralogical impact on the maturity seems unlikely, since all samples are marine siliciclastic sediments. The C_{29} sterane epimer ratios are also considered as important maturity parameters and most of the samples show maturities within their thermodynamic equilibrium thresholds (Fig. 5.7B).

In general, the four maturity parameters show that two Llandovery shale samples (Gen and Ruk) and one Alum Shale (B7) sample are in the "oil window" whereas all other shale samples are immature or in the early stage of oil generation (Fig. 5.7).

The maturity parameters show that the oils in the Ordovician reefs were mainly charged from source rocks during the early "oil window" except for the two samples from Brattefors. Oils in Middle Cambrian reservoirs are generally more mature. Of these the C9 and Gec oils are suggested to represent in peak "oil window" (Fig. 5.7B).

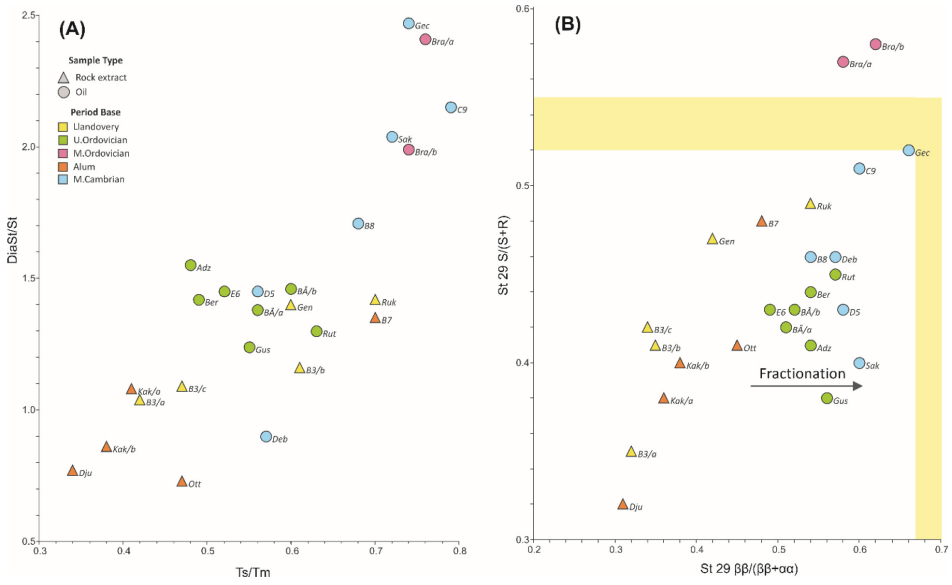

Fig. 5.7. Cross plots of terpane and sterane biomarkers show the maturities of source rock and oil samples. Yellow stripes in panel B manifest the thermodynamic equilibrium intervals of the sterane isomer.

5.6.2 Volcanic Intrusion Induced Maturation

The Bra/a and Bra/b oil samples taken from Middle Ordovician limestones in the Brattefors quarry present 20S/(20S+20R) sterane ratios which are significantly higher than the thermodynamic equilibrium threshold (Fig. 5.7B). This implies that these samples are likely to have experienced abnormally fast heating during maturation (Strachan et al., 1989). Furthermore, only these two samples have high pyrene/phenanthrene ratios. The pyrene/phenanthrene ratio in petroleum is generally low, and elevated values for this ratio are suggested to be caused by pyrolytic maturation (Budzinski et al., 1997). Because rapid heating and high temperatures can cause the breaking of bonds in organic matter leading to small molecular fragments, mostly free radicals recombine to form PAHs by pyrosynthesis as the temperature drops (Huang et al., 2015b). For instance, PAHs are enriched in artificial pyrolysates (Brocks et al., 2003), hydrothermally generated oil (Simoneit and Lonsdale, 1982), sediments influenced by forest fires (Venkatesan and Dahl, 1989), or oils generated by near volcanic intrusions (Huang et al., 2015b).

The regional maturity pattern reveals that potential source rocks are immature in south central Sweden (Fig. 5.1), and that there is a lack of pathways for the oil to migrate from the basin centre. Due to the widespread occurrence of Permo-Carboniferous diabases in this area, oil samples from the Middle Ordovician Brattefors limestone are genetically related to this volcanic intrusion period (Dahl et al., 1989). Sterane maturity and PAHs characteristics similar to the Brattefors oil is missing in the other investigated samples, so that oil formation in the Baltic State area is the result of geological burial.

5.6.3 Correlation

5.6.3.1 Acyclic Isoprenoids

Traditionally Pr/Ph was applied to differ oxic from anoxic depositional environments (Didyk, 1978). However, palaeosalinity (ten Haven et al., 1987), maturity (Dzou et al., 1995), and organic matter type input (Goossens et al., 1984) were also considered as influencing factors. Thus, Pr/Ph values between 0.8-3.0 offer a broad interpretation window, and are not exclusively indicative for a depositional environment assignment (Peters et al., 2005).

In our sample set, three Llandovery shale samples from well B3 have Pr/Ph ratios higher than 3.0 (Table 5.1 and Fig. 5.3), and, despite other considerations, could refer to terrestrial organic matter input under oxic conditions (Peters et al., 2005). However, advanced

terrestrial plant community is widely believed not to flourish before the Devonian time (Kenrick and Crane, 1997), but recent studies reveal the occurrence of first eutracheophytes in the Late Ordovician (Gerrienne et al., 2016), and that sediments across the Late Ordovician-Early Silurian boundary in Sweden host spores (Badawy et al., 2014). Accordingly, some terrestrial organic matter can have been admixed into marine depositional environments during the foreland basin stage. In summary, the high Pr/Ph ratios in some Llandovery shale samples are reasonable indications that the depositional environment during the early Silurian time was stronger oxidized than during deposition of the Alum Shale.

5.6.3.2 Terpanes

The routine BNH/H ratio, Gammacerane index and C35 homohopane index are not indicative in differentiating the Lower Palaeozoic samples in this study, because most of these biomarkers were not detected by GC-MS and GC-MS/MS analyses. As suggested by PCA, ETR and the C_{24} tetracyclic/C_{26} tricyclic terpane (C_{24}TeT/C_{26}TT) ratio were compared and a nice correlation can be found (Fig. 5.8). The Llandovery shale extracts show very low ETR values and enrichments in C_{24} tetracyclic terpanes, whereas the Alum Shale extracts and oil samples from Upper Ordovician limestone reservoirs plot in the lower right part of the template (Fig. 5.8).

ETR (ETR=[C_{28}+ C_{29}]/ [C_{28}+ C_{29}+Ts]) was taken as an age-related biomarker ratio in differentiating Jurassic reservoired oil from Triassic (Hanson et al., 2007; Holba et al., 2001) and is relatively resistant to thermal maturation and biodegradation (Holba et al., 2002). The ETR values correlate well with the Gammacerane Index and Pr/Ph ratio (De Grande et al., 1993; Hao et al., 2011), and are thus considered indicators for salinity and alkalinity.

The C_{24} tetracyclic terpane is considered as a biomarker in evaluating depositional environments (Tao et al., 2015; Volk et al., 2005) and can be enriched in carbonate rocks (Palacas et al., 1984), evaporites (Clark and Philp, 1989), or rocks with terrestrial organic matter input (Philp and Gilbert, 1986). Furthermore, the tetracyclic terpanes are regarded to be more resistant against biodegradation than tricyclic terpanes due to the more stable stereoisomerism (Aquino Neto et al., 1981; Williams et al., 1986). Thus, the C_{24}TeT/C_{26}TT ratio would increase with intensified biodegradation level. However, the application of the PM scale (Peters and Moldowan, 1991) shows that the bitumen in the Llandovery shale has undergone very slight biodegradation (Table 5.1), i.e. only a few *n*-alkanes have been

depleted (see GC-FID traces in Fig. 5.3). The more biodegraded oil samples, e.g. "Adz" and "Ber" exhibit only very low C_{24}TeT/C_{26}TT ratios (Table 5.1 and Fig. 5.8). In summary, the biodegradation of these samples is not as pronounced as to control the tetracyclic/tricyclic terpane distribution.

The scattered distribution of oil samples and the Alum Shale extracts in Fig. 5.8 can be explained by the combination of facies variations and maturity changes. Deposited in a vast area the Alum Shale is characterized by vertical and horizontal variations during deposition across the area. With increasing maturity, the ETR is anticipated to be decreased, because of the relative Ts enrichment in the denominator of the ratio. Also, Farrimond et al. (1999) and Huang et al. (2015a) pointed out that the C_{24}TeT/C_{26}TT ratio would slightly increase especially after peak oil generation although this is not the case in our sample set. These maturation controls can partly explain why the more mature oil samples in the Middle Cambrian sandstone reservoir have lower ETR and higher C_{24}TeT/C_{26}TT ratios than the oil from the Upper Ordovician limestone. Summarising the above, the oil samples can be regarded as genetically closer to the Alum Shale than to the Llandovery shale.

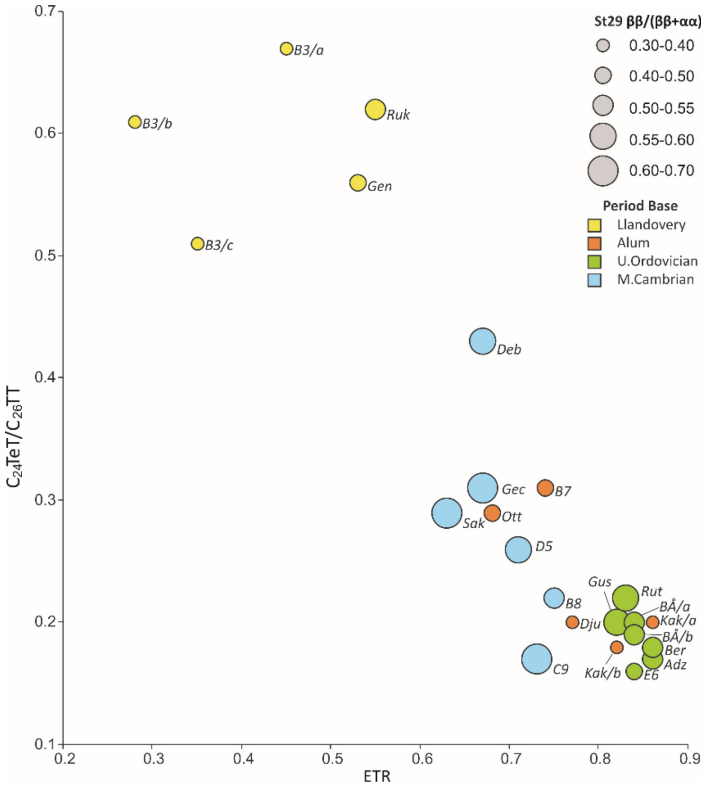

Fig 5.8. The terpane biomarker cross-plot can efficiently separate Llandovery source rocks from the rest. C_{24} TeT and C_{26} TT are abbreviations for C_{24} tetracyclic terpane and C_{26} tricyclic terpane respectively. The extended tricyclic terpane ratio (ETR) (Holba et al., 2001) is calculated from $(C_{28}+C_{29})/(C_{28}+C_{29}+T_s)$ in m/z 191. The size of the dot demonstrates the maturity of each sample to evaluate the maturity dependency of the biomarkers.

Although both were deposited below wave base under dysoxic to anoxic conditions, the Alum Shale and Llandovery shales differ in depositional features. The Alum Shale was deposited in a large and shallow epicontinental sea (Schovsbo, 2002; Thickpenny, 1984), while the Llandovery shale was formed in a foreland basin with open circulation to the ocean. The salinity differences indicated from biomarkers might reflect differences in water column stratification between the two settings, and the Alum Shale was deposited in water column with stratification. In general, organic lean shale, sandstone and carbonate intercalations can be found more frequently in Lower Silurian shales than in the Alum Shale (Lazauskiene et al., 2003; Modliński and Podhalańska, 2010) which implies a less stratified, more unstable, and shallower-water prevailed environment during deposition.

5.6.3.3 Steranes

The ternary diagram about the C_{27}, C_{28}, and C_{29} distribution is meant to enable the distinction of source rocks or oils from different ecosystems or depositional settings (Huang and Meinschein, 1979).

The Llandovery shale samples can be clearly separated from the rest of the samples due to their elevated C_{29} proportions. The Alum Shale extracts and the oil samples overlap (Fig. 5.9) and thus confirm marine depositional conditions (Moldowan et al., 1985). The oil sample Gec could be partly co-sourced by the Llandovery shale which is indicated by very similar sterane distributions (Fig. 5.9). With an elevated C_{29} concentration, the C9 oil could also be influenced by Llandovery shale (Fig. 5.9). Samples with C_{29} sterane concentrations larger than 60% are typically referred to an organic material dominated by terrestrial precursors (Huang and Meinschein, 1979), and may be related to the early advanced plant development in this area. Alternatively, the C_{29} steranes can also be retraced to green algae, e.g. Chlorophyceae (Grantham and Wakefield, 1988; Katz and Everett, 2016; Kelly et al., 2011). Consequently, the precursor of the organic matter in the Llandovery shale can be clearly differentiated from those organisms which delivered the organic matter preserved in the Alum Shale and most of the oil samples.

The Deb oil is the only sample with identifiable 24-*iso*-/*n*-propylcholestanes. This C_{30} sterane is interpreted as an indicator of marine algae (Moldowan et al., 1990) or demosponges (Love et al., 2009). C_{30} steranes were not found in the Alum Shale and in oils in Cambrian reservoirs (Moldowan et al., 1990). These data are based on the analyses of a limited sample set and lead to the conclusion that the precursor sterols for the formation of

C_{30} steranes appeared between the Early Ordovician and the Devonian. However, the detection of C_{30} steranes is dependent on the instrumental sensitivity and often due to contamination from lubricating oil during drilling (Antcliffe and Stouge, 2013). Since the C_{30} sterane signals in the "Deb" oil sample are generally weak, it is hard to explicit the geological meaning of these compounds in this sample so far.

To briefly summarize the above findings, the Lower Palaeozoic oil found in the Baltic Basin is primarily generated from the Alum Shale. The Llandovery shale could add only a subordinate contribution to these oils in the area.

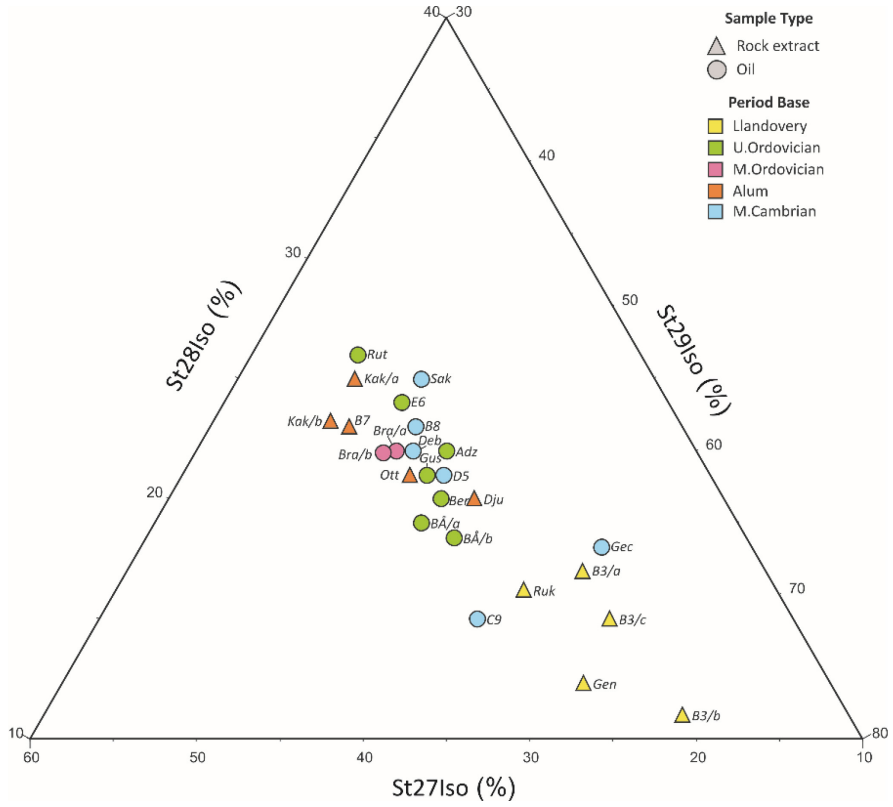

Fig. 5.9. Ternary diagram showing the relative distribution of C_{27}, C_{28} and C_{29} iso-steranes [5α,14β,17β(H) 20S+20R]. The Llandovery shale extracts and oil sample Gec are featured by high concentrations in C_{29} iso-sterane.

5.6.4 Heterogeneity within Alum Shale

The Alum Shale is vertically and horizontally highly heterogenous in terms of lithology (Thickpenny, 1984), depositional environment (Schovsbo, 2001), rock types (Schovsbo et al., 2015), mineralogy (Snäll, 1988), artificial pyrolysates (Bharati et al., 1995; Horsfield et al., 1992a), and uranium concentrations (Kosakowski et al., 2016; Schovsbo, 2002). For example, the Upper Cambrian and Lower Ordovician Alum Shale in the northern part of

the basin are rich in uranium (> 100ppm) (Schovsbo, 2002) which was either induced by hydrothermal activity (Mossman et al., 1993; Oliver et al., 1999) or controlled by the depositional environments (Schovsbo, 2002), while the Middle Cambrian Alum Shale is generally poor in uranium. However, only minor variations in source-related and age-related aliphatic biomarker compositions can be found among the three sub-stages. Nevertheless, triaromatic steroids distribution could be helpful in differentiating them.

Two Alum Shale extracts lack in or have very low C_{26}-C_{28} triaromatic steroid concentrations although C_{20}-C_{21} triaromatic steroids can be identified in all samples (Table 5.1 and Fig. 5.5) and the strong resistance of triaromatic steroids against biodegradation (Larter et al., 2012; Peters and Moldowan, 1991) argues against a removal by biodegradation. In general, triaromatic steroids are considered as aromatization products from monoaromatic steroids. During thermal maturation the C_{26}-C_{28} / C_{20}-C_{21} triaromatic steroid concentrations will decrease due to the preferential degradation of the long-chain triaromatic steroids (Beach et al., 1989; Mackenzie et al., 1981). The C_{26}-C_{28} triaromatic steroids are expected to be entirely cracked to shorter chained compounds during condensate or wet gas generation stages (Peters et al., 2005). The Baltic samples without C_{26}-C_{28} triaromatic steroids are either immature or in the peak oil generation stage which implies that those compounds were not thermally cracked. Dahl et al. (1988a) and Lewan and Buchardt (1989) found that the C_{26}-C_{28} triaromatic steroid concentrations in the Alum Shale are inversely proportional to its uranium content and concluded that the uranium irradiation initiates the cleavage of the aliphatic side chains of high molecular weight steroids to form lower molecular weight steroids. This theory fits the results of our work as the two Alum Shale extracts without C_{26}-C_{28} triaromatic steroids are from the uranium-rich Upper Cambrian and Lower Ordovician Alum Shale (Table 5.1), and as the Middle Cambrian Alum Shale samples with significantly higher C_{26}-C_{28} triaromatic steroid responses are generally lean in uranium concentrations (Schovsbo, 2002). Importantly, the oil sample from the Middle Cambrian sandstone reservoirs contains no C_{26}-C_{28} triaromatic steroids and is probably sourced from the uranium-rich Alum Shale interval. In contrast, the oil samples in the Upper Ordovician reef reservoirs all have high triaromatic steroid compounds and thus can be genetically linked with the Middle Cambrian Alum Shale. However, further geological or geochemical evidence is required to support this hypothesis. The weak response of C_{26}-C_{28} triaromatic steroids in the Brattefors oil samples is either an original one or caused by the high temperature influence during volcanic intrusions.

5.6.5 Migration and Mixing

The distribution of pyrrolic nitrogen compounds is considered to reflect migration distances, the abundance of carbazoles and the benzo[a]carbazole/benzo[c]carbazole isomer ratio both decrease with increasing migration distance (Larter et al., 1996; Li et al., 1995). However, Horsfield et al. (1998) and Bakr and Wilkes (2002) have pointed out that the benzocarbazole isomer ratio is also influenced by maturity and depositional environment. Nevertheless, the carbazole concentration seems to reflect the migration distance because the NSO compounds undergo retention due to geochromatographic effects and their less affinity to hydrocarbons (Silliman et al., 2002; van Duin and Larter, 1998). All oil samples from Upper Ordovician limestone reservoirs are depleted in carbazole compounds (Table 5.1). Only four oil samples from Middle Cambrian reservoirs (C9, B8, Deb, and Gec) have clear carbazole signal responses (Table 5.1), and indicate relatively short migration distances from the source rock. This conclusion is supported by the Biomarker Migration Index theory suggested by Seifert and Moldowan (1981) and Carlson and Chamberlain (1986)Carlson and Chamberlain (1986) as these four oil samples plot along the source sample maturity trend line in the C_{29} sterane isomer maturity diagram (Fig. 5.7B). This feature corresponds to the First Order Kinetic Conversion lines and oil samples Sak and Gus are shifted to the right of the trend line due to strong fractionation during migration (Fig. 5.7B). In other words, the source rock for the oil in the reservoirs is "close by" and this phenomenon fits the regional maturity trend (Fig. 5.1).

Although the Alum Shale is regarded to be the main source rock for the Lower Palaeozoic petroleum, contributions from the Llandovery shales to some reservoirs is possible. For example, the Gec oil sample is generally grouped between the Alum Shale and the Llandovery shale in the chemometric analysis (Fig. 5.6), and is characterized by a similar terpane distribution as the Alum Shale (Fig. 5.8) while the C_{29} sterane ratio resembles the Llandovery shale (Fig. 5.9). The Deb oil sample is among the least mature samples considering Ts/Tm and Diasterane/sterane ratios (Fig. 5.7A), but C_{29} sterane isomers indicate a higher maturity than most of the oil in Upper Ordovician reef reservoirs. This inconsistency in maturity could also be caused by multi-charging processes from the same source through time, since carbonate-rich source rocks are not involved here. Most likely the oil in the Middle Cambrian sandstone reservoirs is exclusively sourced by the uranium-rich Alum Shale, because C_{26}-C_{28} triaromatic steroids would occur in this oil if other source rock were involved.

5.7 Conclusions

1. Chemometric tools are efficient in screening decisive oil-source rock correlation biomarkers and showing genetic affinity relationship of samples.
2. Oil samples from Brattefors quarry in south central Sweden were heated by volcanic intrusions with high pyrene/phenanthrene ratios and have C_{29} S/R sterane ratios significantly beyond the normal thermodynamic threshold. Oil reservoired in basinal areas is generated by normal geological burial processes.
3. ETR, C_{24} tetracyclic terpane/C_{26} tricyclic terpane, and relative C_{29} sterane concentrations are the most useful biomarkers in differentiating Llandovery shale from Alum Shale. The uranium irradiation induced decrease of C_{26}-C_{28} triaromatic steroids in Alum Shale can be a practical key signal to link oil to the specific sub-stages of the Alums Shale.
4. Alum Shale is the main source rock for the oil in the Lower Palaeozoic sandstone and reef reservoirs in the Baltic Basin. A contribution from the Middle Cambrian Alum Shale to the oil in Upper Ordovician limestone reservoirs is noticeable. In contrast, oil in Middle Cambrian siliciclastic reservoirs was mainly sourced from more mature Upper Cambrian and Lower Ordovician Alum Shale.
5. The evaluation of migration distances can help in understanding the accumulation processes. Possible oil mixing occurs in some Lithuanian wells where the Llandovery shale occurs with good source rock properties.

5.8 Acknowledgement

The authors thank Gripen Oil & Gas AB, the Geological Survey of Sweden and Dr. Jurga Lazauskiene for providing rock and oil samples. Cornelia Karger and Anke Kaminsky (both from GFZ Potsdam) are acknowledged for their technical support during laboratory work.

Reviews and constructive comments from Pawel Kosakowski and Jon H. Pedersen are much appreciated. Kind thanks are extended to AAPG Bulletin Editor Barry Katz for his comments and suggestions.

6. SUMMARY AND PESPECTIVES

6.1 Summary

6.1.1 MME

The extent of the MME on the Bowland Shale is significant and can be attributed to its high clay content. Previous findings of sedimentological features, biomarkers, and stable carbon isotope data revealed that the Bowland Shale was deposited in a marine environment, and these results fit the Rock-Eval data of kerogen samples rather than whole rock samples in this dissertation. Compared with data of kerogen concentrates, the whole rock samples have lower HI and higher OI, and thus, point to type III kerogen. Also, the GOR and aromaticity data gained from analyses of the pyrolysates are significantly high in the whole rock samples suggesting a gas and a condensate potential; this is furthermore confirmed by phase predictions based on MSSV data. The bulk kinetic and secondary kinetic features of the Bowland Shale were also influenced by the complex mineral matrix effects. As a result, questionable predictions of the secondary gas generation in basin modelling studies can be induced by the application of such kinetic data. Thus, the MME strongly impacts the quantity, quality, and timing of the petroleum generation of the Bowland Shale, and especially regarding the quantitative modelling of secondary gas generation. It is important to note that secondary gas generation contributes the major part of thermogenic shale gas production.

The extent of MME in shale varies according to the mineralogical composition. In contrast to the Bowland Shale, the calcite-rich Toolebuc Oil Shale and the quartz-rich Alum Shale are not or only slightly affected by MME. Furthermore, the interface area between clay minerals and organic matter could be another factor that influences the extent of MME.

The heating rate dependency of MME on the Bowland Shale is obvious as revealed by MSSV experiments. A lower heating rate weakens the MME on aromaticity and generation amount. A calibration sequence with natural samples manifests that neither the kerogen nor the whole-rock pyrolysates show a similar gross elemental composition as natural products. However, kerogen pyrolysates resemble natural products more in certain NSO class ratios compared with whole-rock pyrolysates, which implies that MME on NSO

compounds is diminished under geological situations. In brief, the MME is speculated to only exist in the laboratory environment and not during a geological maturation process.

6.1.2 Uranium

Immature Alum Shale samples generally contain higher uranium concentrations, up to 20 times more than other typical marine shales. Pyrolysates, solvent extracts, and kerogen structures of the Alum Shale were all changed by the uranium irradiation.

Atypical pyrolysis products can be generated from the marine Alum Shale. GOR, aromaticity, and gas quantity are significantly higher compared with typical marine shales. The HI and OI are not well correlated with uranium contents compared with data from previous publications. HI seems to be controlled by original depositional rates and OI is typically low (<5 mgHC/gTOC). In contrast, GOR and aromaticity of pyrolysates are exponentially correlated with U contents in the source rock. These findings imply that the original kerogen structures are uniform and irradiation caused a higher aromaticity and gas-prone character.

The *o*-xylene/*n*-C_9 alkane ratios gained by thermovaporisation resemble laboratory pyrolysates. Also, the GORs from thermovaporisation can be generally correlated with pyrolysates. Some discrepancies are likely caused by the random decrease of GOR through weathering, sampling and storage. The hydrocarbons in the immature shale samples reflect early generated bitumen or were formed by the bombardment of uranium radiation. These findings confirm that uranium irradiation effects do influence the petroleum generation in natural environments.

The FT-ICR MS data reveal that the NSO compounds in the uranium-rich Alum Shale samples are less alkylated, and reflect the kerogen structures. This could be the reason why a significant amount of gas can be generated from such kind of samples. Basin modelling investigations suggest that most of the Alum Shale reached peak petroleum generation from Late Devonian to Early Carboniferous (360-385 Myr ago) in the basin centre (Kosakowski et al., 2010), thus, the source rocks at that time have experienced 20%-30% dosage of irradiation compared with nowadays samples which undergone irradiation for 478-500 Myr. Based on the correlations between irradiation damage, irradiation time and uranium contents, the Alum Shale hydrocarbon generation properties, e.g., GOR and aromaticity are calculated for the oil window time. This reconstruction plays a crucial role in predicting the quality and quantity of petroleum that has been generated.

The unique distribution of triaromatic steroids in uranium-rich Alum Shale samples was found in its petroleum. The absence of the high molecular weight (C_{26}-C_{28}) compounds is not a matter of thermal maturity, biodegradation, or migration fractionation, but is more likely due to uranium irradiation.

To summarise, uranium irradiation decreases the alkylation of kerogen structures and also plays an important catalytic role in converting the kerogen into gaseous and aromatic hydrocarbons in pyrolysis experiments through condensation and cross-linking mechanisms.

6.1.3 Comparison

Marine source rock samples with high contents of clay minerals or uranium may present similar features in pyrolysis experiments, i.e., high GOR and high aromaticity in the pyrolysates which are similar to type III kerogens. But they still have fundamental differences. For example, phenol and cresol which are dominant compounds in the pyrolysates of terrestrial organic matter are nearly absent in pyrolysates of the clay-rich and uranium-rich marine shale.

Excluding those similarities, clay minerals and uranium have intrinsic differences in influencing petroleum generation and occurrence through different processes. The interactions between solids and organic matter during diagenesis are limited due to few interface reactions, and the catalytic effect of clay minerals is only effective under very high temperatures. However, the irradiation is penetrative and the spontaneous fission of uranium is independent of temperature and pressure. Therefore, the kerogen structure of clay-rich shale would not significantly be changed during diagenesis, but uranium irradiation can severely alter the molecular structure of kerogen during geological time scales. A removal of minerals by acidic dissolution can easily avoid the MME in the laboratory, while the influence of uranium during pyrolysis is impossible to be eliminated. Both clay minerals and uranium have certain impacts on biomarkers used for maturity assessments. Reactive clay mineral entities mainly increase aliphatic biomarkers applied as maturity indicators, e.g., Ts/Tm or diasteranes/steranes ratios. By contrast, the influence of uranium on biomarkers is mainly focused on aromatic biomarkers, e.g., TA(I)/TA(I + II).

6.2 Perspectives

6.2.1 MME

Although MME result in an artefact during laboratory pyrolysis, possible false appearances of HI, OI, kinetics, and open-pyrolysis results, which are crucially important in evaluating source rock type and maturity, can finally cause significant risks in petroleum exploration.

The prepararion of kerogen concentrates from each sample before pyrolysis for a screening purpose is time consuming, but shale samples poor in organic matter or rich in clay contents must be re-examined. Special attention has to be paid on kinetic data regarding the MME, because the timing of petroleum generation in basin modelling is very sensitive to the kinetic result. For example, a 1 °C error caused during laboratory work would result in a 3 °C uncertainty in the geological extrapolation (Burnham, 1994b).

Results gained from the application of pyrolysis techniques allow an estimate about the petroleum generation and reflect the kerogen structure, whereas the heating rate dependency of MME emphasises the differences between laboratory heating and geological maturation. For example, the NSO compound concentrations in pyrolysates are significantly higher than those in natural products (Horsfield, 1997). High temperatures (>300 °C) and fast heating rates used in the laboratory would enable certain reactions which would not happen efficiently through geological environments. Therefore, some data gained from pyrolytic techniques should not be over-interpreted, but critically re-evaluated.

6.2.2 Uranium

Based on the application of pyrolytic methodologies, evidence for the shale gas potential of the Alum Shale was highlighted and that the oil potential is anticipated to be very limited (Kotarba et al., 2014a; Sanei et al., 2014). In addition, the gas sorption capacity of the Alum Shale was also expected to be very high due to the high aromatic kerogen structures. However, the shale gas explorations in Sweden and Denmark were unsuccessful which can be partly attributed to gas leakages in the response of tectonic movements (Pool et al., 2012). Furthermore, oil discoveries in the Baltic Basin can be traced back to the Alum Shale as a source rock by meaningful biomarkers and isotope characteristics which counteract the predictions based on pyrolysis experiments.

The reconstruction of the kerogen structure during the time span of petroleum generation could avoid an over-estimation of the gas potential and gas sorption capacity, and an under-estimation of the oil potential, and would thus reduce the exploration risks significantly.

The unique distribution of triaromatic biomarkers in both Alum Shale extracts and petroleum caused by irradiation can serve as a new parameter for correlation, especially when aliphatic biomarkers are absent due to irradiation.

REFERENCES

Abelson, P.H. (1963) Organic geochemistry and the formation of petroleum, 6th World Petroleum Congress. World Petroleum Congress.

Abouelresh, M.O. and Slatt, R.M. (2012) Lithofacies and sequence stratigraphy of the Barnett Shale in east-central Fort Worth Basin, Texas. AAPG bulletin 96, 1-22.

Abu-Ali, M., Rudkiewicz, J., McGillivray, J. and Behar, F. (1999) Paleozoic petroleum system of central Saudi Arabia. GeoArabia 4, 321-336.

Al-Sammerrai, F., Al-Sammerrai, D. and Al-Rawi, J. (1987) The use of thermogravimetry and NMR spectroscopy in the attempted identification of the source of babylonian building asphalt. Thermochimica Acta 115, 181-188.

Allen, R.G., Pereira, L.S., Raes, D. and Smith, M. (1998) Crop evapotranspiration-Guidelines for computing crop water requirements-FAO Irrigation and drainage paper 56. FAO, Rome 300, D05109.

Alloway, B.J. (2013) Bioavailability of elements in soil, Essentials of medical geology. Springer, pp. 351-373.

Amyx, J.W., Bass, D.M. and Whiting, R.L. (1960) Petroleum reservoir engineering: physical properties. McGraw-Hill College.

Anderson, R.F., Fleisher, M.Q. and LeHuray, A.P. (1989) Concentration, oxidation state, and particulate flux of uranium in the Black Sea. Geochimica et Cosmochimica Acta 53, 2215-2224.

Andersson, A. (1985) The Scandinavian alum shales. Sveriges geologiska undersökning.

Andrews, I. (2013) The Carboniferous Bowland Shale gas study: geology and resource estimation.

Antcliffe, J.B. and Stouge, S. (2013) Questioning the evidence of organic compounds called sponge biomarkers. Palaeontology 56, 917-925.

Aquino Neto, F.d., Trendel, J., Restle, A., Connan, J. and Albrecht, P. (1981) Occurrence and formation of tricyclic and tetracyclic terpanes in sediments and petroleums. Advances in organic geochemistry 10, 659-676.

Armstrong, J.P., Smith, J., D'Elia, V.A. and Trueblood, S.P. (1997) The occurrence and correlation of oils and Namurian source rocks in the Liverpool Bay-North Wales area. Geological Society, London, Special Publications 124, 195-211.

Arnold, R. and van Vleck Anderson, R. (1907) Geology and oil resources of the Santa Maria oil district, Santa Barbara County, California. US Government Printing Office.

Arthur Stankiewicz, B., van Bergen, P.F., Duncan, I.J., Carter, J.F., Briggs, D.E. and Evershed, R.P. (1996) Recognition of chitin and proteins in invertebrate cuticles using analytical pyrolysis/gas chromatography

and pyrolysis/gas chromatography/mass spectrometry. Rapid Commun Mass Sp 10, 1747-1757.

Badawy, A.S., Mehlqvist, K., Vajda, V., Ahlberg, P. and Calner, M. (2014) Late Ordovician (Katian) spores in Sweden: oldest land plant remains from Baltica. GFF 136, 16-21.

Bae, E., Na, J.-G., Chung, S.H., Kim, H.S. and Kim, S. (2010) Identification of about 30 000 Chemical Components in Shale Oils by Electrospray Ionization (ESI) and Atmospheric Pressure Photoionization (APPI) Coupled with 15 T Fourier Transform Ion Cyclotron Resonance Mass Spectrometry (FT-ICR MS) and a Comparison to. Energy & Fuels 24, 2563-2569.

Baker, E. (1959) Origin and migration of oil. Science 129, 871-874.

Bakr, M.M. and Wilkes, H. (2002) The influence of facies and depositional environment on the occurrence and distribution of carbazoles and benzocarbazoles in crude oils: a case study from the Gulf of Suez, Egypt. Organic Geochemistry 33, 561-580.

Barrett, P.A. (1988) Early Carboniferous of the Solway Basin: a tectonostratigraphic model and its bearing on hydrocarbon potential. Marine and petroleum geology 5, 271-281.

Barrow, M.P., Headley, J.V., Peru, K.M. and Derrick, P.J. (2004) Fourier transform ion cyclotron resonance mass spectrometry of principal components in oilsands naphthenic acids. J Chromatogr A 1058, 51-59.

Bates, T.F. (1958) An investigation of the mineralogy, petrography and paleobotany of uranium-bearing shales and lignites. United States Atomic Energy Commission, Technical Information Service., Oak Ridge, Tennessee, p. volume.

Baur, F., Littke, R., Wielens, H., Lampe, C. and Fuchs, T. (2010) Basin modeling meets rift analysis – A numerical modeling study from the Jeanne d'Arc basin, offshore Newfoundland, Canada. Marine and Petroleum Geology 27, 585-599.

Beach, F., Peakman, T., Abbott, G., Sleeman, R. and Maxwell, J. (1989) Laboratory thermal alteration of triaromatic steroid hydrocarbons. Organic geochemistry 14, 109-111.

Behar, F., Kressmann, S., Rudkiewicz, J.L. and Vandenbroucke, M. (1992) Experimental simulation in a confined system and kinetic modelling of kerogen and oil cracking. Organic Geochemistry 19, 173-189.

Behar, F., Roy, S. and Jarvie, D. (2010) Artificial maturation of a Type I kerogen in closed system: Mass balance and kinetic modelling. Organic Geochemistry 41, 1235-1247.

Behar, F., Vandenbroucke, M., Tang, Y., Marquis, F. and Espitalie, J. (1997) Thermal cracking of kerogen in open and closed systems : determination of kinetic parameters and stoichiometric coefficients for oil and gas generation. Organic Geochemistry 26, 321-339.

Belonoshko, A.B., Lukinov, T., Rosengren, A., Bryk, T. and Litasov, K.D. (2015) Synthesis of heavy hydrocarbons at the core-mantle boundary. Sci Rep-Uk 5.

Bernard, S., Horsfield, B., Schulz, H.-M., Wirth, R., Schreiber, A. and Sherwood, N. (2012) Geochemical evolution of organic-rich shales with increasing maturity: A STXM and TEM study of the Posidonia Shale (Lower Toarcian, northern Germany). Marine and Petroleum Geology 31, 70-89.

Berry, W.B., Wilde, P., Quinby-Hunt, M.S. and Orth, C.J. (1986) Trace element signatures in Dictyonema Shales and their geochemical and stratigraphic significance. Norsk Geol. Tidsskr 66, 45-51.

Bethke, C.M., Vergo, N. and ALTANER, S.P. (1986) Pathways of smectite illitization. CLAYS CLAY MINER. Clays Clay Miner. 34, 125.

Bharati, S., Patience, R.L. and Larter, S.R. (1995) Elucidation of the Alum Shale kerogen structure using a multi-disciplinary approach. Organic Geochemistry 23, 1043-1058.

Bloch, S. (1980) Some factors controlling the concentration of uranium in the world ocean. Geochimica et Cosmochimica Acta 44, 373-377.

Bojesen-Koefoed, J.A., N., H.P., R., P., B., B., Weiss, H., Kanev, K., Zdanavičiūtė, O., Khubldikov, A. and Pokorski, J. (2001) Petroleum in the Baltic syneclise and the peribaltic region composition and variability. 20th International Meeting on Organic Geochemistry 1, 419-420.

Boreham, C. and Powell, T. (1987) Sources and preservation of organic matter in the Cretaceous Toolebuc Formation, eastern Australia. Organic Geochemistry 11, 433-449.

Bowker, K.a. (2007) Barnett Shale gas production, Fort Worth Basin: Issues and discussion. AAPG Bulletin 91, 523-533.

Brangulis, A., Kanev, S., Margulis, L. and Pomerantseva, R. (1993) Geology and hydrocarbon prospects of the Paleozoic in the Baltic region. Geological Society, London, Petroleum Geology Conference series 4, 651-656.

Braun, R. and Burnham, A. (1987) Analysis of chemical reaction kinetics using a distribution of activation energies and simpler models. Energy & Fuels 1, 153-161.

Bray, E. and Evans, E. (1961) Distribution of n-paraffins as a clue to recognition of source beds. Geochimica et Cosmochimica Acta 22, 2-15.

Breger, I. (1974) The role of organic matter in the accumulation of uranium: the organic geochemistry of the coal-uranium association. Formation of uranium ore deposits, 99-124.

Breger, I.A. and Brown, A. (1962) Kerogen in the Chattanooga shale. Science 137, 221-224.

Brocks, J.J., Love, G.D., Snape, C.E., Logan, G.A., Summons, R.E. and Buick, R. (2003) Release of bound aromatic hydrocarbons from late

Archean and Mesoproterozoic kerogens via hydropyrolysis. Geochimica et Cosmochimica Acta 67, 1521-1530.

Brooks, B.T. (1948) Active-surface catalysts in formation of petroleum. AAPG Bulletin 32, 2269-2286.

Brooks, B.T. (1952) Evidence of catalytic action in petroleum formation. Industrial & Engineering Chemistry 44, 2570-2577.

Bruce, C.H. (1984) Smectite dehydration--its relation to structural development and hydrocarbon accumulation in northern Gulf of Mexico basin. AAPG Bulletin 68, 673-683.

Buchardt, B. (1999) Gas Potential of the Cambro-Ordovician Alum Shale in Southern Scandinavia and the Baltic Region. The Search for Deep Gas.

Buchardt, B., Nielsen, A.T., Schovsbo, N.H. and Bojesen-Kofoed, J. (1997) Alun skiferen i Skandinavien. Geologisk Tidsskrift 1997, 1-30.

Budzinski, H., Jones, I., Bellocq, J., Pierard, C. and Garrigues, P. (1997) Evaluation of sediment contamination by polycyclic aromatic hydrocarbons in the Gironde estuary. Marine chemistry 58, 85-97.

Burnham, A.K. (1994a) Comments on "The effects of the mineral matrix on the determination of kinetic parameters using modified Rock-Eval pyrolysis" by H. Dembicki Jr, and the resulting comment by R. Pelet. Organic Geochemistry 21, 985-986.

Burnham, A.K. (1994b) Comments on The effects of the mineral matrix on the determination of kinetic parameters using modified Rock-Eval pyrolysis" by H. Dembicki Jr, and the resulting comment. Organic Geochemistry 21, 985-986.

Burnham, A.K. (2015) A Simple Kinetic Model of Oil Generation, Vaporization, Coking, and Cracking. Energy & Fuels.

Burnham, A.K., Braun, R.L., Gregg, H.R. and Samoun, A.M. (1987) Comparison of methods for measuring kerogen pyrolysis rates and fitting kinetic parameters. Energy & Fuels 1, 452-458.

Burnham, A.K., Braun, R.L. and Samoun, A.M. (1988) Further comparison of methods for measuring kerogen pyrolysis rates and fitting kinetic parameters. Organic geochemistry 13, 839-845.

Burnham, A.K. and Singleton, M.F. (1983) High-pressure pyrolysis of Green River oil shale, ACS Symp. Ser.;(United States). Lawrence Livermore National Lab., CA.

Burnham, A.K. and Sweeney, J.J. (1989) A chemical kinetic model of vitrinite maturation and reflectance. Geochimica et Cosmochimica Acta 53, 2649-2657.

Burst, J.F. (1969) Diagenesis of Gulf Coast clayey sediments and its possible relation to petroleum migration. AAPG bulletin 53, 73-93.

Burtner, R.L. and Warner, M.A. (1986) Relationship between illite/smectite diagenesis and hydrocarbon generation in Lower Cretaceous Mowry and Skull Creek shales of the northern Rocky Mountain area. Clays and Clay Minerals 34, 390-402.

Carlson, R. and Chamberlain, D. (1986) Steroid biomarker-clay mineral adsorption free energies: implications to petroleum migration indices. Organic geochemistry 10, 163-180.

Charlesby, A. (1954) The cross-linking and degradation of paraffin chains by high-energy radiation, Proceedings of the Royal Society of London A: Mathematical, Physical and Engineering Sciences. The Royal Society, pp. 60-74.

Chatzis, C. (2014) Description of pore systems from a vuggy Palaeozoic carbonate, Gotland, Sweden. The University of Manchester, p. 54.

Chiaberge, S., Fiorani, T., Savoini, A., Bionda, A., Ramello, S., Pastori, M. and Cesti, P. (2013) Classification of crude oil samples through statistical analysis of APPI FTICR mass spectra. Fuel Processing Technology 106, 181-185.

Chisholm, J.I., Charsley, T.J. and Aitkenhead, N. (1988) Geology of the country around Ashbourne and Cheadle. HMSO.

Clark, J. and Philp, R. (1989) Geochemical characterization of evaporite and carbonate depositional environments and correlation of associated crude oils in the Black Creek Basin, Alberta. Bulletin of Canadian Petroleum Geology 37, 401-416.

Claxton, M., Patience, R. and Park, P. (1993) Molecular modelling of bond energies in potential kerogen sub-units. Organic Geochemistry, 198-201.

Cohen, K., Finney, S., Gibbard, P. and Fan, J.-X. (2013) The ICS international chronostratigraphic chart. Episodes 36, 199-204.

Colombo, U., Sironi, G. and Denti, E. (1964) A geochemical investigation upon the effects of ionizing radiation on hydrocarbons. J. Inst. Petrol. 50.

Constable, F. (1925) The mechanism of catalytic decomposition. Proceedings of the Royal Society of London. Series A, Containing Papers of a Mathematical and Physical Character 108, 355-378.

Cooper, J. and Bray, E. (1963) A postulated role of fatty acids in petroleum formation. Geochimica et Cosmochimica Acta 27, 1113-1127.

Corbett, C.S. (1955) In situ origin of McMurray oil of northeastern Alberta and its relevance to general problem of origin of oil. AAPG Bulletin 39, 1601-1621.

Court, R.W., Sephton, M.A., Parnell, J. and Gilmour, I. (2006) The alteration of organic matter in response to ionising irradiation: Chemical trends and implications for extraterrestrial sample analysis. Geochimica et cosmochimica acta 70, 1020-1039.

Craig, H. (1953) The geochemistry of the stable carbon isotopes. Geochimica et Cosmochimica Acta 3, 53-92.

Curiale, J.A. and Frolov, E.B. (1998) Occurrence and origin of olefins in crude oils. A critical review. Organic geochemistry 29, 397-408.

Curtis, J.B. (2002) Fractured shale-gas systems. AAPG bulletin 11, 1921-1938.

Dahl, J., Chen, R. and Kaplan, I. (1989) Alum Shale bitumen maturation and migration: implications for Gotland's oil. Journal of Petroleum Geology 12, 465-476.

Dahl, J., Hallberg, R. and Kaplan, I. (1988a) Effects of irradiation from uranium decay on extractable organic matter in the Alum Shales of Sweden. Organic geochemistry 12, 559-571.

Dahl, J., Hallberg, R. and Kaplan, I. (1988b) The effects of radioactive decay of uranium on elemental and isotopic ratios of Alum Shale kerogen. Applied geochemistry 3, 583-589.

Dahlkamp, F.J. (2013) Uranium ore deposits. Springer Science & Business Media.

Damsté, J.S.S., de las Heras, F.X.C., van Bergen, P.F. and de Leeuw, J.W. (1993) Characterization of Tertiary Catalan lacustrine oil shales: discovery of extremely organic sulphur-rich Type I kerogens. Geochimica et Cosmochimica Acta 57, 389-415.

De Grande, S., Neto, F.A. and Mello, M. (1993) Extended tricyclic terpanes in sediments and petroleums. Organic geochemistry 20, 1039-1047.

DECC (2011) The unconventional hydrocarbon resources of Britain’s onshore basins - shale gas. DECC Promote website, December 2010.

Dembicki, H. (1990) Mineral matrix effect during analytical pyrolysis of source rocks. Association of Petroleum Geochemist and Explorer Bulletin 6, 78-105.

Dembicki, H. (1992) The effects of the mineral matrix on the determination of kinetic parameters using modified Rock Eval pyrolysis. Organic Geochemistry 18, 531-539.

Dembicki, H. (1994) Reply to comments by R. Pelet on the paper “The effects of the mineral matrix on the determination of kinetic parameters using modified Rock-Eval pyrolysis” by H. Dembicki Jr, Org. Geochem., 18, 531–539 (1992). Organic Geochemistry 21, 982-984.

Dembicki, H., Horsfield, B. and Ho, T.T. (1983) Source rock evaluation by pyrolysis-gas chromatography. AAPG Bulletin 67, 1094-1103.

Derenne, S., Largeau, C. and Berkaloff, C. (1996) First example of an algaenan yielding an aromatic-rich pyrolysate. Possible geochemical implications on marine kerogen formation. Organic Geochemistry 24, 617-627.

Dessort, D., Connan, J., Derenne, S. and Largeau, C. (1997) Comparative studies of the kinetic parameters of various algaenans and kerogens via open-system pyrolyses. Organic Geochemistry 26, 705-720.

di Primio, R., Dieckmann, V. and Mills, N. (1998) PVT and phase behaviour analysis in petroleum exploration. Organic Geochemistry 29, 207-222.

di Primio, R. and Horsfield, B. (1996) Predicting the generation of heavy oils in carbonate/evaporitic environments using pyrolysis methods. Organic Geochemistry 6380.

di Primio, R. and Horsfield, B. (2006) From petroleum-type organofacies to hydrocarbon phase prediction. AAPG Bulletin 90, 1031-1058.

Didyk, B. (1978) Organic geochemical indicators of palaeoenvnonmental conditions of sedimentation. Nature 272, 216-222.

Dieckmann, V. (2005) Modelling petroleum formation from heterogeneous source rocks: the influence of frequency factors on activation energy distribution and geological prediction. Marine and Petroleum Geology 22, 375-390.

Dieckmann, V., Horsfield, B. and Schenk, H.J. (2000a) Heating rate dependency of petroleum-forming reactions: implications for compositional kinetic predictions. Organic Geochemistry 31.

Dieckmann, V. and Keym, M. (2006) A new approach to bridge the effect of organofacies variations on kinetic modelling and geological extrapolations. Organic Geochemistry 37, 728-739.

Dieckmann, V., Schenk, H.J. and Horsfield, B. (2000b) Assessing the overlap of primary and secondary reactions by closed- versus open-system pyrolysis of marine kerogens. Journal of Analytical and Applied Pyrolysis 56, 33-46.

Dieckmann, V., Schenk, H.J., Horsfield, B. and Welte, D.H. (1998) Kinetics of petroleum generation and cracking by programmed-temperature closed-system pyrolysis of Toarcian Shales. Fuel 77, 23-31.

Disnar, J. and Sureau, J. (1990) Organic matter in ore genesis: Progress and perspectives. Organic Geochemistry 16, 577-599.

Dole, M. (1958) The Effects of Ionizing Radiation on Natural and Synthetic High Polymers. J Am Chem Soc 80, 6694-6694.

Douglas, A., Coates, R., Bowler, B. and Hall, K. (1975) Alkanes from the pyrolysis of recent sediments. Advances in Organic Geochemistry, 357-374.

Down, A. and Himus, G. (1941) A preliminary study of the chemical constitution of kerogen. Journal of the Institute of Petroleum 27, 426-445.

Dronov, A. and Holmer, L. (1999) Depositional sequences in the Ordovician of Baltoscandia. Acta-Universitatis Carolinae Geologica, 133-136.

Düppenbecker, S. and Horsfield, B. (1990) Compositional information for kinetic modelling and petroleum type prediction. Organic Geochemistry 16, 259-266.

Duran, E.R., di Primio, R., Anka, Z., Stoddart, D. and Horsfield, B. (2013) 3D-basin modelling of the Hammerfest Basin (southwestern Barents Sea): A quantitative assessment of petroleum generation, migration and leakage. Marine and petroleum geology 45, 281-303.

Durand, B. (2003) A history of organic geochemistry. Oil & gas science and technology 58, 203-231.

Durand, B. and Espitalié, J. (1973) Evolution de la matière organique au cours de l'enfouissement des sédiments. Compte rendus de l'Académie des Sciences (Paris) 276, 2253-2256.

Dyni, J. (2006) Geology and resources of some world oil shale deposits: scientific investigations report 2005–5294, US Department of the Interior. US Geological Survey, 49.

Dzou, L., Noble, R. and Senftle, J. (1995) Maturation effects on absolute biomarker concentration in a suite of coals and associated vitrinite concentrates. Organic Geochemistry 23, 681-697.

Eglinton, G. and Calvin, M. (1967) Chemical fossils. Scientific American 216, 32-43.

Eglinton, T., Rowland, S., Curtis, C. and Douglas, A. (1986) Kerogen-mineral reactions at raised temperatures in the presence of water. Organic Geochemistry 10, 1041-1052.

Eglinton, T.I., Damsté, J.S.S., Kohnen, M.E. and de Leeuw, J.W. (1990) Rapid estimation of the organic sulphur content of kerogens, coals and asphaltenes by pyrolysis-gas chromatography. Fuel 69, 1394-1404.

EIA (2015) Technically Recoverable Shale Oil and Shale Gas Resources.

EIA, U. (2011) World shale gas resources: an initial assessment of 14 regions outside the United States.

Emery, K.O. and Hoggan, D. (1958) Gases in marine sediments. AAPG Bulletin 42, 2174-2188.

Ericsson, I. and Lattimer, R. (1989) Pyrolysis nomenclature. Journal of analytical and applied pyrolysis 14, 219-221.

Espitalie, J., Madec, M. and Tissot, B. (1980) Role of mineral matrix in kerogen pyrolysis: influence on petroleum generation and migration. AAPG Bulletin 64, 59-66.

Espitalie, J., Madec, M., Tissot, B., Mennig, J. and Leplat, P. (1977) Source rock characterization method for petroleum exploration, Offshore Technology Conference. Offshore Technology Conference.

Espitalié, J., Makadi, K.S. and Trichet, J. (1984) Role of the mineral matrix during kerogen pyrolysis. Organic Geochemistry 6, 365-382.

Espitalie, J., Ungerer, P., Irwin, I. and Marquis, F. (1988) Primary cracking of kerogens. Experimenting and modelling C 1, C 2–C 5, C 6–C 15 and C 15+ classes of hydrocarbons formed. Organic Geochemistry 13, 893-899.

Ewbank, G., Manning, D.A.C. and Abbott, G.D. (1993) An organic geochemical study of bitumens and their potential source rocks from the South Pennine Orefield, Central England. Organic geochemistry 20, 579-598.

Farrimond, P., Bevan, J.C. and Bishop, A.N. (1999) Tricyclic terpane maturity parameters: response to heating by an igneous intrusion. Organic Geochemistry 30, 1011-1019.

Fischer, F. and Tropsch, H. (1930) Process for the production of paraffin-hydrocarbons with more than one carbon atom. Google Patents.

Fisher, D.E. and Bostrom, K. (1969) Uranium rich sediments on the East Pacific Rise. Nature 224, 64-65.

Forbes, P., Landais, P., Bertrand, P., Brosse, E., Espitalie, J. and Yahaya, M. (1988) Chemical transformations of type-III organic matter associated with the Akouta uranium deposit (Niger): geological implications. Chemical geology 71, 267-282.

Foscolos, A. and Powell, T. (1979) Catagenesis in shales and occurrence of authigenic clays in sandstones, North Sabine H-49 well, Canadian Arctic Islands. Canadian Journal of Earth Sciences 16, 1309-1314.

Foscolos, A., Powell, T. and Gunther, P. (1976) The use of clay minerals and inorganic and organic geochemical indicators for evaluating the degree of diagenesis and oil generating potential of shales. Geochimica et cosmochimica acta 40, 953-966.

Fowler, M. and Douglas, A. (1984) Distribution and structure of hydrocarbons in four organic-rich Ordovician rocks. Organic Geochemistry 6, 105-114.

Fraser, A.J. and Gawthorpe, R.L. (2003) An atlas of Carboniferous basin evolution in Northern England. Geological Society, London, Memoirs 28, NP-NP.

Frolov, E., Melikhov, V. and Smirnov, M. (1996) Radiolytic nature of n-alkene/n-alkane distributions in Russian Precambrian and Palaeozoic oils. Organic geochemistry 24, 1061-1064.

Frolov, E. and Smirnov, M. (1994) Unsaturated hydrocarbons in crude oils. Organic geochemistry 21, 189-208.

Frost, A. (1945) The role of clays in the formation of petroleum. Uspekhi. Khim 14, 501.

Gasparik, M., Bertier, P., Gensterblum, Y., Ghanizadeh, A., Krooss, B.M. and Littke, R. (2014) Geological controls on the methane storage capacity in organic-rich shales. International Journal of Coal Geology 123, 34-51.

Gautschi, A. (2001) Hydrogeology of a fractured shale (Opalinus Clay): Implications for deep geological disposal of radioactive wastes. Hydrogeol J 9, 97-107.

Gerrienne, P., Servais, T. and Vecoli, M. (2016) Plant evolution and terrestrialization during Palaeozoic times—the phylogenetic context. Review of Palaeobotany and Palynology 227, 4-18.

Gibbins-Matham, J. and Kandiyoti, R. (1988) Coal pyrolysis yields from fast and slow heating in a wire-mesh apparatus with a gas sweep. Energy & fuels 2, 505-511.

Gold, T. (1985) The origin of natural gas and petroleum, and the prognosis for future supplies. Annual Review of Energy 10, 53-77.

Gold, T. and Soter, S. (1982) Abiogenic methane and the origin of petroleum. Energ Explor Exploit 1, 89-104.

Goldschmidt, V.M. (1937) The principles of distribution of chemical elements in minerals and rocks. The seventh Hugo Müller Lecture, delivered before the Chemical Society on March 17th, 1937. Journal of the Chemical Society (Resumed), 655-673.

Goodwin, J., Golovko, V., Iacob, V. and Hardy, J.C. (2009) Half-life of the electron-capture decay of Ru 97: Precision measurement shows no temperature dependence. Phys Rev C 80, 045501.

Goossens, H.d., De Leeuw, J., Schenck, P. and Brassell, S. (1984) Tocopherols as likely precursors of pristane in ancient sediments and crude oils. Nature 312, 440-442.

Gradstein, F., Ogg, J. and Smith, A. A geologic time scale 2004. Cambridge, Cambridge University Press.

Grantham, P. and Wakefield, L. (1988) Variations in the sterane carbon number distributions of marine source rock derived crude oils through geological time. Organic Geochemistry 12, 61-73.

Green, C.A., Styles, P. and Baptie, B.J. (2012) Preese Hall shale gas fracturing review and recommendations for induced seismic mitigation. London, UK: Department of Energy and Climate Change.

Grim, R.E. (1947) Relation of clay mineralogy to origin and recovery of petroleum. AAPG Bulletin 31, 1491-1499.

Gross, D., Sachsenhofer, R., Bechtel, A., Pytlak, L., Rupprecht, B. and Wegerer, E. (2015) Organic geochemistry of Mississippian shales (Bowland Shale Formation) in central Britain: Implications for depositional environment, source rock and gas shale potential. Marine and Petroleum Geology 59, 1-21.

Groysman, A. (2014) History of Crude Oil and Petroleum Products, Corrosion in Systems for Storage and Transportation of Petroleum Products and Biofuels. Springer, pp. 221-226.

Gussow, W.C. (1954) Differential entrapment of oil and gas: a fundamental principle. AAPG bulletin 38, 816-853.

Hanson, A.D., Ritts, B.D. and Moldowan, J.M. (2007) Organic Geochemistry of oil and source rock strata of the Ordos Basin, north-central China. AAPG bulletin 91, 1273-1293.

Hao, F., Zhou, X., Zhu, Y. and Yang, Y. (2011) Lacustrine source rock deposition in response to co-evolution of environments and organisms controlled by tectonic subsidence and climate, Bohai Bay Basin, China. Organic Geochemistry 42, 323-339.

Hartwig, A., di Primio, R., Anka, Z. and Horsfield, B. (2012) Source rock characteristics and compositional kinetic models of Cretaceous organic rich black shales offshore southwestern Africa. Organic Geochemistry 51, 17-34.

Hedberg, H.D. (1964) Geologic aspects of origin of petroleum. AAPG Bulletin 48, 1755-1803.

Heller-Kallai, L., Aizenshtat, Z. and Miloslavski, I. (1984) The effect of various clay minerals on the thermal decomposition of stearic acid under 'bulk flow'conditions. Clay Miner 19, 779-788.

Hill, R.J., Zhang, E., Katz, B.J. and Tang, Y. (2007) Modeling of gas generation from the Barnett Shale, Fort Worth Basin, Texas. AAPG Bulletin 91, 501-521.

Hoering, T. (1984) Thermal reactions of kerogen with added water, heavy water and pure organic substances. Organic Geochemistry 5, 267-278.

Hoering, T.C. and Navale, V. (1987) A search for molecular fossils in the kerogen of Precambrian sedimentary rocks. Precambrian Res 34, 247-267.

Hoffmann, C., Foster, C., Powell, T. and Summons, R. (1987) Hydrocarbon biomarkers from Ordovician sediments and the fossil alga Gloeocapsomorpha prisca Zalessky 1917. Geochimica et Cosmochimica Acta 51, 2681-2697.

Högström, A.E.S. and Ebbestad, J.O.R. (2004) Preservational aspects of the Upper Ordovician Fjäcka Shale, central Sweden–exemplified by a medusoid problematicum. WOGOGOB-2004 8th Meeting on the Working Group on the Ordovician Geology of Baltoscandia 1, 45-46.

Holba, A., Ellis, L., Dzou, I., Hallam, A., Masterson, W., Francu, J. and Fincannon, A. (2001) Extended tricyclic terpanes as age discriminators between Triassic, Early Jurassic and Middle-Late Jurassic oils. 20th International Meeting on Organic Geochemistry 1, 464.

Holba, A., Masterson, W., Ellis, L. and Dzou, L. (2002) Triassic source facies in high paleo-latitude petroleum systems, Pacific Section AAPG/Western Region SPE Conference, Anchorage Alaska, p. 1146.

Horsfield, B. (1989) Practical criteria for classifying kerogens: some observations from pyrolysis-gas chromatography. Geochimica et Cosmochimica Acta 53, 891-901.

Horsfield, B. (1997) The bulk composition of first-formed petroleum in source rocks. Petroleum and basin evolution.

Horsfield, B., Bharati, S. and Larter, S.R. (1992a) On the atypical petroleum-generating characteristics of alginite in the Cambrian Alum Shale, in: Schidlowski, M., Golubic, S., Kimberley, M.M., Sr, D.M.M., Trudinger, P.A. (Eds.), Early Organic Evolution. Springer Berlin Heidelberg, pp. 257-266.

Horsfield, B., Bharati, S. and Larter, S.R. (1992b) On the atypical petroleum-generating characteristics of alginite in the Cambrian Alum Shale. Early Organic Evolution.

Horsfield, B., Clegg, H., Wilkes, H. and Santamaria-Orozco, D. (1998) Effect of maturity on carbazole distributions in petroleum systems: new insights from the Sonda de Campeche, Mexico, and Hils Syncline, Germany. The Science of Nature 85, 233-237.

Horsfield, B., Dembicki, H. and Ho, T. (1983) Some potential applications of pyrolysis to basin studies. Journal of the Geological Society 140, 431-443.

Horsfield, B., Disko, U. and Leistner, F. (1989) The micro-scale simulation of maturation: outline of a new technique and its potential applications. Geologische Rundschau 78, 361-373.

Horsfield, B. and Douglas, A. (1980) The influence of minerals on the pyrolysis of kerogens. Geochimica et Cosmochimica Acta 44, 1119-1131.

Horsfield, B., Leistner, F. and Hall, K. (2014) Microscale sealed vessel pyrolysis. Principles and Practice of Analytical Techniques in Geosciences 4, 209.

Horsfield, B., Schenk, H.J., Mills, N. and Welte, D.H. (1992c) An investigation of the in-reservoir conversion of oil to gas: compositional and kinetic findings from closed-system programmed-temperature pyrolysis. Organic Geochemistry 19, 191-204.

Hough, E. and Vane, C.H. (2014) The Bowland Shale in the Roosecote Borehole of the Lancaster Fells Sub-Basin Craven Basin UK: A Potential UK Shale gas Play? SPE/EAGE European …, 25-27.

Hu, M., Cheng, Z., Zhang, M., Liu, M., Song, L., Zhang, Y. and Li, J. (2014) Effect of Calcite, Kaolinite, Gypsum, and Montmorillonite on Huadian Oil Shale Kerogen Pyrolysis. Energy & Fuels 28, 1860-1867.

Huang, H., Zhang, S. and Su, J. (2015a) Geochemistry of Tri- and Tetracyclic Terpanes in the Palaeozoic Oils from the Tarim Basin, Northwest China. Energy & Fuels 29, 7014-7025.

Huang, H., Zhang, S. and Su, J. (2015b) Pyrolytically derived polycyclic aromatic hydrocarbons in marine oils from the Tarim Basin, NW China. Energy & Fuels 29, 5578-5586.

Huang, W.-Y. and Meinschein, W. (1979) Sterols as ecological indicators. Geochimica et Cosmochimica Acta 43, 739-745.

Hughes, W.B. (1984) Use of thiophenic organosulfur compounds in characterizing crude oils derived from carbonate versus siliciclastic sources.

Hughey, C.A., Hendrickson, C.L., Rodgers, R.P., Marshall, A.G. and Qian, K. (2001) Kendrick mass defect spectrum: a compact visual analysis for ultrahigh-resolution broadband mass spectra. Analytical Chemistry 73, 4676-4681.

Hughey, C.A., Rodgers, R.P., Marshall, A.G., Qian, K. and Robbins, W.K. (2002) Identification of acidic NSO compounds in crude oils of different geochemical origins by negative ion electrospray Fourier transform ion cyclotron resonance mass spectrometry. Organic Geochemistry 33, 743-759.

Huizinga, B.J., Tannenbaum, E. and Kaplan, I. (1987) The role of minerals in the thermal alteration of organic matter—III. Generation of bitumen in laboratory experiments. Organic Geochemistry 11, 591-604.

Hunt, J.M. (1961) Distribution of hydrocarbons in sedimentary rocks. Geochimica et cosmochimica Acta 22, 37-49.

Hunt, J.M. (1996) Petroleum geochemistry and geology. WH Freeman New York.

Hunt, J.M., Lewan, M. and Hennet, R.J. (1991) Modeling Oil Generation with Time-Temperature Index Graphs Based on the Arrhenius Equation (1). AAPG Bulletin 75, 795-807.

Hunt, T.S. (1863) Report on the geology of Canada. Canadian Geological Survey Report: Progress to 1863. Canadian Geological Survey.

Imber, J., Armstrong, H. and Clancy, S. (2014) Natural fractures in a UK shale reservoir analogue, Cleveland Basin, NE England. AAPG Bulletin.

Jaraula, C.M., Schwark, L., Moreau, X., Pickel, W., Bagas, L. and Grice, K. (2015) Radiolytic alteration of biopolymers in the Mulga Rock (Australia) uranium deposit. Applied Geochemistry 52, 97-108.

Jarvie, D.M., Behar, F. and Mazéas, L. (2010) Decomposition of Organic Matter and Impact on Shale Resource Play Assessments. 11-14.

Jarvie, D.M., Hill, R.J., Ruble, T.E. and Pollastro, R.M. (2007) Unconventional shale-gas systems: The Mississippian Barnett Shale of north-central Texas as one model for thermogenic shale-gas assessment. AAPG Bulletin 91, 475-499.

Jarvis, G.T. and McKenzie, D.P. (1980) Sedimentary basin formation with finite extension rates. Earth and Planetary Science Letters 48, 42-52.

Johns, W.D. and Shimoyama, A. (1972) Clay minerals and petroleum-forming reactions during burial and diagenesis. AAPG Bulletin 56, 2160-2167.

Jones, R. (1984) Comparison of carbonate and shale source rocks.

Jurg, J. and Eisma, E. (1964) Petroleum hydrocarbons: generation from fatty acid. Science 144, 1451-1452.

Kanev, S., Margulis, L., Bojesen-Koefoed, J., Weil, W., Merta, H. and Zdanavičiūtė, O. (1994) Oils and hydrocarbon source rocks of the Baltic syneclise. Oil and Gas Journal 92, 1-4.

Karabakan, A. and Yürüm, Y. (1998) Effect of the mineral matrix in the reactions of oil shales: 1. Pyrolysis reactions of Turkish Göynük and US Green River oil shales. Fuel 77, 1303-1309.

Karnkowski, P.H., Pikulski, L. and Wolnowski, T. (2010) Petroleum geology of the Polish part of the Baltic region-an overview. Geological Quarterly 54, 143-158.

Katz, B.J. (1983) Limitations of 'Rock-Eval'pyrolysis for typing organic matter. Organic Geochemistry 4, 195-199.

Katz, B.J. and Everett, M.A. (2016) An overview of pre-Devonian petroleum systems–Unique characteristics and elevated risks. Marine and Petroleum Geology 73, 492-516.

Kelly, A.E., Love, G.D., Zumberge, J.E. and Summons, R.E. (2011) Hydrocarbon biomarkers of Neoproterozoic to Lower Cambrian oils from eastern Siberia. Organic Geochemistry 42, 640-654.

Kenney, J., Shnyukov, Y.F., Krayishkin, V., Tchebanenko, I. and Klochko, V. (2001) Dismissal of claims of a biological connection for natural petroleum. Energia 22, 26-34.

Kenrick, P. and Crane, P.R. (1997) The origin and early evolution of plants on land. Nature 389, 33-39.

Killops, S.D. and Killops, V.J. (2013) Introduction to organic geochemistry. John Wiley & Sons.

Kim, S., Stanford, L.A., Rodgers, R.P., Marshall, A.G., Walters, C.C., Qian, K., Wenger, L.M. and Mankiewicz, P. (2005) Microbial alteration of the acidic and neutral polar NSO compounds revealed by Fourier transform ion cyclotron resonance mass spectrometry. Organic Geochemistry 36, 1117-1134.

Kissin, Y. (1987) Catagenesis and composition of petroleum: origin of n-alkanes and isoalkanes in petroleum crudes. Geochimica et Cosmochimica Acta 51, 2445-2457.

Klein, G.C., Kim, S., Rodgers, R.P., Marshall, A.G. and Yen, A. (2006) Mass spectral analysis of asphaltenes. II. Detailed compositional comparison of asphaltenes deposit to its crude oil counterpart for two geographically different crude oils by ESI FT-ICR MS. Energy & fuels 20, 1973-1979.

Koczy, F.F., Tomic, E. and Hecht, F. (1957) Zur geochemie des urans im ostseebecken. Geochimica et Cosmochimica Acta 11, 86-102.

Kolesnikov, A., Kutcherov, V.G. and Goncharov, A.F. (2009) Methane-derived hydrocarbons produced under upper-mantle conditions. Nature Geoscience 2, 566-570.

Konitzer, S.F., Davies, S.J., Stephenson, M.H. and Leng, M.J. (2014) Depositional Controls On Mudstone Lithofacies In A Basinal Setting: Implications for the Delivery of Sedimentary Organic Matter. Journal of Sedimentary Research 84, 198-214.

Kosakowski, P., Kotarba, M.J., Piestrzyński, A., Shogenova, A. and Więcław, D. (2016) Petroleum source rock evaluation of the Alum and Dictyonema Shales (Upper Cambrian–Lower Ordovician) in the Baltic Basin and Podlasie Depression (eastern Poland). International Journal of Earth Sciences 105, 1-19.

Kosakowski, P., Wróbel, M. and Poprawa, P. (2010) Hydrocarbon generation and expulsion modelling of the lower Paleozoic source rocks in the Polish part of the Baltic region. Geological Quarterly 54, 241-256.

Kotarba, M. and Lewan, M. (2013) Sources of natural gases in Middle Cambrian reservoirs in Polish and Lithuanian Baltic Basin as determined by stable isotopes and hydrous pyrolysis of Lower Palaeozoic source rocks. Chemical Geology 345, 62-76.

Kotarba, M., Lewan, M. and Więcław, D. (2014a) Shale Gas and Oil Potential of Lower Palaeozoic Strata in the Polish Baltic Basin by Hydrous Pyrolysis. Conference: Fourth EAGE Shale Workshop.

Kotarba, M., Więcław, D., Dziadzio, P., Kowalski, A., Kosakowski, P. and Bilkiewicz, E. (2014b) Organic geochemical study of source rocks and natural gas and their genetic correlation in the eastern part of the Polish Outer Carpathians and Palaeozoic–Mesozoic basement. Marine and Petroleum Geology 56, 97-122.

Kribek, B., Zak, K., Spangenberg, J.E., Jehlicka, J., Prokes, S. and Kominek, J. (1999) Bitumens in the late Variscan hydrothermal vein-type uranium deposit of Pribram, Czech Republic; sources, radiation-induced alteration, and relation to mineralization. Economic Geology 94, 1093-1114.

Kudryavtsev, N. (1951) Against the organic hypothesis of the origin of petroleum. Neftianoye Khozyaistvo 9, 17-29.

Kuhn, P.P., di Primio, R., Hill, R., Lawrence, J.R. and Horsfield, B. (2012) Three-dimensional modeling study of the low-permeability petroleum system of the Bakken Formation. AAPG Bulletin 96, 1867-1897.

Kvenvolden, K.A. (1966) Evidence for transformations of normal fatty acids in sediments. Advances in organic geochemistry 1968, 355-366.

Lakshmanan, C.C., Bennett, M.L. and White, N. (1991) Implications of multiplicity in kinetic parameters to petroleum exploration: distributed activation energy models. Energy & Fuels 5, 110-117.

Landais, P. (1993) Bitumens in uranium deposits, Bitumens in ore deposits. Springer, pp. 213-238.

Landais, P. (1996) Organic geochemistry of sedimentary uranium ore deposits. Ore Geol Rev 11, 33-51.

Lange, G. and Freyhoff, G. (1991) GEOLOGIE UND BERGBAU IN DER URANLAGERSTATTE RONNEBURG/THURINGEN. Erzmetall 44, 264-269.

Larsen, J.W. and Hu, J. (2006) Kerogen chemistry. 8. Hydrous pyrolysis of rundle kerogen: Source of the oxygen in CO2 and mineral catalysis. Energy & fuels 20, 278-280.

Larter, S. (1984) Application of analytical pyrolysis techniques to kerogen characterization and fossil fuel exploration/exploitation, Analytical pyrolysis. Butterworths London, pp. 212-272.

Larter, S., Huang, H., Adams, J., Bennett, B. and Snowdon, L.R. (2012) A practical biodegradation scale for use in reservoir geochemical studies of biodegraded oils. Organic Geochemistry 45, 66-76.

Larter, S.R., Bowler, B.F.J., Li, M. and Chen, M. (1996) Molecular indicators of secondary oil migration distances. Nature 383, 593-597.

Law, B.E. (1988) Coal-bed methane. Petroleum Systems of the United States, 52.

Lawrence, S., Coster, P. and Ireland, R. (1987) Structural development and petroleum potential of the northern flanks of the Bowland Basin (Carboniferous) Northwest England. Petroleum geology of north-west Europe 1, 225-233.

Lazauskiene, J., Sliaupa, S., Brazauskas, A. and Musteikis, P. (2003) Sequence stratigraphy of the Baltic Silurian succession: tectonic control on the foreland infill. Geological Society, London, Special Publications 208, 95-115.

Leckie, D.A., Singh, C., Goodarzi, F. and Wall, J.H. (1990) Organic-rich, radioactive marine shale: a case study of a shallow-water condensed section, Cretaceous Shaftesbury Formation, Alberta, Canada. Journal of Sedimentary Research 60.

Lecomte, A., Cathelineau, M., Michels, R., Peiffert, C. and Brouand, M. (2017) Uranium mineralization in the Alum Shale Formation (Sweden): Evolution of a U-rich marine black shale from sedimentation to metamorphism. Ore Geol Rev 88, 71-98.

Leeder, M. (1988) Recent developments in Carboniferous geology: a critical review with implications for the British Isles and NW Europe. Proceedings of the Geologists' Association 99, 73-100.

Leventhal, J. (1991) Comparison of organic geochemistry and metal enrichment in two black shales: Cambrian Alum Shale of Sweden and Devonian Chattanooga Shale of United States. Mineralium Deposita 26, 104-112.

Leventhal, J.S. (1981) Pyrolysis gas chromatography-mass spectrometry to characterize organic matter and its relationship to uranium content of Appalachian Devonian black shales. Geochimica et Cosmochimica Acta 45, 883-889.

Leventhal, J.S., Daws, T.A. and Frye, J.S. (1986) Organic geochemical analysis of sedimentary organic matter associated with uranium. Applied geochemistry 1, 241-247.

Leventhal, J.S. and Threlkeld, C.N. (1978) Carbon-13/carbon-12 isotope fractionation of organic matter associated with uranium ores induced by alpha irradiation. Science 202, 430-432.

Lewan, B.M.D. and Henry, A.A. (1999) Gas : Oil Ratios for Source Rocks Containing Type-I , -II , -IIS , and -III Kerogens as Determined by Hydrous Pyrolysis. USGS report.

Lewan, M. and Buchardt, B. (1989) Irradiation of organic matter by uranium decay in the Alum Shale, Sweden. Geochimica et Cosmochimica Acta 53, 1307-1322.

Lewan, M., Kotarba, M., Więcław, D. and Piestrzyński, A. (2008) Evaluating transition-metal catalysis in gas generation from the Permian Kupferschiefer by hydrous pyrolysis. Geochimica et Cosmochimica Acta 72, 4069-4093.

Lewan, M., Spiro, B., Illich, H., Raiswell, R., Mackenzie, A., Durand, B., Manning, D., Comet, P., Berner, R. and De Leeuw, J. (1985) Evaluation of petroleum generation by hydrous pyrolysis experimentation [and discussion]. Philosophical Transactions of the Royal Society of London A: Mathematical, Physical and Engineering Sciences 315, 123-134.

Lewan, M., Winters, J. and McDonald, J. (1979) Generation of oil-like pyrolyzates from organic-rich shales. Science 203, 897-899.

Lewan, M.D. (1997) Experiments on the role of water in petroleum formation. Geochimica et Cosmochimica Acta 61, 3691-3723.

Lewan, M.D., Dolan, M.P. and Curtis, J.B. (2014) Effects of smectite on the oil-expulsion efficiency of the Kreyenhagen Shale, San Joaquin Basin, California, based on hydrous-pyrolysis experiments. AAPG Bulletin 98, 1091-1109.

Lewan, M.D. and Ruble, T.E. (2002) Comparison of petroleum generation kinetics by isothermal hydrous and nonisothermal open-system pyrolysis. Organic Geochemistry 33, 1457-1475.

Li, M., Larter, S., Stoddart, D. and Bjorøy, M. (1995) Fractionation of pyrrolic nitrogen compounds in petroleum during migration: derivation of migration-related geochemical parameters. Geological Society, London, Special Publications 86, 103-123.

Liao, Y., Shi, Q., Hsu, C.S., Pan, Y. and Zhang, Y. (2012) Distribution of acids and nitrogen-containing compounds in biodegraded oils of the Liaohe Basin by negative ion ESI FT-ICR MS. Organic Geochemistry 47, 51-65.

Lind, S. and Bardwell, D. (1926) The chemical action of gaseous ions produced by alpha particles. IX. Saturated hydrocarbons. J Am Chem Soc 48, 2335-2351.

Lindgreen, H. and Drits, V.A. (2000) Illite-smectite structural changes during metamorphism in black Cambrian Alum shales from the Baltic area. American Mineralogist 85, 1223-1238.

Liu, P., Li, M., Jiang, Q., Cao, T. and Sun, Y. (2015) Effect of secondary oil migration distance on composition of acidic NSO compounds in crude oils determined by negative-ion electrospray Fourier transform ion cyclotron resonance mass spectrometry. Organic Geochemistry 78, 23-31.

Loog, A., Kurvits, T., Aruvali, J. and Petersell, V. (2001) Grain size analysis and mineralogy of the Tremadocian Dictyonema shale in Estonia. Oil Shale 18, 281-297.

Loucks, R.G. and Ruppel, S.C. (2007) Mississippian Barnett Shale: Lithofacies and depositional setting of a deep-water shale-gas succession in the Fort Worth Basin, Texas. AAPG Bulletin 91, 579-601.

Love, G.D., Grosjean, E., Stalvies, C., Fike, D.A., Grotzinger, J.P., Bradley, A.S., Kelly, A.E., Bhatia, M., Meredith, W., Snape, C.E., Bowring, S.A., Condon, D.J. and Summons, R.E. (2009) Fossil steroids record the appearance of Demospongiae during the Cryogenian period. Nature 457, 718-721.

Loydell, D., Butcher, A., Frýda, J., Lüning, S. and Fowler, M. (2009) Lower Silurian "hot shales" in Jordan: a new depositional model. Journal of Petroleum Geology 32, 261-270.

Lu, S.-T. and Kaplan, I.R. (1989) Pyrolysis of kerogens in the absence and presence of montmorillonite—II. Aromatic hydrocarbons generated at 200 and 300° C. Organic geochemistry 14, 501-510.

Lu, S.-T., Ruth, E. and Kaplan, I.R. (1989) Pyrolysis of kerogens in the absence and presence of montmorillonite—I. The generation,

degradation and isomerization of steranes and triterpanes at 200 and 300° C. Organic Geochemistry 14, 491-499.

Lüning, S., Shahin, Y.M., Loydell, D., Al-Rabi, H.T., Masri, A., Tarawneh, B. and Kolonic, S. (2005) Anatomy of a world-class source rock: Distribution and depositional model of Silurian organic-rich shales in Jordan and implications for hydrocarbon potential. AAPG Bulletin 89, 1397-1427.

Lutz, M., Kaasschieter, P. and van Wijhe, H. (1975) PD 2 (3) geological factors controlling Rotliegend gas accumulations in the Mid-European Basin, 9th World Petroleum Congress. World Petroleum Congress.

Mackenzie, A., Hoffmann, C. and Maxwell, J. (1981) Molecular parameters of maturation in the Toarcian shales, Paris Basin, France—III. Changes in aromatic steroid hydrocarbons. Geochimica et Cosmochimica Acta 45, 1345-1355.

Mackenzie, A., Leythaeuser, D., Muller, P., Quigley, T. and Radke, M. (1988) The movement of hydrocarbons in shales. Nature.

Mahlstedt, N., di Primio, R. and Horsfield, B. (2013) GOR-Fit-From Liquids to Late Gas: Deconvoluting Primary from Secondary Gas Generation Kinetics. Book of Abstracts of the Communications, 26th International Meeting on Organic Geochemistry - IMOG (Costa Adeje, Tenerife Spain 2013), pp. 193-194.

Mahlstedt, N., Horsfield, B., Wilkes, H. and Poetz, S. (2016) Tracing the Impact of Fluid Retention on Bulk Petroleum Properties Using Nitrogen-Containing Compounds. Energy & Fuels 30, 6290-6305.

Mahlstedt, N.L. (2012) Evaluating the late gas potential of source rocks stemming from different sedimentary environments genehmigte Dissertation, pp. 370pp-370pp.

Makadi, K.S. (1983) Étude expérimentale des interactions entre matière organique-matrice minérale au cours de la pyrolyse. IFP.

Mango, F.D. (1987) An invariance in the isoheptanes of petroleum. Science 237, 514-517.

Mango, F.D. (1990) The origin of light hydrocarbons in petroleum: a kinetic test of the steady-state catalytic hypothesis. Geochimica et Cosmochimica Acta 54, 1315-1323.

Mango, F.D. (1991) The stability of hydrocarbons under the time–temperature conditions of petroleum genesis. Nature.

Mango, F.D. (1992) Transition metal catalysis in the generation of petroleum: A genetic anomaly in Ordovician oils. Geochimica et Cosmochimica Acta 56, 3851-3854.

Mango, F.D. (1994) The origin of light hydrocarbons in petroleum: Ring preference in the closure of carbocyclic rings. Geochimica et Cosmochimica Acta 58, 895-901.

Mango, F.D. (1997) Review paper: The light hydrocarbons in petroleum: a critical review. Organic Geochemistry 26, 417-440.

Mango, F.D. (2007) In situ conversion of heavy hydrocarbons to catalytic gas. US Patent App. 11/856,566 2.

Mango, F.D. (2010) "Distinguishing gases derived from oil cracking and kerogen maturation: Insights from laboratory pyrolysis experiments." Guo Liguo, Xiao Xianming, Tian Hui, Song Zhiguang, 2009, Organic Geochemistry 40, 1074–1084. Organic Geochemistry 41, 719-720.

Mango, F.D. and Hightower, J. (1997) The catalytic decomposition of petroleum into natural gas. Geochimica et Cosmochimica Acta 61, 5347-5350.

Marshall, A.G., Hendrickson, C.L. and Jackson, G.S. (1998) Fourier transform ion cyclotron resonance mass spectrometry: a primer. Mass spectrometry reviews 17, 1-35.

Marshall, A.G. and Rodgers, R.P. (2004) Petroleomics: The next grand challenge for chemical analysis. Accounts of Chemical Research 37, 53-59.

Mayer, L.M. (1994) Surface area control of organic carbon accumulation in continental shelf sediments. Geochimica et Cosmochimica Acta 58, 1271-1284.

McCain, W.D. (1990) The properties of petroleum fluids. PennWell Books.

McKenzie, D., Mackenzie, A.S., Maxwell, J. and Sajgo, C. (1983) Isomerization and aromatization of hydrocarbons in stretched sedimentary basins.

McKirdy, D., Aldridge, A. and Ypma, P. (1981) A geochemical comparison of some crude oils from pre-Ordovician carbonate rocks, in: Bjorøy, M. (Ed.), Advances in organic geochemistry. John Wiley & Sons Ltd, University of Bergen, Norway, pp. 99-107.

Meinschein, W. (1961) Significance of hydrocarbons in sediments and petroleum. Geochimica et Cosmochimica Acta 22, 58-64.

Mendeleev, D. (1877) L'origine du petrole. Revue Scientifique 8, 409-416.

Michels, R., Landais, P., Torkelson, B.E. and Philp, R.P. (1995) Effects of effluents and water pressure on oil generation during confined pyrolysis and high-pressure hydrous pyrolysis. Geochimica et Cosmochimica Acta 59, 1589-1604.

Modliński, Z. and Podhalańska, T. (2010) Outline of the lithology and depositional features of the lower Paleozoic strata in the Polish part of the Baltic region. Geological Quarterly 54, 109-121.

Modliński, Z. and Szymański, B. (1997) The Ordovician lithostratigraphy of the Peribaitic Depression (NE Poland). Geological Quarterly 41, 273-288.

Moldowan, J.M., Dahl, J., Huizinga, B.J., Fago, F.J., Hickey, L.J., Peakman, T.M. and Taylor, D.W. (1994) The molecular fossil record of oleanane and its relation to angiosperms. Science, 768-771.

Moldowan, J.M., Fago, F.J., Lee, C.Y., Jacobson, S.R., Watt, D.S., Slougui, N.-E., Jeganathan, A. and Young, D.C. (1990) Sedimentary 24-n-

propylcholestanes, molecular fossils diagnostic of marine algae. Science 247, 309-312.

Moldowan, J.M., Seifert, W.K. and Gallegos, E.J. (1985) Relationship between petroleum composition and depositional environment of petroleum source rocks. AAPG bulletin 69, 1255-1268.

Møller, L.N. and Friis, H. (1999) Petrographic evidence for hydrocarbon migration in Lower Cambrian sandstones, Bornholm, Denmark. Bulletin of the Geological Society of Denmark 45, 117-127.

Momper, J.A. (1979) Domestic Oil Reserves Forecasting Method and Assessment of Regional Potentials: ABSTRACT. AAPG Bulletin 63, 497-498.

Monthioux, M., Landais, P. and Monin, J.-C. (1985) Comparison between natural and artificial maturation series of humic coals from the Mahakam delta, Indonesia. Organic Geochemistry 8, 275-292.

Mossman, D.J., Nagy, B. and Davis, D.W. (1993) Hydrothermal alteration of organic matter in uranium ores, Elliot Lake, Canada: implications for selected organic-rich deposits. Geochimica et cosmochimica acta 57, 3251-3259.

Motuza, G., Kepezinskas, P. and Šliaupa, S. (1994) Diabases from the well D-1 in the Baltic Sea. Geologija 16, 16-20.

Motuzaa, G., Šliaupab, S. and Timmermanc, M.J. (2015) Geochemistry and 40Ar/39Ar age of Early Carboniferous dolerite sills in the southern Baltic Sea. Estonian Journal of Earth Sciences 64, 3.

Mullen, J. (2010) Petrophysical characterization of the Eagle Ford Shale in south Texas, Canadian Unconventional Resources and International Petroleum Conference. Society of Petroleum Engineers.

Muntendam-Bos, A.G. (2009) Inventory non-conventional gas. TNO Built Environment and Geosciences.

Nielsen, A.T. and Schovsbo, N.H. (2006) Cambrian to basal Ordovician lithostratigraphy in southern Scandinavia. Bulletin of the Geological Society of Denmark 53, 47-92.

Oakwood, T., Shriver, D., Fall, H., McAleer, W. and Wunz, P. (1952) Optical activity of petroleum. Industrial & Engineering Chemistry 44, 2568-2570.

Obst, K. (2000) Permo-Carboniferous dyke magmatism on the Danish island Bornholm. Neues Jahrbuch Fur Geologie Und Palaontologie-Abhandlungen 218, 243-266.

Oldenburg, T.B.P., Brown, M., Bennett, B. and Larter, S.R. (2014) The impact of thermal maturity level on the composition of crude oils, assessed using ultra-high resolution mass spectrometry. Organic Geochemistry 75, 151-168.

Oliver, N., Pearson, P., Holcombe, R. and Ord, A. (1999) Mary Kathleen metamorphic – hydrothermal uranium – rare - earth element deposit: ore genesis and numerical model of coupled deformation and fluid flow. Australian Journal of Earth Sciences 46, 467-484.

Osborne, M.J. and Swarbrick, R.E. (1997) Mechanisms for generating overpressure in sedimentary basins: a reevaluation. AAPG bulletin 81, 1023-1041.

Osmond, J. and Cowart, J. (1976) The theory and uses of natural uranium isotopic variations in hydrology. Atomic Energy Review 14, 621-679.

Öztaş, N. and Yürüm, Y. (2000) Pyrolysis of Turkish Zonguldak bituminous coal. Part 1. Effect of mineral matter. Fuel 79, 1221-1227.

Pakarinen, J.M., Teräväinen, M.J., Pirskanen, A., Wickström, K. and Vainiotalo, P. (2007) A positive-ion electrospray ionization Fourier transform ion cyclotron resonance mass spectrometry study of Russian and North Sea crude oils and their six distillation fractions. Energy & Fuels 21, 3369-3374.

Palacas, J.G., Anders, D.E. and King, J.D. (1984) South Florida basin--a prime example of carbonate source rocks of petroleum, in: Palacas, J.G. (Ed.), Petroleum Geochemistry and Source Rock Potential of Carbonate Rocks. American Association of Petroleum Geologists, Tulsa, Oklahoma, pp. 71-96.

Pan, C., Geng, A., Zhong, N. and Liu, J. (2010) Kerogen pyrolysis in the presence and absence of water and minerals: Steranes and triterpenoids. Fuel 89, 336-345.

Pan, C., Geng, A., Zhong, N., Liu, J. and Yu, L. (2007) Kerogen pyrolysis in the presence and absence of water and minerals. 1. Gas components. Energy & Fuels, 416-427.

Pan, Y., Liao, Y., Shi, Q. and Hsu, C.S. (2013) Acidic and Neutral Polar NSO Compounds in Heavily Biodegraded Oils Characterized by Negative-Ion ESI FT-ICR MS. Energy & Fuels 27, 2960-2973.

Pater, C.J.D. and Baisch, S. (2011) Geomechanical study of Bowland Shale seismicity. Synthesis Report.

Patterson, J., Ramsden, A., Dale, L. and Fardy, J. (1986) Geochemistry and mineralogical residences of trace elements in oil shales from Julia Creek, Queensland, Australia. Chemical geology 55, 1-16.

Pedersen, J.H., Karlsen, D.A., Spjeldnæs, N., Backer-Owe, K., Lie, J.E. and Brunstad, H. (2007) Lower Paleozoic petroleum from southern Scandinavia: Implications to a Paleozoic petroleum system offshore southern Norway. AAPG Bulletin 91, 1189-1212.

Pelet, R. (1994) Comments on the paper "The effects of the mineral matrix on the determination of kinetic parameters using modified Rock-Eval pyrolysis" by H. Dembicki Jr, Org. Organic geochemistry 21, 979-981.

Pepper, A.S. and Corvi, P.J. (1995) Simple kinetic models of petroleum formation.Part I:oil and gas generation from kerogen. Marine and Petroleum Geology 12, 291-319.

Pepper, A.S. and Dodd, T.a. (1995) Simple kinetic models of petroleum formation. Part II: oil-gas cracking. Marine and Petroleum Geology 12, 321-340.

Perry Jr, E.A. and Hower, J. (1972) Late-stage dehydration in deeply buried pelitic sediments. AAPG Bulletin 56, 2013-2021.

Peters, K. (1986) Guidelines for evaluating petroleum source rock using programmed pyrolysis. AAPG Bulletin 70, 318-329.

Peters, K. and Moldowan, J. (1991) Effects of source, thermal maturity, and biodegradation on the distribution and isomerization of homohopanes in petroleum. Organic geochemistry 17, 47-61.

Peters, K.E. and Cassa, M.R. (1994) Applied source rock geochemistry. AAPG Memoir.

Peters, K.E., Coutrot, D., Nouvelle, X., Ramos, L.S., Rohrback, B.G., Magoon, L.B. and Zumberge, J.E. (2013) Chemometric differentiation of crude oil families in the San Joaquin Basin, California. AAPG bulletin 97, 103-143.

Peters, K.E., Fraser, T.H., Amris, W., Rustanto, B. and Hermanto, E. (1999) Geochemistry of crude oils from eastern Indonesia. AAPG Bulletin 83, 1927-1942.

Peters, K.E., Walters, C.C. and Mankiewicz, P.J. (2006) Evaluation of kinetic uncertainty in numerical models of petroleum generation. AAPG Bulletin 90, 387-403.

Peters, K.E., Walters, C.C. and Moldowan, J.M. (2005) The biomarker guide: biomarkers and isotopes in the environment and human history. Cambridge University Press, New York.

Peters, K.E., Wright, T.L., Ramos, L.S., Zumberge, J.E. and Magoon, L.B. (2016) Chemometric recognition of genetically distinct oil families in the Los Angeles basin, California. AAPG Bulletin 100, 115-135.

Petersen, H.I., Schovsbo, N.H. and Nielsen, A.T. (2013) Reflectance measurements of zooclasts and solid bitumen in Lower Paleozoic shales, southern Scandinavia: Correlation to vitrinite reflectance. International Journal of Coal Geology 114, 1-18.

Philippi, G. (1965) On the depth, time and mechanism of petroleum generation. Geochimica et Cosmochimica Acta 29, 1021-1049.

Philp, R.t. and Gilbert, T. (1986) Biomarker distributions in Australian oils predominantly derived from terrigenous source material. Organic Geochemistry 10, 73-84.

Pierce, A.P., Mytton, J.W. and Barnett, P.R. (1958) Geochemistry of uranium in organic substances in petroliferous rocks. Geological Survey, Washington, DC.

Poetz, S., Horsfield, B. and Wilkes, H. (2014) Maturity-Driven Generation and Transformation of Acidic Compounds in the Organic-Rich Posidonia Shale as Revealed by Electrospray Ionization Fourier Transform Ion Cyclotron Resonance Mass Spectrometry. Energy & Fuels 28, 4877-4888.

Pollastro, R.M. (2007) Total petroleum system assessment of undiscovered resources in the giant Barnett Shale continuous (unconventional) gas accumulation, Fort Worth Basin, Texas. AAPG Bulletin 91, 551-578.

Pompeckj, J. (1901) Der Jura zwischen Regensburg und Regenstauf: Geognostische Jahreshefte, v. 14.

Pool, W., Geluk, M., Abels, J. and Tiley, G. (2012) Assessment of an unusual European shale gas play: the Cambro-Ordovician alum shale, southern Sweden. SPE/EAGE European ….

Poprawa, P., Šliaupa, S., Stephenson, R. and Lazauskien, J. (1999) Late Vendian–Early Palaeozoic tectonic evolution of the Baltic Basin: regional tectonic implications from subsidence analysis. Tectonophysics 314, 219-239.

Powers, M.C. (1967) Fluid-release mechanisms in compacting marine mudrocks and their importance in oil exploration. AAPG bulletin 51, 1240-1254.

Pratt, W.E. (1947) Petroleum on continental shelves. AAPG Bulletin 31, 657-672.

Price, L.C. and Schoell, M. (1995) Constraints on the origins of hydrocarbon gas from compositions of gases at their site of origin. Nature 378, 368.

Priem, H., Mulder, F., Boelrijk, N., Hebeda, E., Verschure, R. and Verdurmen, E.T. (1968) Geochronological and palaeomagnetic reconnaissance survey in parts of central and southern Sweden. Physics of the Earth and Planetary Interiors 1, 373-380.

Quigley, T., Mackenzie, A. and Gray, J. (1987) Kinetic theory of petroleum generation. Collection colloques et séminaires-Institut français du pétrole, 649-665.

Radke, M., Willsch, H. and Welte, D.H. (1980) Preparative hydrocarbon group type determination by automated medium pressure liquid chromatography. Analytical Chemistry 52, 406-411.

Raji, M., Cornford, C., Pather, A. and Satterfield, D. (2013) Unconventional oil and gas potential of the Widmerpool Gulf in the East Midlands Province of England. Unconventional Resources Technology Conference (URTEC).

Reynolds, J.G. and Burnham, A.K. (1995) Comparison of kinetic analysis of source rocks and kerogen concentrates. Organic Geochemistry.

Reynolds, J.G., Burnham, A.K. and Mitchell, T.O. (1995) Kinetic analysis of California petroleum source rocks by programmed temperature micropyrolysis. Organic geochemistry 23, 109-120.

Rice, D.D. and Claypool, G.E. (1981) Generation, accumulation, and resource potential of biogenic gas. AAPG Bulletin 65, 5-25.

Rice, F. (1931) The thermal decomposition of organic compounds from the standpoint of free radicals. I. Saturated hydrocarbons. J Am Chem Soc 53, 1959-1972.

Robl, T.L. and Davis, B.H. (1993) Comparison of the HF-HCl and HF-BF 3 maceration techniques and the chemistry of resultant organic concentrates. Organic Geochemistry 20, 249-255.

Romer, R.L. and Hahne, K. (2010) Life of the Rheic Ocean: scrolling through the shale record. Gondwana Res 17, 236-253.

Rubinstein, I., Sieskind, O. and Albrecht, P. (1975) Rearranged sterenes in a shale: occurrence and simulated formation. Journal of the Chemical Society, Perkin Transactions 1 1, 1833-1836.

Rudakov, G. (1967) Recent developments in the theory of the non-biogenic origin of petroleum. Chemical Geology 2, 179-185.

Salmon, V., Derenne, S., Lallier-Verges, E., Largeau, C. and Beaudoin, B. (2000) Protection of organic matter by mineral matrix in a Cenomanian black shale. Organic Geochemistry 31, 463-474.

Sandström, B., Tullborg, E.L., Torres, T.D. and Ortiz, J.E. (2006) The occurrence and potential origin of asphaltite in bedrock fractures, Forsmark, central Sweden. GFF 128, 233-242.

Sanei, H., Petersen, H.I., Schovsbo, N.H., Jiang, C. and Goodsite, M.E. (2014) Petrographic and geochemical composition of kerogen in the Furongian (U. Cambrian) Alum Shale, central Sweden: Reflections on the petroleum generation potential. International Journal of Coal Geology 132, 158-169.

Saxby, J. (1970) Isolation of kerogen in sediments by chemical methods. Chemical Geology 6, 173-184.

Saxby, J. and Riley, K. (1984) Petroleum generation by laboratory-scale pyrolysis over six years simulating conditions in a subsiding basin. Nature.

Schenk, H.J. and Horsfield, B. (1993) Kinetics of petroleum generation by programmed-temperature closed-versus open-system pyrolysis. Geochimica et Cosmochimica Acta 57, 623-630.

Schenk, H.J., Horsfield, B. and Krooss, B. (1997) Kinetics of petroleum formation and cracking. Petroleum and basin evolution.

Schleicher, M., Koster, J., Kulke, H. and Weil, W. (1998) Reservoir and source-rock characterisation of the early Palaeozoic interval in the peribaltic syneclise, northern Poland. Journal of Petroleum Geology 21, 33-56.

Schmoker, J.W. (1981) Determination of organic-matter content of Appalachian Devonian shales from gamma-ray logs. AAPG Bulletin 65, 1285-1298.

Schoell, M. (1980) The hydrogen and carbon isotopic composition of methane from natural gases of various origins. Geochimica et Cosmochimica Acta 44, 649-661.

Schovsbo, N.H. (2001) Why barren intervals? A taphonomic case study of the Scandinavian Alum Shale and its faunas. Lethaia 34, 271-285.

Schovsbo, N.H. (2002) Uranium enrichment shorewards in black shales: A case study from the Scandinavian Alum Shale. GFF 124, 107-115.

Schovsbo, N.H. (2003) The geochemistry of Lower Palaeozoic sediments deposited on the margins of Baltica. Bulletin of the Geological Society of Denmark 50, 11-27.

Schovsbo, N.H., Esbensen, K.H., Nielsen, A.T., Derbez, E., Gaucher, E.C., Poirier-Coutansais, X., Riou, A., Tallone, P. and Milton-Taylor, D. (2015) Rock Types in the Scandinavian Alum Shale Resource Play: Definitions and Predictions, 77th EAGE Conference & Exhibition 2015, IFEMA, Madrid, Spain, pp. 1-5.

Schovsbo, N.H., Nielsen, A.T. and Gautier, D.L. (2014) The Lower Palaeozoic shale gas play in Denmark. Geological Survey of Denmark and Greenland Bulletin 31, 19-22.

Schovsbo, N.H., Nielsen, A.T., Klitten, K., Mathiesen, A. and Rasmussen, P. (2011) Shale gas investigations in Denmark: Lower Palaeozoic shales on Bornholm. Geological Survey of Denmark and Greenland Bulletin 23, 9-12.

Schulz, H.-M., Biermann, S., van Berk, W., Krüger, M., Straaten, N., Bechtel, A., Wirth, R., Lüders, V., Schovsbo, N.H. and Crabtree, S. (2015) From shale oil to biogenic shale gas: Retracing organic–inorganic interactions in the Alum Shale (Furongian–Lower Ordovician) in southern Sweden. AAPG Bulletin 99, 927-956.

Schulz, H.-M., Horsfield, B. and Sachsenhofer, R. (2010) Shale gas in Europe: a regional overview and current research activities, in: Vining, B.A., Pickering, S.C. (Eds.), Geological Society, London, Petroleum Geology Conference series. Geological Society of London, London, pp. 1079-1085.

Seifert, W.K. and Moldowan, J.M. (1981) Paleoreconstruction by biological markers. Geochimica et Cosmochimica Acta 45, 783-794.

Selley, R. (1987) British shale gas potential scrutinized. Oil Gas J 85, 62-64.

Selley, R.C. (2005) UK shale-gas resources. Geological Society, London, Petroleum Geology Conference series 6, 707-714.

Selley, R.C. (2012) UK shale gas: the story so far. Marine and petroleum geology 31, 100-109.

Semyrka, G., Jarzyna, J., Semyrka, R., Kaźmierczuk, M. and Pikulski, L. (2010) Reservoir parameters of lithostratigraphic successions of the lower Paleozoic strata in the Polish part of the Baltic region based on laboratory studies and well logs. Geological Quarterly 54, 227-240.

Serra, O. (1983) Fundamentals of well-log interpretation.

Shaw, D.B. and Weaver, C.E. (1965) The mineralogical composition of shales. Journal of Sedimentary Research 35.

Sheppard, C.W. and Burton, V.L. (1946) The Effects of Radioactivity on Fatty Acids1, 1a. J Am Chem Soc 68, 1636-1639.

Shimoyama, A. and Johns, W.D. (1971) Catalytic conversion of fatty acids to petroleum-like paraffins and their maturation. Nature 232, 140-144.

Silliman, J.E., Li, M., Yao, H. and Hwang, R. (2002) Molecular distributions and geochemical implications of pyrrolic nitrogen compounds in the Permian Phosphoria Formation derived oils of Wyoming. Organic Geochemistry 33, 527-544.

Simoneit, B.R. and Lonsdale, P.F. (1982) Hydrothermal petroleum in mineralized mounds at the seabed of Guaymas Basin. Nature 295, 198-202.

Sing, K.S. (1985) Reporting physisorption data for gas/solid systems with special reference to the determination of surface area and porosity (Recommendations 1984). Pure and applied chemistry 57, 603-619.

Sinninghe Damsté, J.S., Rijpstra, W.I.C., Kock-van Dalen, A., De Leeuw, J.W. and Schenck, P. (1989) Quenching of labile functionalised lipids by inorganic sulphur species: evidence for the formation of sedimentary organic sulphur compounds at the early stages of diagenesis. Geochimica et Cosmochimica Acta 53, 1343-1355.

Sivhed, U. (2004) Upper Ordovician carbonate mounds on Gotland, central Baltic Sea: distribution, composition and reservoir characteristics. Journal of Petroleum Geology 27, 115-140.

Šliaupa, S. and Hoth, P. (2011) Geological evolution and resources of the Baltic Sea area from the Precambrian to the Quaternary, in: Harff, J., Björck, S., Hoth, P. (Eds.), The Baltic Sea Basin. Springer Berlin Heidelberg, pp. 13-51.

Smith, N. (1995) Unconventional hydrocarbons: changing exploration strategies. Earthwise, 14-15.

Smith, N., Turner, P. and Williams, G. (2010) UK data and analysis for shale gas prospectivity. Geological Society, London, Petroleum Geology Conference series.

Smith, P.V. (1952) The occurrence of hydrocarbons in recent sediments from the Gulf of Mexico. Science 116, 437-439.

Snäll, S. (1988) Mineralogy and maturity of the alum shales of south-central Jamtland, Sweden. Sveriges geologiska undersökning, Uppsala.

Snowdon, L.R. (2001) Natural gas composition in a geological environment and the implications for the processes of generation and preservation. Organic Geochemistry 32, 913-931.

Sopher, D., Erlström, M., Bell, N. and Juhlin, C. (2016) The structure and stratigraphy of the sedimentary succession in the Swedish sector of the Baltic Basin: New insights from vintage 2D marine seismic data. Tectonophysics 676, 90-111.

Spears, D. and Amin, M. (1981) Geochemistry and mineralogy of marine and non - marine Namurian black shales from the Tansley Borehole, Derbyshire. Sedimentology 28, 407-417.

Stahl, W.J. and Carey, B.D. (1975) Source-rock identification by isotope analyses of natural gases from fields in the Val Verde and Delaware basins, west Texas. Chemical Geology 16, 257-267.

Stainforth, J.G. (2009) Practical kinetic modeling of petroleum generation and expulsion. Marine and Petroleum Geology 26, 552-572.

Stouge, S. and Nielsen, A.T. (2003) An integrated biostratigraphical analysis of the Volkhov-Kunda (Lower Ordovician) succession at Fågelsång,

Scania, Sweden. Bulletin of the Geological Society of Denmark 50, 75-94.

Strachan, M., Alexander, R., Van Bronswijk, W. and Kagi, R. (1989) Source and heating rate effects upon maturity parameters based on ratios of 24-ethylcholestane diastereomers. Journal of Geochemical Exploration 31, 285-294.

Swanson, V.E. (1960) Oil yield and uranium content of black shales. Geological Survey, Washington, DC (USA).

Swanson, V.E. and Swanson, V.E. (1961) Geology and geochemistry of uranium in marine black shales: a review. US Government Printing Office Washington, DC.

Tan, J., Horsfield, B., Mahlstedt, N., Zhang, J., di Primio, R., Vu, T.A.T., Boreham, C.J., van Graas, G. and Tocher, B.A. (2013) Physical properties of petroleum formed during maturation of Lower Cambrian shale in the upper Yangtze Platform, South China, as inferred from PhaseKinetics modelling. Marine and Petroleum Geology 48, 47-56.

Tannenbaum, E., Huizinga, B.J. and Kaplan, I. (1986a) Role of minerals in thermal alteration of organic matter--II: a material balance. AAPG bulletin 70, 1156-1165.

Tannenbaum, E. and Kaplan, I.R. (1985a) Low-Mr hydrocarbons generated during hydrous and dry pyrolysis of kerogen.

Tannenbaum, E. and Kaplan, I.R. (1985b) Role of minerals in the thermal alteration of organic matter—I: Generation of gases and condensates under dry condition. Geochimica et Cosmochimica Acta 49, 2589-2604.

Tannenbaum, E., Ruth, E. and Kaplan, I.R. (1986b) Steranes and triterpanes generated from kerogen pyrolysis in the absence and presence of minerals. Geochimica et cosmochimica acta 50, 805-812.

Tao, S., Wang, C., Du, J., Liu, L. and Chen, Z. (2015) Geochemical application of tricyclic and tetracyclic terpanes biomarkers in crude oils of NW China. Marine and Petroleum Geology 67, 460-467.

Tarafa, M.E., Hunt, J.M. and Ericsson, I. (1983) Effect of hydrocarbon volatility and adsorption on source-rock pyrolysis. Journal of Geochemical Exploration 18, 75-85.

Tegelaar, E., De Leeuw, J., Derenne, S. and Largeau, C. (1989) A reappraisal of kerogen formation. Geochimica et Cosmochimica Acta 53, 3103-3106.

Tegelaar, E.W. and Noble, R.a. (1994) Kinetics of hydrocarbon generation as a function of the molecular structure of kerogen as revealed by pyrolysis-gas chromatography. Organic Geochemistry 22, 543-574.

ten Haven, H., de Leeuw, J., Rullkotter, J. and Sinninghe Damsté, J. (1987) Restricted utility of the pristane/phytane ratio as a palaeoenvironmental indicator? Nature 330, 641-643.

Teräväinen, M.J., Pakarinen, J.M., Wickström, K. and Vainiotalo, P. (2007) Comparison of the composition of Russian and North Sea crude oils

and their eight distillation fractions studied by negative-ion electrospray ionization Fourier transform ion cyclotron resonance mass spectrometry: The effect of suppression. Energy & fuels 21, 266-273.

Thickpenny, A. (1984) The sedimentology of the Swedish Alum Shales. Geological Society, London, Special Publications 15, 511-525.

Tian, Y. (2010) An Investigation of regional variations of Barnett shale reservoir properties, and resulting variability of hydrocarbon composition and well performance. Texas A&M University.

Tissot, B.P. and Welte, D.H. (1984) Petroleum formation and occurrence.

Tolmacheva, T.J., Koren, T.N., Holmer, L.E., Popov, L.E. and Raevskaya, E. (2001) The Hunneberg Stage (Ordovician) in the area east of St. Petersburg, north-western Russia. Paläontologische Zeitschrift 74, 543-561.

Treibs, A. (1934) Chlorophyll - und Häminderivate in bituminösen Gesteinen, Erdölen, Erdwachsen und Asphalten. Ein Beitrag zur Entstehung des Erdöls. Eur J Org Chem 510, 42-62.

Tuuling, I. and Flodén, T. (2009) The Llandovery–lowermost Wenlock sequence in the Baltic Sea between Saaremaa and Gotland; subdivision, thicknesses and correlation, based on marine seismic studies. Mar Geol 267, 55-70.

Ulmishek, G. (1990) Geologic evolution and petroleum resources of the Baltic Basin, in: Leighton, M.W., Kolata, D.R., Oltz, D.F., Eidel, J.J. (Eds.), Interior Cratonic Basins. American Association of Petroleum Geologists, Tulsa, Oklahoma, pp. 603-632.

Ungerer, P. (1990) State of the art of research in kinetic modelling of oil formation and expulsion. Organic Geochemistry 16, 1-25.

Ungerer, P., Behar, F., Villalba, M., Heum, O.R. and Audibert, A. (1988) Kinetic modelling of oil cracking. Organic Geochemistry 13, 857-868.

Ungerer, P. and Pelet, R. (1987) Extrapolation of the kinetics of oil and gas formation from laboratory experiments to sedimentary basins. Nature 327, 52-54.

Ūsaityt, D. (2000) The geology of the southeastern Baltic Sea: a review. Earth-Science Reviews 50, 137-225.

Van de Meent, D., Brown, S.C., Philp, R.P. and Simoneit, B.R. (1980) Pyrolysis-high resolution gas chromatography and pyrolysis gas chromatography-mass spectrometry of kerogens and kerogen precursors. Geochimica et Cosmochimica Acta 44, 999-1013.

van Duin, A.C. and Larter, S.R. (1997) Unravelling Mango's mysteries: a kinetic scheme describing the diagenetic fate of C 7-alkanes in petroleum systems. Organic geochemistry 27, 597-599.

van Duin, A.C. and Larter, S.R. (1998) Application of molecular dynamics calculations in the prediction of dynamical molecular properties. Organic Geochemistry 29, 1043-1050.

van Kaam-Peters, H.M., Köster, J., van der Gaast, S.J., Dekker, M., de Leeuw, J.W. and Damsté, J.S.S. (1998) The effect of clay minerals on diasterane/sterane ratios. Geochimica et Cosmochimica Acta 62, 2923-2929.

Van Krevelen, D. (1950) Graphical-statistical method for the study of structure and reaction processes of coal. Fuel 29, 269-284.

Vandenbroucke, M., Behar, F. and Rudkiewicz, J.L. (1999) Kinetic modelling of petroleum formation and cracking: implications from the high pressure/high temperature Elgin Field (UK, North Sea). Organic Geochemistry 30, 1105-1125.

Vandenbroucke, M. and Largeau, C. (2007) Kerogen origin, evolution and structure. Organic Geochemistry 38, 719-833.

Veeh, H., Calvert, S. and Price, N. (1974) Accumulation of uranium in sediments and phosphorites on the South West African shelf. Marine Chemistry 2, 189-202.

Vejbæk, G., Stouge, S. and Poulsen, K.D. (1994) Palaeozoic tectonic and sedimentary evolution and hydrocarbon prospectivity in the Bornholm area. Geological Survey of Denmark.

Velde, B. and Espitalié, J. (1989) Comparison of kerogen maturation and illite/smectite composition in diagenesis. Journal of Petroleum Geology 12, 103-110.

Venkatesan, M. and Dahl, J. (1989) Organic geochemical evidence for global fires at the Cretaceous/Tertiary boundary. Nature 338, 57-60.

Vine, J.D. and Tourtelot, E.B. (1970) Geochemistry of black shale deposits; a summary report. Economic Geology 65, 253-272.

Volk, H., George, S.C., Middleton, H. and Schofield, S. (2005) Geochemical comparison of fluid inclusion and present-day oil accumulations in the Papuan Foreland–evidence for previously unrecognised petroleum source rocks. Organic Geochemistry 36, 29-51.

Walters, C. (2006) The origin of petroleum. Practical Advances in Petroleum Processing, 79-101.

Walters, C.C., Wang, F.C., Qian, K., Wu, C., Mennito, A.S. and Wei, Z. (2015) Petroleum alteration by thermochemical sulfate reduction–A comprehensive molecular study of aromatic hydrocarbons and polar compounds. Geochimica et Cosmochimica Acta 153, 37-71.

Waples, D.W. (2000) The kinetics of in-reservoir oil destruction and gas formation: constraints from experimental and empirical data, and from thermodynamics. Organic Geochemistry 31, 553-575.

Waples, D.W. (2010) SOURCE-ROCK KINETICS. Unpublished.

Waples, D.W. and Marzi, R.W. (1998) The universality of the relationship between vitrinite reflectance and transformation ratio. Organic Geochemistry 28, 383-388.

Waples, D.W., Suizu, M. and Kamata, H. (1992) The Art of Maturity Modeling. Part 2: Alternative Models and Sensitivity Analysis. AAPG Bulletin.

Waters, C.N., Waters, R.A., Barclay, W.J. and Davies, J.R. (2009) A lithostratigraphical framework for the Carboniferous successions of southern Great Britain (Onshore). BGS Report.

Weaver, C.E. (1960) Possible uses of clay minerals in search for oil. AAPG Bulletin 44, 1505-1518.

Wei, Z., Moldowan, J.M., Dahl, J., Goldstein, T.P. and Jarvie, D.M. (2006) The catalytic effects of minerals on the formation of diamondoids from kerogen macromolecules. Organic Geochemistry 37, 1421-1436.

Welte, D. and Waples, D. (1973) Über die Bevorzugung geradzahliger n-Alkane in Sedimentgesteinen. Naturwissenschaften 60, 516-517.

Welte, D.H. (1965) Relation between petroleum and source rock. AAPG Bulletin 49, 2246-2268.

Welte, D.H. (1970) Organischer Kohlenstoff und die Entwicklung der Photosynthese auf der Erde. Naturwissenschaften 57, 17-23.

Whitmore, F.C. (1934) Mechanism of the polymerization of olefins by acid catalysts. Industrial & Engineering Chemistry 26, 94-95.

Whyte, G.N. (1973) Principles of radiation dosimetry. John Wiley and Sons, Inc., New York.

Więcław, D., Kotarba, M.J., Kosakowski, P., Kowalski, A. and Grotek, I. (2010a) Habitat and hydrocarbon potential of the lower Paleozoic source rocks in the Polish part of the Baltic region. Geological Quarterly 54, 159-182.

Więcław, D., Kotarba, M.J. and Kowalski, A. (2010b) Origin of oils accumulated in the Middle Cambrian reservoirs of the Polish part of the Baltic region. Geological Quarterly 54, 205-216.

Williams, J., Bjorøy, M., Dolcater, D. and Winters, J. (1986) Biodegradation in South Texas Eocene oils—effects on aromatics and biomarkers. Organic Geochemistry 10, 451-461.

Williams, P.T., Besler, S. and Taylor, D.T. (1990) The pyrolysis of scrap automotive tyres: The influence of temperature and heating rate on product composition. Fuel 69, 1474-1482.

Wróbel, M. and Kosakowski, P. (2010) 2-D modelling of petroleum processes of the lower Paleozoic strata in the Polish part of the Baltic region. Geol. Quart 54, 257-266.

Wu, L.M., Zhou, C.H., Keeling, J., Tong, D.S. and Yu, W.H. (2012) Towards an understanding of the role of clay minerals in crude oil formation, migration and accumulation. Earth-Science Reviews 115, 373-386.

Wu, Z., Jernström, S., Hughey, C.A., Rodgers, R.P. and Marshall, A.G. (2003) Resolution of 10 000 compositionally distinct components in polar coal extracts by negative-ion electrospray ionization Fourier transform ion cyclotron resonance mass spectrometry. Energy & fuels 17, 946-953.

Xiao, Y. and James, A. (1997) Is acid catalyzed isomerization responsible for the invariance in isoheptanes of petroleum, The 18th

International Meeting on Organic Geochemistry, Book of Abstracts, pp. 769-770.

Yang, S. and Horsfield, B. (2016) Some predicted effects of minerals on the generation of petroleum in nature. Energy & Fuels 30, 6677-6687.

Yang, S., Horsfield, B., Mahlstedt, N., Stephenson, M. and Könitzer, S. (2015) On the primary and secondary petroleum generating characteristics of the Bowland Shale, northern England. Journal of the Geological Society.

Yang, S., Horsfield, B., Mahlstedt, N., Stephenson, M.H. and Könitzer, S.F. (2016) On the primary and secondary petroleum generating characteristics of the Bowland Shale, northern England. Journal of the Geological Society 173, 292-305.

Yang, S., Schulz, H.-M., Schovsbo, N.H. and Bojesen-Koefoed, J.A. (2017) Oil-source rock correlation of the Lower Palaeozoic petroleum system in the Baltic Basin (northern Europe). AAPG Bulletin preliminary version published online Ahead of Print May 22, 2017.

Zdanavičiūtė, O. (2012) The Middle Cambrian Succession In The Central Baltic Basin: Geochemistry Of Oils And Sandstone Reservoir Characteristics. Journal of Petroleum Geology 35, 237-254.

Zdanavičiūtė, O. and Lazauskienė, J. (2004) Hydrocarbon migration and entrapment in the Baltic Syneclise. Organic Geochemistry 35, 517-527.

Zdanavičiūtė, O. and Lazauskienė, J. (2009) Organic matter of Early Silurian succession–the potential source of unconventional gas in the Baltic Basin (Lithuania). Baltica 22, 89-99.

Zdanavikiute, O. and Bojesen-Koefoed, J.A. (1997) Geochemistry of Lithuanian oils and source rocks: a preliminary assessment. Journal of Petroleum Geology 20, 381-402.

Zengler, K., Richnow, H.H., Rosselló-Mora, R., Michaelis, W. and Widdel, F. (1999) Methane formation from long-chain alkanes by anaerobic microorganisms. Nature 401, 266-269.

Ziegs, V. (2013) Development of a compositional kinetic model for primary and secondary petroleum generation from Lower Cretaceous Wealden Shales , Lower Saxony Basin , Northern Germany.

Ziegs, V., Horsfield, B., Skeie, J.E. and Rinna, J. (2017) Petroleum retention in the Mandal Formation, Central Graben, Norway. Marine and Petroleum Geology 83, 195-214.

Zobell, C.E. (1945) The role of bacteria in the formation and transformation of petroleum hydrocarbons. Science (New York, NY) 102, 364-369.